Theory Manual Version 2.7

Last Updated: April 11, 2018

Contributors
Steve Maas (steve.maas@utah.edu)
Dave Rawlins (rawlins@sci.utah.edu)
Dr. Jeffrey Weiss (jeff.weiss@utah.edu)
Dr. Gerard Ateshian (ateshian@columbia.edu)

Contact address
Musculoskeletal Research Laboratories, University of Utah
72 S. Central Campus Drive, Room 2646
Salt Lake City, Utah

Website
MRL: `http://mrl.sci.utah.edu`
FEBio: `http://febio.org`

Forum
`https://forums.febio.org/index.php`

Contents

Chapter 1

Introduction

1.1   Overview of FEBio

FEBio is an implicit, nonlinear finite element solver that is specifically designed for applications in biomechanics. It offers analyses, constitutive models and boundary conditions that are relevant for this particular field. This section describes briefly the available features of FEBio. A more detailed overview of features can be found in the *FEBio User's Manual*.

FEBio supports two analysis types, namely *quasi-static* and *quasi-static poroelastic*. In a *quasi-static* analysis the (quasi-) static response of the system is sought; inertial terms are ignored. In a *quasi-static poroelastic* analysis a coupled solid-fluid problem is solved. The latter analysis type is useful for modeling tissues that have high water content and the explicit modeling of fluid movement relative to the solid phase is important.

Several nonlinear constitutive models are available to allow the user to model the often complicated biological tissue behavior. Several isotropic constitutive models are supported such as Neo-Hookean, Mooney-Rivlin, Veronda-Westmann, Arruda-Boyce and Ogden. These models have a nonlinear stress-strain response. In addition to the isotropic models, there are several anisotropic models available. These materials show anisotropic behavior in at least one preferred direction and are useful for modeling biological tissues such as tendons, muscles and other tissues that contain fibers. FEBio also contains a *rigid body* material model, which can be used to model rigid structures whose deformation is negligible compared to the deformable geometry.

Biological tissues can interact in very complicated ways. Therefore FEBio supports a wide range of boundary conditions to model these interactions. These include prescribed displacements, nodal forces, and pressure forces. Deformable models can also be connected to rigid bodies so that the user can model prescribed rotations and torques. Rigid bodies can be connected with rigid joints. Even more complicated interactions can be modeled using FEBio's contact interfaces. The user can choose between different types of contact interfaces, such as sliding interfaces, tied interfaces and rigid wall interfaces. A sliding interface is defined between two surfaces that are allowed to separate and slide across each other but are not allowed to penetrate. The rigid wall interface is also similar to the sliding interface, except that one of the contacting surfaces is a movable rigid wall. As of version 1.2, there is an implementation of a sliding interface that allows for fluid flow crossing the contact interface. The tied interface is similar to the sliding interface, but in this case, the surfaces are not allowed to slide or separate. In addition, the user may specify a body force which can be used to model the effects of gravity or base acceleration.

1.2   About this document

This document is a part of a set of three manuals that accompany FEBio: the *FEBio User's Manual*, describing how to use FEBio, the *FEBio Developer's Manual* for users who wish to modify or add features to the code, and this manual, which describes the theory behind most of the FEBio algorithms.

The purpose of this manual is to provide theoretical background on many of the algorithms that are implemented in FEBio. In this way the user can develop a better understanding of how the program works and how it can be used to create well defined biomechanical simulations. The authors have tried to be as detailed as possible to make the text coherent and comprehensible, but due to the complexity of some of the topics, some descriptions only skim the surface. Many of the theoretical ideas discussed in this manual can and have filled entire bookshelves. The explanations contained herein should be sufficient to give the reader a basic understanding of the theoretical developments. References to textbooks and the primary literature are provided for further reading.

Chapter 2 starts with a brief overview of some of the important concepts in continuum mechanics. Readers who are already familiar with this field can skip this chapter, although the material may be useful to get familiar with the notation and terminology used in this manual.

Chapter 3 describes the nonlinear finite element method. It also explains the Newton-Raphson method, which is the basis for most implementations of the nonlinear finite element method. A more specialized version of this algorithm, the BFGS method, is described as well since it is used in FEBio.

In Chapter 4 the different element types that are available in FEBio are described in detail. FEBio currently supports 3D solid elements, such as the linear hexahedral, pentahedral and tetrahedral elements, as well as quadrilateral and triangular shell elements.

Chapter 5 contains a detailed description of the material models in FEBio. Most of these models are based on hyperelasticity, which is introduced in chapter 2. Several transversely isotropic materials are described as well. This also discusses the biphasic material and its implementation in FEBio.

Chapter 6 describes the basics of the theory of contact and coupling. In FEBio the user can connect the different parts of the geometry in a variety of ways. There are rigid interfaces where a deformable model is attached to a rigid model, rigid joints where two or more rigid bodies connect, and sliding interfaces where two surfaces are allowed to separate and slide across each other but are not allowed to penetrate. The various contact and coupling algorithms are discussed as well together with their implementation in FEBio.

Chapter 2

Continuum Mechanics

This chapter contains an overview of some of the important concepts from continuum mechanics and establishes some of the notation and terminology that will be used in the rest of this document. The section begins by introducing the important concepts of deformation, stress and strain. Next the concept of hyperelasticity is discussed. Finally the concept of virtual work is discussed. This concept will be used later to derive the nonlinear finite element equations. For a more thorough introduction to the mathematics needed for continuum mechanics, the user can consult [19].

2.1 Vectors and Tensors

It is assumed that the reader is familiar with the concepts of vectors and tensors. This section summarizes the notation and some useful relations that will be used throughout the manual.

Vectors are denoted by small, bold letters, e.g. $\mathbf{v}$. Their components will be denoted by v_i, where, unless otherwise stated, Latin under scripts such as i or I will range from 1 to 3. In matrix form a vector will be represented as a column vector and its transpose as a row vector:

$$\mathbf{v} = \begin{pmatrix} v_1 \\ v_2 \\ v_3 \end{pmatrix}, \qquad \mathbf{v}^T = \begin{pmatrix} v_1, & v_2, & v_3 \end{pmatrix} . \tag{2.1.1}$$

The following products are defined between vectors. Assume $\mathbf{u}$, $\mathbf{v}$ are vectors. Also note that the Einstein summation convention is used throughout this manual [38].

The *dot* or *scalar product*:

$$\mathbf{u} \cdot \mathbf{v} = u_i v_i . \tag{2.1.2}$$

The *cross product*:

$$\mathbf{u} \times \mathbf{v} = \begin{bmatrix} u_2 v_3 - u_3 v_2 \\ u_3 v_1 - u_1 v_3 \\ u_1 v_2 - u_2 v_1 \end{bmatrix} . \tag{2.1.3}$$

The *vector outer product*:

$$(\mathbf{u} \otimes \mathbf{v})_{ij} = u_i v_j . \tag{2.1.4}$$

Note that vectors are also known as first order tensors. Scalars are known as zero order tensors. The outer product, defined by equation (2.1.4), is a second order tensor.

Second order tensors are denoted by bold, capital letters, e.g. $\mathbf{A}$. Some exceptions will be made to remain consistent with the literature. For instance, the Cauchy stress tensor is denoted

by σ. However, the nature of the objects will always be clear from the context. The following operations on tensors are defined. Assume $\mathbf{A}$ and $\mathbf{B}$ are second-order tensors.

The *double contraction* or *tensor inner product* is defined as:

$$\mathbf{A} : \mathbf{B} = A_{ij} B_{ij} \,. \tag{2.1.5}$$

The *trace* is defined as:

$$\operatorname{tr} \mathbf{A} = \mathbf{I} : \mathbf{A} = A_{ii} \,. \tag{2.1.6}$$

Here $\mathbf{I}$ is the second order identity tensor with components δ_{ij}.

In general the components of tensors will change under a change of coordinate system. Nevertheless, certain intrinsic quantities associated with them will remain invariant under such a transformation. The scalar product between two vectors is such an example. The double contraction between two second-order tensors is another example. The following set of invariants for second-order tensors is commonly used:

$$\begin{aligned}
I_1 &= \operatorname{tr} \mathbf{A}, \\
I_2 &= \frac{1}{2} \left((\operatorname{tr} \mathbf{A})^2 - \operatorname{tr} \mathbf{A}^2 \right). \\
I_3 &= \det \mathbf{A}.
\end{aligned} \tag{2.1.7}$$

A tensor $\mathbf{S}$ is called symmetric if it is equal to its transpose:

$$\mathbf{S} = \mathbf{S}^T \,. \tag{2.1.8}$$

A tensor $\mathbf{W}$ is called anti-symmetric if it is equal to the negative of its transpose:

$$\mathbf{W} = -\mathbf{W}^T \,. \tag{2.1.9}$$

Any second order tensor $\mathbf{A}$ can be written as the sum of a symmetric tensor $\mathbf{S}$ and an anti-symmetric tensor $\mathbf{W}$:

$$\mathbf{A} = \mathbf{S} + \mathbf{W}, \tag{2.1.10}$$

where

$$\mathbf{S} = \frac{1}{2} \left(\mathbf{A} + \mathbf{A}^T \right), \text{ and } \mathbf{W} = \frac{1}{2} \left(\mathbf{A} - \mathbf{A}^T \right). \tag{2.1.11}$$

Also note that for any tensor $\mathbf{B}$ the following holds:

$$\mathbf{B} : \mathbf{A} = \mathbf{B} : \mathbf{S}, \quad \mathbf{B} : \mathbf{W} = \mathbf{0} \,. \tag{2.1.12}$$

With any anti-symmetric tensor a dual vector $\mathbf{w}$ can be associated such that,

$$\hat{\mathbf{w}} \cdot \mathbf{u} = \mathbf{w} \times \mathbf{u} \,, \tag{2.1.13}$$

where the second order tensor $\hat{\mathbf{w}}$ is defined as,

$$\hat{\mathbf{w}} = \begin{bmatrix} 0 & -w_3 & w_2 \\ w_3 & 0 & -w_1 \\ -w_2 & w_1 & 0 \end{bmatrix}. \tag{2.1.14}$$

A second order $\mathbf{Q}$ tensor is called *orthogonal* if $\mathbf{Q}^{-1} = \mathbf{Q}^T$.

In the implementation of the FE method it is often convenient to write symmetric second-order tensors using *Voigt notation*. In this notation the components of a 2nd order symmetric tensor $\mathbf{A}$ are arranged as a column vector:

$$[\mathbf{A}] = \begin{bmatrix} A_{11} \\ A_{22} \\ A_{33} \\ A_{12} \\ A_{23} \\ A_{13} \end{bmatrix} . \tag{2.1.15}$$

Higher order tensors will be denoted by bold, capital, script symbols, e.g. $\mathcal{A}$. An example of a third-order tensor is the *permutation tensor* $\mathcal{E}_{ijk}$, whose components are 1 for an even permutation of $(1, 2, 3)$, -1 for an odd permutation of $(1, 2, 3)$ and zero otherwise. The permutation symbol is useful for expressing the cross-product of two vectors in index notation:

$$(\mathbf{u} \times \mathbf{v})_i = \mathcal{E}_{ijk} u_j v_k . \tag{2.1.16}$$

An example of a fourth-order tensor is the elasticity tensor $\mathcal{C}$ which, in linear elasticity theory, relates the small strain tensor ε and the Cauchy stress tensor $\sigma = \mathcal{C} : \varepsilon$.

Higher order tensors can be constructed from second order tensors in a similar way as second order tensors can be constructed from vectors. If $\mathbf{A}$ and $\mathbf{B}$ are second order tensors, then the following fourth order tensors can be defind by requiring that the following must hold for any second order tensor $\mathbf{X}$:

$$(\mathbf{A} \otimes \mathbf{B}) : \mathbf{X} = (\mathbf{B} : \mathbf{X}) \, \mathbf{A} , \tag{2.1.17}$$

$$(\mathbf{A} \underline{\otimes} \mathbf{B}) : \mathbf{X} = \mathbf{A} \cdot \mathbf{X} \cdot \mathbf{B}^T , \tag{2.1.18}$$

$$(\mathbf{A} \overline{\otimes} \mathbf{B}) : \mathbf{X} = \mathbf{A} \cdot \mathbf{X}^T \cdot \mathbf{B}^T , \tag{2.1.19}$$

$$(\mathbf{A} \underline{\overline{\otimes}} \mathbf{B}) : \mathbf{X} = \frac{1}{2} \left(\mathbf{A} \cdot \mathbf{X} \cdot \mathbf{B}^T + \mathbf{A} \cdot \mathbf{X}^T \cdot \mathbf{B}^T \right) . \tag{2.1.20}$$

The Cartesian component forms of the operators $\otimes$, $\underline{\otimes}$, $\overline{\otimes}$ and $\underline{\overline{\otimes}}$ are defined as follows:

$$(\mathbf{A} \otimes \mathbf{B})_{ijkl} = \mathbf{A}_{ij} \mathbf{B}_{kl} , \tag{2.1.21}$$

$$(\mathbf{A} \underline{\otimes} \mathbf{B})_{ijkl} = \mathbf{A}_{ik} \mathbf{B}_{jl} , \tag{2.1.22}$$

$$(\mathbf{A} \overline{\otimes} \mathbf{B})_{ijkl} = A_{il} B_{jk} , \tag{2.1.23}$$

$$(\mathbf{A} \underline{\overline{\otimes}} \mathbf{B})_{ijkl} = \frac{1}{2} \left(A_{ik} B_{jl} + A_{il} B_{jk} \right) . \tag{2.1.24}$$

The fourth order identity tensors are defined as:

$$\begin{aligned} \mathbf{A} &= \mathcal{I} : \mathbf{A} , \\ \mathbf{A}^T &= \overline{\mathcal{I}} : \mathbf{A} , \end{aligned} \tag{2.1.25}$$

where $\mathcal{I} = \mathbf{I} \underline{\otimes} \mathbf{I}$ and $\overline{\mathcal{I}} = \mathbf{I} \overline{\otimes} \mathbf{I}$. The components are given by:

$$\begin{aligned} \mathcal{I}_{ijkl} &= \delta_{ik} \delta_{jl} , \\ \overline{\mathcal{I}}_{ijkl} &= \delta_{il} \delta_{jk} . \end{aligned} \tag{2.1.26}$$

2.2   The Directional Derivative

In later sections the nonlinear finite element method will be formulated. Anticipating an iterative solution method to solve the nonlinear equations, it will be necessary to linearize the quantities involved. This linearization process will utilize a construction called the *directional derivative* [19].

The directional derivative of a function $f(\mathbf{x})$ is defined as follows:

$$Df(\mathbf{x})[\mathbf{u}] = \left.\frac{d}{d\varepsilon}\right|_{\varepsilon=0} f(\mathbf{x} + \varepsilon\mathbf{u}) . \tag{2.2.1}$$

The quantity $\mathbf{x}$ may be a scalar, a vector or even a vector of unknown functions. For instance, consider a scalar function $f(\mathbf{x})$, where $\mathbf{x}$ is the position vector in $\mathbb{R}^3$. In this case the directional derivative is given by:

$$\begin{aligned} Df(\mathbf{x})[\mathbf{u}] &= \left.\frac{d}{d\varepsilon}\right|_{\varepsilon=0} f(\mathbf{x} + \varepsilon\mathbf{u}) \\ &= \frac{\partial f}{\partial x_i} u_i \\ &= \nabla f \cdot \mathbf{u} . \end{aligned} \tag{2.2.2}$$

Here, the symbol ∇("nabla") depicts the gradient operator.

The linearization of a function implies that it is approximated by a linear function. Using the directional derivative, a function f can be linearized as follows:

$$f(\mathbf{x} + \mathbf{u}) \cong f(\mathbf{x}) + Df(\mathbf{x})[\mathbf{u}] . \tag{2.2.3}$$

The directional derivative obeys the usual properties for derivatives.

1. *sum rule*: If $f = f_1 + f_2$, then

$$Df(\mathbf{x})[\mathbf{u}] = Df_1(\mathbf{x})[\mathbf{u}] + Df_2(\mathbf{x})[\mathbf{u}] . \tag{2.2.4}$$

2. *product rule*: If $f = f_1 \cdot f_2$, then

$$Df(\mathbf{x})[\mathbf{u}] = f_1(\mathbf{x}) \cdot Df_2(\mathbf{x})[\mathbf{u}] + f_2 \cdot Df_1(\mathbf{x})[\mathbf{u}] . \tag{2.2.5}$$

3. *chain rule*: If $f = g(h(\mathbf{x}))$, then

$$Df(\mathbf{x})[\mathbf{u}] = Dg(h(\mathbf{x}))[Dh(\mathbf{x})[\mathbf{u}]] . \tag{2.2.6}$$

2.3   Deformation, Strain and Stress

2.3.1   The deformation gradient tensor

Consider the deformation of an object from an initial or *reference configuration* to a deformed or *current configuration*. The location of the material particles in the reference configuration are denoted by $\mathbf{X}$ and are known as the *material coordinates.* Their location in the current configuration is denoted by $\mathbf{x}$ and known as the *spatial coordinates.* The *deformation map φ*, which is a mapping from $\mathbb{R}^3$to$\mathbb{R}^3$, maps the coordinates of a material point to the spatial configuration:

$$\mathbf{x} = \varphi(\mathbf{X}) . \tag{2.3.1}$$
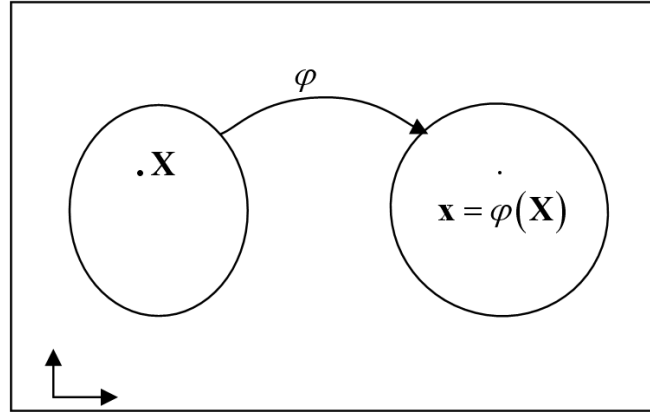
The deformation map

The displacement map $\mathbf{u}$ is defined as the difference between the spatial and material coordinates:

$$\mathbf{x} = \mathbf{X} + \mathbf{u}\left(\mathbf{X}\right).\tag{2.3.2}$$

The *deformation gradient* is defined as

$$\mathbf{F} = \frac{\partial \varphi}{\partial \mathbf{X}}.\tag{2.3.3}$$

The deformation gradient relates an infinitesimal vector in the reference configuration $d\mathbf{X}$ to the corresponding vector in the current configuration:

$$d\mathbf{x} = \mathbf{F} \cdot d\mathbf{X}.\tag{2.3.4}$$

The determinant of the deformation tensor $J = \det \mathbf{F}$ is called the *volume ratio*; it gives the volume change, or equivalently the change in density:

$$\rho_0 = \rho J.\tag{2.3.5}$$

Here ρ_0 is the density in the reference configuration and ρ is the current density.

When dealing with incompressible and nearly incompressible materials it will prove useful to separate the volumetric and the deviatoric (distortional) components of the deformation gradient. Such a separation must ensure that the deviatoric part of the deformation gradient, namely $\tilde{\mathbf{F}}$, does not produce any change in volume. Noting that the determinant of the deformation gradient gives the volume ratio, the determinant of $\tilde{\mathbf{F}}$ must therefore satisfy,

$$\det \tilde{\mathbf{F}} = 1.\tag{2.3.6}$$

This condition can be achieved by choosing $\tilde{\mathbf{F}}$ as,

$$\tilde{\mathbf{F}} = J^{-1/3}\mathbf{F}.\tag{2.3.7}$$

Using the polar decomposition of a second order tensor, the deformation gradient can be written as a product of a positive definite symmetric tensor $\mathbf{V}$ (or $\mathbf{U}$) and a proper orthogonal tensor $\mathbf{R}$:

$$\mathbf{F} = \mathbf{V} \cdot \mathbf{R} = \mathbf{R} \cdot \mathbf{U}.\tag{2.3.8}$$

$\mathbf{V}$ is called the *left stretch tensor*, $\mathbf{U}$ is called the *right stretch tensor* and the orthogonal tensor $\mathbf{R}$ is called the *rotation*.

2.3.2 Strain

The *right Cauchy-Green deformation tensor* is defined as follows:

$$\mathbf{C} = \mathbf{F}^T \cdot \mathbf{F}\,. \tag{2.3.9}$$

This tensor is an example of a *material tensor* and is typically expressed a function of the material coordinates $\mathbf{X}$. The *left Cauchy-Green deformation tensor* is defined as follows:

$$\mathbf{b} = \mathbf{F} \cdot \mathbf{F}^T\,. \tag{2.3.10}$$

This tensor is an example of a *spatial tensor* and is typically expressed as a function of the spatial coordinates $\mathbf{x}$. The implementation of the updated Lagrangian finite element method used by FEBio is described in the spatial configuration.

The left and right deformation tensors can also be split into volumetric and deviatoric components. With the use of,(2.3.7) the deviatoric deformation tensors are:

$$\begin{aligned}
\tilde{\mathbf{C}} &= \tilde{\mathbf{F}}^T \cdot \tilde{\mathbf{F}} = J^{-2/3}\mathbf{C}\,, \\
\tilde{\mathbf{b}} &= \tilde{\mathbf{F}} \cdot \tilde{\mathbf{F}}^T = J^{-2/3}\mathbf{b}\,.
\end{aligned} \tag{2.3.11}$$

The deformation tensors defined above are not good candidates for strain measures since in the absence of strain they become the identity tensor $\mathbf{I}$. However, they can be used to define strain measures. The *Green-Lagrange strain tensor* is defined as:

$$\mathbf{E} = \frac{1}{2}\left(\mathbf{C} - \mathbf{I}\right)\,. \tag{2.3.12}$$

This tensor is a material tensor. Its spatial equivalent is known as the *Almansi strain tensor* and is defined as:

$$\mathbf{e} = \frac{1}{2}\left(\mathbf{I} - \mathbf{b}^{-1}\right)\,. \tag{2.3.13}$$

In the limit of small displacement gradients, the components of both strain tensors are identical, resulting in the *small strain tensor* or *infinitesimal strain tensor*:

$$\varepsilon = \frac{1}{2}\left(\frac{\partial \mathbf{u}}{\partial \mathbf{x}} + \left(\frac{\partial \mathbf{u}}{\partial \mathbf{x}}\right)^T\right)\,. \tag{2.3.14}$$

Note that the small strain tensor is also the linearization of the Green Lagrange strain,

$$D\mathbf{E}\left[\mathbf{u}\right] = \mathbf{F}^T \cdot \varepsilon \cdot \mathbf{F}\,. \tag{2.3.15}$$

2.3.3 Stress

The traction $\mathbf{t}$ on a plane bisecting the body is given by,

$$\mathbf{t} = \boldsymbol{\sigma} \cdot \mathbf{n}, \tag{2.3.16}$$

where $\boldsymbol{\sigma}$ is the *Cauchy stress tensor* and $\mathbf{n}$ is the outward unit normal vector to the plane. It can be shown that by the conservation of angular momentum that this tensor is symmetric ($\sigma_{ij} = \sigma_{ji}$) [57]. The Cauchy stress tensor, a spatial tensor, is the actual physical stress, that is, the force per unit deformed area. To simplify the equations of continuum mechanics, especially when working

in the material configuration, several other stress measures are often used. The *Kirchhoff stress tensor* is defined as

$$\boldsymbol{\tau} = J\boldsymbol{\sigma}\,. \qquad (2.3.17)$$

The *first Piola-Kirchhoff stress tensor* is given as

$$\mathbf{P} = J\boldsymbol{\sigma} \cdot \mathbf{F}^{-T}\,. \qquad (2.3.18)$$

Note that $\mathbf{P}$, like $\mathbf{F}$, is not symmetric. Also, like $\mathbf{F}$, $\mathbf{P}$ is known as a *two-point* tensor, meaning it is neither a material nor a spatial tensor. Since we have two strain tensors, one spatial and one material tensor, it would be useful to have similar stress measures. The Cauchy stress is a spatial tensor and the *second Piola-Kirchhoff (2nd PK) stress tensor*, defined as

$$\mathbf{S} = J\mathbf{F}^{-1} \cdot \boldsymbol{\sigma} \cdot \mathbf{F}^{-T}\,, \qquad (2.3.19)$$

is a material tensor. The inverse relations are:

$$\boldsymbol{\sigma} = \frac{1}{J}\boldsymbol{\tau}\,, \quad \boldsymbol{\sigma} = \frac{1}{J}\mathbf{P} \cdot \mathbf{F}^{T}\,, \quad \boldsymbol{\sigma} = \frac{1}{J}\mathbf{F} \cdot \mathbf{S} \cdot \mathbf{F}^{T}\,. \qquad (2.3.20)$$

In many practical applications it is physically relevant to separate the hydrostatic stress and the deviatoric stress $\tilde{\boldsymbol{\sigma}}$ of the Cauchy stress tensor:

$$\boldsymbol{\sigma} = \tilde{\boldsymbol{\sigma}} + p\mathbf{I}\,. \qquad (2.3.21)$$

Here, the pressure is defined as $p = \frac{1}{3}\operatorname{tr}\boldsymbol{\sigma}$. Note that the deviatoric Cauchy stress tensor satisfies $\operatorname{tr}\tilde{\boldsymbol{\sigma}} = 0$.

The directional derivative of the 2nd PK stress tensor needs to be calculated for the linearization of the finite element equations. For a hyperelastic material, a linear relationship between the directional derivative of $\mathbf{S}$ and the linearized strain $D\mathbf{E}\left[\mathbf{u}\right]$ can be obtained:

$$D\mathbf{S}\left[\mathbf{u}\right] = \mathbb{C} : D\mathbf{E}\left[\mathbf{u}\right]\,. \qquad (2.3.22)$$

Here, $\mathbb{C}$ is a fourth-order tensor known as the *material elasticity tensor*. Its components are given by, $\sum$

$$\mathbb{C}_{IJKL} = \frac{\partial S_{IJ}}{\partial E_{KL}} = \frac{4\partial^2\Psi}{\partial C_{IJ}\partial C_{KL}}\,, \qquad (2.3.23)$$

where Ψ is the strain-energy density function for the hyperelastic material. The spatial equivalent – the *spatial elasticity tensor $\mathcal{C}$* – can be obtained by,

$$\mathcal{C}_{ijkl} = \frac{1}{J}F_{iI}F_{jJ}F_{kK}F_{lL}\mathcal{C}_{IJKL}. \qquad (2.3.24)$$

2.4 Hyperelasticity

When the constitutive behavior is only a function of the current state of deformation, the material is *elastic*. In the special case when the work done by the stresses during a deformation is only dependent on the initial state and the final state, the material is termed *hyperelastic* and its behavior is path-independent. As a consequence of the path-independence a *strain energy function*

per unit undeformed volume can be defined as the work done by the stresses from the initial to the final configuration:

$$\Psi\left(\mathbf{F}\left(\mathbf{X}\right),\mathbf{X}\right) = \int_{t_0}^{t} \mathbf{P}\left(\mathbf{F}\left(\mathbf{X}\right),\mathbf{X}\right) : \dot{\mathbf{F}}\, dt\,. \tag{2.4.1}$$

The rate of change of the potential is then given by

$$\dot{\Psi}\left(\mathbf{F}\left(\mathbf{X}\right),\mathbf{X}\right) = \mathbf{P} : \dot{\mathbf{F}}\,. \tag{2.4.2}$$

Or alternatively,

$$P_{iJ} = \sum_{i,J=1}^{3} \frac{\partial \Psi}{\partial F_{iJ}} \dot{F}_{iJ}\,. \tag{2.4.3}$$

Comparing (2.4.2) with (2.4.3) reveals that

$$\mathbf{P}\left(\mathbf{F}\left(\mathbf{X}\right),\mathbf{X}\right) = \frac{\partial \Psi\left(\mathbf{F}\left(\mathbf{X}\right),\mathbf{X}\right)}{\partial \mathbf{F}}\,. \tag{2.4.4}$$

This general constitutive equation can be further simplified by observing that, as a consequence of the objectivity requirement, Ψ may only depend on $\mathbf{F}$ through the stretch tensor $\mathbf{U}$ and must be independent of the rotation component $\mathbf{R}$. For convenience, however, Ψ is often expressed as a function of $\mathbf{C} = \mathbf{U}^2 = \mathbf{F}^T \cdot \mathbf{F}$. Noting that $\frac{1}{2}\dot{\mathbf{C}} = \dot{\mathbf{E}}$ is work conjugate to the second Piola-Kirchhoff stress $\mathbf{S}$, establishes the following general relationships for hyperelastic materials:

$$\dot{\Psi} = \frac{\partial \Psi}{\partial \mathbf{C}} : \dot{\mathbf{C}} = \frac{1}{2}\mathbf{S} : \dot{\mathbf{C}}, \quad \boxed{\mathbf{S}\left(\mathbf{C}\left(\mathbf{X}\right),\mathbf{X}\right) = 2\frac{\partial \Psi}{\partial \mathbf{C}} = \frac{\partial \Psi}{\partial \mathbf{E}}}\,. \tag{2.4.5}$$

2.4.1   Isotropic Hyperelasticity

The hyperelastic constitutive equations discussed so far are unrestricted in their application. Isotropic material symmetry is defined by requiring the constitutive behavior to be independent of the material axis chosen and, consequently, Ψ must only be a function of the invariants of $\mathbf{C}$,

$$\Psi\left(\mathbf{C}\left(\mathbf{X}\right),\mathbf{X}\right) = \Psi\left(I_1, I_2, I_3, \mathbf{X}\right)\,, \tag{2.4.6}$$

where the invariants of **C** are defined here as,

$$I_1 = \operatorname{tr}\mathbf{C} = \mathbf{C} : \mathbf{I},\ I_2 = \frac{1}{2}\left[\left(\operatorname{tr}\mathbf{C}\right)^2 - \operatorname{tr}\mathbf{C}^2\right],\ I_3 = \det\mathbf{C} = J^2\,. \tag{2.4.7}$$

As a result of the isotropic restriction, the second Piola-Kirchhoff stress tensor can be written as,

$$\mathbf{S} = 2\frac{\partial \Psi}{\partial \mathbf{C}} = 2\frac{\partial \Psi}{\partial I_1}\frac{\partial I_1}{\partial \mathbf{C}} + 2\frac{\partial \Psi}{\partial I_2}\frac{\partial I_2}{\partial \mathbf{C}} + 2\frac{\partial \Psi}{\partial I_3}\frac{\partial I_3}{\partial \mathbf{C}}\,. \tag{2.4.8}$$

The second order tensors formed by the derivatives of the invariants with respect to **C** can be evaluated as follows:

$$\frac{\partial I_1}{\partial \mathbf{C}} = \mathbf{I},\ \frac{\partial I_2}{\partial \mathbf{C}} = I_1\mathbf{I} - \mathbf{C},\ \frac{\partial I_3}{\partial \mathbf{C}} = I_3\mathbf{C}^{-1}\,. \tag{2.4.9}$$

Introducing expressions (2.4.9) into equation (2.4.8) enables the second Piola-Kirchhoff stress to be evaluated as,

$$\mathbf{S} = 2\left\{\left(\Psi_1 + I_1\Psi_2 + I_2\Psi_3\right)\right)\mathbf{I} - \left(\Psi_2 + I_1\Psi_3\right)\mathbf{C}\right\} + \Psi_3\mathbf{C}^2\,, \tag{2.4.10}$$

where $\Psi_I = \partial\Psi/\partial I_1$, $\Psi_2 = \partial\Psi/\partial I_2$, and $\Psi_3 = \partial\Psi/\partial I_3$.

The Cauchy stresses can now be obtained from the second Piola-Kirchhoff stresses by using (2.3.20):

$$\boldsymbol{\sigma} = \frac{2}{J}\left\{(\Psi_1 + I_1\Psi_2 + I_2\Psi_3))\,\mathbf{b} - (\Psi_2 + I_1\Psi_3)\,\mathbf{b}^2\right\} + \frac{1}{J}\Psi_3\mathbf{b}^3. \tag{2.4.11}$$

Note that in this equation Ψ_1, Ψ_2, and Ψ_3 still involve derivatives with respect to the invariants of $\mathbf{C}$. However, since the invariants of $\mathbf{b}$ are identical to those of $\mathbf{C}$, the quantities Ψ_1, Ψ_2 and Ψ_3 may also be considered to be the derivatives with respect to the invariants of $\mathbf{b}$.

2.4.2 Isotropic Elasticity in Principal Directions

For isotropic materials, the principal directions of the strain and stress tensors are the same. Let the eigenvalues of $\mathbf{C}$ be denoted by λ_i^2 $(i = 1, 2, 3)$, then the strain energy density may be given as a function of these eigenvalues, $\Psi\left(\lambda_1^2, \lambda_2^2, \lambda_3^2\right)$. To derive the expression for the stress, recognize that

$$\frac{\partial\lambda_i^2}{\partial\mathbf{C}} = \mathbf{N}_i \otimes \mathbf{N}_i \equiv \mathbf{A}_i, \tag{2.4.12}$$

where the $\mathbf{N}_i$ are the eigenvectors of $\mathbf{C}$. It follows that the second Piola-Kirchhoff stress may be represented as

$$\mathbf{S} = \sum_{i=1}^{3} S_i\mathbf{A}_i, \tag{2.4.13}$$

where

$$S_i = 2\frac{\partial\Psi}{\partial\lambda_i^2}. \tag{2.4.14}$$

To evaluate the material elasticity tensor, recognize that

$$\frac{\partial\mathbf{A}_i}{\partial\mathbf{C}} = \frac{1}{\lambda_i^2 - \lambda_j^2}\left(\mathbf{A}_i\,\overline{\underline{\otimes}}\,\mathbf{A}_j + \mathbf{A}_j\,\overline{\underline{\otimes}}\,\mathbf{A}_i\right) + \frac{1}{\lambda_i^2 - \lambda_k^2}\left(\mathbf{A}_i\,\overline{\underline{\otimes}}\,\mathbf{A}_k + \mathbf{A}_k\,\overline{\underline{\otimes}}\,\mathbf{A}_i\right), \tag{2.4.15}$$

where i, j, k form a permutation over $1, 2, 3$. Then it can be shown that the material elasticity tensor is given by

$$\begin{aligned}
\mathbb{C} = &\sum_{i=1}^{3} 4\frac{\partial^2\Psi}{\partial\lambda_i^2\partial\lambda_i^2}\mathbf{A}_i \otimes \mathbf{A}_i \\
&+ \sum_{i=1}^{3}\sum_{j=i+1}^{3} 4\frac{\partial^2\Psi}{\partial\lambda_i^2\partial\lambda_j^2}\left(\mathbf{A}_i \otimes \mathbf{A}_j + \mathbf{A}_j \otimes \mathbf{A}_i\right). \\
&+ \sum_{i=1}^{3}\sum_{j=i+1}^{3} 2\frac{S_i - S_j}{\lambda_i^2 - \lambda_j^2}\left(\mathbf{A}_i\,\overline{\underline{\otimes}}\,\mathbf{A}_j + \mathbf{A}_j\,\overline{\underline{\otimes}}\,\mathbf{A}_i\right)
\end{aligned} \tag{2.4.16}$$

When eigenvalues coincide, L'Hospital's rule may be used to evalue the coefficient in the last term,

$$\lim_{\lambda_j^2 \to \lambda_i^2} 2\frac{S_i - S_j}{\lambda_i^2 - \lambda_j^2} = 4\left(\frac{\partial^2\Psi}{\partial\lambda_j^2\partial\lambda_j^2} - \frac{\partial^2\Psi}{\partial\lambda_i^2\partial\lambda_j^2}\right). \tag{2.4.17}$$

The double summations in (2.4.16) are arranged such that the summands represent fourth-order tensors with major and minor symmetries.

In the spatial frame, the Cauchy stress is given by

$$\boldsymbol{\sigma} = \sum_{i=1}^{3} \sigma_i \mathbf{a}_i \,, \tag{2.4.18}$$

where

$$\mathbf{a}_i = \mathbf{n}_i \otimes \mathbf{n}_i \,, \tag{2.4.19}$$

and $\mathbf{n}_i = (\mathbf{F} \cdot \mathbf{N}_i) / \lambda_i$ are the eigenvectors of $\mathbf{b}$. The principal normal stresses are

$$\sigma_i = \frac{\lambda_i}{J} \frac{\partial \Psi}{\partial \lambda_i} \,. \tag{2.4.20}$$

The spatial elasticity tensor is given by

$$\begin{aligned}
\mathcal{C} = &\sum_{i=1}^{3} \left(J^{-1} \lambda_i^2 \frac{\partial^2 \Psi}{\partial \lambda_i^2} - \sigma_i \right) \mathbf{a}_i \otimes \mathbf{a}_i \\
&+ \sum_{i=1}^{3} \sum_{j=i+1}^{3} J^{-1} \lambda_i \lambda_j \frac{\partial^2 \Psi}{\partial \lambda_i \partial \lambda_j} \left(\mathbf{a}_i \otimes \mathbf{a}_j + \mathbf{a}_j \otimes \mathbf{a}_i \right) . \\
&+ \sum_{i=1}^{3} \sum_{j=i+1}^{3} 2 \frac{\lambda_j^2 \sigma_i - \lambda_i^2 \sigma_j}{\lambda_i^2 - \lambda_j^2} \left(\mathbf{a}_i \, \overline{\underline{\otimes}} \, \mathbf{a}_j + \mathbf{a}_j \, \overline{\underline{\otimes}} \, \mathbf{a}_i \right)
\end{aligned} \tag{2.4.21}$$

2.4.3 Nearly-Incompressible Hyperelasticity

A material is considered incompressible if it shows no change in volume during deformation, or otherwise stated, if $J = 1$ holds throughout the entire body. It can be shown [19] that if the material is incompressible the hyperelastic constitutive equation becomes

$$\mathbf{S} = 2 \frac{\partial \tilde{\Psi}}{\partial \mathbf{C}} + pJ\mathbf{C}^{-1} \,, \tag{2.4.22}$$

where $\tilde{\Psi} = \Psi \left(\tilde{\mathbf{C}} \right)$ is the deviatoric strain energy function and p is the hydrostatic pressure. The presence of J may seem unnecessary, but retaining J has the advantage that equation (2.4.22) remains valid in the nearly incompressible case. Further, in practical terms, a finite element analysis rarely enforces $J = 1$ in a pointwise manner, and hence its retention may be important for the evaluation of stresses.

The process of defining constitutive equations in the case of nearly incompressible hyperelasticity is simplified by adding a volumetric energy component $U(J)$ to the distortional component $\tilde{\Psi}(\mathbf{C})$:

$$\Psi(\mathbf{C}) = \tilde{\Psi}(\mathbf{C}) + U(J) \,. \tag{2.4.23}$$

The second Piola-Kirchhoff tensor for a material defined by (2.4.23) is obtained in the standard manner with the help of equation (2.4.8).

$$\begin{aligned}
\mathbf{S} &= 2 \frac{\partial \Psi}{\partial \mathbf{C}} \\
&= 2 \frac{\partial \tilde{\Psi}}{\partial \mathbf{C}} + 2 \frac{dU}{dJ} \frac{\partial J}{\partial \mathbf{C}} \,, \\
&= 2 \frac{\partial \tilde{\Psi}}{\partial \mathbf{C}} + pJ\mathbf{C}^{-1}
\end{aligned} \tag{2.4.24}$$

where the pressure p is defined as

$$p = \frac{dU}{dJ} \, . \tag{2.4.25}$$

An example for U that will be used later in the definition of the constitutive models is

$$U(J) = \frac{1}{2}\kappa \left(\ln J\right)^2 \, . \tag{2.4.26}$$

The parameter κ will be used later as a penalty factor that will enforce the (nearly-) incompressible constraint. However, κ can represent a true material coefficient, namely the bulk modulus, for a compressible material that happens to have a hyperelastic strain energy function in the form of (2.4.23). In the case where the dilatational energy is given by (2.4.26), the pressure is

$$p = \kappa \frac{\ln J}{J} \, . \tag{2.4.27}$$

Equation (2.4.24) can be further developed by applying the chain rule to the first term:

$$\mathbf{S} = pJ\mathbf{C}^{-1} + J^{-2/3}\operatorname{dev}\tilde{\mathbf{S}} \, , \tag{2.4.28}$$

where the *fictitious second Piola-Kirchoff* tensor [31] is defined by,

$$\tilde{\mathbf{S}} = 2\frac{\partial\tilde{\Psi}}{\partial\tilde{\mathbf{C}}} \, , \tag{2.4.29}$$

and Dev is the deviator operator in the reference frame:

$$\operatorname{Dev}(\cdot) = (\cdot) - \frac{1}{3}\left((\cdot):\mathbf{C}\right)\mathbf{C}^{-1}. \tag{2.4.30}$$

The Cauchy stress can then be obtained from equation $(2.3.20)_3$:

$$\boldsymbol{\sigma} = p\mathbf{I} + \operatorname{dev}\tilde{\boldsymbol{\sigma}} \, , \tag{2.4.31}$$

where

$$\tilde{\boldsymbol{\sigma}} = \frac{2}{J}\tilde{\mathbf{F}} \cdot \frac{\partial\tilde{\Psi}}{\partial\tilde{\mathbf{C}}} \cdot \tilde{\mathbf{F}}^T \, . \tag{2.4.32}$$

The following expression will be useful in the following development.

$$\frac{d\tilde{C}_{IJ}}{dC_{KL}} = J^{-2/3}\left(\frac{1}{2}\left(\delta_{IK}\delta_{JL} + \delta_{IL}\delta_{JK}\right) - \frac{1}{3}\tilde{C}_{IJ}\tilde{C}_{KL}^{-1}\right) \, . \tag{2.4.33}$$

Notice that the contraction with a symmetric tensor $\mathbf{A}$ results in,

$$\frac{d\tilde{C}_{IJ}}{dC_{KL}}A_{IJ} = J^{-2/3}\operatorname{Dev}A_{KL} \, . \tag{2.4.34}$$

The elasticity tensor, defined in (2.3.23), takes on the following form.

$$\begin{aligned}
\mathbb{C}_{IJKL} &= \left(J^2\frac{dp}{dJ} + Jp\right)C_{IJ}^{-1}C_{KL}^{-1} - 2pJ\mathcal{I}_{IJKL} \\
&\quad - \frac{2}{3}J^{-2/3}\left(\operatorname{Dev}\tilde{S}_{IJ}C_{KL}^{-1} + C_{IJ}^{-1}\operatorname{Dev}\tilde{S}_{KL}\right) \\
&\quad + \frac{2}{3}\tilde{S}_{RS}\tilde{C}_{RS}\left(\mathcal{I}_{IJKL} - \frac{1}{3}C_{KL}^{-1}C_{IJ}^{-1}\right) + J^{-4/3}\hat{\mathbb{C}}_{IJKL}
\end{aligned} \tag{2.4.35}$$

where

$$\hat{\mathbb{C}}_{IJKL} = \tilde{\mathbb{C}}_{IJKL} - \frac{1}{3}\left(\tilde{\mathbb{C}}_{IJRS}\tilde{C}_{RS}\tilde{C}_{KL}^{-1} + \tilde{\mathbb{C}}_{RSKL}C_{RS}C_{IJ}^{-1}\right) + \frac{1}{9}\tilde{C}_{IJ}^{-1}\tilde{C}_{RS}\tilde{\mathbb{C}}_{RSMN}\tilde{C}_{MN}\tilde{C}_{KL}^{-1}. \quad (2.4.36)$$

The spatial elasticity tensor follows from,

$$\begin{aligned}
\mathcal{C}_{ijkl} = &\left(J\frac{dp}{dJ} + p\right)\delta_{ij}\delta_{kl} - p\left(\delta_{ik}\delta_{jl} + \delta_{il}\delta_{jk}\right) \\
&- \frac{2}{3}\left(\mathrm{dev}\,\tilde{\sigma}_{ij}\delta_{kl} + \delta_{ij}\,\mathrm{dev}\,\tilde{\sigma}_{kl}\right) \\
&+ \frac{1}{3}\tilde{\sigma}_{rs}\delta_{rs}\left(\left(\delta_{ik}\delta_{jl} + \delta_{il}\delta_{jk}\right) - \frac{2}{3}\delta_{ij}\delta_{kl}\right) + \hat{\mathcal{C}}_{ijkl}
\end{aligned} \quad (2.4.37)$$

where

$$\hat{\mathcal{C}}_{ijkl} = \frac{1}{J}\tilde{F}_{iI}\tilde{F}_{jJ}\tilde{F}_{kK}\tilde{F}_{lL}\hat{\mathbb{C}}_{IJKL}. \quad (2.4.38)$$

2.4.4 Transversely Isotropic Hyperelasticity

Transverse isotropy can be introduced by adding a vector field representing the material preferred direction explicitly into the strain energy [64]. We require that the strain energy depends on a unit vector field $\mathbf{A}$, which describes the local fiber direction in the undeformed configuration. When the material undergoes deformation, the vector $\mathbf{A}(\mathbf{X})$ may be described by a unit vector field $\mathbf{a}(\varphi(\mathbf{X}))$. In general, the fibers will also undergo length change. The fiber stretch, λ, can be determined in terms of the deformation gradient and the fiber direction in the undeformed configuration,

$$\lambda\mathbf{a} = \mathbf{F}\cdot\mathbf{A}. \quad (2.4.39)$$

Also, since $\mathbf{a}$ is a unit vector,

$$\lambda^2 = \mathbf{A}\cdot\mathbf{C}\cdot\mathbf{A}. \quad (2.4.40)$$

The strain energy function for a transversely isotropic material, $\Psi(\mathbf{C}, \mathbf{A}, \mathbf{X})$ is an isotropic function of $\mathbf{C}$ and $\mathbf{A}\otimes\mathbf{A}$. It can be shown [57] that the following set of invariants are sufficient to describe the material fully:

$$I_1 = \mathrm{tr}\,\mathbf{C}, \quad I_2 = \frac{1}{2}\left[(\mathrm{tr}\,\mathbf{C})^2 - \mathrm{tr}\,\mathbf{C}^2\right], \quad I_3 = \det C = J^2, \quad (2.4.41)$$

$$I_4 = \mathbf{A}\cdot\mathbf{C}\cdot\mathbf{A}, \quad I_5 = \mathbf{A}\cdot\mathbf{C}^2\cdot\mathbf{A}. \quad (2.4.42)$$

The strain energy function can be written in terms of these invariants such that

$$\Psi(\mathbf{C}, \mathbf{A}, \mathbf{X}) = \Psi(I_1(\mathbf{C}), I_2(\mathbf{C}), I_3(\mathbf{C}), I_4(\mathbf{C}, \mathbf{A}), I_5(\mathbf{C}, \mathbf{A})). \quad (2.4.43)$$

The second Piola-Kirchhoff can now be obtained in the standard manner:

$$\mathbf{S} = 2\frac{\partial\Psi}{\partial\mathbf{C}} = 2\sum_{i=1}^{5}\frac{\partial\Psi}{\partial I_i}\frac{\partial I_i}{\partial\mathbf{C}}. \quad (2.4.44)$$

In the transversely isotropic constitutive models described in Chapter 5 it is further assumed that the strain energy function can be split into the following terms:

$$\Psi(\mathbf{C}, \mathbf{A}) = \Psi_1(I_1, I_2, I_3) + \Psi_2(I_4) + \Psi_3(I_1, I_2, I_3 I_4). \quad (2.4.45)$$

The strain energy function Ψ_1 represents the material response of the isotropic ground substance matrix, Ψ_2 represents the contribution from the fiber family (e.g. collagen), and Ψ_3 is the contribution from interactions between the fibers and matrix. The form (2.4.45) generalizes many constitutive equations that have been successfully used in the past to describe biological soft tissues e.g. [32, 34, 35]. While this relation represents a large simplification when compared to the general case, it also embodies almost all of the material behavior that one would expect from transversely isotropic, large deformation matrix-fiber composites.

2.5   Biphasic Material

Biphasic materials may be used to model deformable porous media. A biphasic material represents a mixture of a porous permeable solid and an interstitial fluid. Each constituent is intrinsically incompressible, but the mixture may change volume as interstitial fluid is exchanged with the pore space of the solid. Biphasic materials require the explicit modeling of fluid that permeates the solid. The biphasic material model is useful to simulate materials that show flow-dependent viscoelastic behavior resulting from the frictional interactions of the fluid and solid. Several biological materials such as cartilage can be described more accurately this way.

2.5.1   Governing Equations

Consider a mixture consisting of a solid constituent and a fluid constituent. Both constituents are considered to be intrinsically incompressible, but the mixture can change volume when fluid enters or leaves the porous solid matrix [20, 46]. According to the kinematics of the continuum [60], each constituent α of a mixture ($\alpha = s$ for the solid and $\alpha = w$ for the fluid) has a separate motion $\boldsymbol{\chi}^\alpha\left(\mathbf{X}^\alpha, t\right)$ which places particles of each mixture constituent, originally located at $\mathbf{X}^\alpha$, in the current configuration $\mathbf{x}$ according to

$$\mathbf{x} = \boldsymbol{\chi}^\alpha\left(\mathbf{X}^\alpha, t\right) . \tag{2.5.1}$$

For the purpose of finite element analyses, the motion of the solid matrix, $\alpha = s$, is of particular interest.

   The governing equations that enter into the statement of virtual work are the conservation of linear momentum and the conservation of mass, for the mixture as a whole. Under quasi-static conditions, the conservation of momentum reduces to

$$\operatorname{div}\boldsymbol{\sigma} + \rho\mathbf{b} = \mathbf{0} , \tag{2.5.2}$$

where σ is the Cauchy stress for the mixture, ρ is the mixture density and $\mathbf{b}$ is the external mixture body force per mass. Since the mixture is porous, this stress may also be written as

$$\boldsymbol{\sigma} = -p\mathbf{I} + \boldsymbol{\sigma}^e , \tag{2.5.3}$$

where p is the fluid pressure and σ^e is the effective or extra stress, resulting from the deformation of the solid matrix. Conservation of mass for the mixture requires that

$$\operatorname{div}\left(\mathbf{v}^s + \mathbf{w}\right) = 0 , \tag{2.5.4}$$

where $\mathbf{v}^s = \partial\boldsymbol{\chi}^s/\partial t$ is the solid matrix velocity and $\mathbf{w}$ is the flux of the fluid relative to the solid matrix. Let the solid matrix displacement be denoted by $\mathbf{u}$, then $\mathbf{v}^s = \dot{\mathbf{u}}$.

   To relate the relative fluid flux $\mathbf{w}$ to the fluid pressure and solid deformation, it is necessary to employ the equation of conservation of linear momentum for the fluid,

$$-\varphi^w\operatorname{grad}p + \rho^w\mathbf{b}^w + \hat{\mathbf{p}}_d^w = \mathbf{0} , \tag{2.5.5}$$

where φ^w is the solid matrix porosity, $\rho^w = \varphi^w\rho_T^w$ is the apparent fluid density and ρ_T^w is the true fluid density, $\mathbf{b}^w$ is the external body force per mass acting on the fluid, and $\hat{\mathbf{p}}_d^w$ is the momentum exchange between the solid and fluid constituents, typically representing the frictional interaction between these constituents. This equation neglects the viscous stress of the fluid in comparison

to $\hat{\mathbf{p}}_d^w$. The most common constitutive relation is $\hat{\mathbf{p}}_d^w = -\varphi^w \mathbf{k}^{-1} \cdot \mathbf{w}$, where the second order, symmetric tensor $\mathbf{k}$ is the hydraulic permeability of the mixture. When combined with Eq.(2.5.5), it produces

$$\mathbf{w} = -\mathbf{k} \cdot (\operatorname{grad} p - \rho_T^w \mathbf{b}^w) \ , \tag{2.5.6}$$

which is equivalent to Darcy's law. In general, $\mathbf{k}$ may be a function of the deformation.

2.6 Biphasic-Solute Material

A biphasic-solute material is an extension of the biphasic material model that also includes transport and mechano-chemical effects of a neutral solute. Transport of a solute in a porous medium includes diffusion, resulting from gradients in the solute concentration, and convection of the solute by the solvent, as a result of fluid pressure gradients. Mechano-chemical effects describe phenomena such as osmotic pressurization and swelling.

2.6.1 Governing Equations

The governing equations adopted in this finite element implementation of neutral solute transport in deformable porous media are based on the framework of mixture theory [60, 21]. A single solute is considered in this presentation for notational simplicity, though the extension of equations to multiple solutes is straightforward. Various forms of the governing equations have been presented in the prior literature [45, 6], though a presentation that incorporates all the desired features of this implementation has not been reported previously and is thus detailed here.

The fundamental modeling assumptions adopted in this treatment are quasi-static conditions for momentum balance (negligible effects of inertia), intrinsic incompressibility of all constituents (invariant true densities), isothermal conditions, negligible volume fraction of solute relative to the solid and solvent, and negligible effects of solute and solvent viscosities (friction within constituents) relative to frictional interactions between constituents. These assumptions are often made in studies of biological tissues and cells. External body forces and chemical reactions are not considered.

The three constituents of the mixture are the porous-permeable solid matrix ($\alpha = s$), the solvent ($\alpha = w$), and the solute ($\alpha = u$). The motion of the solid matrix is described by the displacement vector $\mathbf{u}$, the pressure of the interstitial fluid (solvent+solute) is p, and the solute concentration (on a solution-volume basis) is c. The total (or mixture) stress may be described by the Cauchy stress tensor $\boldsymbol{\sigma} = -p\mathbf{I} + \boldsymbol{\sigma}^e$, where $\mathbf{I}$ is the identity tensor and $\boldsymbol{\sigma}^e$ is the stress arising from the strain in the porous solid matrix. Because it is porous, the solid matrix is compressible since the volume of pores changes as interstitial fluid enters or leaves the matrix. Under the conditions outlined above, the balance of linear momentum for the mixture reduces to

$$\operatorname{div} \boldsymbol{\sigma} = -\operatorname{grad} p + \operatorname{div} \boldsymbol{\sigma}^e = \mathbf{0}\,. \tag{2.6.1}$$

Similarly, the equations of balance of linear momentum for the solvent and solute are given by

$$\begin{aligned}
\rho^w \operatorname{grad} \tilde{\mu}^w + \mathbf{f}^{ws} \cdot (\mathbf{v}^s - \mathbf{v}^w) + \mathbf{f}^{wu} \cdot (\mathbf{v}^u - \mathbf{v}^w) = \mathbf{0}\,, \\
-\rho^u \operatorname{grad} \tilde{\mu}^u + \mathbf{f}^{us} \cdot (\mathbf{v}^s - \mathbf{v}^u) + \mathbf{f}^{uw} \cdot (\mathbf{v}^w - \mathbf{v}^u) = \mathbf{0}\,,
\end{aligned} \tag{2.6.2}$$

where ρ^α is the apparent density (mass of α per volume of the mixture), $\tilde{\mu}^\alpha$ is the mechano-chemical potential and $\mathbf{v}^\alpha$ is the velocity of constituent α. $\mathbf{f}^{\alpha\beta}$ is the diffusive drag tensor between constituents α and β representing momentum exchange via frictional interactions, which satisfies $\mathbf{f}^{\beta\alpha} = \mathbf{f}^{\alpha\beta}$. An important feature of these relations is the incorporation of momentum exchange term between the solute and solid matrix, $\mathbf{f}^{us} \cdot (\mathbf{v}^s - \mathbf{v}^u)$, which is often neglected in other treatments but plays an important role for describing solid-solute interactions [45, 1, 2]. These momentum equations show that the driving force for the transport of solvent or solute is the gradient in its mechano-chemical potential, which is resisted by frictional interactions with other constituents.

The mechano-chemical potential is the sum of the mechanical and chemical potentials. The chemical potential μ^α of α represents the rate at which the mixture free energy changes with

increasing mass of α. The mechanical potential represents the rate at which the mixture free energy density changes with increasing volumetric strain of α. In a mixture of intrinsically incompressible constituents, where the volumetric strain is idealized to be zero, this potential is given by $(p - p_0)/\rho_T^\alpha$, where ρ_T^α is the true density of α (mass of α per volume of α), which is invariant for incompressible constituents, and p_0 is some arbitrarily set reference pressure (e.g., ambient pressure).

From classical physical chemistry, the general form of a constitutive relation for the chemical potential is $\mu^\alpha = \mu_0^\alpha(\theta) + (R\theta/M^\alpha)\ln a^\alpha$ [59], where R is the universal gas constant, θ is the absolute temperature, M^α is the molecular weight (invariant) and a^α is the activity of constituent α (a non-dimensional quantity); $\mu_0^\alpha(\theta)$ is the chemical potential at some arbitrary reference state, at a given temperature. For solutes, physical chemistry treatments let $a^u = \gamma c/c_0$, where c_0 is the solute concentration in some standard reference state (an invariant, typically $c_0 = 1\,\text{M}$), and γ is the non-dimensional activity coefficient, which generally depends on the current state (e.g., concentration) but reduces to unity under the assumption of ideal physico-chemical behavior [59]. Since this representation is strictly valid for free solutions only, whereas solutes may be partially excluded from some of the interstitial space of a porous solid matrix, Mauck et al. [45] extended this representation of the solute activity to let $a^u = \gamma c/\kappa c_0$, where the solubility κ represents the fraction of the pore space which is accessible to the solute ($0 < \kappa \leqslant 1$). In this extended form, it becomes clear that even under ideal behavior ($\gamma = 1$), the solute activity may be affected by the solubility. Indeed, for neutral solutes, the solubility also represents the partition coefficient of the solute between the tissue and external bath [40, 47].

When accounting for the fact that the solute volume fraction is negligible compared to the solvent volume fraction [59, 5], the general expressions for $\tilde{\mu}^w$ and $\tilde{\mu}^u$ take the form

$$\tilde{\mu}^w = \mu_0^w(\theta) + \frac{1}{\rho_T^w}(p - p_0 - R\theta\,\Phi\,c)\,,$$
$$\tilde{\mu}^u = \mu_0^u(\theta) + \frac{R\theta}{M}\ln\frac{\gamma c}{\kappa c_0}\,,$$

(2.6.3)

where Φ is the osmotic coefficient (a non-dimensional function of the state), which deviates from unity under non-ideal physico-chemical behavior. Therefore, a complete description of the physico-chemical state of solvent and solute requires constitutive relations for Φ and the effective solubility $\tilde{\kappa} = \kappa/\gamma$, which should generally depend on the solid matrix strain and the solute concentration.

It is also necessary to satisfy the balance of mass for each of the constituents. In the absence of chemical reactions, the statement of balance of mass for constituent α reduces to

$$\frac{\partial\rho^\alpha}{\partial t} + \text{div}\,(\rho^\alpha\mathbf{v}^\alpha) = 0\,.$$

(2.6.4)

The apparent density may be related to the true density via $\rho^\alpha = \varphi^\alpha\rho_T^\alpha$, where φ^α is the volume fraction of α in the mixture. Due to mixture saturation (no voids), the volume fractions add up to unity. Since the volume fraction of solute is considered negligible ($\varphi^u \ll \varphi^s, \varphi^w$), it follows that $\sum_\alpha \varphi^\alpha \approx \varphi^s + \varphi^w = 1$. Since ρ_T^α of an incompressible constituent is invariant in space and time, these relations may be combined to produce the mixture balance of mass relation,

$$\text{div}\,(\mathbf{v}^s + \mathbf{w}) = 0,$$

(2.6.5)

where $\mathbf{w} = \varphi^w(\mathbf{v}^w - \mathbf{v}^s)$ is the volumetric flux of solvent relative to the solid. The balance of mass for the solute may also be written as

$$\frac{\partial(\varphi^w c)}{\partial t} + \text{div}\,(\mathbf{j} + \varphi^w c\,\mathbf{v}^s) = 0\,,$$

(2.6.6)

where $\mathbf{j} = \varphi^w c \left(\mathbf{v}^u - \mathbf{v}^s \right)$ is the molar flux of solute relative to the solid. This mass balance relation is obtained by recognizing that the solute apparent density (mass per mixture volume) is related to its concentration (moles per solution volume) via $\rho^u = (1 - \varphi^s) Mc \approx \varphi^w Mc$. Finally, it can be shown via standard arguments that the mass balance for the solid matrix reduces to

$$\varphi^s = \frac{\varphi_r^s}{J}, \tag{2.6.7}$$

where φ_r^s is the solid volume fraction in the reference state, $J = \det \mathbf{F}$ and $\mathbf{F} = \mathbf{I} + \operatorname{grad} \mathbf{u}$ is the deformation gradient of the solid matrix.

Inverting the momentum balance equations in (2.6.2), it is now possible to relate the solvent and solute fluxes to the driving forces according to

$$\mathbf{w} = -\tilde{\mathbf{k}} \cdot \left(\rho_T^w \operatorname{grad} \tilde{\mu}^w + Mc \frac{\mathbf{d}}{d_0} \operatorname{grad} \tilde{\mu}^u \right),$$

$$\mathbf{j} = \mathbf{d} \cdot \left(-\frac{M}{R\theta} \varphi^w c \operatorname{grad} \tilde{\mu}^u + \frac{c}{d_0} \mathbf{w} \right), \tag{2.6.8}$$

where $\mathbf{d}$ is the solute diffusivity tensor in the mixture (solid+solution), d_0 is its (isotropic) diffusivity in free solution; $\tilde{\mathbf{k}}$ is the hydraulic permeability tensor of the solution (solvent+solute) through the porous solid matrix, which depends explicitly on concentration according to

$$\tilde{\mathbf{k}} = \left[\mathbf{k}^{-1} + \frac{R\theta c}{\varphi^w d_0} \left(\mathbf{I} - \frac{\mathbf{d}}{d_0} \right) \right]^{-1}, \tag{2.6.9}$$

where $\mathbf{k}$ represents the hydraulic permeability tensor of the solvent through the solid matrix. The permeability and diffusivity tensors are related to the diffusive drag tensors appearing in (2.6.2) according to

$$\mathbf{k} = (\varphi^w)^2 (\mathbf{f}^{ws})^{-1},$$

$$\mathbf{d}_0 = R\theta \varphi^w c (\mathbf{f}^{uw})^{-1} \equiv d_0 \mathbf{I}, \tag{2.6.10}$$

$$\mathbf{d} = R\theta \varphi^w c (\mathbf{f}^{us} + \mathbf{f}^{uw})^{-1},$$

though these explicit relationships are not needed here since $\mathbf{k}$, $\mathbf{d}$ and d_0 may be directly specified in a particular analysis. Since the axiom of entropy inequality requires that the tensors $\mathbf{f}^{\alpha\beta}$ be positive semi-definite (see appendix of [9]), it follows that d_0 must be greater than or equal to the largest eigenvalue of $\mathbf{d}$. Constitutive relations are needed for these transport properties, which relate them to the solid matrix strain and solute concentration. Note that the relations in (2.6.10) represent generalizations of Darcy's law for fluid permeation through porous media, and Fick's law for solute diffusion in porous media or free solution.

2.6.2 Continuous Variables

In principle, the objective of the finite element analysis is to solve for the three unknowns, $\mathbf{u}$, p and c, using the partial differential equations that enforce mixture momentum balance in (2.6.1), mixture mass balance in (2.6.5), and solute mass balance in (2.6.6). The remaining solvent and solute momentum balances in (2.6.8), and solid mass balance in (2.6.7), have been reduced to relations that may be substituted into the three partial differential equations as needed. Solving these equations requires the application of suitable boundary conditions that are consistent with mass, momentum and energy balances across boundary surfaces or interfaces. When defining

boundaries or interfaces on the solid matrix (the conventional approach in solid mechanics), whose outward unit normal is $\mathbf{n}$, mass and momentum balance relations demonstrate that the mixture traction $\mathbf{t} = \boldsymbol{\sigma} \cdot \mathbf{n}$ and normal flux components $w_n = \mathbf{w} \cdot \mathbf{n}$ and $j_n = \mathbf{j} \cdot \mathbf{n}$ must be continuous across the interface [5, 24]. Therefore, $\mathbf{t}$, w_n and j_n may be prescribed as boundary conditions.

Combining momentum and energy balances across an interface also demonstrates that $\tilde{\mu}^w$ and $\tilde{\mu}^u$ must be continuous [5, 37], implying that these mechano-chemical potentials may be prescribed as boundary conditions. However, because of the arbitrariness of the reference states μ_0^w, μ_0^u, p_0 and c_0, and the ill-conditioning of the logarithm function in the limit of small solute concentration, the mechano-chemical potentials do not represent practical choices for primary variables in a finite element implementation. An examination of (2.6.3) also shows that continuity of these potentials across an interface does not imply continuity of the fluid pressure p or solute concentration c. Therefore, pressure and concentration are also unsuitable as nodal variables in a finite element analysis and they must be replaced by alternative choices. Based on the similar reasoning presented by Sun et al. [58], an examination of the expressions in (2.6.3) shows that continuity may be enforced by using

$$\tilde{p} = p - R\theta \, \Phi \, c \,,$$
$$\tilde{c} = \frac{c}{\tilde{\kappa}} \,, \tag{2.6.11}$$

where $\tilde{p}$ is the effective fluid pressure and $\tilde{c}$ is the effective solute concentration in the mixture. Note that $\tilde{p}$ represents that part of the fluid pressure which does not result from osmotic effects (since the term $R\theta \, \Phi \, c$ may be viewed as the osmotic pressure contribution to p), and $\tilde{c}$ is a straightforward measure of the solute activity, since $a^u = \tilde{c}/c_0$. Therefore these alternative variables have clear physical meanings.

Since the unknowns are now given by $\mathbf{u}$, $\tilde{p}$ and $\tilde{c}$, the governing partial differential equations may be rewritten in the form

$$\operatorname{grad} (\tilde{p} + R\theta \, \Phi \, \tilde{\kappa}\tilde{c}) + \operatorname{div} \boldsymbol{\sigma}^e = \mathbf{0} \,,$$
$$\operatorname{div} (\mathbf{v}^s + \mathbf{w}) = 0 \,, \tag{2.6.12}$$
$$\frac{\partial (\varphi^w \tilde{\kappa}\tilde{c})}{\partial t} + \operatorname{div} (\mathbf{j} + \varphi^w \tilde{\kappa}\tilde{c} \, \mathbf{v}^s) = 0 \,,$$

where

$$\mathbf{w} = -\tilde{\mathbf{k}} \cdot \left(\operatorname{grad} \tilde{p} + R\theta \frac{\tilde{\kappa}}{d_0} \mathbf{d} \cdot \operatorname{grad} \tilde{c} \right) \,,$$
$$\mathbf{j} = \tilde{\kappa} \mathbf{d} \cdot \left(-\varphi^w \operatorname{grad} \tilde{c} + \frac{\tilde{c}}{d_0} \mathbf{w} \right) \,, \tag{2.6.13}$$
$$\tilde{\mathbf{k}} = \left[\mathbf{k}^{-1} + \frac{R\theta}{\varphi^w} \frac{\tilde{\kappa}\tilde{c}}{d_0} \left(\mathbf{I} - \frac{\mathbf{d}}{d_0} \right) \right]^{-1} \,.$$

Constitutive equations are needed to relate $\boldsymbol{\sigma}^e$, $\mathbf{k}$, $\mathbf{d}$, d_0, $\tilde{\kappa}$ and Φ to the solid matrix strain and effective solute concentration.

2.7 Triphasic and Multiphasic Materials

Multiphasic materials represent an extension of the biphasic-solute material, where the mixture may contain a multitude of solutes. These solutes may be either electrically charged (ionized) or neutral. Similarly, the solid matrix may either carry electrical charge (a fixed charge density) or be neutral. A triphasic material is a special case of a multiphasic material, having two solutes

that carry opposite charges. Triphasic and multiphasic materials may be used to model porous deformable biological tissues whose solid matrix may be charged and whose interstitial fluid may contain any number of charged or neutral solutes. When mixture constituents are electrically charged, the response of the tissue to various loading conditions may encompass a range of mechano-electrochemical phenomena, including permeation, diffusion, osmosis, streaming potentials and streaming currents. To better understand multiphasic materials, the reader is encouraged to review the descriptions of biphasic (Section 2.5) and biphasic-solute materials (Section 2.6).

2.7.1   Governing Equations

In multiphasic materials the solvent is assumed to be neutral, whereas the solid and solutes may carry charge. The mixture is isothermal and all constituents are considered to be intrinsically incompressible. Since the viscosity of the fluid constituents (solvent and solutes) is considered negligible relative to the frictional interactions among constituents, the stress tensor σ for the mixture includes only a contribution from the fluid pressure p and the stress $\boldsymbol{\sigma}^e$ in the solid,

$$\boldsymbol{\sigma} = -p\mathbf{I} + \boldsymbol{\sigma}^e \,. \tag{2.7.1}$$

The mechano-chemical potential of the solvent is given by

$$\tilde{\mu}^w = \mu_0^w\left(\theta\right) + \frac{1}{\rho_T^w}\left(p - p_0 - R\theta\Phi\sum_\alpha c^\alpha\right)\,, \tag{2.7.2}$$

where $\mu_0^w\left(\theta\right)$ is the solvent chemical potential in the solvent standard state, θ is the absolute temperature, ρ_T^w is the true density of the solvent (which is invariant since the solvent is assumed intrinsically incompressible), p is the fluid pressure, p_0 is the corresponding pressure in the standard state, R is the universal gas constant, Φ is the non-dimensional osmotic coefficient, and c^α is the solution volume-based concentration of solute α. The summation is taken over all solutes in the mixture. The mechano-electrochemical potential of each solute is similarly given by

$$\tilde{\mu}^\alpha = \mu_0^\alpha\left(\theta\right) + \frac{R\theta}{M^\alpha}\left(\frac{z^\alpha F_c}{R\theta}\left(\psi - \psi_0\right) + \ln\frac{\gamma^\alpha c^\alpha}{\kappa^\alpha c_0^\alpha}\right)\,, \tag{2.7.3}$$

where M^α is the molar mass of the solute, γ^α is its activity coefficient, κ^α is its solubility, z^α is its charge number, and c_0^α is its concentration in the solute standard state; F_c is Faraday's constant, ψ is the electrical potential of the mixture, and ψ_0 is the corresponding potential in the standard state.

In these relations, Φ and γ^α are functions of state that describe the deviation of the mixture from ideal physico-chemical behavior; κ^α represents the fraction of the pore volume which may be occupied by solute α. The standard state represents an arbitrary set of reference conditions for the physico-chemical state of each constituent. Therefore, the values of $\mu_0^w\left(\theta\right)$, p_0, ψ_0, $\mu_0^\alpha\left(\theta\right)$, and c_0^α, remain invariant over the entire domain of definition of an analysis. Since κ^α and γ^α appear together as a ratio, they may be combined into a single material function, $\hat{\kappa}^\alpha = \kappa^\alpha/\gamma^\alpha$, called the effective solubility.

In multiphasic mixtures, it is also assumed that electroneutrality is satisfied at every point in the continuum. Therefore, the net electrical charge summed over all constituents must reduce to zero, and no net charge accumulation may occur at any time. Denoting the fixed charge density of the solid by c^F (moles of equivalent charge per solution volume), and recognizing that the solvent is always considered neutral, the electroneutrality condition may be written as

$$c^F + \sum_\alpha z^\alpha c^\alpha = 0\,. \tag{2.7.4}$$

This condition represents a constraint on a mixture of charged constituents. If none of the constituents are charged ($c^F = 0$ and $z^\alpha = 0$ for all α), the constraint disappears.

Each constituent of the mixture must satisfy the axiom of mass balance. In the absence of chemical reactions involving constituent α, its mass balance equation is

$$\frac{\partial \rho^\alpha}{\partial t} + \text{div}\,(\rho^\alpha \mathbf{v}^\alpha) = 0\,, \tag{2.7.5}$$

where ρ^α is the apparent density and $\mathbf{v}^\alpha$ is the velocity of that constituent. For solutes, the apparent density is related to the concentration according to $\rho^\alpha = (1 - \varphi^s)\,M^\alpha c^\alpha$, where φ^s is the volume fraction of the solid. When the solute volume fractions are negligible, it follows that $1 - \varphi^s \approx \varphi^w$, where φ^w is the solvent volume fraction. The molar flux of the solute relative to the solid is given by $\mathbf{j}^\alpha = \varphi^w c^\alpha\,(\mathbf{v}^\alpha - \mathbf{v}^s)$, where $\mathbf{v}^\alpha$ is the solute velocity. Using these relations, the mass balance relation for the solute may be rewritten as

$$\frac{1}{J}\frac{D^s}{Dt}\,(J\varphi^w c^\alpha) + \text{div}\,\mathbf{j}^\alpha = 0\,, \tag{2.7.6}$$

where $D^s\,(\cdot)\,/Dt$ represents the material time derivative in the spatial frame, following the solid; $J = \det \mathbf{F}$, where $\mathbf{F}$ is the deformation gradient of the solid. This form of the mass balance for the solute is convenient for a finite element formulation where the mesh is defined on the solid matrix.

The volume flux of solvent relative to the solid is given by $\mathbf{w} = \varphi^w\,(\mathbf{v}^w - \mathbf{v}^s)$, where $\mathbf{v}^w$ is the solvent velocity. When solute volume fractions are negligible, the mass balance equation for the mixture reduces to

$$\text{div}\,(\mathbf{v}^s + \mathbf{w}) = 0\,. \tag{2.7.7}$$

Finally, the mass balance for the solid may be reduced to the form $D^s\,(J\varphi^s)\,/Dt = 0$, which may be integrated to produce the algebraic relation $\varphi^s = \varphi_r^s/J$, where φ_r^s is the solid volume fraction in the stress-free reference state of the solid.

Differentiating the electroneutrality condition in (2.7.4) using the material time derivative following the solid, and substituting the mass balance relations into the resulting expressions, produces a constraint on the solute fluxes:

$$\text{div}\sum_{\alpha \neq s,w} z^\alpha \mathbf{j}^\alpha = 0\,. \tag{2.7.8}$$

Recognizing that $\mathbf{I}_e = F_c \sum_{\alpha \neq s,w} z^\alpha \mathbf{j}^\alpha$ is the current density in the mixture, with F_c representing Faraday's constant, the relation of (2.7.8) reduces to one of the Maxwell's equation, $\text{div}\,\mathbf{I}_e = 0$, in the special case when there can be no charge accumulation (electroneutrality).

As described in Section 2.6.2, the fluid pressure p and solute concentrations c^α are not continuous across boundaries of a mixture, whereas $\tilde{\mu}^w$ and $\tilde{\mu}^\alpha$'s for the solutes do satisfy continuity. Therefore, in a finite element implementation, the following continuous variables are used as nodal degrees of freedom:

$$\tilde{p} = p - R\theta\Phi \sum_{\alpha \neq s,w} c^\alpha\,, \tag{2.7.9}$$

which represents the effective fluid pressure, and

$$\tilde{c}^\alpha = c^\alpha/\tilde{\kappa}^\alpha\,, \tag{2.7.10}$$

which represents the effective solute concentration. In the last expression, $\tilde{\kappa}^\alpha$ is the partition coefficient of the solute, which is related to the effective solubility and electric potential according to

$$\tilde{\kappa}^\alpha = \hat{\kappa}^\alpha \exp\left(-\frac{z^\alpha F_c \psi}{R\theta}\right)\,. \tag{2.7.11}$$

Physically, since $R\theta\,\Phi\sum_{\alpha\neq s,w}c^\alpha$ is the osmotic (chemical) contribution to the fluid pressure, $\tilde{p}$ may be interpreted as that part of the total (mechano-chemical) fluid pressure which does not result from osmotic effects; thus, it is the mechanical contribution to p. Similarly, the effective solute concentration $\tilde{c}^\alpha$ represents the true contribution of the molar solute content to its electrochemical potential.

When using these variables instead of mechano-electrochemical potentials, the momentum equations for the solvent and solutes may be inverted to produce the following flux relations:

$$\mathbf{w} = -\tilde{\mathbf{k}} \cdot \left(\mathrm{grad}\tilde{p} + R\theta \sum_{\beta\neq s,w} \frac{\tilde{\kappa}^\beta}{d_0^\beta} \mathbf{d}^\beta \cdot \mathrm{grad}\tilde{c}^\beta \right) , \tag{2.7.12}$$

and

$$\mathbf{j}^\alpha = \tilde{\kappa}^\alpha \mathbf{d}^\alpha \cdot \left(-\varphi^w \mathrm{grad}\tilde{c}^\alpha + \frac{\tilde{c}^\alpha}{d_0^\alpha} \mathbf{w} \right) , \tag{2.7.13}$$

where

$$\tilde{\mathbf{k}} = \left[\mathbf{k}^{-1} + \frac{R\theta}{\varphi^w} \sum_{\alpha\neq s,w} \frac{c^\alpha}{d_0^\alpha} \left(\mathbf{I} - \frac{\mathbf{d}^\alpha}{d_0^\alpha} \right) \right]^{-1} \tag{2.7.14}$$

is the effective hydraulic permeability of the solution (solvent+solutes) in the mixture. The momentum equation for the mixture is

$$\mathrm{div}\,\boldsymbol{\sigma} = \mathbf{0} . \tag{2.7.15}$$

2.8   Mixture of Solids

A solid material may consist of a heterogeneous mixture of various solid constituents that are constrained to move together. If each constituent is denoted by the superscript σ, a constrained mixture satisfies $\mathbf{v}^\sigma = \mathbf{v}^s$ for all σ, where $\mathbf{v}^s$ is the velocity of the solid mixture. For example, a fiber-reinforced material may consist of a mixture of fibers and a ground matrix. In general, the constitutive relation for such a constrained mixture of solids may be a complex function of the mass fraction of each constituent as well as the ultrastructure of the constituents and their mutual interactions. The mass fraction of each constituent may be represented by the apparent density ρ_r^σ, which is the ratio of the mass of σ to the volume of the mixture in the reference configuration, in an elemental region. In the framework of hyperelasticity, the general representation for the strain energy density for such a solid mixture may have the form

$$\Psi = \Psi\left(\mathbf{F}^{(1)}, \cdots, \mathbf{F}^{(n)}, \rho_r^{(1)}, \cdots, \rho_r^{(n)} \right) , \tag{2.8.1}$$

where $\mathbf{F}^\sigma$ is the deformation gradient of constituent σ and n is the number of solid constituents in the mixture. Though the solid constituents are constrained to move together, their deformation gradients are not necessarily the same, depending on how the various solid constituents of a constrained mixture were assembled [8].

With no loss of generality, it may be assumed that the strain energy density of the mixture is the summation of the strain energy densities of all the constituents,

$$\Psi\left(\mathbf{F}^{(1)}, \cdots, \mathbf{F}^{(n)}, \rho_r^{(1)}, \cdots, \rho_r^{(n)} \right) = \sum_{\sigma=1}^{n} \Psi^\sigma\left(\mathbf{F}^{(1)}, \cdots, \mathbf{F}^{(n)}, \rho_r^{(1)}, \cdots, \rho_r^{(n)} \right) , \tag{2.8.2}$$

where Ψ^σ is the strain energy density of constituent σ.

Now, *as a special case*, we may assume that the simplest form of the constitutive relation for a mixture of constrained solids is

$$\Psi\left(\mathbf{F}^{(1)}, \cdots, \mathbf{F}^{(n)}, \rho_r^{(1)}, \cdots, \rho_r^{(n)}\right) = \sum_{\sigma=1}^{n} \Psi^\sigma\left(\mathbf{F}^\sigma, \rho_r^\sigma\right) . \qquad (2.8.3)$$

This special form assumes that there are no explicit dependencies among the various solid constituents of the mixture. Thus, Ψ^σ depends only on the deformation gradient and mass content of σ.

Furthermore, if we assume that $\mathbf{F}^\sigma = \mathbf{F}$ for all σ (implying no residual stresses in the solid mixture), then the general form for Ψ further reduces to

$$\Psi = \sum_{\sigma=1}^{n} \Psi^\sigma\left(\mathbf{F}, \rho_r^\sigma\right) . \qquad (2.8.4)$$

Consequently, the stress tensor for the mixture becomes

$$\boldsymbol{\sigma} = J^{-1}\frac{\partial \Psi}{\partial \mathbf{F}} \cdot \mathbf{F}^T = \sum_{\sigma=1}^{n} J^{-1}\frac{\partial \Psi^\sigma}{\partial \mathbf{F}} \cdot \mathbf{F}^T = \sum_{\sigma=1}^{n} \boldsymbol{\sigma}^\sigma . \qquad (2.8.5)$$

In other words, the stress in the solid mixture may be evaluated from the sum of the stresses in each mixture constituent using the same hyperelasticity relation as for a single, pure solid constituent. The fact that Ψ^σ also depends on ρ_r^σ implies that the material properties appearing in the constitutive relation for $\boldsymbol{\sigma}^\sigma$ are dependent on the mass content of solid σ in the mixture.

For nearly-incompressible solids, using a reasoning similar to that which led to (2.8.4), the uncoupled strain energy density for the solid mixture may be of the form

$$\Psi = U(J) + \sum_{\sigma=1}^{n} \tilde{\Psi}^\sigma\left(\tilde{\mathbf{F}}, \rho_r^\sigma\right) , \qquad (2.8.6)$$

where $U(J)$ is the volumetric energy component, $\tilde{\Psi} = \sum_{\sigma} \tilde{\Psi}^\sigma$ is the distortional energy component, and $\tilde{\mathbf{F}}$ is the distortional part of the deformation gradient, as described in Section 2.4.3.

2.9 Equilibrium Swelling

When the interstitial fluid of a porous medium contains one or more solutes, an osmotic pressure may be produced in the fluid if the osmolarity of the interstitial fluid is non-uniform, or if it is different from that of the external bathing solution surrounding the porous medium. In general, since the osmolarity of the interstitial fluid may vary over time in transient problems, the analysis of such swelling effects may be addressed using, for example, the biphasic-solute material model described in Section 2.6. However, if we are only interested in the steady-state response for such types of materials, when solvent and solute fluxes have subsided, the analysis may be simplified considerably.

The Cauchy stress tensor for a mixture of a porous solid and interstitial fluid is given by

$$\boldsymbol{\sigma} = -p\mathbf{I} + \boldsymbol{\sigma}^e \,, \tag{2.9.1}$$

where p is he fluid pressure and $\boldsymbol{\sigma}^e$ is the stress in the solid matrix resulting from solid strain. When steady-state conditions are achieved, the fluid pressure p results exclusively from osmotic effects and ambient conditions (i.e., it does not depend on the loading history). Thus, in analogy to (2.6.11), $p = \tilde{p} + R\theta\Phi c$ where $\tilde{p}$ is the mechanical pressure resulting from ambient conditions and $R\theta\Phi c$ is the osmotic pressure resulting from the osmolarity c of the solution.

The osmotic pressure p may produce swelling of the solid matrix, which is opposed by the solid matrix stress. This becomes more apparent when considering, for example, the case of a traction-free body. The traction is given by $\mathbf{t} = \boldsymbol{\sigma} \cdot \mathbf{n}$, where $\mathbf{n}$ is the unit outward normal to the boundary. When $\mathbf{t} = \mathbf{0}$, the relation of (2.9.1) produces $p = \mathbf{n} \cdot \boldsymbol{\sigma}^e \cdot \mathbf{n}$, clearly showing that the osmotic pressure p is balanced by the swelling solid matrix.

The interstitial osmolarity (number of moles of solute per volume of interstitial fluid) may be related to the solute and solid content according to

$$c = \frac{c_r}{J - \varphi_r^s} \,, \tag{2.9.2}$$

where c_r is the number of moles of solute per volume of the mixture in the reference configuration, φ_r^s is the volume fraction of the solid in the reference configuration, and $J = \det \mathbf{F}$ is the volume ratio of the porous solid matrix. Neither c_r nor φ_r^s depend on the solid matrix deformation, thus (2.9.2) provides the explicit dependence of c on J. This relation shows that the osmolarity of the interstitial fluid is dependent on the relative change in volume of the solid matrix with deformation. Effectively, under equilibrium swelling conditions, the term $-p\mathbf{I}$ in (2.9.1) represents an elastic stress and may be treated in this manner when analyzing equilibrium swelling conditions.

Since p also depends on the osmotic coefficient, if we assume that Φ depends on the solid strain at most via a dependence on J, we may thus state generically that $p = p\,(J)$ under equilibrium swelling. It follows that the elasticity tensor for $\boldsymbol{\sigma}$ is

$$\mathcal{C} = -\left(p + J\frac{dp}{dJ}\right)\mathbf{I} \otimes \mathbf{I} + 2p\mathbf{I}\,\overline{\otimes}\,\mathbf{I} + \mathcal{C}^e \,, \tag{2.9.3}$$

where $\mathcal{C}^e$ is the elasticity tensor of $\boldsymbol{\sigma}^e$.

2.9.1 Perfect Osmometer

Consider a porous medium with an interstitial fluid that consists of a solvent and one or more solutes, whose boundary is permeable to the solvent but not to the solutes (e.g., a biological cell).

Since solutes are trapped within such a medium, c_r is a constant in this type of problem. Since the boundary is permeable to the solvent, $\tilde{p}$ must be continuous across the boundary. Assuming ideal physicochemical conditions, $\Phi = 1$, and zero ambient pressure, this continuity requirement implies that $p = R\theta (c - c^*)$, where c^* is the osmolarity of the external environment. Using (2.9.2), it follows that

$$p = R\theta \left(\frac{c_r}{J - \varphi_r^s} - c^* \right) . \tag{2.9.4}$$

The reference configuration (the stress-free configuration of the solid) is achieved when $J = 1$ and $p = 0$, from which it follows that $c_r = (1 - \varphi_r^s) c_0^*$, where c_0^* is the value of c^* in the reference state. Therefore (2.9.4) may also be written as

$$p = R\theta c^* \left(\frac{1 - \varphi_r^s}{J - \varphi_r^s} \frac{c_0^*}{c^*} - 1 \right) , \tag{2.9.5}$$

and this expression may be substituted into (2.9.3) to evaluate the corresponding elasticity tensor.

A perfect osmometer is a porous material whose interstitial fluid behaves ideally and whose solid matrix exhibits negligible resistance to swelling ($\boldsymbol{\sigma}^e \approx \mathbf{0}$). In that case $p = 0$ and (2.9.5) may be rearranged to yield

$$J = (1 - \varphi_r^s) \frac{c_0^*}{c^*} + \varphi_r^s. \tag{2.9.6}$$

This equation is known as the Boyle-van't Hoff relation for a perfect osmometer. It predicts that variations in the relative volume of such as medium with changes in external osmolarity c^* is an affine function of c_0^*/c^*, with the intercept at the origin representing the solid volume fraction and the slope representing the fluid volume fraction, in the reference configuration.

FEBio implements the relation of (2.9.5) for the purpose of modeling equilibrium swelling even when solid matrix stresses are not negligible. The name "perfect osmometer" is adopted for this model because it reproduces the Boyle-van't Hoff response in the special case when $\boldsymbol{\sigma}^e = \mathbf{0}$.

2.9.2 Cell Growth

The growth of cells requires the active uptake of soluble mass to provide the building blocks for various intracellular structures, such as the cytoskeleton or chromosomes, and growth contributes to the osmolarity of the intracellular space. The resulting mechano-chemical gradient drives solvent into the cell as well, contributing to its volumetric growth.

Cell growth may be modeled using the "perfect osmometer" framework by simply increasing the mass of the intracellular solid matrix and membrane-impermeant solute. This is achieved by using (2.9.4) to model the osmotic pressure and allowing the parameters φ_r^s and c_r (normally constant) to increase over time as a result of growth. Since cell growth is often accompanied by cell division, and since daughter cells typically achieve the same solid and solute content as their parent, it may be convenient to assume that φ_r^s and c_r increase proportionally, though this is not an obligatory relationship. To ensure that the initial configuration is a stress-free reference configuration, let $c_r = (1 - \varphi_r^s) c^*$ in the initial state prior to growth.

2.9.3 Donnan Equilibrium Swelling

Consider a porous medium whose solid matrix holds a fixed electrical charge and whose interstitial fluid consists of a solvent and two monovalent counter-ions (such as Na$^+$ and Cl$^-$). The

boundaries of the medium are permeable to the solvent and ions. The fixed charge density is denoted by c^F; it is a measure of the number of fixed charges per volume of the interstitial fluid in the current configuration. This charge density may be either negative or positive, thereby producing an imbalance in the concentration of anions and cations in the interstitial fluid. To determine the osmolarity of the interstitial fluid, it is necessary to equate the mechano-chemical potential of the solvent and the mechano-electrochemical potential of the ions between the porous medium and its surrounding bath. When assuming ideal physicochemical behavior, the interstitial osmolarity (resulting from the interstitial ions) is given by

$$c = \sqrt{(c^F)^2 + (2c^*)^2}, \qquad (2.9.7)$$

where c^* is the salt concentration in the bath. Alternatively, we note that the osmolarity of the bath is $\bar{c}^* = 2c^*$. Though this expression may be equated with (2.9.2), the resulting value of c_r is not constant in this case, since ions may transport into or out of the pore space; therefore that relation is not useful here.

However, since the number of charges fixed to the solid matrix is invariant, we may manipulate (2.9.2) to produce a relation between the fixed charge density in the current configuration, c^F, and the corresponding value in the reference configuration, c_r^F,

$$c^F = \frac{1 - \varphi_r^s}{J - \varphi_r^s} c_r^F \ . \qquad (2.9.8)$$

Now the osmotic pressure resulting from the difference in osmolarity between the porous medium and its surrounding bath is given by

$$p = R\theta \left(\sqrt{\left(\frac{1 - \varphi_r^s}{J - \varphi_r^s} c_r^F \right)^2 + (\bar{c}^*)^2} - \bar{c}^* \right) \ . \qquad (2.9.9)$$

This expression may be substituted into (2.9.3) to evaluate the corresponding elasticity tensor.

When the osmotic pressure results from an imbalance in osmolarity produced by a fixed charge density, it is called a Donnan osmotic pressure. The analysis associated with this relation is called Donnan equilibrium.

2.10 Chemical Reactions

Chemical reactions may be incorportated into a multiphasic mixture by adding a mass supply term to the equation of mass balance,

$$\frac{\partial \rho^\alpha}{\partial t} + \operatorname{div}\left(\rho^\alpha \mathbf{v}^\alpha\right) = \hat{\rho}^\alpha, \tag{2.10.1}$$

Where $\hat{\rho}^\alpha$ is the volume density of mass supply to α resulting from chemical reactions with all other mixture constitutents. Since mass must be conserved over all constituents, mass supply terms are constrained by

$$\sum_\alpha \hat{\rho}^\alpha = 0. \tag{2.10.2}$$

In a mixture containing a solid constituent (denoted by $\alpha = s$), it is conveniemt to define the mixture domain (and thus the finite element mesh) on the solid and evaluate mass fluxes of constituents relative to the solid,

$$\mathbf{m}^\alpha = \rho^\alpha\left(\mathbf{v}^\alpha - \mathbf{v}^s\right). \tag{2.10.3}$$

Substituting (2.10.3) into (2.10.1), the differential form of the mass balance may be rewritten as

$$\frac{D^s \rho_r^\alpha}{Dt} + J \operatorname{div} \mathbf{m}^\alpha = \hat{\rho}_r^\alpha, \tag{2.10.4}$$

Where $D^s\left(\cdot\right)/Dt$ represents the material time derivative in the spatial frame, following the solid, $J = \det \mathbf{F}$, where $\mathbf{F}$ is the deformation gradient of the solid matrix; ρ_r^α is the apparent density and $\hat{\rho}_r^\alpha$ is the volume density of mass supply to α normalized to the mixture volume in the reference configuration,

$$\rho_r^\alpha = J\rho^\alpha, \quad \hat{\rho}_r^\alpha = J\hat{\rho}^\alpha. \tag{2.10.5}$$

Since ρ_r^α is the mass of α in the current configuration per volume of the mixture in the reference configuration (an invariant quantity), this parameter represents a direct measure of the mass content of α in the mixture, which may thus be used as a state variable in a framework that accounts for chemical reactions. A distinction is now made between solid and solute species in the mixture, since they are often treated differential in an analysis.

2.10.1 Solid Matrix and Solid-Bound Molecular Constituents

For constituents constrained to move with the solid (denoted generically by $\alpha = \sigma$ and satisfying $\mathbf{v}^s = \mathbf{v}^\sigma$, $\forall\sigma$), the statement of mass balance in (2.10.4) reduces to the special form

$$D^s \rho_r^\sigma / Dt = \hat{\rho}_r^\sigma. \tag{2.10.6}$$

This representation makes it easy to see that alterations in ρ_r^σ can occur only as a result of chemical reactions (such as synthesis, degradation, or binding). In contrast, as seen in (2.10.4), alterations in ρ_r^α for solutes or solvent ($\alpha \neq \sigma$) may also occur as a result of mass transport into or out of the pore space of the solid matrix. Therefore, ρ_r^σ is the natural choice of state variable for describing the content of solid constituents in a reactive mixture.

When multiple solid species are present, the net solid mass content may be given by $\rho_r^s = \sum_\sigma \rho_r^\sigma$ whereas the net mass supply of solid is $\hat{\rho}_r^s = \sum_\sigma \hat{\rho}_r^\sigma$ such that $D^s \rho_r^s / Dt = \hat{\rho}_r^s$. The referential solid volume fraction, φ_r^s, may be evaluated from

$$\varphi_r^s = \varphi_0^s + \sum_\sigma \rho_r^\sigma / \rho_T^\sigma, \tag{2.10.7}$$

where ρ_T^σ is the true density of solid constituent σ (mass of σ per volume of σ) and φ_0^s is the referential solid volume fraction of solid constituents not explicitly modeled by solid-bound molecules (a user-defined parameter). According to (2.10.5), it follows that the solid volume fraction in the current configuration is given by $\varphi^s = \varphi_r^s / J$. Note that $0 \leqslant \varphi^s \leqslant 1$ under all circumstances, while $0 \leqslant \varphi_r^s \leqslant J$, implying that φ_r^s may exceed unity when solid growth occurs. In this study, it is assumed that all mixture constituents are intrinsically incompressible, implying that their true density is invariant.

The various constituents of the solid matrix may be electrically charged. Let z^σ be the charge number (equivalent charge per mole) of solid constituent σ, then the net referential fixed charge density of the solid matrix (equivalent charge per fluid volume in the referential configuration) is given by

$$c_r^F = \frac{1}{1 - \varphi_r^s} \sum_\sigma \frac{z^\sigma \rho_r^\sigma}{M^\sigma} \, , \tag{2.10.8}$$

where M^σ is the molar mass of σ (an invariant quantity) and $1 - \varphi_r^s$ represents the referential volume fraction of all fluid constituents (solvent + solutes) in a saturated mixture. Based on the kinematics of the continuum, the fixed charge density in the current configuration is

$$c^F = \frac{1 - \varphi_r^s}{J - \varphi_r^s} c_r^F \, . \tag{2.10.9}$$

2.10.2 Solutes

Solutes are denoted generically by $\alpha = \iota$. In chemistry solute content is often represented in units of molar concentration (moles per fluid volume). It follows that solute molar concentration c^ι and molar supply $\hat{c}^\iota$ are related to ρ^ι and $\hat{\rho}^\iota$ via

$$c^\iota = \frac{\rho^\iota}{(1 - \varphi^s) M^\iota}, \quad \hat{c}^\iota = \frac{\hat{\rho}^\iota}{(1 - \varphi^s) M^\iota} \, . \tag{2.10.10}$$

The molar flux of constituent ι relative to the solid is given by

$$\mathbf{j}^\iota = (1 - \varphi^s) c^\iota (\mathbf{v}^\iota - \mathbf{v}^s) \, , \tag{2.10.11}$$

where it may be noted that $\mathbf{m}^\iota = M^\iota \mathbf{j}^\iota$. Combining these relations with (2.10.4)-(2.10.5) produces the desired form of the mass balance for the solutes,

$$\frac{1}{J} \frac{D^s [J (1 - \varphi^s) c^\iota]}{Dt} + \mathsf{div} \mathbf{j}^\iota = (1 - \varphi^s) \hat{c}^\iota \, . \tag{2.10.12}$$

This form is suitable for implementation in a finite element analysis where the mesh is defined on the solid matrix.

2.10.3 Mixture with Negligible Solute Volume Fraction

The volume fraction of each constituent is given by $\varphi^\alpha = \rho^\alpha / \rho_T^\alpha$. In a saturated mixture these volume fractions satisfy $\sum_\alpha \varphi^\alpha = 1$. Substituting $\rho^\alpha = \varphi^\alpha \rho_T^\alpha$ into (2.10.1), dividing across by ρ_T^α (invariant for intrinsically incompressible constituents), and taking the sum of the resulting expression over all constituents produces

$$\mathrm{div} \left(\sum_\alpha \varphi^\alpha \mathbf{v}^\alpha \right) = \sum_\alpha \frac{\hat{\rho}^\alpha}{\rho_T^\alpha} \, . \tag{2.10.13}$$

This mass balance relation for the mixture expresses the fact that the mixture volume will change as a result of chemical reactions where the true density of products is different from that of reactants. Indeed, assuming that ρ_T^α is the same for all α would nullify the right-hand-side of (2.10.13) based on (2.10.2). We now adopt the assumption that solutes occupy a negligible volume fraction of the mixture ($\varphi^\iota \ll 1$), from which it follows that $\varphi^s + \varphi^w \approx 1$ and $\sum_\alpha \varphi^\alpha \mathbf{v}^\alpha \approx \mathbf{v}^s + \mathbf{w}$, where $\mathbf{w} = \varphi^w (\mathbf{v}^w - \mathbf{v}^s)$ is the volumetrix flux of solvent relative to the solid. Thus, the mixture mass balance may be reduced to

$$\operatorname{div}(\mathbf{v}^s + \mathbf{w}) = \sum_\alpha \frac{\hat{\rho}^\alpha}{\rho_T^\alpha} \,. \tag{2.10.14}$$

In the special case of the solvent ($\alpha = w$), FEBio uses a solvent supply, $\hat{\varphi}^w = \hat{\rho}^w / \hat{\rho}_T^w$, which may be incorporated in (2.10.14) as

$$\operatorname{div}(\mathbf{v}^s + \mathbf{w}) = \hat{\varphi}^w + \sum_{\alpha \neq w} \frac{\hat{\rho}^\alpha}{\rho_T^\alpha} \,. \tag{2.10.15}$$

2.10.4 Chemical Kinetics

Productions rates are described by constitutive relations which are functions of the state variables. In a biological mixture under isothermal conditions, the minimum set of state variables needed to describe reactive mixtures that include a solid matrix are: the (uniform) temperature θ, the solid matrix deformation gradient $\mathbf{F}$ (or related strain measures), and the molar content c^α of the various constituents. This set differs from the classical treatment of chemical kinetics in fluid mixtures by the inclusion of $\mathbf{F}$ and the subset of constituents bound to the solid matrix. To maintain a consistent notation in this section, solid-bound molecular species are described by their molar concentrations and molar supplies which may be related to their referential mass density and referential mass supply according to

$$c^\sigma = \frac{\rho_r^\sigma}{(J - \varphi_r^s) M^\sigma}, \quad \hat{c}^\sigma = \frac{\hat{\rho}_r^\sigma}{(J - \varphi_r^s) M^\sigma} \,. \tag{2.10.16}$$

Consider a general chemical reaction,

$$\sum_\alpha \nu_R^\alpha \mathcal{E}^\alpha \to \sum_\alpha \nu_P^\alpha \mathcal{E}^\alpha \,, \tag{2.10.17}$$

where $\mathcal{E}^\alpha$ is the chemical species representing constituent α; ν_R^α and ν_P^α represent stoichiometric coefficients of the reactants and products, respectively. Since the molar supply of reactants and products is constrained by stoichiometry, it follows that all molar supplies $\hat{c}^\alpha$ in a specific chemical reaction may be related to a production rate $\hat{\zeta}$ according to

$$\hat{c}^\alpha = \nu^\alpha \hat{\zeta} \,, \tag{2.10.18}$$

where ν^α represents the net stoichiometric coefficient for $\mathcal{E}^\alpha$,

$$\nu^\alpha = \nu_P^\alpha - \nu_R^\alpha \,. \tag{2.10.19}$$

Thus, formulating constitutive relations for $\hat{c}^\alpha$ is equivalent to providing a single relation for $\hat{\zeta}(\theta, \mathbf{F}, c^\alpha)$. When the chemical reaction is reversible,

$$\sum_\alpha \nu_R^\alpha \mathcal{E}^\alpha \rightleftharpoons \sum_\alpha \nu_P^\alpha \mathcal{E}^\alpha \,, \tag{2.10.20}$$

the relations of (2.10.18)-(2.10.19) still apply but the form of $\hat{\zeta}$ would be different.

Using the relations of (2.10.10), (2.10.16) and (2.10.18), it follows in general that $\hat{\rho}^\alpha = (1 - \varphi^s) M^\alpha \nu^\alpha \hat{\zeta}$, so that the constraint of (2.10.2) is equivalent to enforcing stoichiometry, namely,

$$\sum_\alpha \nu^\alpha M^\alpha = 0 \,. \tag{2.10.21}$$

Thus, properly balancing a chemical reaction satisfies this constraint.

The mixture mass balance in (2.10.15) may now be rewritten as

$$\operatorname{div} (\mathbf{v}^s + \mathbf{w}^w) = \hat{\varphi}^w + (1 - \varphi^s) \hat{\zeta} \overline{\mathcal{V}} \,, \tag{2.10.22}$$

where $\overline{\mathcal{V}} = \sum_{\alpha \neq w} \nu^\alpha \mathcal{V}^\alpha$ and $\mathcal{V}^\alpha = M^\alpha / \rho_T^\alpha$ is the molar volume of α. (Currently in FEBio, $\hat{\varphi}^w$ is specified independently of $\hat{\zeta}$, because users may choose to neglect the contribution from $\overline{\mathcal{V}}$ in (2.10.22); therefore, if one desires to model chemical reactions, (2.10.17) or (2.10.20), that involve the solvent, it is necessary to explicitly provide a solvent supply function compatible with the above relations, namely $\hat{\varphi}^w = (1 - \varphi^s) \hat{\zeta} \nu^w \mathcal{V}^w$.) Similarly, the solute mass balance in (2.10.12) becomes

$$\frac{1}{J} \frac{D^s \left[J \left(1 - \varphi^s\right) c^\iota \right]}{Dt} + \operatorname{div} \mathbf{j}^\iota = (1 - \varphi^s) \nu^\iota \hat{\zeta} \,. \tag{2.10.23}$$

These mass balance equations reduce to those of non-reactive mixtures when $\hat{\zeta} = 0$.

2.11   Fluid Mechanics

2.11.1   Mass and Momentum Balance

In a spatial (Eulerian) frame, the momentum balance equation for a continuum is

$$\rho \mathbf{a} = \operatorname{div} \boldsymbol{\sigma} + \rho \mathbf{b} \,, \tag{2.11.1}$$

where ρ is the density, $\boldsymbol{\sigma}$ is the Cauchy stress, $\mathbf{b}$ is the body force per mass, and $\mathbf{a}$ is the acceleration, given by the material time derivative of the velocity $\mathbf{v}$ in the spatial frame,

$$\mathbf{a} = \dot{\mathbf{v}} = \frac{\partial \mathbf{v}}{\partial t} + \mathbf{L} \cdot \mathbf{v} \,, \tag{2.11.2}$$

where $\mathbf{L} = \operatorname{grad} \mathbf{v}$ is the spatial velocity gradient. The mass balance equation is

$$\dot{\rho} + \rho \operatorname{div} \mathbf{v} = 0 \,, \tag{2.11.3}$$

where the material time derivative of the density in the spatial frame is

$$\dot{\rho} = \frac{\partial \rho}{\partial t} + \operatorname{grad} \rho \cdot \mathbf{v} \,. \tag{2.11.4}$$

Let $\mathbf{F}$ denote the deformation gradient (the gradient of the motion with respect to the material coordinate). The material time derivative of $\mathbf{F}$ is related to $\mathbf{L}$ via

$$\dot{\mathbf{F}} = \mathbf{L} \cdot \mathbf{F} \,. \tag{2.11.5}$$

Let $J = \det \mathbf{F}$ denote the Jacobian of the motion (the volume ratio, or ratio of current to referential volume, $J > 0$); then, the dilatation (relative change in volume between current and reference configurations) is given by $e = J - 1$. Using the chain rule, J's material time derivative is $\dot{J} = J\mathbf{F}^{-T} : \dot{\mathbf{F}}$ which, when combined with eq.(2.11.5), produces a kinematic constraint between $\dot{J}$ and $\operatorname{div} \mathbf{v}$,

$$\dot{J} = J \operatorname{div} \mathbf{v} . \tag{2.11.6}$$

Substituting this relation into the mass balance, eq.(2.11.3), produces $\dot{\overline{\rho J}} = 0$, which may be integrated directly to yield

$$\rho = \rho_r / J , \tag{2.11.7}$$

where ρ_r is the density in the reference configuration (when $J = 1$). Since ρ_r is obtained by integrating the above material time derivative of ρJ, it is an intrinsic material property that must be invariant in time and space.

The Cauchy stress is given by

$$\boldsymbol{\sigma} = -p\mathbf{I} + \boldsymbol{\tau} , \tag{2.11.8}$$

where $\mathbf{I}$ is the identity tensor, $\boldsymbol{\tau}$ is the viscous stress, p is the pressure arising from the elastic response,

$$p = -\frac{d\Psi_r(J)}{dJ} , \tag{2.11.9}$$

and Ψ_r is the free energy density of the fluid (free energy per volume of the continuum in the reference configuration). The axiom of entropy inequality dictates that Ψ_r cannot be a function of the rate of deformation $\mathbf{D} = (\mathbf{L} + \mathbf{L}^T)/2$. In contrast, the viscous stress $\boldsymbol{\tau}$ is generally a function of J and $\mathbf{D}$.

Boundary conditions may be derived by satisfying mass and momentum balance across a moving interface Γ. Let Γ divide the material domain V into subdomains V_+ and V_- and let the outward normal to V_+ on Γ be denoted by $\mathbf{n}$. The jump condition across Γ derived from the axiom of mass balance requires that

$$[[\rho \mathbf{u}_\Gamma]] \cdot \mathbf{n} = 0 , \tag{2.11.10}$$

where $\mathbf{u}_\Gamma \equiv \mathbf{v} - \mathbf{v}_\Gamma$ on Γ and $\mathbf{v}_\Gamma$ is the velocity of the interface Γ. Thus, $\mathbf{u}_\Gamma$ represents the velocity of the fluid relative to Γ. The double bracket notation denotes $[[f]] = f_+ - f_-$, where f_+ and f_- represent the value of f on Γ in V_+ and V_-, respectively. This jump condition implies that the mass flux normal to Γ must be continuous. In particular, if V_+ is a fluid domain and V_- is a solid domain, and Γ denotes the solid boundary (e.g., a wall), we use $\rho_+ = \rho$, $\mathbf{v}_+ = \mathbf{v}$ for the fluid, and $\mathbf{v}_- = \mathbf{v}_\Gamma$ for the solid, such that eq.(2.11.10) reduces to $\rho(\mathbf{v} - \mathbf{v}_\Gamma) \cdot \mathbf{n} = 0$. The jump condition derived from the axiom of linear momentum balance similarly requires that

$$[[\boldsymbol{\sigma} - \rho \mathbf{u}_\Gamma \otimes \mathbf{u}_\Gamma]] \cdot \mathbf{n} = \mathbf{0} . \tag{2.11.11}$$

This condition implies that the jump in the traction $\boldsymbol{\sigma} \cdot \mathbf{n}$ across Γ must be balanced by the jump in momentum flux normal to Γ. In addition to jump conditions dictated by axioms of conservation, viscous fluids require the satisfaction of the no-slip condition,

$$(\mathbf{I} - \mathbf{n} \otimes \mathbf{n}) \cdot [[\mathbf{u}_\Gamma]] = \mathbf{0} , \tag{2.11.12}$$

which implies that the velocity component tangential to Γ is continuous across that interface.

In our finite element treatment we use $\mathbf{v}$ and J as nodal variables, implying that our formulation automatically enforces continuity of these variables across element boundaries, thus $[[\mathbf{v}]] = [[\mathbf{u}_\Gamma]] = \mathbf{0}$ and $[[J]] = 0$. Based on eqs.(2.11.7) and (2.11.9), it follows that the density

and elastic pressure are continuous across element boundaries in this formulation, $[[\rho]] = 0$ and $[[p]] = 0$. Thus, the mass jump in eq.(2.11.10) is automatically satisfied, and the momentum jump in eq.(2.11.11) reduces to $[[\boldsymbol{\sigma}]] \cdot \mathbf{n} = \mathbf{0}$, requiring continuity of the traction, or more specifically according to (2.11.8), the continuity of the viscous traction $\boldsymbol{\tau} \cdot \mathbf{n}$, since p is automatically continuous.

2.11.2   Energy Balance

The energy balance for a continuum may be written in integral form over a control volume V as

$$
\frac{d}{dt} \int_V \rho \left(\varepsilon + \frac{1}{2} \mathbf{v} \cdot \mathbf{v} \right) dV = - \int_S \rho \left(\varepsilon + \frac{1}{2} \mathbf{v} \cdot \mathbf{v} \right) (\mathbf{v} \cdot \mathbf{n}) \, dS + \int_S \mathbf{t} \cdot \mathbf{v} \, dS + \int_V \rho \mathbf{b} \cdot \mathbf{v} \, dV
$$
$$
- \int_S \mathbf{q} \cdot \mathbf{n} \, dS + \int_V \rho r \, dV
$$

$$(2.11.13)$$

where S is the control surface bounding V, ε is the specific internal energy, $\mathbf{q}$ is the heat flux across S, and r is the heat supply per mass to the material in V resulting from other sources. Bringing the time derivative inside the integral on the left-hand-side, and using the divergence theorem, this integral statement of the energy balance may be written as

$$
\int_V \left[\rho \left(\dot{\varepsilon} + \mathbf{v} \cdot \mathbf{a} \right) + \rho \left(\varepsilon + \frac{1}{2} \mathbf{v} \cdot \mathbf{v} \right) \left(\operatorname{div} \mathbf{v} - \frac{\dot{J}}{J} \right) \right] dV
$$
$$
= \int_V \left[\boldsymbol{\sigma} : \mathbf{D} - \operatorname{div} \mathbf{q} + \rho r + \mathbf{v} \cdot \left(\operatorname{div} \boldsymbol{\sigma} + \rho \mathbf{b} \right) \right] dV
$$

$$(2.11.14)$$

This statement must be valid for arbitrary control volumes and arbitrary processes, from which we conventionally derive the differential form of the axioms of mass, momentum and energy balance.

For the specialized conditions of a viscous fluid at constant temperature assumed in our treatment, the only state variables for the functions of state ε, $\boldsymbol{\sigma}$ and $\mathbf{q}$ are J and $\mathbf{D}$ (i.e., the temperature is not a state variable since it is assumed constant). Under these conditions the entropy inequality shows that the specific entropy η and the heat flux $\mathbf{q}$ must be zero, and the Cauchy stress $\boldsymbol{\sigma}$ must have the form of (2.11.8) where p is given by(2.11.9) as a function of J only, leaving the residual dissipation statement $\boldsymbol{\tau} : \mathbf{D} \geq 0$ as a constraint that must be satisfied by constitutive relations for $\boldsymbol{\tau}$. (For a Newtonian fluid, this constraint is satisfied when the viscosities μ and κ are positive.) From these thermodynamic restrictions we conclude that $\varepsilon = \psi$, where ψ is the specific (Helmholtz) free energy, with $\Psi_r = \rho_r \psi$.

For the conditions adopted here (isothermal viscous fluid), the axiom of energy balance reduces to $\rho \dot{\psi} = \boldsymbol{\sigma} : \mathbf{D} + \rho r$; since ψ is only a function of J, this expression may be further simplified using (2.11.6)-(2.11.9) to produce $\boldsymbol{\tau} : \mathbf{D} + \rho r = 0$. In other words, isothermal conditions may be maintained only if heat dissipated by the viscous stress is emitted in the form of a heat supply density $\rho r = -\boldsymbol{\tau} : \mathbf{D}$ (heat leaving the system). Now, the integral form of the energy balance in (2.11.14) simplifies to

$$
\int_V \left[\mathbf{v} \cdot \left(\operatorname{div} \boldsymbol{\sigma} + \rho \left(\mathbf{b} - \mathbf{a} \right) \right) + \rho \left(\psi + \frac{1}{2} \mathbf{v} \cdot \mathbf{v} \right) \left(\frac{\dot{J}}{J} - \operatorname{div} \mathbf{v} \right) \right] dV = 0 \, . \qquad (2.11.15)
$$

A comparison of this statement with the statement of virtual work, presented below in (3.5.1), establishes a clear correspondence between the virtual velocity $\delta \mathbf{v}$ and $\mathbf{v}$, and between the virtual energy density δJ and $\rho \left(\psi + \frac{1}{2} \mathbf{v} \cdot \mathbf{v} \right)$, with the latter representing the sum of the internal (free) and kinetic energy densities.

Chapter 3

The Nonlinear FE Method

This chapter discusses the basic principles of the nonlinear finite element method. The chapter begins with a short introduction to the weak formulation and the principle of virtual work. Next, the important concept of linearization is discussed and applied to the principle of virtual work. Finally the Newton-Raphson procedure and its application to the nonlinear finite element method are described.

3.1   Weak formulation for Solid Materials

Generally, the finite element formulation is established in terms of a weak form of the differential equations under consideration. In the context of solid mechanics this implies the use of the virtual work equation:

$$\delta W = \int_v \boldsymbol{\sigma} : \delta \mathbf{d} \, dv - \int_v \mathbf{f} \cdot \delta \mathbf{v} \, dv - \int_{\partial v} \mathbf{t} \cdot \delta \mathbf{v} \, da = 0 \,. \tag{3.1.1}$$

Here, $\delta \mathbf{v}$ is a virtual velocity and $\delta \mathbf{d}$ is the virtual rate of deformation tensor. This equation is known as the *spatial virtual work equation* since it is formulated using spatial quantities only. We can also define the *material virtual work equation* by expressing the principle of virtual work using only material quantities.

$$\delta W = \int_V \mathbf{S} : \delta \dot{\mathbf{E}} \, dV - \int_V \mathbf{f}_0 \cdot \delta \mathbf{v} \, dV - \int_{\partial V} \mathbf{t}_0 \cdot \delta \mathbf{v} \, dA = 0 \,. \tag{3.1.2}$$

Here, $\mathbf{f}_0 = J\mathbf{f}$ is the body force per unit undeformed volume and $\mathbf{t}_0 = \mathbf{t} \, (da/dA)$ is the traction vector per unit initial area.

3.1.1   Linearization

Equation (3.1.1) is the starting point for the nonlinear finite element method. It is highly nonlinear and any method attempting to solve this equation, such as the Newton-Raphson method, necessarily has to be iterative.

To linearize the finite element equations, the directional derivative of the virtual work in equation (3.1.1) must be calculated. In an iterative procedure, the quantity ϕ will be approximated by a trial solution ϕ_k. Linearization of the virtual work equation around this trial solution gives

$$\delta W \left(\phi_k, \delta \mathbf{v} \right) + D\delta W \left(\phi_k, \delta \mathbf{v} \right) \left[\mathbf{u} \right] = 0 \,. \tag{3.1.3}$$

The directional derivative of the virtual work will eventually lead to the definition of the stiffness matrix. In order to proceed, it is convenient to split the virtual work into an internal and external virtual work component:

$$D\delta W\left(\boldsymbol{\phi}, \delta\mathbf{v}\right)[\mathbf{u}] = D\delta W_{int}\left(\boldsymbol{\phi}, \delta\mathbf{v}\right)[\mathbf{u}] - D\delta W_{ext}\left(\boldsymbol{\phi}, \delta\mathbf{v}\right)[\mathbf{u}] ,\qquad(3.1.4)$$

where

$$\delta W_{int}\left(\boldsymbol{\phi}, \delta\mathbf{v}\right) = \int_v \boldsymbol{\sigma} : \delta\mathbf{d}\, dv ,\qquad(3.1.5)$$

and

$$\delta W_{ext}\left(\boldsymbol{\phi}, \delta\mathbf{v}\right) = \int_v \mathbf{f}\cdot\delta\mathbf{v}\, dv + \int_{\partial v} \mathbf{t}\cdot\delta\mathbf{v}\, da .\qquad(3.1.6)$$

The result is listed here without details of the derivation – see [19] for details. The linearization of the internal virtual work is given by

$$D\delta W_{int}\left(\boldsymbol{\phi}, \delta\mathbf{v}\right)[\mathbf{u}] = \int_v \delta\mathbf{d} : \boldsymbol{\mathcal{C}} : \boldsymbol{\varepsilon}\, dv + \int_v \boldsymbol{\sigma} : \left[(\nabla\mathbf{u})^T\cdot\nabla\delta\mathbf{v}\right]\, dv .\qquad(3.1.7)$$

Notice that this equation is symmetric in $\delta\mathbf{v}$ and $\mathbf{u}$. This symmetry will, upon discretization, yield a symmetric tangent matrix.

The external virtual work has contributions from both body forces and surface tractions. The precise form of the linearized external virtual work depends on the form of these forces. For surface tractions, normal pressure forces may be represented in FEBio. The linearized external work for this type of traction is given by

$$\begin{aligned}
D\delta W_{ext}^{p}\left(\boldsymbol{\phi}, \delta\mathbf{v}\right)[\mathbf{u}] &= \frac{1}{2}\int_{A_\xi} p\frac{\partial\mathbf{x}}{\partial\xi}\cdot\left[\left(\frac{\partial\mathbf{u}}{\partial\eta}\times\delta\mathbf{v}\right) + \left(\frac{\partial\delta\mathbf{v}}{\partial\eta}\times\mathbf{u}\right)\right] d\xi\, d\eta \\
&\quad -\frac{1}{2}\int_{A_\xi} p\frac{\partial\mathbf{x}}{\partial\eta}\cdot\left[\left(\frac{\partial\mathbf{u}}{\partial\xi}\times\delta\mathbf{v}\right) + \left(\frac{\partial\delta\mathbf{v}}{\partial\xi}\times\mathbf{u}\right)\right] d\xi\, d\eta .
\end{aligned}\qquad(3.1.8)$$

Discretization of this equation will also lead to a symmetric component of the tangent matrix.

FEBio currently supports gravity as a body force, $\mathbf{f} = \rho\mathbf{g}$. Since this force is independent of the geometry, the contribution to the linearized external work is zero. Another type of body force implemented in FEBio is the centrifugal force. For a body rotating with a constant angular speed ω, about an axis passing through the point $\mathbf{c}$ and directed along the unit vector $\mathbf{n}$, the body force is given by $\mathbf{f} = \rho\omega^2\mathbf{r}$, where $\mathbf{r}$ is the vector distance from a point $\mathbf{x}$ to the axis of rotation,

$$\mathbf{r} = (\mathbf{I} - \mathbf{n}\otimes\mathbf{n})\cdot(\mathbf{x} - \mathbf{c}) .\qquad(3.1.9)$$
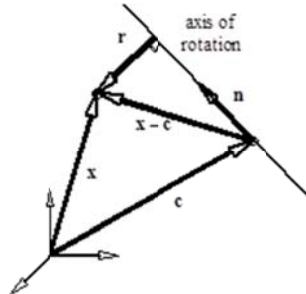
The resulting linearized external work is given by

$$D\delta W_{ext}^{f}\left(\boldsymbol{\phi},\delta\mathbf{v}\right)\left[\mathbf{u}\right]=\int_{v}\rho\omega^{2}\delta\mathbf{v}\cdot\left(\mathbf{I}-\mathbf{n}\otimes\mathbf{n}\right)\cdot\mathbf{u}\,dv,\tag{3.1.10}$$

which produces a symmetric expression that will yield a symmetric matrix.

3.1.2 Discretization

The basis of the finite element method is that the domain of the problem (that is, the volume of the object under consideration) is divided into smaller subunits, called *finite elements*. In the case of *isoparametric elements* it is further assumed that each element has a local coordinate system, named the *natural coordinates*, and the coordinates and shape of the element are discretized using the same functions. The discretization process is established by interpolating the geometry in terms of the coordinates $\mathbf{X}_a$ of the *nodes* that define the geometry of a finite element, and the *shape functions*:

$$\mathbf{X}=\sum_{a=1}^{n}N_{a}\left(\xi_{1},\xi_{2},\xi_{3}\right)\mathbf{X}_{a}\,,\tag{3.1.11}$$

where n is the number of nodes and ξ_{i} are the natural coordinates. Similarly, the motion is described in terms of the current position $\mathbf{x}_{a}\left(t\right)$ of the *same* particles:

$$\mathbf{x}\left(t\right)=\sum_{a=1}^{n}N_{a}\mathbf{x}_{a}\left(t\right)\,.\tag{3.1.12}$$

Quantities such as displacement, velocity and virtual velocity can be discretized in a similar way.

In deriving the discretized equilibrium equations, the integrations performed over the entire volume can be written as a sum of integrations constrained to the volume of an element. For this reason, the discretized equations are defined in terms of integrations over a particular element e. The discretized equilibrium equations for this particular element per node is given by

$$\delta W^{(e)}\left(\boldsymbol{\phi},N_{a}\delta\mathbf{v}\right)=\delta\mathbf{v}_{a}\cdot\left(\mathbf{T}_{a}^{(e)}-\mathbf{F}_{a}^{(e)}\right)\,,\tag{3.1.13}$$

where

$$\begin{aligned}T_{a}^{(e)}&=\int_{v^{(e)}}\boldsymbol{\sigma}\cdot\nabla N_{a}\,dv\,,\\F_{a}^{(e)}&=\int_{v^{(e)}}N_{a}\mathbf{f}\,dv+\int_{\partial v^{(e)}}N_{a}\mathbf{t}\,da\,.\end{aligned}\tag{3.1.14}$$

The linearization of the internal virtual work can be split into a *material* and an *initial stress* component [19]:

$$\begin{aligned}D\delta W_{int}^{(e)}\left(\boldsymbol{\phi},\delta\mathbf{v}\right)\left[\mathbf{u}\right]&=\int_{v^{(e)}}\delta\mathbf{d}:\boldsymbol{\mathcal{C}}:\boldsymbol{\varepsilon}\,dv+\int_{v^{(e)}}\boldsymbol{\sigma}:\left[\left(\nabla\mathbf{u}\right)^{T}\cdot\nabla\delta\mathbf{v}\right]\,dv\\&=D\delta W_{c}^{(e)}\left(\boldsymbol{\phi},\delta\mathbf{v}\right)\left[\mathbf{u}\right]+D\delta W_{\sigma}^{(e)}\left(\boldsymbol{\phi},\delta\mathbf{v}\right)\left[\mathbf{u}\right]\,.\end{aligned}\tag{3.1.15}$$

The constitutive component can be discretized as follows:

$$D\delta W_{c}^{(e)}\left(\boldsymbol{\phi},\delta\mathbf{v}\right)\left[\mathbf{u}\right]=\delta\mathbf{v}_{a}\cdot\left(\int_{v^{(e)}}\mathbf{B}_{a}^{T}\mathbf{D}\mathbf{B}_{b}\,dv\right)\mathbf{u}_{b}\,.\tag{3.1.16}$$

The term in parentheses defines the constitutive component of the tangent matrix relating node a to node b in element e:

$$\mathbf{K}_{c,ab}^{(e)} = \int_{v^{(e)}} \mathbf{B}_a^T \mathbf{D} \mathbf{B}_b \, dv \,. \tag{3.1.17}$$

Here, the linear strain-displacement matrix $\mathbf{B}$ relates the displacements to the small-strain tensor in Voigt Notation:

$$\varepsilon = \sum_{a=1}^{n} \mathbf{B}_a \mathbf{u}_a \,. \tag{3.1.18}$$

Or, written out completely,

$$\mathbf{B}_a = \begin{bmatrix} \partial N_a/\partial x & 0 & 0 \\ 0 & \partial N_a/\partial y & 0 \\ 0 & 0 & \partial N_a/\partial z \\ \partial N_a/\partial y & \partial N_a/\partial x & 0 \\ 0 & \partial N_a/\partial z & \partial N_a/\partial y \\ \partial N_a/\partial z & 0 & \partial N_a/\partial z \end{bmatrix} \,. \tag{3.1.19}$$

The spatial constitutive matrix $\mathbf{D}$ is constructed from the components of the fourth-order tensor $\mathcal{C}$ using the following table; $D_{IJ} = \mathcal{C}_{ijkl}$ where

I/J	i/k	j/l
1	1	1
2	2	2
3	3	3
4	1	2
5	2	3
6	1	3

The initial stress component can be written as follows:

$$D\delta W_\sigma^{(e)} \left(\phi, N_a \delta \mathbf{v} \right) [N_b \mathbf{u}_b] = \int_{v^{(e)}} \left(\nabla N_a \cdot \boldsymbol{\sigma} \cdot \nabla N_b \right) \mathbf{I} \, dv. \tag{3.1.20}$$

For the pressure component of the external virtual work, we find

$$D\delta W_p^{(e)} \left(\phi, N_a \delta \mathbf{v}_a \right) [N_b \mathbf{u}_b] = \delta \mathbf{v}_a \cdot \mathbf{K}_{p,ab}^{(e)} \cdot \mathbf{u}_b \,, \tag{3.1.21}$$

where,

$$\begin{aligned} \mathbf{K}_{p,ab}^{(e)} &= \mathcal{E} \mathbf{k}_{p,ab}^{(e)}, \\ \mathbf{k}_{p,ab}^{(e)} &= \frac{1}{2} \int_{A_\xi} p \frac{\partial \mathbf{x}}{\partial \xi} \left(\frac{\partial N_a}{\partial \eta} N_b - \frac{\partial N_b}{\partial \eta} N_a \right) d\xi \, d\eta \\ &+ \frac{1}{2} \int_{A_\xi} p \frac{\partial \mathbf{x}}{\partial \eta} \left(\frac{\partial N_a}{\partial \xi} N_b - \frac{\partial N_b}{\partial \xi} N_a \right) d\xi \, d\eta \,. \end{aligned} \tag{3.1.22}$$

3.2 Weak formulation for biphasic materials

A weak form of the statement conservation of linear momemtum for the quasi-static case is obtained by using Eqs.(2.5.2) and (2.5.4):

$$\delta W = \int_b \left[\delta \mathbf{v}^s \cdot (\mathrm{div}\,\boldsymbol{\sigma} + \rho \mathbf{b}) + \delta p\,\mathrm{div}\,(\mathbf{v}^s + \mathbf{w}) \right] dv = 0 \,, \tag{3.2.1}$$

where b is the domain of interest defined on the solid matrix, $\delta \mathbf{v}^s$ is a virtual velocity of the solid and δp is a virtual pressure of the fluid [61]. dv is an elemental volume of b. Using the divergence theorem, this expression may be rearranged as

$$\begin{aligned}
\delta W = &\int_{\partial b} \delta \mathbf{v}^s \cdot \mathbf{t}\,da + \int_{\partial b} \delta p\,w_n\,da + \int_b \delta \mathbf{v}^s \cdot \rho \mathbf{b}\,dv \\
&- \int_b \boldsymbol{\sigma} : \mathrm{grad}\,\delta \mathbf{v}^s\,dv - \int_b (\mathbf{w} \cdot \mathrm{grad}\,\delta p - \delta p\,\mathrm{div}\,\mathbf{v}^s)\,dv
\end{aligned}, \tag{3.2.2}$$

where $\delta \mathbf{d}^s = \left(\mathrm{grad}\,\delta \mathbf{v}^s + \mathrm{grad}^T \delta \mathbf{v}^s \right)/2$ is the virtual rate of deformation tensor, $\mathbf{t} = \boldsymbol{\sigma} \cdot \mathbf{n}$ is the total traction on the surface ∂b, and $w_n = \mathbf{w} \cdot \mathbf{n}$ is the component of the fluid flux normal to ∂b, with $\mathbf{n}$ representing the unit outward normal to ∂b. da represents an elemental area of ∂b. In this type of problem, essential boundary conditions are prescribed for $\mathbf{u}$ and p, and natural boundary conditions are prescribed for $\mathbf{t}$ and w_n. In the expression of Eq.(3.2.2), $\delta W\,(\boldsymbol{\chi}^s, p, \delta \mathbf{v}^s, \delta p)$ represents the virtual work.

3.2.1 Linearization

Since the system of equations in Eq.(3.2.2) is highly nonlinear, its solution requires an iterative scheme such as Newton's method. This requires the linearization of δW at some trial solution $(\boldsymbol{\chi}^s_k, p_k)$, along an increment $\Delta \mathbf{u}$ in $\boldsymbol{\chi}^s$ and an increment Δp in p,

$$\delta W + D\delta W\,[\Delta \mathbf{u}] + D\delta W\,[\Delta p] = 0, \tag{3.2.3}$$

where $Df\,[\Delta q]$ represents the directional derivative of f along Δq. For convenience, the virtual work may be separated into its internal and external parts,

$$\delta W = \delta W_{\mathrm{ext}} - \delta W_{\mathrm{int}}, \tag{3.2.4}$$

where

$$\delta W_{\mathrm{int}} = \int_b \boldsymbol{\sigma} : \delta \mathbf{d}^s\,dv + \int_b \left(\mathbf{w} \cdot \mathrm{grad}\,\delta p - \delta p\,\frac{\dot{J}}{J} \right) dv, \tag{3.2.5}$$

where we have substituted $\mathrm{div}\,\mathbf{v}^s = \dot{J}/J$, and

$$\delta W_{\mathrm{ext}} = \int_{\partial b} \delta \mathbf{v}^s \cdot \mathbf{t}\,da + \int_{\partial b} \delta p\,w_n\,da + \int_b \delta \mathbf{v}^s \cdot \rho \mathbf{b}\,dv \,. \tag{3.2.6}$$

The evaluation of the directional derivatives can be performed following a standard approach [19]. In particular, a backward difference scheme is used to evaluate $\dot{J} \approx \left(J - J^{-\Delta t} \right)/\Delta t$, where $J^{-\Delta t}$

is the value of J at the previous time step. For the internal part of the virtual work, the directional derivative along $\Delta\mathbf{u}$ yields

$$
\begin{aligned}
D\delta W_{\text{int}}\left[\Delta\mathbf{u}\right] = {} & \int_b \delta\mathbf{d}^s : \boldsymbol{\mathcal{C}} : \Delta\boldsymbol{\varepsilon}\,dv + \int_b \boldsymbol{\sigma} : \left(\text{grad}^T\,\Delta\mathbf{u}\cdot\text{grad}\,\delta\mathbf{v}^s\right)\,dv \\
& - \int_b \frac{\delta p}{\Delta t}\,\text{div}\,\Delta\mathbf{u}\,dv \\
& - \int_b \text{grad}\,\delta p\cdot\left(\boldsymbol{\mathcal{K}} : \Delta\boldsymbol{\varepsilon}\right)\cdot\left(\text{grad}\,p - \rho_T^w\mathbf{b}^w\right)\,dv \\
& + \int_b \text{grad}\,\delta p\cdot\mathbf{k}\cdot\rho_T^w\left(\text{grad}^T\,\Delta\mathbf{u}\cdot\mathbf{b}^w + \text{grad}\,\mathbf{b}^w\cdot\Delta\mathbf{u}\right)\,dv\,,
\end{aligned}
\tag{3.2.7}
$$

where $\boldsymbol{\mathcal{C}}$ is the fourth-order spatial elasticity tensor for the mixture and $\Delta\boldsymbol{\varepsilon} = \left(\text{grad}\,\Delta\mathbf{u} + \text{grad}^T\,\Delta\mathbf{u}\right)/2$. Based on the relation of Eq.(2.5.3), the spatial elasticity tensor may also be expanded as

$$
\boldsymbol{\mathcal{C}} = \boldsymbol{\mathcal{C}}^e + p\left(-\mathbf{I}\otimes\mathbf{I} + 2\mathbf{I}\,\overline{\underline{\otimes}}\,\mathbf{I}\right),
\tag{3.2.8}
$$

where $\boldsymbol{\mathcal{C}}^e$ is the spatial elasticity tensor for the solid matrix [23]. It is related to the material elasticity tensor $\mathbb{C}^e$ via

$$
\boldsymbol{\mathcal{C}}^e = J^{-1}\left(\mathbf{F}\,\underline{\otimes}\,\mathbf{F}\right) : \mathbb{C}^e : \left(\mathbf{F}^T\,\underline{\otimes}\,\mathbf{F}^T\right),
\tag{3.2.9}
$$

where $\mathbf{F}$ is the deformation gradient of the solid matrix, $\mathbb{C}^e = \partial\mathbf{S}^e/\partial\mathbf{E}$ where $\mathbf{E}$ is the Lagrangian strain tensor and $\mathbf{S}^e$ is the second Piola-Kirchhoff stress tensor, related to the Cauchy stress tensor via $\boldsymbol{\sigma}^e = J^{-1}\mathbf{F}\cdot\mathbf{S}^e\cdot\mathbf{F}^T$.

Similarly, $\boldsymbol{\mathcal{K}}$ is a fourth-order tensor that represents the spatial measure of the rate of change of permeability with strain. It is related to its material frame equivalent $\mathbb{K}$ via

$$
\boldsymbol{\mathcal{K}} = J^{-1}\left(\mathbf{F}\,\underline{\otimes}\,\mathbf{F}\right) : \mathbb{K} : \left(\mathbf{F}^T\,\underline{\otimes}\,\mathbf{F}^T\right),
\tag{3.2.10}
$$

where $\mathbb{K} = \partial\mathbf{K}/\partial\mathbf{E}$ and $\mathbf{K}$ is the permeability tensor in the material frame, such that $\mathbf{k} = J^{-1}\mathbf{F}\cdot\mathbf{K}\cdot\mathbf{F}^T$. Since $\mathbf{K}$ and $\mathbf{E}$ are symmetric tensors, it follows that $\boldsymbol{\mathcal{K}}$ and $\mathbb{K}$ exhibit two minor symmetries (e.g., $\mathcal{K}_{jikl} = \mathcal{K}_{ijkl}$ and $\mathcal{K}_{ijlk} = \mathcal{K}_{ijkl}$). However, unlike the elasticity tensor, it is not necessary that these tensors exhibit major symmetry (e.g., $\mathcal{K}_{klij} \neq \mathcal{K}_{ijkl}$ in general).

The directional derivative of δW_{int} along Δp is given by

$$
D\delta W_{\text{int}}\left[\Delta p\right] = -\int_b \text{grad}\,\delta p\cdot\mathbf{k}\cdot\text{grad}\,\Delta p\,dv - \int_b \Delta p\,\text{div}\,\delta\mathbf{v}^s\,dv\,.
\tag{3.2.11}
$$

Note that letting $p = 0$ and $\delta p = 0$ in the above equations recovers the virtual work relations for nonlinear elasticity of compressible solids. The resulting simplified equation emerging from Eq.(3.2.7) is symmetric to interchanges of $\Delta\mathbf{u}$ and $\delta\mathbf{v}^s$, producing a symmetric stiffness matrix in the finite element formulation [19]. However, the general relations of Eqs.(3.2.7) and (3.2.11) do not exhibit symmetry to interchanges of $(\Delta\mathbf{u}, \Delta p)$ and $(\delta\mathbf{v}^s, \delta p)$, implying that the finite element stiffness matrix for a solid-fluid mixture is not symmetric under general conditions.

The directional derivatives of the external virtual work δW_{ext} depend on the type of boundary conditions being considered. For a prescribed total normal traction t_n, where $\mathbf{t} = t_n\mathbf{n}$,

$$
\delta W_{\text{ext}}^t = \int_{\partial b} \delta\mathbf{v}^s\cdot t_n\mathbf{n}\,da,
\tag{3.2.12}
$$

and

$$D\delta W_{\text{ext}}^t [\Delta \mathbf{u}] = \int_{\partial b} \delta \mathbf{v}^s \cdot t_n \left(\mathbf{g}_1 \times \frac{\partial \Delta \mathbf{u}}{\partial \eta^2} - \mathbf{g}_2 \times \frac{\partial \Delta \mathbf{u}}{\partial \eta^1} \right) \frac{da}{|\mathbf{g}_1 \times \mathbf{g}_2|} \,,$$

$$D\delta W_{\text{ext}}^t [\Delta p] = 0,$$

(3.2.13)

where

$$\mathbf{g}_\alpha = \frac{\partial \mathbf{x}}{\partial \eta^\alpha}, \quad \alpha = 1, 2$$

(3.2.14)

are covariant basis (tangent) vectors on ∂b, such that

$$\mathbf{n} = \frac{\mathbf{g}_1 \times \mathbf{g}_2}{|\mathbf{g}_1 \times \mathbf{g}_2|} \,.$$

(3.2.15)

For a prescribed normal effective traction t_n^e, where $\mathbf{t} = (-p + t_n^e) \, \mathbf{n}$ and p is not prescribed, then

$$\delta W_{\text{ext}}^e = \int_{\partial b} \delta \mathbf{v}^s \cdot (-p + t_n^e) \, \mathbf{n} \, da \,,$$

(3.2.16)

and

$$D\delta W_{\text{ext}}^e [\Delta \mathbf{u}] = \int_{\partial b} \delta \mathbf{v}^s \cdot (-p + t_n^e) \left(\mathbf{g}_1 \times \frac{\partial \Delta \mathbf{u}}{\partial \eta^2} - \mathbf{g}_2 \times \frac{\partial \Delta \mathbf{u}}{\partial \eta^1} \right) \frac{da}{|\mathbf{g}_1 \times \mathbf{g}_2|} \,,$$

$$D\delta W_{\text{ext}}^e [\Delta p] = - \int_{\partial b} \delta \mathbf{v}^s \cdot \Delta p \, \mathbf{n} \, da \,.$$

(3.2.17)

For a prescribed normal fluid flux $w_n = \mathbf{w} \cdot \mathbf{n}$,

$$\delta W_{\text{ext}}^w = \int_{\partial b} \delta p \, w_n \, da \,,$$

(3.2.18)

and

$$D\delta W_{\text{ext}}^w [\Delta \mathbf{u}] = \int_{\partial b} \delta p \, w_n \, \mathbf{n} \cdot \left(\mathbf{g}_1 \times \frac{\partial \Delta \mathbf{u}}{\partial \eta^2} - \mathbf{g}_2 \times \frac{\partial \Delta \mathbf{u}}{\partial \eta^1} \right) \frac{da}{|\mathbf{g}_1 \times \mathbf{g}_2|} \,,$$

$$D\delta W_{\text{ext}}^w [\Delta p] = 0 \,.$$

(3.2.19)

Finally, for a prescribed external body force, recognizing that $\rho \mathbf{b} = \rho^s \mathbf{b}^s + \rho^w \mathbf{b}^w$ and assuming that the body forces $\mathbf{b}^s$ and $\mathbf{b}^w$ do not depend on p,

$$D\left(\delta W_{\text{ext}}^b \right) [\Delta \mathbf{u}] = \int_b \delta \mathbf{v}^s \cdot [(\rho^s \, grad \mathbf{b}^s + \rho^w \, grad \mathbf{b}^w) \cdot \Delta \mathbf{u} + (\text{div} \, \Delta \mathbf{u}) \, \rho_T^w \mathbf{b}^w] \, dv \,,$$

$$D\left(\delta W_{\text{ext}}^b \right) [\Delta p] = 0 \,.$$

(3.2.20)

3.2.2 Discretization

Let

$$\delta \mathbf{v}^s = \sum_{a=1}^m N_a \delta \mathbf{v}_a \,, \quad \delta p = \sum_{a=1}^m N_a \delta p_a \,,$$

$$\Delta \mathbf{u} = \sum_{b=1}^m N_b \Delta \mathbf{u}_b \,, \quad \Delta p = \sum_{b=1}^m N_b \Delta p_b \,,$$

(3.2.21)

where N_a represents the interpolation functions over an element, $\delta\mathbf{v}_a, \delta p_a, \Delta\mathbf{u}_b$ and Δp_b respectively represent nodal values of $\delta\mathbf{v}^s$, δp, $\Delta\mathbf{u}$ and Δp, and m is the number of nodes in an element. Then the discretized form of δW_{int} in Eq.(3.2.5) may be written as

$$\delta W_{\text{int}} = \sum_{e=1}^{n_e} \sum_{k=1}^{n_{\text{int}}^{(e)}} W_k J_\eta \sum_{a=1}^{m} \begin{bmatrix} \delta\mathbf{v}_a & \delta p_a \end{bmatrix} \cdot \begin{bmatrix} \mathbf{r}_a^u \\ r_a^p \end{bmatrix}, \tag{3.2.22}$$

where n_e is the number of elements in b, $n_{\text{int}}^{(e)}$ is the number of integration points in the $e-$th element, W_k is the quadrature weight associated with the $k-$th integration point, and J_η is the Jacobian of the transformation from the spatial frame to the parametric space of the element. In the above expression,

$$\mathbf{r}_a^u = \boldsymbol{\sigma} \cdot \nabla N_a, \quad r_a^p = \mathbf{w} \cdot \nabla N_a - N_a \text{div}\mathbf{v}^s, \tag{3.2.23}$$

and it is understood that J_η, $\mathbf{r}_a^u$ and r_a^p are evaluated at the parametric coordinates of the $k-$th integration point.

Similarly, the discretized form of $D\delta W_{\text{int}}$ in Eqs.(3.2.7) and (3.2.11) may be written as

$$-D\delta W_{\text{int}} = \sum_{e=1}^{n_e} \sum_{k=1}^{n_{\text{int}}^{(e)}} W_k J_\eta \sum_{a=1}^{m} \begin{bmatrix} \delta\mathbf{v}_a & \delta p_a \end{bmatrix} \cdot \sum_{b=1}^{m} \begin{bmatrix} \mathbf{K}_{ab}^{uu} & \mathbf{k}_{ab}^{up} \\ \mathbf{k}_{ab}^{pu} & k_{ab}^{pp} \end{bmatrix} \cdot \begin{bmatrix} \Delta\mathbf{u}_b \\ \Delta p_b \end{bmatrix}, \tag{3.2.24}$$

where

$$\begin{aligned}
\mathbf{K}_{ab}^{uu} &= \nabla N_a \cdot \boldsymbol{\mathcal{C}} \cdot \nabla N_b + (\nabla N_a \cdot \boldsymbol{\sigma} \cdot \nabla N_b)\,\mathbf{I} \\
&\quad - N_a \left[N_b \left(\rho^s \nabla \mathbf{b}^s + \rho^w \nabla \mathbf{b}^w \right) + \rho_T^w \mathbf{b}^w \otimes \nabla N_b \right], \\
\mathbf{k}_{ab}^{up} &= -N_b \nabla N_a, \\
\mathbf{k}_{ab}^{pu} &= - \left(\nabla N_a \cdot \boldsymbol{\mathcal{K}} \cdot \nabla N_b \right) \cdot \left(\nabla p - \rho_T^w \mathbf{b}^w \right) - \frac{1}{\Delta t} N_a \cdot \nabla N_b \\
&\quad + \rho_T^w \left(\mathbf{b}^w \otimes \nabla N_b + N_b \nabla^T \mathbf{b}^w \right) \cdot \mathbf{k} \cdot \nabla N_a, \\
k_{ab}^{pp} &= -\nabla N_a \cdot \mathbf{k} \cdot \nabla N_b,
\end{aligned} \tag{3.2.25}$$

and Δt is a discrete increment in time. In a numerical implementation, it has been found that evaluating $\text{div}\,\mathbf{v}^s$ from $\dot{J}/J$, where $J = \det \mathbf{F}$, yields more accurate solutions than evaluating it from the trace of $\text{grad}\,\mathbf{v}^s$ [12].

For the various types of contributions to the external virtual work, a similar discretization produces

$$\delta W_{\text{ext}} = \sum_{e=1}^{n_e} \sum_{k=1}^{n_{\text{int}}^{(e)}} W_k J_\eta \sum_{a=1}^{m} \begin{bmatrix} \delta\mathbf{v}_a & \delta p_a \end{bmatrix} \cdot \begin{bmatrix} \mathbf{r}_a^u \\ r_a^p \end{bmatrix}, \tag{3.2.26}$$

and

$$-D\delta W_{\text{ext}} = \sum_{e=1}^{n_e} \sum_{k=1}^{n_{\text{int}}^{(e)}} W_k J_\eta \sum_{a=1}^{m} \begin{bmatrix} \delta\mathbf{v}_a & \delta p_a \end{bmatrix} \cdot \sum_{b=1}^{m} \begin{bmatrix} \mathbf{K}_{ab}^{uu} & \mathbf{k}_{ab}^{up} \\ \mathbf{k}_{ab}^{pu} & k_{ab}^{pp} \end{bmatrix} \cdot \begin{bmatrix} \Delta\mathbf{u}_b \\ \Delta p_b \end{bmatrix}, \tag{3.2.27}$$

where

$$J_\eta = |\mathbf{g}_1 \times \mathbf{g}_2|. \tag{3.2.28}$$

In this case, m represents the number of nodes on an element face. For a prescribed normal traction t_n as given in (3.2.12)-(3.2.13),

$$\mathbf{r}_a^u = t_n N_a \mathbf{n}\,, \qquad\qquad\qquad r_a^u = 0\,,$$
$$\mathbf{K}_{ab}^{uu} = t_n N_a \frac{1}{J_\eta} \mathcal{A} \left\{ \frac{\partial N_b}{\partial \eta^1} \mathbf{g}_2 - \frac{\partial N_b}{\partial \eta^2} \mathbf{g}_1 \right\}\,, \quad \mathbf{k}_{ab}^{up} = \mathbf{0}\,, \qquad\qquad (3.2.29)$$
$$\mathbf{k}_{ab}^{pu} = \mathbf{0}\,, \qquad\qquad\qquad k_{ab}^{pp} = 0\,,$$

where $\mathcal{A}\{\mathbf{v}\} = -\mathcal{E} \cdot \mathbf{v}$ is the skew-symmetric tensor whose dual vector is $\mathbf{v}$ and $\mathcal{E}$ is the third-order permutation pseudo-tensor. For a prescribed traction t_n^e as given in (3.2.16)-(3.2.17),

$$\mathbf{r}_a^u = \left(-p + t_n^e \right) N_a \mathbf{n}\,, \qquad\qquad\qquad r_a^u = 0\,,$$
$$\mathbf{K}_{ab}^{uu} = \left(-p + t_n^e \right) N_a \frac{1}{J_\eta} \mathcal{A} \left\{ \frac{\partial N_b}{\partial \eta^1} \mathbf{g}_2 - \frac{\partial N_b}{\partial \eta^2} \mathbf{g}_1 \right\}\,, \quad \mathbf{k}_{ab}^{up} = \mathbf{0}\,, \qquad\qquad (3.2.30)$$
$$\mathbf{k}_{ab}^{pu} = \mathbf{0}\,, \qquad\qquad\qquad k_{ab}^{pp} = 0\,.$$

For a prescribed normal fluid flux w_n as given in (3.2.18)-(3.2.19),

$$\mathbf{r}_a^u = \mathbf{0}\,, \qquad\qquad\qquad r_a^u = w_n N_a\,,$$
$$\mathbf{K}_{ab}^{uu} = \mathbf{0}\,, \qquad\qquad\qquad \mathbf{k}_{ab}^{up} = \mathbf{0}\,,$$
$$\mathbf{k}_{ab}^{pu} = w_n N_a \frac{1}{J_\eta} \mathbf{n} \times \left(\frac{\partial N_b}{\partial \eta^1} \mathbf{g}_2 - \frac{\partial N_b}{\partial \eta^2} \mathbf{g}_1 \right)\,, \quad k_{ab}^{pp} = 0\,. \qquad (3.2.31)$$

3.3 Weak Formulation for Biphasic-Solute Materials

The virtual work integral for this problem is given by

$$\delta W = \int_b \delta \mathbf{v} \cdot \operatorname{div} \boldsymbol{\sigma}\, dv + \int_b \delta \tilde{p} \operatorname{div} \left(\mathbf{v}^s + \mathbf{w} \right)\, dv$$
$$+ \int_b \delta \tilde{c} \left[\frac{\partial \left(\varphi^w \tilde{\kappa} \tilde{c} \right)}{\partial t} + \operatorname{div} \left(\mathbf{j} + \phi^w \tilde{\kappa} \tilde{c}\, \mathbf{v}^s \right) \right]\, dv\,, \qquad (3.3.1)$$

where $\delta \mathbf{v}$ is the virtual velocity of the solid, $\delta \tilde{p}$ is the virtual effective fluid pressure, and $\delta \tilde{c}$ is the virtual molar energy of the solute. b represents the mixture domain in the spatial frame and dv is an elemental mixture volume in b. In the last integral of δW, note that

$$\frac{\partial \left(\varphi^w \tilde{\kappa} \tilde{c} \right)}{\partial t} + \operatorname{div} \left(\varphi^w \tilde{\kappa} \tilde{c}\, \mathbf{v}^s \right) = \frac{1}{J} \frac{D^s}{Dt} \left(J \varphi^w \tilde{\kappa} \tilde{c} \right)\,, \qquad (3.3.2)$$

where $D^s f / Dt \equiv \partial f / \partial t + \mathbf{v}^s \cdot \operatorname{grad} f$ is the material time derivative of a scalar function f in the spatial frame, following the solid. Similarly, note that $\operatorname{div} \mathbf{v}^s = J^{-1} \left(D^s J / Dt \right)$. Using the divergence theorem, the virtual work integral may be separated into internal and external contributions, $\delta W = \delta W_{\text{ext}} - \delta W_{\text{int}}$, where

$$\delta W_{\text{int}} = \int_b \boldsymbol{\sigma} : \delta \mathbf{d}^s\, dv + \int_b \left(\mathbf{w} \cdot \operatorname{grad} \delta \tilde{p} - \frac{\delta \tilde{p}}{J} \frac{D^s J}{Dt} \right) dv$$
$$+ \int_b \left[\mathbf{j} \cdot \operatorname{grad} \delta \tilde{c} - \frac{\delta \tilde{c}}{J} \frac{D^s}{Dt} \left(J \varphi^w \tilde{\kappa} \tilde{c} \right) \right] dv\,, \qquad (3.3.3)$$
$$\delta W_{\text{ext}} = \int_{\partial b} \left(\delta \mathbf{v} \cdot \mathbf{t} + \delta \tilde{p}\, w_n + \delta \tilde{c}\, j_n \right) da\,,$$

with δW_{ext} being evaluated on the domain's boundary surface ∂b. In the first expression $\delta \mathbf{d}^s = \left(\text{grad}\, \delta \mathbf{v} + \text{grad}^T \delta \mathbf{v} \right) / 2$ represents the virtual solid rate of deformation.

To solve this nonlinear system using an iterative Newton scheme, the virtual work must be linearized at trial solutions, along increments in $\mathbf{u}$, $\tilde{p}$ and $\tilde{c}$,

$$\delta W + D\delta W\left[\Delta \mathbf{u}\right] + D\delta W\left[\Delta \tilde{p}\right] + D\delta W\left[\Delta \tilde{c}\right] \approx 0\,, \tag{3.3.4}$$

where, for any function $f(q)$, $Df\left[\Delta q\right]$ represents the directional derivative of f along Δq [19]. To operate the directional derivative on the integrand of δW_{int}, it is first necessary to convert the integrals from the spatial to the material domain [19]:

$$\delta W_{\text{int}} = \int_B \mathbf{S} : \delta \dot{\mathbf{E}}\, dV + \int_B \left(\mathbf{W} \cdot \text{grad}\, \delta \tilde{p} - \delta \tilde{p} \frac{\partial J}{\partial t} \right) dV + \int_B \left[\mathbf{J} \cdot \text{grad}\, \delta \tilde{c} - \delta \tilde{c} \frac{\partial}{\partial t} \left(J \varphi^w \tilde{\kappa} \tilde{c} \right) \right] dV\,, \tag{3.3.5}$$

where B represents the mixture domain in the material frame, dV is an elemental mixture volume in B, and

$$\begin{aligned}
\mathbf{S} &= J\, \mathbf{F}^{-1} \cdot \boldsymbol{\sigma} \cdot \mathbf{F}^{-T}\,, \\
\delta \dot{\mathbf{E}} &= \mathbf{F}^T \cdot \delta \mathbf{d}^s \cdot \mathbf{F}\,, \\
\mathbf{W} &= J\, \mathbf{F}^{-1} \cdot \mathbf{w}\,, \\
\mathbf{J} &= J\, \mathbf{F}^{-1} \cdot \mathbf{j}\,.
\end{aligned} \tag{3.3.6}$$

The second Piola-Kirchhoff stress tensor $\mathbf{S}$, and material flux vectors $\mathbf{W}$ and $\mathbf{J}$, are respectively related to $\boldsymbol{\sigma}$, $\mathbf{w}$ and $\mathbf{j}$ by the Piola transformations for tensors and vectors [19, 43]. Substituting (3.3.6) into (2.6.13) produces

$$\begin{aligned}
\mathbf{W} &= -\tilde{\mathbf{K}} \cdot \left(\text{grad}\, \tilde{p} + R\theta \frac{\tilde{\kappa}}{d_0} J^{-1} \mathbf{C} \cdot \mathbf{D} \cdot \text{grad}\, \tilde{c} \right)\,, \\
\mathbf{J} &= \tilde{\kappa} \mathbf{D} \cdot \left(-\varphi^w \,\text{grad}\, \tilde{c} + \frac{\tilde{c}}{d_0} J^{-1} \mathbf{C} \cdot \mathbf{W} \right)\,,
\end{aligned} \tag{3.3.7}$$

where $\tilde{\mathbf{K}}$ and $\mathbf{D}$ are the material representations of the permeability and diffusivity tensors, related to $\tilde{\mathbf{k}}$ and $\mathbf{d}$ via the Piola transformation,

$$\begin{aligned}
\tilde{\mathbf{K}} &= J\, \mathbf{F}^{-1} \cdot \tilde{\mathbf{k}} \cdot \mathbf{F}^{-T}\,, \\
\mathbf{D} &= J\, \mathbf{F}^{-1} \cdot \mathbf{d} \cdot \mathbf{F}^{-T}\,.
\end{aligned} \tag{3.3.8}$$

The linearization of δW_{int} is rather involved and a summary of the resulting lengthy expressions is provided below. In consideration of the dearth of experimental data relating $\tilde{\kappa}$ and Φ to the complete state of solid matrix strain (such as $\mathbf{C}$), this implementation assumes that the dependence of these functions on the strain is restricted to a dependence on the volume ratio $J = (\det \mathbf{C})^{1/2}$. Furthermore, it is assumed that the free solution diffusivity d_0 is independent of the strain.

The linearization of δW_{ext} is described in Section 3.3.2. Following the linearization procedure, the resulting expressions may be discretized by nodally interpolating $\mathbf{u}$, $\tilde{p}$ and $\tilde{c}$ over finite elements, producing a set of equations in matrix form, as described in Section 3.3.2.

The formulation presented in this study is implemented in FEBio by introducing an additional module dedicated to solute transport in deformable porous media. Classes are implemented to describe material functions for $\boldsymbol{\sigma}^e$, $\mathbf{k}$, $\mathbf{d}$ (and d_0), $\tilde{\kappa}$ and Φ, which allow the formulation of any desired constitutive relation for these functions of $\mathbf{C}$ and $\tilde{c}$, along with corresponding derivatives of

these functions with respect to $\mathbf{C}$ and $\tilde{c}$. The implementation accepts essential boundary conditions on $\mathbf{u}$, $\tilde{p}$ and $\tilde{c}$, or natural boundary conditions on $\mathbf{t}$, w_n and j_n; initial conditions may also be specified for $\tilde{p}$ and $\tilde{c}$. Analysis results for pressure and concentration may be displayed either as $\tilde{p}$ and $\tilde{c}$, or as p and c by inverting the relations of (2.6.11).

3.3.1 Linearization of Internal Virtual Work

The virtual work integral δW_{int} in (3.3.5) may be linearized term by term along increments in $\Delta \mathbf{u}$, $\Delta \tilde{p}$ and $\Delta \tilde{c}$ using the general form

$$D \left(\int_B F \, dV \right) [\Delta q] = \int_B DF \, [\Delta q] \, dV = \int_b f \, dv \,. \tag{3.3.9}$$

For notational simplicity, the integral sign is omitted and the linearization of each term is presented in the form $DF \, [\Delta q] \, dV = f \, dv$.

3.3.1.1 Linearization along $\Delta \mathbf{u}$

The linearization of the first term in δW_{int} along $\Delta \mathbf{u}$ yields

$$\left(\mathbf{S} : \delta \dot{\mathbf{E}} \right) [\Delta \mathbf{u}] \, dV = \left[\delta \mathbf{d}^s : \boldsymbol{\mathcal{C}} : \Delta \boldsymbol{\varepsilon} + \boldsymbol{\sigma} : \left(\text{grad}^T \Delta \mathbf{u} \cdot \text{grad} \, \delta \mathbf{v} \right) \right] \, dv \,, \tag{3.3.10}$$

where $\boldsymbol{\mathcal{C}}$ is the spatial elasticity tensor of the mixture,

$$\boldsymbol{\mathcal{C}} = \boldsymbol{\mathcal{C}}^e - \left(\tilde{p} + R\theta \, \Phi \tilde{\kappa} \tilde{c} \right) \left(\mathbf{I} \otimes \mathbf{I} - 2 \mathbf{I} \, \overline{\underline{\otimes}} \, \mathbf{I} \right) - R\theta \tilde{c} \, J \frac{\partial \left(\Phi \tilde{\kappa} \right)}{\partial J} \mathbf{I} \otimes \mathbf{I} \,, \tag{3.3.11}$$

and $\boldsymbol{\mathcal{C}}^e$ is the spatial elasticity tensor of the solid matrix,

$$\boldsymbol{\mathcal{C}}^e = J^{-1} \left(\mathbf{F} \, \underline{\overline{\otimes}} \, \mathbf{F} \right) : 2 \frac{\partial \mathbf{S}^e}{\partial \mathbf{C}} : \left(\mathbf{F}^T \, \underline{\overline{\otimes}} \, \mathbf{F}^T \right) \,. \tag{3.3.12}$$

The linearization of the second term is

$$D \left(\mathbf{W} \cdot \text{Grad} \, \delta \tilde{p} \right) [\Delta \mathbf{u}] \, dV = \text{grad} \, \delta \tilde{p} \cdot \mathbf{w}'_u \, dv \,, \tag{3.3.13}$$

where

$$\mathbf{w}'_u \equiv J^{-1} \mathbf{F} \cdot D\mathbf{W} \, [\Delta \mathbf{u}] = - \left(\tilde{\boldsymbol{\mathcal{K}}} : \Delta \boldsymbol{\varepsilon} \right) \cdot \left(\text{grad} \, \tilde{p} + R\theta \frac{\tilde{\kappa}}{d_0} \mathbf{d} \cdot \text{grad} \, \tilde{c} \right)$$
$$- \frac{R\theta}{d_0} \tilde{\mathbf{k}} \cdot \left(J^2 \frac{\partial \left(J^{-1} \tilde{\kappa} \right)}{\partial J} \left(\text{div} \, \Delta \mathbf{u} \right) \mathbf{I} + 2 \tilde{\kappa} \, \Delta \boldsymbol{\varepsilon} \right) \cdot \mathbf{d} \cdot \text{grad} \, \tilde{c} - \tilde{\kappa} \frac{R\theta}{d_0} \tilde{\mathbf{k}} \cdot \left(\boldsymbol{\mathcal{D}} : \Delta \boldsymbol{\varepsilon} \right) \cdot \text{grad} \, \tilde{c} \,, \tag{3.3.14}$$

with

$$\tilde{\boldsymbol{\mathcal{K}}} = J^{-1} \left(\mathbf{F} \, \underline{\overline{\otimes}} \, \mathbf{F} \right) : 2 \frac{\partial \tilde{\mathbf{K}}}{\partial \mathbf{C}} : \left(\mathbf{F}^T \, \underline{\overline{\otimes}} \, \mathbf{F}^T \right) \,,$$
$$\boldsymbol{\mathcal{D}} = J^{-1} \left(\mathbf{F} \, \underline{\overline{\otimes}} \, \mathbf{F} \right) : 2 \frac{\partial \mathbf{D}}{\partial \mathbf{C}} : \left(\mathbf{F}^T \, \underline{\overline{\otimes}} \, \mathbf{F}^T \right) \,, \tag{3.3.15}$$

representing the spatial tangents, with respect to the strain, of the effective permeability and solute diffusivity, respectively. These fourth-order tensors exhibit minor symmetries but not major

symmetry, as described recently [9]. Since $\tilde{\mathbf{K}}$ is given by substituting $(2.6.13)_3$ into $(3.3.8)_1$, the evaluation of $\tilde{\mathcal{K}}$ is rather involved and it can be shown that

$$\tilde{\mathcal{K}} = 2\left(\tilde{\mathbf{k}} \otimes \mathbf{I} - 2\tilde{\mathbf{k}} \,\underline{\otimes}\, \mathbf{I}\right) - \left(\tilde{\mathbf{k}} \,\overline{\underline{\otimes}}\, \tilde{\mathbf{k}}\right) : \mathcal{G}\,, \tag{3.3.16}$$

where

$$\begin{aligned}
\mathcal{G} = {}& 2\left(\mathbf{k}^{-1} \otimes \mathbf{I} - 2\mathbf{k}^{-1}\,\overline{\underline{\otimes}}\,\mathbf{I}\right) - \left(\mathbf{k}^{-1} \,\underline{\otimes}\, \mathbf{k}^{-1}\right) : \mathcal{K} \\
& + \frac{R\theta\tilde{c}}{d_0} J \frac{\partial}{\partial J}\left(\frac{\tilde{\kappa}}{\varphi^w}\right)\left(\mathbf{I} - \frac{\mathbf{d}}{d_0}\right) \otimes \mathbf{I} \\
& + \frac{R\theta\tilde{c}}{d_0} \frac{\tilde{\kappa}}{\varphi^w}\left(\mathbf{I} \otimes \mathbf{I} - 2\mathbf{I}\,\underline{\otimes}\,\mathbf{I} - \frac{1}{d_0}\mathcal{D}\right)
\end{aligned} \tag{3.3.17}$$

and

$$\mathcal{K} = J^{-1}\left(\mathbf{F}\,\underline{\otimes}\,\mathbf{F}\right) : 2\frac{\partial\mathbf{K}}{\partial\mathbf{C}} : \left(\mathbf{F}^T\,\underline{\otimes}\,\mathbf{F}^T\right)\,. \tag{3.3.18}$$

The next term in δW_{int} linearizes to

$$-D\left(\delta\tilde{p}\frac{\partial J}{\partial t}\right)[\Delta\mathbf{u}]\,dV = -\delta\tilde{p}\frac{1}{\Delta t}\operatorname{div}\Delta\mathbf{u}\,dv\,, \tag{3.3.19}$$

where we used a backward difference scheme to approximate the time derivative,

$$\frac{\partial J}{\partial t} \approx \frac{1}{\Delta t}\left(J - J^{-\Delta t}\right)\,, \tag{3.3.20}$$

and Δt represents the time increment relative to the previous time point. The next term is given by

$$D\left(\mathbf{J} \cdot \operatorname{Grad}\delta\tilde{c}\right)[\Delta\mathbf{u}]\,dV = \operatorname{grad}\delta\tilde{c}\cdot\mathbf{j}_u'\,dv, \tag{3.3.21}$$

where

$$\begin{aligned}
\mathbf{j}_u' \equiv {}& J^{-1}\mathbf{F}\cdot D\mathbf{J}\,[\Delta\mathbf{u}] = \left(J\frac{\partial\tilde{\kappa}}{\partial J}\left(\operatorname{div}\Delta\mathbf{u}\right)\mathbf{d} + \tilde{\kappa}\mathcal{D}:\Delta\boldsymbol{\varepsilon}\right)\cdot\left(-\varphi^w\operatorname{grad}\tilde{c} + \frac{\tilde{c}}{d_0}\mathbf{w}\right) \\
& + \tilde{\kappa}\mathbf{d}\cdot\left(-\varphi^s\left(\operatorname{div}\Delta\mathbf{u}\right)\operatorname{grad}\tilde{c} + \frac{\tilde{c}}{d_0}\left(2\Delta\boldsymbol{\varepsilon} - \left(\operatorname{div}\Delta\mathbf{u}\right)\mathbf{I}\right)\cdot\mathbf{w}\right) + \tilde{\kappa}\frac{\tilde{c}}{d_0}\mathbf{d}\cdot\mathbf{w}_u'
\end{aligned} \tag{3.3.22}$$

Using a backward difference scheme for the time derivative, the last term is

$$D\left(\delta\tilde{c}\frac{\partial\left(J\varphi^w\tilde{\kappa}\tilde{c}\right)}{\partial t}\right)[\Delta\mathbf{u}]\,dV = \frac{\delta\tilde{c}}{\Delta t}\frac{\partial\left(J\varphi^w\tilde{\kappa}\right)}{\partial J}\tilde{c}\operatorname{div}\Delta\mathbf{u}\,dv\,. \tag{3.3.23}$$

3.3.1.2   Linearization along $\Delta\tilde{p}$

The linearization of the various terms in δW_{int} along $\Delta\tilde{p}$ yields

$$D\left(\mathbf{S}:\delta\dot{\mathbf{E}}\right)[\Delta\tilde{p}]\,dV = -\Delta\tilde{p}\operatorname{div}\delta\mathbf{v}\,dv\,, \tag{3.3.24}$$

$$D\left(\mathbf{W}\cdot\operatorname{Grad}\delta\tilde{p} - \delta\tilde{p}\frac{\partial J}{\partial t}\right)[\Delta\tilde{p}]\,dV = -\operatorname{grad}\delta\tilde{p}\cdot\tilde{\mathbf{k}}\cdot\operatorname{grad}\Delta\tilde{p}\,dv\,, \tag{3.3.25}$$

$$D\left(\mathbf{J}\cdot\operatorname{Grad}\delta\tilde{c} - \delta\tilde{c}\frac{\partial\left(J\varphi^w\tilde{\kappa}\tilde{c}\right)}{\partial t}\right)[\Delta\tilde{p}]\,dV = -\frac{\tilde{\kappa}\tilde{c}}{d_0}\operatorname{grad}\delta\tilde{c}\cdot\mathbf{d}\cdot\tilde{\mathbf{k}}\cdot\operatorname{grad}\Delta\tilde{p}\,dv\,. \tag{3.3.26}$$

3.3.1.3 Linearization along $\Delta\tilde{c}$

The linearization of the first term in δW_{int} along $\Delta\tilde{c}$ yields

$$D\left(\mathbf{S}:\delta\dot{\mathbf{E}}\right)[\Delta\tilde{c}]\,dV = \Delta\tilde{c}\left(\boldsymbol{\sigma}_c':\delta\mathbf{d} - R\theta\frac{\partial\left(\Phi\tilde{\kappa}\tilde{c}\right)}{\partial\tilde{c}}\operatorname{div}\delta\mathbf{v}\right)dv\,, \tag{3.3.27}$$

where

$$\boldsymbol{\sigma}_c' = J^{-1}\mathbf{F}\cdot\frac{\partial\mathbf{S}^e}{\partial\tilde{c}}\cdot\mathbf{F}^T \tag{3.3.28}$$

represents the spatial tangent of the stress with respect to the effective concentration. The next term is

$$D\left(\mathbf{W}\cdot\operatorname{Grad}\delta\tilde{p}\right)[\Delta\tilde{c}]\,dV = \operatorname{grad}\delta\tilde{p}\cdot\mathbf{w}_c'\,dv\,, \tag{3.3.29}$$

where

$$\begin{aligned}
\mathbf{w}_c' &\equiv J^{-1}\mathbf{F}\cdot D\mathbf{W}[\Delta\tilde{c}] = -\Delta\tilde{c}\,\tilde{\mathbf{k}}_c'\cdot\left(\operatorname{grad}\tilde{p} + R\theta\frac{\tilde{\kappa}}{d_0}\mathbf{d}\cdot\operatorname{grad}\tilde{c}\right)\\
&- R\theta\tilde{\mathbf{k}}\cdot\left[\Delta\tilde{c}\left(\frac{\partial}{\partial\tilde{c}}\left(\frac{\tilde{\kappa}}{d_0}\right)\mathbf{d} + \frac{\tilde{\kappa}}{d_0}\mathbf{d}_c'\right)\cdot\operatorname{grad}\tilde{c} + \frac{\tilde{\kappa}}{d_0}\mathbf{d}\cdot\operatorname{grad}\Delta\tilde{c}\right]\,,
\end{aligned} \tag{3.3.30}$$

and

$$\tilde{\mathbf{k}}_c' = J^{-1}\mathbf{F}\cdot\frac{\partial\tilde{\mathbf{K}}}{\partial\tilde{c}}\cdot\mathbf{F}^T \tag{3.3.31}$$

is the spatial tangent of the effective hydraulic permeability with respect to the effective concentration.

The next term reduces to

$$-D\left(\delta\tilde{p}\frac{\partial J}{\partial t}\right)[\Delta\tilde{c}]\,dV = 0\,. \tag{3.3.32}$$

The following term is

$$D\left(\mathbf{J}\cdot\operatorname{Grad}\delta\tilde{c}\right)[\Delta\tilde{c}]\,dV = \operatorname{grad}\delta\tilde{c}\cdot\mathbf{j}_c'\,dv\,, \tag{3.3.33}$$

where

$$\begin{aligned}
\mathbf{j}_c' &\equiv J^{-1}\mathbf{F}\cdot D\mathbf{J}[\Delta\tilde{c}]\\
&= \Delta\tilde{c}\left(\frac{\partial\tilde{\kappa}}{\partial\tilde{c}}\mathbf{d} + \tilde{\kappa}\mathbf{d}_c'\right)\cdot\left(-\varphi^w\operatorname{grad}\tilde{c} + \frac{\tilde{c}}{d_0}\mathbf{w}\right)\\
&- \varphi^w\tilde{\kappa}\mathbf{d}\cdot\operatorname{grad}\Delta\tilde{c} + \tilde{\kappa}\frac{\tilde{c}}{d_0}\mathbf{d}\cdot\mathbf{w}_c'\,,
\end{aligned} \tag{3.3.34}$$

and

$$\mathbf{d}_c' = J^{-1}\mathbf{F}\cdot\frac{\partial\mathbf{D}}{\partial\tilde{c}}\cdot\mathbf{F}^T \tag{3.3.35}$$

is the spatial tangent of the diffusivity with respect to the effective concentration.

The last term is

$$D\left(\frac{\partial\left(J\varphi^w\tilde{\kappa}\tilde{c}\right)}{\partial t}\delta\tilde{c}\right)[\Delta\tilde{c}]\,dV = \delta\tilde{c}\frac{\varphi^w}{\Delta t}\frac{\partial\left(\tilde{\kappa}\tilde{c}\right)}{\partial\tilde{c}}\Delta\tilde{c}\,dv\,, \tag{3.3.36}$$

where we similarly used a backward difference scheme to discretize the time derivative.

3.3.2 Linearization of External Virtual Work

The linearization of δW_{ext} in (3.3.3) depends on whether natural boundary conditions are prescribed as area densities or total net values over an area. Thus, in the case when $\mathbf{t}\, da$ (net force), $w_n da$ (net volumetric flow rate), or $j_n da$ (net molar flow rate) are prescribed over the elemental area da, there is no variation in δW_{ext} and it follows that $D\delta W_{\text{ext}} = 0$. Alternatively, in the case when $\mathbf{t}$, w_n or j_n are prescribed, the linearization may be performed by evaluating the integral in the parametric space of the boundary surface ∂b, with parametric coordinates (η^1, η^2). Accordingly, for a point $\mathbf{x}\,(\eta^1, \eta^2)$ on ∂b, surface tangents (covariant basis vectors) are given by

$$\mathbf{g}_\alpha = \frac{\partial \mathbf{x}}{\partial \eta^\alpha}, \quad (\alpha = 1, 2) \tag{3.3.37}$$

and the outward unit normal is

$$\mathbf{n} = \frac{\mathbf{g}_1 \times \mathbf{g}_2}{|\mathbf{g}_1 \times \mathbf{g}_2|}. \tag{3.3.38}$$

The elemental area on ∂b is $da = |\mathbf{g}_1 \times \mathbf{g}_2|\, d\eta^1 d\eta^2$. Consequently, the external virtual work integral may be rewritten as

$$\delta W_{\text{ext}} = \int_{\partial b} (\delta \mathbf{v} \cdot \mathbf{t} + \delta\tilde{p}\, w_n + \delta\tilde{c}\, j_n)\, |\mathbf{g}_1 \times \mathbf{g}_2|\, d\eta^1 d\eta^2. \tag{3.3.39}$$

The directional derivative of δW_{ext} may then be applied directly to its integrand, since the parametric space is invariant [19].

If we restrict traction boundary conditions to the special case of normal tractions, then $\mathbf{t} = t_n \mathbf{n}$ where t_n is the prescribed normal traction component. Then it can be shown that the linearization of δW_{ext} along $\Delta \mathbf{u}$ produces

$$D\left(\delta W_{\text{ext}}\right)[\Delta \mathbf{u}] = \int_{\partial b} (t_n \delta \mathbf{v} + w_n \delta\tilde{p}\, \mathbf{n} + j_n \delta\tilde{c}\, \mathbf{n}) \cdot \left(\frac{\partial \Delta \mathbf{u}}{\partial \eta^1} \times \mathbf{g}_2 + \mathbf{g}_1 \times \frac{\partial \Delta \mathbf{u}}{\partial \eta^2}\right) d\eta^1 d\eta^2. \tag{3.3.40}$$

The linearizations along $\Delta\tilde{p}$ and $\Delta\tilde{c}$ reduce to zero, $D\left(\delta W_{\text{ext}}\right)[\Delta\tilde{p}] = 0$ and $D\left(\delta W_{\text{ext}}\right)[\Delta\tilde{c}] = 0$.

3.3.3 Discretization

To discretize the virtual work relations, let

$$\delta \mathbf{v} = \sum_{a=1}^{m} N_a \delta \mathbf{v}_a, \quad \Delta \mathbf{u} = \sum_{b=1}^{m} N_b \Delta \mathbf{u}_b,$$

$$\delta\tilde{p} = \sum_{a=1}^{m} N_a \delta\tilde{p}_a, \quad \Delta\tilde{p} = \sum_{b=1}^{m} N_b \Delta\tilde{p}_b, \tag{3.3.41}$$

$$\delta\tilde{c} = \sum_{a=1}^{m} N_a \delta\tilde{c}_a, \quad \Delta\tilde{c} = \sum_{b=1}^{m} N_b \Delta\tilde{c}_b,$$

where N_a represents the interpolation functions over an element, $\delta \mathbf{v}_a$, $\delta\tilde{p}_a$, $\delta\tilde{c}_a$, $\Delta \mathbf{u}_a$, $\Delta\tilde{p}_a$ and $\Delta\tilde{c}_a$ respectively represent the nodal values of $\delta \mathbf{v}$, $\delta\tilde{p}$, $\delta\tilde{c}$, $\Delta \mathbf{u}$, $\Delta\tilde{p}$ and $\Delta\tilde{c}$; m is the number of nodes in an element.

The discretized form of δW_{int} in (3.3.3) may be written as

$$\delta W_{\text{int}} = \sum_{e=1}^{n_e} \sum_{k=1}^{n_{\text{int}}^{(e)}} W_k J_\eta \sum_{a=1}^{m} \begin{bmatrix} \delta \mathbf{v}_a & \delta \tilde{p}_a & \delta \tilde{c}_a \end{bmatrix} \cdot \begin{bmatrix} \mathbf{r}_a^u \\ r_a^p \\ r_a^c \end{bmatrix}, \tag{3.3.42}$$

where n_e is the number of elements in b, $n_{\text{int}}^{(e)}$ is the number of integration points in the $e-$th element, W_k is the quadrature weight associated with the $k-$th integration point, and J_η is the Jacobian of the transformation from the current spatial configuration to the parametric space of the element. In the above expression,

$$\mathbf{r}_a^u = \boldsymbol{\sigma} \cdot \operatorname{grad} N_a,$$
$$r_a^p = \mathbf{w} \cdot \operatorname{grad} N_a - N_a \frac{1}{J} \frac{\partial J}{\partial t}, \tag{3.3.43}$$
$$r_a^c = \mathbf{j} \cdot \operatorname{grad} N_a - N_a \frac{1}{J} \frac{\partial}{\partial t} \left(J \varphi^w \tilde{\kappa} \tilde{c} \right),$$

and it is understood that J_η, $\mathbf{r}_a^u$, r_a^p and r_a^c are evaluated at the parametric coordinates of the $k-$th integration point. Since the parametric space is invariant, time derivatives are evaluated in a material frame. For example, the time derivative $D^s J(\mathbf{x}, t) / Dt$ appearing in (3.3.3) becomes $\partial J(\eta_k, t) / \partial t$ when evaluated at the parametric coordinates $\eta_k = \left(\eta_k^1, \eta_k^2, \eta_k^3 \right)$ of the $k-$th integration point.

Similarly, the discretized form of $D\delta W_{\text{int}} = D\delta W_{\text{int}}[\Delta \mathbf{u}] + D\delta W_{\text{int}}[\Delta \tilde{p}] + D\delta W_{\text{int}}[\Delta \tilde{c}]$ may be written as

$$D\delta W_{\text{int}} = \sum_{e=1}^{n_e} \sum_{k=1}^{n_{\text{int}}^{(e)}} W_k J_\eta \sum_{a=1}^{m} \sum_{b=1}^{m} \begin{bmatrix} \delta \mathbf{v}_a & \delta \tilde{p}_a & \delta \tilde{c}_a \end{bmatrix} \cdot \begin{bmatrix} \mathbf{K}_{ab}^{uu} & \mathbf{k}_{ab}^{up} & \mathbf{k}_{ab}^{uc} \\ \mathbf{k}_{ab}^{pu} & k_{ab}^{pp} & k_{ab}^{pc} \\ \mathbf{k}_{ab}^{cu} & k_{ab}^{cp} & k_{ab}^{cc} \end{bmatrix} \cdot \begin{bmatrix} \Delta \mathbf{u}_b \\ \Delta \tilde{p}_b \\ \Delta \tilde{c}_b \end{bmatrix}, \tag{3.3.44}$$

where the terms in the first column are the discretized form of the linearization along $\Delta \mathbf{u}$:

$$\mathbf{K}_{ab}^{uu} = \operatorname{grad} N_a \cdot \boldsymbol{\mathcal{C}} \cdot \operatorname{grad} N_b + (\operatorname{grad} N_a \cdot \boldsymbol{\sigma} \cdot \operatorname{grad} N_b) \, \mathbf{I}, \tag{3.3.45}$$

$$\mathbf{k}_{ab}^{pu} = (\mathbf{w}_b^u)^T \cdot \operatorname{grad} N_a + N_a \mathbf{q}_b^{pu}, \tag{3.3.46}$$

$$\mathbf{k}_{ab}^{cu} = (\mathbf{j}_b^u)^T \cdot \operatorname{grad} N_a + N_a \mathbf{q}_b^{cu}, \tag{3.3.47}$$

where

$$\mathbf{j}_b^u = J \frac{\partial \tilde{\kappa}}{\partial J} \left[\mathbf{d} \cdot \left(-\varphi^w \operatorname{grad} \tilde{c} + \frac{\tilde{c}}{d_0} \mathbf{w} \right) \right] \otimes \operatorname{grad} N_b + \tilde{\kappa} \left(-\varphi^w \operatorname{grad} \tilde{c} + \frac{\tilde{c}}{d_0} \mathbf{w} \right) \cdot \mathbf{d} \cdot \operatorname{grad} N_b$$
$$+ \tilde{\kappa} \left(-\varphi^s (\mathbf{d} \cdot \operatorname{grad} \tilde{c}) \otimes \operatorname{grad} N_b + \frac{\tilde{c}}{d_0} \left[2 (\operatorname{grad} N_b \cdot \mathbf{w}) \mathbf{d} - (\mathbf{d} \cdot \mathbf{w}) \otimes \operatorname{grad} N_b \right] \right) + \tilde{\kappa} \frac{\tilde{c}}{d_0} \mathbf{d} \cdot \mathbf{w}_b^u, \tag{3.3.48}$$

$$\mathbf{q}_b^{pu} = -\frac{1}{\Delta t} \operatorname{grad} N_b, \tag{3.3.49}$$

$$\mathbf{q}_b^{cu} = \tilde{c} \frac{\partial (J \phi^w \tilde{\kappa})}{\partial J} \mathbf{q}_b^{pu}. \tag{3.3.50}$$

The terms in the second column of the stiffness matrix in (3.3.44) are the discretized form of the linearization along $\Delta \tilde{p}$:

$$\mathbf{k}_{ab}^{up} = -N_b \operatorname{grad} N_a, \tag{3.3.51}$$

$$k_{ab}^{pp} = -\operatorname{grad} N_a \cdot \tilde{\mathbf{k}} \cdot \operatorname{grad} N_b, \tag{3.3.52}$$

$$k_{ab}^{cp} = -\frac{\tilde{\kappa}\tilde{c}}{d_0} \operatorname{grad} N_a \cdot \mathbf{d} \cdot \tilde{\mathbf{k}} \cdot \operatorname{grad} N_b. \tag{3.3.53}$$

The terms in the third column of the stiffness matrix in (3.3.44) are the discretized form of the linearization along $\Delta \tilde{c}$:

$$\mathbf{k}_{ab}^{uc} = N_b \left(\boldsymbol{\sigma}_c' \cdot \operatorname{grad} N_a - R\theta \frac{\partial \left(\Phi \tilde{\kappa} \tilde{c} \right)}{\partial \tilde{c}} \operatorname{grad} N_a \right), \tag{3.3.54}$$

$$k_{ab}^{pc} = \operatorname{grad} N_a \cdot \mathbf{w}_b^c, \tag{3.3.55}$$

$$k_{ab}^{cc} = \operatorname{grad} N_a \cdot \mathbf{j}_b^c + N_a q_b^c, \tag{3.3.56}$$

where

$$\begin{aligned}
\mathbf{w}_b^c = -N_b \tilde{\mathbf{k}}_c' \cdot &\left(\operatorname{grad} \tilde{p} + R\theta \frac{\tilde{\kappa}}{d_0} \mathbf{d} \cdot \operatorname{grad} \tilde{c} \right) \\
&- R\theta \tilde{\mathbf{k}} \cdot \left[N_b \left(\frac{\partial}{\partial \tilde{c}} \left(\frac{\tilde{\kappa}}{d_0} \right) \mathbf{d} + \frac{\tilde{\kappa}}{d_0} \mathbf{d}_c' \right) \cdot \operatorname{grad} \tilde{c} + \frac{\tilde{\kappa}}{d_0} \mathbf{d} \cdot \operatorname{grad} N_b \right],
\end{aligned} \tag{3.3.57}$$

$$\mathbf{j}_b^c = N_b \left(\frac{\partial \tilde{\kappa}}{\partial \tilde{c}} \mathbf{d} + \tilde{\kappa} \mathbf{d}_c' \right) \cdot \left(-\varphi^w \operatorname{grad} \tilde{c} + \frac{\tilde{c}}{d_0} \mathbf{w} \right) + \tilde{\kappa} \mathbf{d} \cdot \left(-\varphi^w \operatorname{grad} N_b + \frac{\tilde{c}}{d_0} \mathbf{w}_b^c \right), \tag{3.3.58}$$

$$q_b^c = -N_b \frac{\phi^w}{\Delta t} \frac{\partial \left(\tilde{\kappa} \tilde{c} \right)}{\partial \tilde{c}}. \tag{3.3.59}$$

The discretization of δW_{ext} in (3.3.3) has the form

$$\delta W_{\text{ext}} = \sum_{e=1}^{n_e} \sum_{k=1}^{n_{\text{int}}^{(e)}} W_k J_\eta \sum_{a=1}^{m} \begin{bmatrix} \delta \mathbf{v}_a & \delta \tilde{p}_a & \delta \tilde{c}_a \end{bmatrix} \cdot \begin{bmatrix} N_a t_n \mathbf{n} \\ N_a w_n \\ N_a j_n \end{bmatrix}, \tag{3.3.60}$$

where $J_\eta = |\mathbf{g}_1 \times \mathbf{g}_2|$. The summation is performed over all surface elements on which these boundary conditions are prescribed. The discretization of $-D\delta W_{\text{ext}}$ has the form

$$-D\delta W_{\text{ext}} = \sum_{e=1}^{n_e} \sum_{k=1}^{n_{\text{int}}^{(e)}} W_k J_\eta \sum_{a=1}^{m} \sum_{b=1}^{m} \begin{bmatrix} \delta \mathbf{v}_a & \delta \tilde{p}_a & \delta \tilde{c}_a \end{bmatrix} \cdot \begin{bmatrix} \mathbf{K}_{ab}^{uu} & \mathbf{0} & \mathbf{0} \\ \mathbf{k}_{ab}^{pu} & 0 & 0 \\ \mathbf{k}_{ab}^{cu} & 0 & 0 \end{bmatrix} \cdot \begin{bmatrix} \Delta \mathbf{u}_b \\ \Delta \tilde{p}_b \\ \Delta \tilde{c}_b \end{bmatrix}, \tag{3.3.61}$$

where

$$\begin{aligned}
\mathbf{K}_{ab}^{uu} &= t_n N_a \boldsymbol{\mathcal{A}} \left\{ \frac{\partial N_b}{\partial \eta^1} \mathbf{g}_2 - \frac{\partial N_b}{\partial \eta^2} \mathbf{g}_1 \right\}, \\
\mathbf{k}_{ab}^{pu} &= -w_n N_a \left(\frac{\partial N_b}{\partial \eta^1} \mathbf{g}_2 - \frac{\partial N_b}{\partial \eta^2} \mathbf{g}_1 \right) \times \mathbf{n}, \\
\mathbf{k}_{ab}^{cu} &= -j_n N_a \left(\frac{\partial N_b}{\partial \eta^1} \mathbf{g}_2 - \frac{\partial N_b}{\partial \eta^2} \mathbf{g}_1 \right) \times \mathbf{n}.
\end{aligned} \tag{3.3.62}$$

In this expression, $\boldsymbol{\mathcal{A}} \{\mathbf{v}\}$ is the antisymmetric tensor whose dual vector is $\mathbf{v}$ (such that $\boldsymbol{\mathcal{A}} \{\mathbf{v}\} \cdot \mathbf{q} = \mathbf{v} \times \mathbf{q}$ for any vector $\mathbf{q}$).

3.4 Weak Formulation for Multiphasic Materials

The virtual work integral for a mixture of intrinsically incompressible constituents combines the balance of momentum for the mixture, the balance of mass for the mixture, and the balance of mass for each of the solutes. In addition, for charged mixtures, the condition of (2.7.8) may be enforced as a penalty constraint on each solute mass balance equation:

$$
\begin{aligned}
\delta W = & \int_b \delta \mathbf{v} \cdot \mathsf{div}\boldsymbol{\sigma}\, dv \\
& + \int_b \delta\tilde{p}\,\mathsf{div}\,(\mathbf{v}^s + \mathbf{w})\; dv \\
& + \sum_{\alpha \neq s,w} \int_b \delta\tilde{c}^\alpha \left[\frac{1}{J^s}\frac{D^s}{Dt}\left(J^s\varphi^w\tilde{\kappa}^\alpha\tilde{c}^\alpha\right) + \mathsf{div}\mathbf{j}^\alpha + \sum_{\beta\neq s,w} z^\beta\mathsf{div}\mathbf{j}^\beta \right]\, dv\,,
\end{aligned}
\tag{3.4.1}
$$

where $\delta\mathbf{v}$ is the virtual velocity of the solid, $\delta\tilde{p}$ is the virtual effective fluid pressure, and $\delta\tilde{c}^\alpha$ is the virtual molar energy of solute α. Here, b represents the mixture domain in the spatial frame and dv is an elemental volume in b. Applying the divergence theorem, δW may be split into internal and external contributions to the virtual work, $\delta W = \delta W_{\text{ext}} - \delta W_{\text{int}}$, where

$$
\begin{aligned}
\delta W_{\text{int}} = & \int_b \boldsymbol{\sigma} : \delta\mathbf{D}\, dv + \int_b \left(\mathbf{w}\cdot\mathsf{grad}\delta\tilde{p} - \frac{\delta\tilde{p}}{J^s}\frac{D^s J^s}{Dt} \right) dv \\
& + \sum_{\alpha\neq s,w} \int_b \left[\mathbf{j}^\alpha\cdot\mathsf{grad}\delta\tilde{c}^\alpha - \frac{\delta\tilde{c}^\alpha}{J^s}\frac{D^s}{Dt}\left(J^s\varphi^w\tilde{\kappa}^\alpha\tilde{c}^\alpha\right) \right] dv \\
& + \sum_{\alpha\neq s,w} \int_b \mathsf{grad}\delta\tilde{c}^\alpha \cdot \sum_{\beta\neq s,w} z^\beta\mathbf{j}^\beta\, dv\,,
\end{aligned}
\tag{3.4.2}
$$

and

$$
\delta W_{\text{ext}} = \int_{\partial b} \left[\delta\mathbf{v}\cdot\mathbf{t} + \delta\tilde{p}\,w_n + \sum_{\alpha\neq s,w} \delta\tilde{c}^\alpha\left(j_n^\alpha + \sum_{\beta\neq s,w} z^\beta j_n^\beta \right) \right] da\,.
\tag{3.4.3}
$$

In these expressions, $\delta\mathbf{D} = \left(\mathsf{grad}\delta\mathbf{v} + \mathsf{grad}^T\delta\mathbf{v}\right)/2$, ∂b is the boundary of b, and da is an elemental area on ∂b. In this finite element formulation, $\mathbf{u}$, $\tilde{p}$ and $\tilde{c}^\alpha$ are used as nodal variables, and essential boundary conditions may be prescribed on these variables. Natural boundary conditions are prescribed to the mixture traction, $\mathbf{t} = \boldsymbol{\sigma}\cdot\mathbf{n}$, normal fluid flux, $w_n = \mathbf{w}\cdot\mathbf{n}$, and normal solute flux, $j_n^\alpha = \mathbf{j}^\alpha\cdot\mathbf{n}$, where $\mathbf{n}$ is the outward unit normal to ∂b. To solve the system $\delta W = 0$ for nodal values of $\mathbf{u}$, $\tilde{p}$ and $\tilde{c}^\alpha$, it is necessary to linearize these equations, as shown for example in Sections 3.3.1-3.3.2 for biphasic-solute materials. If the mixture is charged, it is also necessary to solve for the electric potential ψ by solving the algebraic relation of the electroneutrality condition in (2.7.4), which may be rewritten as

$$
c^F + \sum_{\beta\neq s,w} z^\beta\tilde{\kappa}^\beta\tilde{c}^\beta = 0\,.
\tag{3.4.4}
$$

In the special case of a triphasic mixture, where solutes consist of two counter-ions ($\alpha = +,-$), this equation may be solved in closed form to produce

$$
\psi = \frac{1}{z^\alpha}\frac{R\theta}{F_c}\ln\left(\frac{2z^\alpha\hat{\kappa}^\alpha\tilde{c}^\alpha}{-c^F \pm \sqrt{\left(c^F\right)^2 + 4\left(z^\alpha\right)^2\left(\hat{\kappa}^+\tilde{c}^+\right)\left(\hat{\kappa}^-\tilde{c}^-\right)}} \right),\quad \alpha = +,-,
\tag{3.4.5}
$$

Only the positive root is valid in the argument of the logarithm function.

3.4.1 Linearization along $\Delta \mathbf{u}$

The linearization of the first term in δW_{int} along $\Delta \mathbf{u}$ yields

$$\left(\mathbf{S} : \delta \dot{\mathbf{E}} \right) [\Delta \mathbf{u}] \, dV = \left[\delta \mathbf{d}^s : \boldsymbol{\mathcal{C}} : \Delta \boldsymbol{\varepsilon} + \boldsymbol{\sigma} : \left(\text{grad}^T \Delta \mathbf{u} \cdot \text{grad} \, \delta \mathbf{v} \right) \right] dv \,, \tag{3.4.6}$$

where $\boldsymbol{\mathcal{C}}$ is the spatial elasticity tensor of the mixture,

$$\boldsymbol{\mathcal{C}} = \boldsymbol{\mathcal{C}}^e - \left(\tilde{p} + R\theta \, \Phi \sum_\beta \tilde{\kappa}^\beta \tilde{c}^\beta \right) (\mathbf{I} \otimes \mathbf{I} - 2\mathbf{I} \,\overline{\underline{\otimes}}\, \mathbf{I}) - R\theta \sum_\beta \tilde{c}^\beta \, J \frac{\partial \left(\Phi \tilde{\kappa}^\beta \right)}{\partial J} \mathbf{I} \otimes \mathbf{I} \,, \tag{3.4.7}$$

and $\boldsymbol{\mathcal{C}}^e$ is the spatial elasticity tensor of the solid matrix,

$$\boldsymbol{\mathcal{C}}^e = J^{-1} \left(\mathbf{F} \,\underline{\otimes}\, \mathbf{F} \right) : 2 \frac{\partial \mathbf{S}^e}{\partial \mathbf{C}} : \left(\mathbf{F}^T \,\underline{\otimes}\, \mathbf{F}^T \right) \,. \tag{3.4.8}$$

The linearization of the second term is

$$D \left(\mathbf{W} \cdot \text{Grad} \, \delta \tilde{p} \right) [\Delta \mathbf{u}] \, dV = \text{grad} \, \delta \tilde{p} \cdot \mathbf{w}'_u \, dv \,, \tag{3.4.9}$$

where

$$\mathbf{w}'_u \equiv J - \left(\tilde{\boldsymbol{\mathcal{K}}} : \Delta \boldsymbol{\varepsilon} \right) \cdot \left(\text{grad} \, \tilde{p} + R\theta \sum_\beta \frac{\tilde{\kappa}^\beta}{d_0^\beta} \mathbf{d}^\beta \cdot \text{grad} \, \tilde{c}^\beta \right)$$

$$- \tilde{\mathbf{k}} \cdot R\theta \sum_\beta \left(\left[J \frac{\partial}{\partial J} \left(\frac{\tilde{\kappa}^\beta}{d_0^\beta} \right) - \frac{\tilde{\kappa}^\beta}{d_0^\beta} \right] (\text{div} \, \Delta \mathbf{u}) \, \mathbf{d}^\beta + \frac{\tilde{\kappa}^\beta}{d_0^\beta} \left(2\Delta \boldsymbol{\varepsilon} \cdot \mathbf{d}^\beta + \boldsymbol{\mathcal{D}}^\beta : \Delta \boldsymbol{\varepsilon} \right) \right) \cdot \text{grad} \, \tilde{c}^\beta$$

$$\tag{3.4.10}$$

with

$$\tilde{\boldsymbol{\mathcal{K}}} = J^{-1} \left(\mathbf{F} \,\underline{\otimes}\, \mathbf{F} \right) : 2 \frac{\partial \tilde{\mathbf{K}}}{\partial \mathbf{C}} : \left(\mathbf{F}^T \,\underline{\otimes}\, \mathbf{F}^T \right) \,,$$

$$\boldsymbol{\mathcal{D}}^\alpha = J^{-1} \left(\mathbf{F} \,\underline{\otimes}\, \mathbf{F} \right) : 2 \frac{\partial \mathbf{D}^\alpha}{\partial \mathbf{C}} : \left(\mathbf{F}^T \,\underline{\otimes}\, \mathbf{F}^T \right) \,, \tag{3.4.11}$$

representing the spatial tangents, with respect to the strain, of the effective permeability and solute diffusivity, respectively. These fourth-order tensors exhibit minor symmetries but not major symmetry, as described recently [9]. Since $\tilde{\mathbf{K}}$ is given by substituting $(2.6.13)_3$ into $(3.3.8)_1$, the evaluation of $\tilde{\boldsymbol{\mathcal{K}}}$ is rather involved and it can be shown that

$$\tilde{\boldsymbol{\mathcal{K}}} = 2 \left(\tilde{\mathbf{k}} \otimes \mathbf{I} - 2\tilde{\mathbf{k}} \,\overline{\underline{\otimes}}\, \mathbf{I} \right) - \left(\tilde{\mathbf{k}} \,\underline{\otimes}\, \tilde{\mathbf{k}} \right) : \boldsymbol{\mathcal{G}} \,, \tag{3.4.12}$$

where

$$\boldsymbol{\mathcal{G}} = 2 \left(\mathbf{k}^{-1} \otimes \mathbf{I} - 2\mathbf{k}^{-1} \,\overline{\underline{\otimes}}\, \mathbf{I} \right) - \left(\mathbf{k}^{-1} \otimes \mathbf{k}^{-1} \right) : \mathbf{k}$$

$$+ R\theta \sum_\beta \frac{\tilde{c}^\beta}{d_0^\beta} J \frac{\partial}{\partial J} \left(\frac{\tilde{\kappa}^\beta}{\varphi^w} \right) \left(\mathbf{I} - \frac{\mathbf{d}^\beta}{d_0^\beta} \right) \otimes \mathbf{I}$$

$$+ R\theta \sum_\beta \frac{\tilde{c}^\beta}{d_0} \frac{\tilde{\kappa}^\beta}{\varphi^w} \left(\mathbf{I} \otimes \mathbf{I} - 2\mathbf{I} \,\underline{\otimes}\, \mathbf{I} - \frac{1}{d_0^\beta} \boldsymbol{\mathcal{D}}^\beta \right) \tag{3.4.13}$$

and

$$\mathcal{K} = J^{-1} \left(\mathbf{F} \,\underline{\otimes}\, \mathbf{F} \right) : 2 \frac{\partial \mathbf{K}}{\partial \mathbf{C}} : \left(\mathbf{F}^T \,\underline{\otimes}\, \mathbf{F}^T \right) . \tag{3.4.14}$$

The next term in δW_{int} linearizes to

$$- D \left(\delta \tilde{p} \frac{\partial J}{\partial t} \right) [\Delta \mathbf{u}] \, dV = -\delta \tilde{p} \frac{1}{\Delta t} \operatorname{div} \Delta \mathbf{u} \, dv , \tag{3.4.15}$$

where we used a backward difference scheme to approximate the time derivative,

$$\frac{\partial J}{\partial t} \approx \frac{1}{\Delta t} \left(J - J^{-\Delta t} \right) , \tag{3.4.16}$$

and Δt represents the time increment relative to the previous time point. The next term is given by

$$D \left(\mathbf{J}^\alpha \cdot \operatorname{Grad} \delta \tilde{c}^\alpha \right) [\Delta \mathbf{u}] \, dV = \operatorname{grad} \delta \tilde{c}^\alpha \cdot \mathbf{j}_u^{\alpha\prime} \, dv , \tag{3.4.17}$$

where

$$\begin{aligned}
\mathbf{j}_u^{\alpha\prime} &\equiv J^{-1} \mathbf{F} \cdot D\mathbf{J} \left[\Delta \mathbf{u}\right] = \left(J \frac{\partial \tilde{\kappa}^\alpha}{\partial J} \left(\operatorname{div} \Delta \mathbf{u} \right) \mathbf{d}^\alpha + \tilde{\kappa}^\alpha \boldsymbol{\mathcal{D}}^\alpha : \Delta \boldsymbol{\varepsilon} \right) \cdot \mathbf{g}^\alpha \\
&\quad + \tilde{\kappa}^\alpha \mathbf{d}^\alpha \cdot \left(-\varphi^s \left(\operatorname{div} \Delta \mathbf{u} \right) \operatorname{grad} \tilde{c}^\alpha + \left(2\Delta \boldsymbol{\varepsilon} - \left(\operatorname{div} \Delta \mathbf{u} \right) \mathbf{I} \right) \cdot \frac{\tilde{c}^\alpha}{d_0^\alpha} \mathbf{w} + \frac{\tilde{c}^\alpha}{d_0^\alpha} \mathbf{w}_u' \right)
\end{aligned} \tag{3.4.18}$$

where

$$\mathbf{g}^\alpha = -\varphi^w \operatorname{grad} \tilde{c}^\alpha + \frac{\tilde{c}^\alpha}{d_0^\alpha} \mathbf{w} . \tag{3.4.19}$$

Using a backward difference scheme for the time derivative, the last term is

$$D \left(\delta \tilde{c}^\alpha \frac{\partial \left(J\varphi^w \tilde{\kappa}^\alpha \tilde{c}^\alpha \right)}{\partial t} \right) [\Delta \mathbf{u}] \, dV = \frac{\delta \tilde{c}^\alpha}{\Delta t} \frac{\partial \left(J\varphi^w \tilde{\kappa}^\alpha \right)}{\partial J} \tilde{c}^\alpha \operatorname{div} \Delta \mathbf{u} \, dv . \tag{3.4.20}$$

3.4.2 Linearization along $\Delta \tilde{p}$

The linearization of the various terms in δW_{int} along $\Delta \tilde{p}$ yields

$$D \left(\mathbf{S} : \delta \dot{\mathbf{E}} \right) [\Delta \tilde{p}] \, dV = -\Delta \tilde{p} \operatorname{div} \delta \mathbf{v} \, dv , \tag{3.4.21}$$

$$D \left(\mathbf{W} \cdot \operatorname{Grad} \delta \tilde{p} - \delta \tilde{p} \frac{\partial J}{\partial t} \right) [\Delta \tilde{p}] \, dV = - \operatorname{grad} \delta \tilde{p} \cdot \tilde{\mathbf{k}} \cdot \operatorname{grad} \Delta \tilde{p} \, dv , \tag{3.4.22}$$

$$D \left(\mathbf{J}^\alpha \cdot \operatorname{Grad} \delta \tilde{c}^\alpha - \delta \tilde{c}^\alpha \frac{\partial \left(J\varphi^w \tilde{\kappa}^\alpha \tilde{c}^\alpha \right)}{\partial t} \right) [\Delta \tilde{p}] \, dV = -\frac{\tilde{\kappa}^\alpha \tilde{c}^\alpha}{d_0^\alpha} \operatorname{grad} \delta \tilde{c}^\alpha \cdot \mathbf{d}^\alpha \cdot \tilde{\mathbf{k}} \cdot \operatorname{grad} \Delta \tilde{p} \, dv . \tag{3.4.23}$$

3.4.3 Linearization along $\Delta \tilde{c}^\gamma$

The linearization of the first term in δW_{int} along $\Delta \tilde{c}^\gamma$ yields

$$D \left(\mathbf{S} : \delta \dot{\mathbf{E}} \right) [\Delta \tilde{c}^\gamma] \, dV = \Delta \tilde{c}^\gamma \left(\boldsymbol{\sigma}_\gamma' : \delta \mathbf{d} - R\theta \frac{\partial \left(\Phi \tilde{\kappa}^\alpha \tilde{c}^\alpha \right)}{\partial \tilde{c}^\gamma} \operatorname{div} \delta \mathbf{v} \right) dv , \tag{3.4.24}$$

where

$$\boldsymbol{\sigma}_\gamma' = J^{-1} \mathbf{F} \cdot \frac{\partial \mathbf{S}^e}{\partial \tilde{c}^\gamma} \cdot \mathbf{F}^T \tag{3.4.25}$$

represents the spatial tangent of the stress with respect to the effective concentration. The next term is

$$D\left(\mathbf{W}\cdot\operatorname{Grad}\delta\tilde{p}\right)\left[\Delta\tilde{c}^\gamma\right]dV = \operatorname{grad}\delta\tilde{p}\cdot\mathbf{w}'_\gamma\,dv\,,\tag{3.4.26}$$

where

$$\begin{aligned}
\mathbf{w}'_\gamma &\equiv J^{-1}\mathbf{F}\cdot D\mathbf{W}\left[\Delta\tilde{c}^\gamma\right] = -\tilde{\mathbf{k}}'_\gamma\cdot\left(\operatorname{grad}\tilde{p} + R\theta\sum_\beta\frac{\tilde{\kappa}^\beta}{d_0^\beta}\mathbf{d}^\beta\cdot\operatorname{grad}\tilde{c}^\beta\right)\Delta\tilde{c}^\gamma \\
&- R\theta\tilde{\mathbf{k}}\cdot\frac{\tilde{\kappa}^\gamma}{d_0^\gamma}\mathbf{d}^\gamma\cdot\operatorname{grad}\Delta\tilde{c}^\gamma - \Delta\tilde{c}^\gamma R\theta\tilde{\mathbf{k}}\cdot\sum_\beta\left(\frac{\partial}{\partial\tilde{c}^\gamma}\left(\frac{\tilde{\kappa}^\beta}{d_0^\beta}\right)\mathbf{d}^\beta + \frac{\tilde{\kappa}^\beta}{d_0^\beta}\mathbf{d}_\gamma^{\beta\prime}\right)\cdot\operatorname{grad}\tilde{c}^\beta
\end{aligned}\tag{3.4.27}$$

and

$$\tilde{\mathbf{k}}'_\gamma = J^{-1}\mathbf{F}\cdot\frac{\partial\tilde{\mathbf{K}}}{\partial\tilde{c}^\gamma}\cdot\mathbf{F}^T,\quad \mathbf{d}_\gamma^{\beta\prime} = J^{-1}\mathbf{F}\cdot\frac{\partial\mathbf{d}^\beta}{\partial\tilde{c}^\gamma}\cdot\mathbf{F}^T\tag{3.4.28}$$

are the spatial tangents of the effective hydraulic permeability and solute diffusivity with respect to the effective concentration.

The next term reduces to

$$-D\left(\delta\tilde{p}\frac{\partial J}{\partial t}\right)\left[\Delta\tilde{c}^\gamma\right]dV = 0\,.\tag{3.4.29}$$

The following term is

$$D\left(\mathbf{J}^\alpha\cdot\operatorname{Grad}\delta\tilde{c}^\alpha\right)\left[\Delta\tilde{c}^\gamma\right]dV = \operatorname{grad}\delta\tilde{c}^\alpha\cdot\mathbf{j}_\gamma^{\alpha\prime}\,dv\,,\tag{3.4.30}$$

where

$$\begin{aligned}
\mathbf{j}_\gamma^{\alpha\prime} &\equiv J^{-1}\mathbf{F}\cdot D\mathbf{J}^\alpha\left[\Delta\tilde{c}^\gamma\right] = \Delta\tilde{c}^\gamma\left(\frac{\partial\tilde{\kappa}^\alpha}{\partial\tilde{c}^\gamma}\mathbf{d}^\alpha + \tilde{\kappa}^\alpha\mathbf{d}_\gamma^{\alpha\prime}\right)\cdot\mathbf{g}^\alpha \\
&+ \tilde{\kappa}^\alpha\mathbf{d}^\alpha\cdot\left(-\varphi^w\delta_{\alpha\gamma}\operatorname{grad}\Delta\tilde{c}^\gamma + \frac{\Delta\tilde{c}^\gamma}{d_0^\alpha}\left(\delta_{\alpha\gamma} - \frac{\tilde{c}^\alpha}{d_0^\alpha}\frac{\partial d_0^\alpha}{\partial\tilde{c}^\gamma}\right)\mathbf{w} + \frac{\tilde{c}^\alpha}{d_0^\alpha}\mathbf{w}'_\gamma\right)\,.
\end{aligned}\tag{3.4.31}$$

The last term is

$$D\left(\frac{\partial\left(J\varphi^w\tilde{\kappa}^\alpha\tilde{c}^\alpha\right)}{\partial t}\delta\tilde{c}^\alpha\right)\left[\Delta\tilde{c}^\gamma\right]dV = \delta\tilde{c}^\alpha\frac{\varphi^w}{\Delta t}\frac{\partial\left(\tilde{\kappa}^\alpha\tilde{c}^\alpha\right)}{\partial\tilde{c}^\gamma}\Delta\tilde{c}^\gamma\,dv\,,\tag{3.4.32}$$

where we similarly used a backward difference scheme to discretize the time derivative.

3.4.4   Linearization of External Virtual Work

The linearization of δW_{ext} in (3.4.3) depends on whether natural boundary conditions are prescribed as area densities or total net values over an area. Thus, in the case when $\mathbf{t}\,da$ (net force), $w_n da$ (net volumetric flow rate), or $\tilde{j}_n^\alpha da$ (net effective molar flow rate) are prescribed over the elemental area da, there is no variation in δW_{ext} and it follows that $D\delta W_{\text{ext}} = 0$. Alternatively, in the case when $\mathbf{t}$, w_n or $\tilde{j}_n^\alpha$ are prescribed, the linearization may be performed by evaluating the integral in the parametric space of the boundary surface ∂b, with parametric coordinates (η^1, η^2). Accordingly, for a point $\mathbf{x}\left(\eta^1, \eta^2\right)$ on ∂b, surface tangents (covariant basis vectors) are given by

$$\mathbf{g}_\alpha = \frac{\partial\mathbf{x}}{\partial\eta^\alpha},\quad(\alpha = 1, 2)\tag{3.4.33}$$

and the outward unit normal is

$$\mathbf{n} = \frac{\mathbf{g}_1 \times \mathbf{g}_2}{|\mathbf{g}_1 \times \mathbf{g}_2|} \,. \tag{3.4.34}$$

The elemental area on ∂b is $da = |\mathbf{g}_1 \times \mathbf{g}_2| \, d\eta^1 d\eta^2$. Consequently, the external virtual work integral may be rewritten as

$$\delta W_{\text{ext}} = \int_{\partial b} \left(\delta \mathbf{v} \cdot \mathbf{t} + \delta \tilde{p} \, w_n + \sum_{\alpha \neq s,w} \delta \tilde{c}^\alpha \tilde{j}_n^\alpha \right) |\mathbf{g}_1 \times \mathbf{g}_2| \, d\eta^1 d\eta^2 \,, \tag{3.4.35}$$

where

$$\tilde{j}_n^\alpha = j_n^\alpha + \sum_{\beta \neq s,w} z^\beta j_n^\beta \,. \tag{3.4.36}$$

The directional derivative of δW_{ext} may then be applied directly to its integrand, since the parametric space is invariant [19].

If we restrict traction boundary conditions to the special case of normal tractions, then $\mathbf{t} = t_n \mathbf{n}$ where t_n is the prescribed normal traction component. Then it can be shown that the linearization of δW_{ext} along $\Delta \mathbf{u}$ produces

$$D \left(\delta W_{\text{ext}} \right) [\Delta \mathbf{u}] = \int_{\partial b} \left(t_n \delta \mathbf{v} + w_n \delta \tilde{p} \, \mathbf{n} + \sum_{\alpha \neq s,w} \delta \tilde{c}^\alpha \tilde{j}_n^\alpha \, \mathbf{n} \right) \cdot \left(\frac{\partial \Delta \mathbf{u}}{\partial \eta^1} \times \mathbf{g}_2 + \mathbf{g}_1 \times \frac{\partial \Delta \mathbf{u}}{\partial \eta^2} \right) d\eta^1 d\eta^2 \,. \tag{3.4.37}$$

The linearizations along $\Delta \tilde{p}$ and $\Delta \tilde{c}^\gamma$ reduce to zero, $D \left(\delta W_{\text{ext}} \right) [\Delta \tilde{p}] = 0$ and $D \left(\delta W_{\text{ext}} \right) [\Delta \tilde{c}^\gamma] = 0$.

3.4.5 Discretization

To discretize the virtual work relations, let

$$\delta \mathbf{v} = \sum_{a=1}^{m} N_a \delta \mathbf{v}_a \,, \quad \Delta \mathbf{u} = \sum_{b=1}^{m} N_b \Delta \mathbf{u}_b \,,$$

$$\delta \tilde{p} = \sum_{a=1}^{m} N_a \delta \tilde{p}_a \,, \quad \Delta \tilde{p} = \sum_{b=1}^{m} N_b \Delta \tilde{p}_b \,, \tag{3.4.38}$$

$$\delta \tilde{c}^\alpha = \sum_{a=1}^{m} N_a \delta \tilde{c}_a^\alpha \,, \quad \Delta \tilde{c}^\gamma = \sum_{b=1}^{m} N_b \Delta \tilde{c}_b^\gamma \,,$$

where N_a represents the interpolation functions over an element, $\delta \mathbf{v}_a$, $\delta \tilde{p}_a$, $\delta \tilde{c}_a^\alpha$, $\Delta \mathbf{u}_a$, $\Delta \tilde{p}_a$ and $\Delta \tilde{c}_a^\gamma$ respectively represent the nodal values of $\delta \mathbf{v}$, $\delta \tilde{p}$, $\delta \tilde{c}^\alpha$, $\Delta \mathbf{u}$, $\Delta \tilde{p}$ and $\Delta \tilde{c}^\gamma$; m is the number of nodes in an element.

The discretized form of δW_{int} in (3.3.3) may be written as

$$\delta W_{\text{int}} = \sum_{e=1}^{n_e} \sum_{k=1}^{n_{\text{int}}^{(e)}} W_k J_\eta \sum_{a=1}^{m} \begin{bmatrix} \delta \mathbf{v}_a & \delta \tilde{p}_a & \delta \tilde{c}_a^\alpha & \delta \tilde{c}_a^\beta \end{bmatrix} \cdot \begin{bmatrix} \mathbf{r}_a^u \\ r_a^p \\ r_a^\alpha \\ r_a^\beta \end{bmatrix} \,, \tag{3.4.39}$$

where n_e is the number of elements in b, $n_{\text{int}}^{(e)}$ is the number of integration points in the $e-$th element, W_k is the quadrature weight associated with the $k-$th integration point, and J_η is the

Jacobian of the transformation from the current spatial configuration to the parametric space of the element. In the above expression,

$$\mathbf{r}_a^u = \boldsymbol{\sigma} \cdot \operatorname{grad} N_a \,,$$

$$r_a^p = \mathbf{w} \cdot \operatorname{grad} N_a - N_a \frac{1}{J} \frac{\partial J}{\partial t} \,, \tag{3.4.40}$$

$$r_a^\alpha = \mathbf{j}^\alpha \cdot \operatorname{grad} N_a - N_a \frac{1}{J} \frac{\partial}{\partial t} \left(J \varphi^w \tilde{\kappa}^\alpha \tilde{c}^\alpha \right) \,,$$

and it is understood that J_η, $\mathbf{r}_a^u$, r_a^p and r_a^α are evaluated at the parametric coordinates of the $k-$th integration point. Since the parametric space is invariant, time derivatives are evaluated in a material frame. For example, the time derivative $D^s J\left(\mathbf{x}, t\right)/Dt$ appearing in (3.3.3) becomes $\partial J\left(\eta_k, t\right)/\partial t$ when evaluated at the parametric coordinates $\eta_k = \left(\eta_k^1, \eta_k^2, \eta_k^3\right)$ of the $k-$th integration point. All time derivatives are discretized using a backward difference scheme.

Similarly, the discretized form of $D\delta W_{\text{int}} = D\delta W_{\text{int}}\left[\Delta \mathbf{u}\right] + D\delta W_{\text{int}}\left[\Delta \tilde{p}\right] + \sum_\gamma D\delta W_{\text{int}}\left[\Delta \tilde{c}^\gamma\right]$ may be written as

$$D\delta W_{\text{int}} = \sum_{e=1}^{n_e} \sum_{k=1}^{n_{\text{int}}^{(e)}} W_k J_\eta \sum_{a=1}^{m} \sum_{b=1}^{m} \begin{bmatrix} \delta \mathbf{v}_a & \delta \tilde{p}_a & \delta \tilde{c}_a^\alpha & \delta \tilde{c}_a^\beta \end{bmatrix} \cdot \begin{bmatrix} \mathbf{K}_{ab}^{uu} & \mathbf{k}_{ab}^{up} & \mathbf{k}_{ab}^{u\alpha} & \mathbf{k}_{ab}^{u\beta} \\ \mathbf{k}_{ab}^{pu} & k_{ab}^{pp} & k_{ab}^{p\alpha} & k_{ab}^{p\beta} \\ \mathbf{k}_{ab}^{\alpha u} & k_{ab}^{\alpha p} & k_{ab}^{\alpha\alpha} & k_{ab}^{\alpha\beta} \\ \mathbf{k}_{ab}^{\beta u} & k_{ab}^{\beta p} & k_{ab}^{\beta\alpha} & k_{ab}^{\beta\beta} \end{bmatrix} \cdot \begin{bmatrix} \Delta \mathbf{u}_b \\ \Delta \tilde{p}_b \\ \Delta \tilde{c}_b^\alpha \\ \Delta \tilde{c}_b^\beta \end{bmatrix} \,, \tag{3.4.41}$$

where the terms in the first column are the discretized form of the linearization along $\Delta \mathbf{u}$:

$$\mathbf{K}_{ab}^{uu} = \operatorname{grad} N_a \cdot \boldsymbol{\mathcal{C}} \cdot \operatorname{grad} N_b + \left(\operatorname{grad} N_a \cdot \boldsymbol{\sigma} \cdot \operatorname{grad} N_b\right) \mathbf{I} \,, \tag{3.4.42}$$

$$\mathbf{k}_{ab}^{pu} = \left(\mathbf{w}_b^u\right)^T \cdot \operatorname{grad} N_a + N_a \mathbf{q}_b^{pu} \,, \tag{3.4.43}$$

$$\mathbf{k}_{ab}^{\alpha u} = \left(\mathbf{j}_b^{\alpha u} + \sum_\beta z^\beta \mathbf{j}_b^{\beta u}\right)^T \cdot \operatorname{grad} N_a + N_a \mathbf{q}_b^{\alpha u} \,, \tag{3.4.44}$$

where

$$\mathbf{j}_b^{\alpha u} = J \frac{\partial \tilde{\kappa}^\alpha}{\partial J} \mathbf{d}^\alpha \cdot \mathbf{g}^\alpha \otimes \operatorname{grad} N_b + \tilde{\kappa}^\alpha \mathbf{g}^\alpha \cdot \mathbf{d}^\alpha \cdot \operatorname{grad} N_b$$

$$+ \tilde{\kappa}^\alpha \frac{\mathbf{d}^\alpha}{d_0^\alpha} \cdot \tilde{c}^\alpha \left(\operatorname{grad} N_b \otimes \mathbf{w} - \mathbf{w} \otimes \operatorname{grad} N_b + \left(\operatorname{grad} N_b \cdot \mathbf{w}\right)\mathbf{I} + \mathbf{w}_b^u\right) \tag{3.4.45}$$

$$- \varphi^s \tilde{\kappa}^\alpha \mathbf{d}^\alpha \cdot \operatorname{grad} \tilde{c}^\alpha \otimes \operatorname{grad} N_b \,,$$

$$\mathbf{q}_b^{pu} = -\frac{1}{\Delta t} \operatorname{grad} N_b \,, \tag{3.4.46}$$

$$\mathbf{q}_b^{\alpha u} = \tilde{c}^\alpha \frac{\partial \left(J \varphi^w \tilde{\kappa}^\alpha\right)}{\partial J} \mathbf{q}_b^{pu} \,. \tag{3.4.47}$$

The terms in the second column of the stiffness matrix in (3.3.44) are the discretized form of the linearization along $\Delta \tilde{p}$:

$$\mathbf{k}_{ab}^{up} = -N_b \operatorname{grad} N_a \,, \tag{3.4.48}$$

$$k_{ab}^{pp} = -\operatorname{grad} N_a \cdot \tilde{\mathbf{k}} \cdot \operatorname{grad} N_b \,, \tag{3.4.49}$$

$$k_{ab}^{\alpha p} = \operatorname{grad} N_a \cdot \left(\mathbf{j}_b^{\alpha p} + \sum_\beta z^\beta \mathbf{j}_b^{\beta p}\right) \,, \tag{3.4.50}$$

where

$$\mathbf{j}_b^{\alpha p} = -\frac{\tilde{\kappa}^\alpha \tilde{c}^\alpha}{d_0^\alpha} \mathbf{d}^\alpha \cdot \tilde{\mathbf{k}} \cdot \operatorname{grad} N_b \,. \tag{3.4.51}$$

The terms in the third column of the stiffness matrix in (3.3.44) are the discretized form of the linearization along $\Delta \tilde{c}^\gamma$:

$$\mathbf{k}_{ab}^{u\alpha} = N_b \left(\boldsymbol{\sigma}_\alpha' - R\theta \left[\Phi \tilde{\kappa}^\alpha + \sum_\beta \left(\frac{\partial \Phi}{\partial \tilde{c}^\alpha} \tilde{\kappa}^\beta + \Phi \frac{\partial \tilde{\kappa}^\beta}{\partial \tilde{c}^\alpha} \right) \tilde{c}^\beta \right] \mathbf{I} \right) \cdot \operatorname{grad} N_a \,, \tag{3.4.52}$$

$$k_{ab}^{p\alpha} = \operatorname{grad} N_a \cdot \mathbf{w}_b^\alpha \,, \tag{3.4.53}$$

$$k_{ab}^{\alpha\gamma} = \operatorname{grad} N_a \cdot \left(\mathbf{j}_b^{\alpha\gamma} + \sum_\beta z^\beta \mathbf{j}_b^{\beta\gamma} \right) + N_a q_b^{\alpha\gamma} \,, \tag{3.4.54}$$

where

$$\mathbf{w}_b^\gamma = N_b \left(\tilde{\mathbf{k}}_\gamma' \cdot \mathbf{g}^p - R\theta \tilde{\mathbf{k}} \cdot \sum_\beta \left(\frac{\partial}{\partial \tilde{c}^\gamma} \left(\frac{\tilde{\kappa}^\beta}{d_0^\beta} \right) \mathbf{d}^\beta + \frac{\tilde{\kappa}^\beta}{d_0^\beta} \mathbf{d}_c^{\beta\gamma} \right) \cdot \operatorname{grad} \tilde{c}^\beta \right)$$
$$- R\theta \tilde{\mathbf{k}} \cdot \frac{\tilde{\kappa}^\gamma}{d_0^\gamma} \mathbf{d}^\gamma \cdot \operatorname{grad} N_b \,, \tag{3.4.55}$$

$$\mathbf{j}_b^{\alpha\gamma} = N_b \left(\frac{\partial \tilde{\kappa}^\alpha}{\partial \tilde{c}^\gamma} \mathbf{d}^\alpha + \tilde{\kappa}^\alpha \mathbf{d}_c^{\alpha\gamma} \right) \cdot \mathbf{g}^\alpha$$
$$+ \frac{\tilde{\kappa}^\alpha}{d_0^\alpha} \mathbf{d}^\alpha \cdot \left[\delta_{\alpha\gamma} \left(N_b \mathbf{w} - \varphi^w d_0^\alpha \operatorname{grad} N_b \right) + \tilde{c}^\alpha \left(\mathbf{w}_b^\gamma - \frac{N_b}{d_0^\alpha} \frac{\partial d_0^\alpha}{\partial \tilde{c}^\gamma} \mathbf{w} \right) \right] \,, \tag{3.4.56}$$

$$q_b^{\alpha\gamma} = -N_b \frac{\varphi^w}{\Delta t} \left(\frac{\partial \tilde{\kappa}^\alpha}{\partial \tilde{c}^\gamma} \tilde{c}^\alpha + \delta_{\alpha\gamma} \tilde{\kappa}^\alpha \right) \,, \tag{3.4.57}$$

and

$$\mathbf{g}^p = -\operatorname{grad} \tilde{p} - R\theta \sum_\beta \frac{\tilde{\kappa}^\beta}{d_0^\beta} \mathbf{d}^\beta \cdot \operatorname{grad} \tilde{c}^\beta \,. \tag{3.4.58}$$

The discretization of δW_{ext} in (3.4.35) has the form

$$\delta W_{\text{ext}} = \sum_{e=1}^{n_e} \sum_{k=1}^{n_{\text{int}}^{(e)}} W_k J_\eta \sum_{a=1}^m \begin{bmatrix} \delta \mathbf{v}_a & \delta \tilde{p}_a & \delta \tilde{c}_a^\alpha & \delta \tilde{c}_a^\beta \end{bmatrix} \cdot \begin{bmatrix} N_a t_n \mathbf{n} \\ N_a w_n \\ N_a \tilde{j}_n^\alpha \\ N_a \tilde{j}_n^\beta \end{bmatrix} \,, \tag{3.4.59}$$

where $J_\eta = |\mathbf{g}_1 \times \mathbf{g}_2|$. The summation is performed over all surface elements on which these boundary conditions are prescribed. The discretization of $-D\delta W_{\text{ext}}$ has the form

$$-D\delta W_{\text{ext}} = \sum_{e=1}^{n_e} \sum_{k=1}^{n_{\text{int}}^{(e)}} W_k J_\eta \sum_{a=1}^m \sum_{b=1}^m \begin{bmatrix} \delta \mathbf{v}_a & \delta \tilde{p}_a & \delta \tilde{c}_a^\alpha & \delta \tilde{c}_a^\beta \end{bmatrix} \cdot \begin{bmatrix} \mathbf{K}_{ab}^{uu} & \mathbf{0} & \mathbf{0} & \mathbf{0} \\ \mathbf{k}_{ab}^{pu} & 0 & 0 & 0 \\ \mathbf{k}_{ab}^{\alpha u} & 0 & 0 & 0 \\ \mathbf{k}_{ab}^{\beta u} & 0 & 0 & 0 \end{bmatrix} \cdot \begin{bmatrix} \Delta \mathbf{u}_b \\ \Delta \tilde{p}_b \\ \Delta \tilde{c}_b^\alpha \\ \Delta \tilde{c}_b^\beta \end{bmatrix} \,, \tag{3.4.60}$$

where

$$\mathbf{K}_{ab}^{uu} = t_n N_a \mathcal{A} \left\{ \frac{\partial N_b}{\partial \eta^1} \mathbf{g}_2 - \frac{\partial N_b}{\partial \eta^2} \mathbf{g}_1 \right\} \,,$$

$$\mathbf{k}_{ab}^{pu} = -w_n N_a \left(\frac{\partial N_b}{\partial \eta^1} \mathbf{g}_2 - \frac{\partial N_b}{\partial \eta^2} \mathbf{g}_1 \right) \times \mathbf{n}, \tag{3.4.61}$$

$$\mathbf{k}_{ab}^{\alpha u} = -\tilde{j}_n^\alpha N_a \left(\frac{\partial N_b}{\partial \eta^1} \mathbf{g}_2 - \frac{\partial N_b}{\partial \eta^2} \mathbf{g}_1 \right) \times \mathbf{n}.$$

In this expression, $\mathcal{A}\{\mathbf{v}\}$ is the antisymmetric tensor whose dual vector is $\mathbf{v}$ (such that $\mathcal{A}\{\mathbf{v}\} \cdot \mathbf{q} = \mathbf{v} \times \mathbf{q}$ for any vector $\mathbf{q}$).

3.4.6 Electric Potential and Partition Coefficient Derivatives

When the mixture is charged it is necessary to solve for the electric potential ψ using the electroneutrality condition in (2.7.4). This equation may be rewritted as a polynomial in ζ,

$$\sum_{i=0}^n a_i \zeta^i \,, \tag{3.4.62}$$

where

$$\zeta = \exp\left(-\frac{F_c \psi}{R\theta} \right) \,, \tag{3.4.63}$$

and

$$a_i = \begin{cases} z^\alpha \hat{\kappa}^\alpha \tilde{c}^\alpha & i = z^\alpha - z^{\min} \\ c^F & i = -z^{\min} \end{cases} . \tag{3.4.64}$$

Here, $z^{\min} = \min_\alpha z^\alpha$ and the polynomial degress is $n = z^{\max} - z^{\min}$ where $z^{\max} = \max_\alpha z^\alpha$. Since more than one solute may carry the same charge z^α, the coefficients a_i should be evaluated from the summation of $z^\alpha \hat{\kappa}^\alpha \tilde{c}^\alpha$ over all such solutes. Only real positive roots are valid, since $\psi = -R\theta \left(\ln \zeta \right) / F_c$ according to (3.4.63). Using Descartes' rule of signs, an inspection of the coefficients a_i shows tht there is only one sign change in the polynomial, regardless of the sign of c^F, implying that there will always be only one positive root ζ, which must thus be real. Therefore, there cannot be any ambiguity in the calculation of ψ, irrespective of the polynomial degree. Newton's method is used to solve for the positive real root when $n > 2$.

Using the above relations, it follows that $\tilde{\kappa}^\alpha = \hat{\kappa}^\alpha \zeta^{z^\alpha}$. An examination of the equations resulting from the linearization of the internal virtual work shows that it is necessary to evaluate derivatives of $\tilde{\kappa}^\alpha$ with respect to J and $\tilde{c}^\gamma$, which are given by

$$\begin{aligned} \frac{\partial \tilde{\kappa}^\alpha}{\partial J} &= \frac{\partial \hat{\kappa}^\alpha}{\partial J} \zeta^{z^\alpha} + z^\alpha \tilde{\kappa}^\alpha \frac{1}{\zeta} \frac{\partial \zeta}{\partial J} \\ \frac{\partial \tilde{\kappa}^\alpha}{\partial \tilde{c}^\gamma} &= \frac{\partial \hat{\kappa}^\alpha}{\partial \tilde{c}^\gamma} \zeta^{z^\alpha} + z^\alpha \tilde{\kappa}^\alpha \frac{1}{\zeta} \frac{\partial \zeta}{\partial \tilde{c}^\gamma} \end{aligned} . \tag{3.4.65}$$

In these expressions, the derivatives of $\hat{\kappa}^\alpha$ are obtained from the user-defined constitutive relations for the solubility. Derivatives of ζ may be evaluated by differentiating the electroneutrality condition to produce

$$\begin{aligned} \frac{1}{\zeta} \frac{\partial \zeta}{\partial J} &= -\frac{\frac{\partial c^F}{\partial J} + \sum_\beta z^\beta \zeta^{z^\beta} \tilde{c}^\beta \frac{\partial \hat{\kappa}^\beta}{\partial J}}{\sum_\beta \left(z^\beta \right)^2 \tilde{\kappa}^\beta \tilde{c}^\beta} \\ \frac{1}{\zeta} \frac{\partial \zeta}{\partial \tilde{c}^\gamma} &= -\frac{z^\gamma \tilde{\kappa}^\gamma + \sum_\beta z^\beta \zeta^{z^\beta} \tilde{c}^\beta \frac{\partial \hat{\kappa}^\beta}{\partial \tilde{c}^\gamma}}{\sum_\beta \left(z^\beta \right)^2 \tilde{\kappa}^\beta \tilde{c}^\beta} \end{aligned} . \tag{3.4.66}$$

The derivative $\partial c^F / \partial J$ may be evaluated from

$$c^F = \frac{1 - \varphi_r^s}{J - \varphi_r^s} c_r^F \,, \tag{3.4.67}$$

where φ_r^s is the referential solid volume fraction (volume of solid in current configuration per volume of the mixture in the reference configuration) and c_r^F is the referential fixed charge density (equivalent charge in current configuration per volume of the mixture in the reference configuration).

3.4.7 Chemical Reactions

3.4.7.1 Virtual Work and Linearization

The contribution to δW due to chemical reactions is given by δG, where

$$\delta G = \int_b \delta \tilde{p} \left[\hat{\varphi}^w + (1 - \varphi^s) \hat{\zeta} \overline{\mathcal{V}} \right] dv + \sum_\iota \nu^\iota \int_b \delta \tilde{c}^\iota \left(1 - \varphi^s \right) \hat{\zeta} \, dv \,. \tag{3.4.68}$$

The linearization of δG along a solid displacement increment $\Delta \mathbf{u}$ is

$$\begin{aligned} D\delta G \left[\Delta \mathbf{u} \right] = & \int_b \delta \tilde{p} \left(\hat{\varphi}^w \operatorname{div} \Delta \mathbf{u} + \hat{\boldsymbol{\varphi}}_\varepsilon^w : \Delta \boldsymbol{\varepsilon} \right) dv \\ & + \overline{\mathcal{V}} \int_b \delta \tilde{p} \left[\hat{\zeta} \operatorname{div} \Delta \mathbf{u} + (J - \varphi_r^s) \hat{\boldsymbol{\zeta}}_\varepsilon : \Delta \boldsymbol{\varepsilon} \right] dv \\ & + \sum_\iota \nu^\iota \int_b \delta \tilde{c}^\iota \left[\hat{\zeta} \operatorname{div} \Delta \mathbf{u} + (J - \varphi_r^s) \hat{\boldsymbol{\zeta}}_\varepsilon : \Delta \boldsymbol{\varepsilon} \right] dv \end{aligned} \quad , \tag{3.4.69}$$

where

$$\hat{\boldsymbol{\varphi}}_\varepsilon^w = \mathbf{F} \cdot \frac{\partial \hat{\varphi}^w}{\partial \mathbf{E}} \cdot \mathbf{F}^T \,, \quad \hat{\boldsymbol{\zeta}}_\varepsilon = J^{-1} \mathbf{F} \cdot \frac{\partial \hat{\zeta}}{\partial \mathbf{E}} \cdot \mathbf{F}^T \,. \tag{3.4.70}$$

Currently, $\hat{\zeta}$ is assumed to be independent of $\tilde{p}$ in FEBio; it follows that the linearization along the effective fluid pressure increment $\Delta \tilde{p}$ is

$$D\delta G \left[\Delta \tilde{p} \right] = \int_b \delta \tilde{p} \, \frac{\partial \hat{\varphi}^w}{\partial \tilde{p}} \Delta p \, dv \,. \tag{3.4.71}$$

Finally, the linearization along a concentration increment $\Delta \tilde{c}^\iota$ is

$$\begin{aligned} D\delta G \left[\Delta \tilde{c}^\iota \right] = & \int_b \delta \tilde{p} \, \frac{\partial \hat{\varphi}^w}{\partial \tilde{c}^\iota} \Delta \tilde{c}^\iota \, dv \\ & + \overline{\mathcal{V}} \int_b \delta \tilde{p} \left(1 - \varphi^s \right) \frac{\partial \hat{\zeta}}{\partial \tilde{c}^\iota} \Delta \tilde{c}^\iota \, dv \\ & + \sum_\gamma \nu^\gamma \int_b \delta \tilde{c}^\gamma \left(1 - \varphi^s \right) \frac{\partial \hat{\zeta}}{\partial \tilde{c}^\iota} \Delta \tilde{c}^\iota \, dv \end{aligned} \quad . \tag{3.4.72}$$

The discretized form of these expressions is given by

$$\delta G = \sum_a \delta \tilde{p}_a r_a^p + \sum_\gamma \sum_a \delta \tilde{c}_a^\gamma r_a^\gamma \,, \tag{3.4.73}$$

where

$$r_a^p = \int_b N_a \left[\hat{\varphi}^w + (1 - \varphi^s) \hat{\zeta} \hat{\mathcal{V}} \right] dv$$
$$r_a^\gamma = \nu^\gamma \int_b N_a (1 - \varphi^s) \hat{\zeta} \, dv \tag{3.4.74}$$

Similarly,

$$D\delta G\left[\Delta\mathbf{u}\right] = \sum_a \delta\tilde{p}_a \sum_b \mathbf{k}_{ab}^{pu} \cdot \Delta\mathbf{u}_b$$
$$+ \sum_\gamma \sum_a \delta\tilde{c}_a^\gamma \sum_b \mathbf{k}_{ab}^{\gamma u} \cdot \Delta\mathbf{u}_b , \tag{3.4.75}$$

where

$$\mathbf{k}_{ab}^{pu} = \int_b N_a \left(\hat{\varphi}^w \mathbf{I} + \hat{\boldsymbol{\varphi}}_\varepsilon^w \right) \cdot \operatorname{grad} N_b \, dv$$
$$+ \bar{\mathcal{V}} \int_a N_a \left[\hat{\zeta}\mathbf{I} + (J - \varphi_r^s) \hat{\boldsymbol{\zeta}}_\varepsilon \right] \cdot \operatorname{grad} N_b \, dv . \tag{3.4.76}$$
$$\mathbf{k}_{ab}^{\gamma u} = \nu^\gamma \int_a N_a \left[\hat{\zeta}\mathbf{I} + (J - \varphi_r^s) \hat{\boldsymbol{\zeta}}_\varepsilon \right] \cdot \operatorname{grad} N_b \, dv$$

Then,

$$D\delta G\left[\Delta\tilde{p}\right] = \sum_a \delta\tilde{p}_a \sum_b k_{ab}^{pp} \Delta\tilde{p}_b , \tag{3.4.77}$$

where

$$k_{ab}^{pp} = \int_b N_a \frac{\partial \hat{\varphi}^w}{\partial \tilde{p}} N_b \, dv . \tag{3.4.78}$$

Finally,

$$D\delta G\left[\Delta\tilde{c}^\iota\right] = \sum_a \delta\tilde{p}_a \sum_b k_{ab}^{p\iota} \Delta\tilde{c}_b^\iota$$
$$+ \sum_\gamma \sum_a \delta\tilde{c}_a^\gamma \sum_b k_{ab}^{\gamma\iota} \Delta\tilde{c}_b^\iota , \tag{3.4.79}$$

where

$$k_{ab}^{p\iota} = \int_b N_a N_b \frac{\partial \hat{\varphi}^w}{\partial \tilde{c}^\iota} \, dv + \bar{\mathcal{V}} \int_b N_a N_b (1 - \varphi^s) \frac{\partial \hat{\zeta}}{\partial \tilde{c}^\iota} \, dv$$
$$k_{ab}^{\gamma\iota} = \nu^\gamma \int_b N_a N_b (1 - \varphi^s) \frac{\partial \hat{\zeta}}{\partial \tilde{c}^\iota} \, dv \tag{3.4.80}$$

3.4.7.2 Updating Solid-Bound Molecule Concentrations

The solid-bound molecule concentrations ρ_r^σ are evaluated at integration points of each element; they do not represent nodal degrees of freedom. The values of ρ_r^σ are updated at the end of each iteration in the solution of the nonlinear equations for the nodal degrees of freedom, using trapezoidal integration on $\hat{\rho}_r^\sigma$ in (2.10.6). According to (2.10.16) and (2.10.18), we have $\hat{\rho}_r^\sigma = (J - \varphi_r^s) M^\sigma \nu^\sigma \hat{\zeta}$, which is evaluated as the average of values at t_n and t_{n+1}, then

$$(\rho_r^\sigma)_{n+1} = (\rho_r^\sigma)_n + (\hat{\rho}_r^\sigma)_{n+\frac{1}{2}} \Delta t \tag{3.4.81}$$

where $\Delta t = t_{n+1} - t_n$.

3.5 Computational Fluid Dynamics

3.5.1 Weak Formulation

The nodal unknowns in this formulation are $\mathbf{v}$ and J (or e), which may be solved using the momentum balance in eq.(2.11.1) and the kinematic constraint between J and $\mathbf{v}$ given in eq.(2.11.6). The virtual work integral for a Galerkin finite element formulation [19] is given by

$$\delta W = \int_\Omega \delta\mathbf{v} \cdot (\operatorname{div}\boldsymbol{\sigma} + \rho\,(\mathbf{b} - \mathbf{a}))\,dv$$
$$+ \int_\Omega \delta J \left(\frac{\dot{J}}{J} - \operatorname{div}\mathbf{v}\right) dv\,, \tag{3.5.1}$$

where $\delta\mathbf{v}$ is a virtual velocity and δJ is a virtual energy density; Ω is the fluid finite element domain and dv is a differential volume in Ω. This virtual work statement may be directly related to the axiom of energy balance, specialized to conditions of isothermal flow of viscous compressible fluids (see Section 2.11.2). Using the divergence theorem, we may rewrite the weak form of this integral as the difference between external and internal virtual work, $\delta W = \delta W_{ext} - \delta W_{int}$, where

$$\delta W_{int} = \int_\Omega \boldsymbol{\tau} : \operatorname{grad}\delta\mathbf{v}\,dv + \int_\Omega \delta\mathbf{v} \cdot (\operatorname{grad}p + \rho\mathbf{a})\,dv$$
$$- \int_\Omega \left(\delta J \frac{\dot{J}}{J} + \operatorname{grad}\delta J \cdot \mathbf{v}\right) dv\,, \tag{3.5.2}$$

and

$$\delta W_{ext} = \int_{\partial\Omega} \delta\mathbf{v} \cdot \mathbf{t}^\tau\,da + \int_\Omega \delta\mathbf{v} \cdot \rho\mathbf{b}\,dv - \int_{\partial\Omega} \delta J\,v_n\,da\,. \tag{3.5.3}$$

Here, $\partial\Omega$ is the boundary of Ω and da is a differential area on $\partial\Omega$, $\mathbf{t}^\tau = \boldsymbol{\tau}\cdot\mathbf{n}$ is the viscous component of the traction $\mathbf{t}$, and $v_n = \mathbf{v}\cdot\mathbf{n}$ is the velocity normal to the boundary $\partial\Omega$, with $\mathbf{n}$ representing the outward normal on $\partial\Omega$. From these expressions, it becomes evident that essential (Dirichlet) boundary conditions may be prescribed on $\mathbf{v}$ and J, while natural (Neumann) boundary conditions may be prescribed on $\mathbf{t}^\tau$ and v_n. The appearance of velocity in both essential and natural boundary conditions may seem surprising at first. To better understand the nature of these boundary conditions, it is convenient to separate the velocity into its normal and tangential components, $\mathbf{v} = v_n\mathbf{n} + \mathbf{v}_t$, where $\mathbf{v}_t = (\mathbf{I} - \mathbf{n}\otimes\mathbf{n})\cdot\mathbf{v}$. In particular, for inviscid flow, the viscous stress $\boldsymbol{\tau}$ and its corresponding traction $\mathbf{t}^\tau$ are both zero, leaving v_n as the sole natural boundary condition; similarly, J becomes the only essential boundary condition in such flows, since $\mathbf{v}_t$ is unknown *a priori* on a frictionless boundary and must be obtained from the solution of the analysis.

In general, prescribing J is equivalent to prescribing the elastic fluid pressure, since p is only a function of J. On a boundary where no conditions are prescribed explicitly, we conclude that $v_n = 0$ and $\mathbf{t}^\tau = \mathbf{0}$, which represents a frictionless wall. Conversely, it is possible to prescribe v_n and $\mathbf{t}^\tau$ on a boundary to produce a desired inflow or outflow while simultaneously stabilizing the flow conditions by prescribing a suitable viscous traction. Prescribing essential boundary conditions $\mathbf{v}_t$ and J determines the tangential velocity on a boundary as well as the elastic fluid pressure p, leaving the option to also prescribe the normal component of the viscous traction, $t_n^\tau = \mathbf{t}^\tau\cdot\mathbf{n}$, to completely determine the normal traction $t_n = \mathbf{t}\cdot\mathbf{n}$ (or else t_n^τ naturally equals zero). Mixed boundary conditions represent common physical features: Prescribing v_n and $\mathbf{v}_t$ completely determines the velocity $\mathbf{v}$ on a boundary; prescribing $\mathbf{t}^\tau$ and J completely determines the traction $\mathbf{t} = \boldsymbol{\sigma}\cdot\mathbf{n}$ on a boundary. Note that v_n and J are mutually exclusive boundary conditions, and the same holds for $\mathbf{v}_t$ and the tangential component of the viscous traction, $\mathbf{t}_t^\tau = (\mathbf{I} - \mathbf{n}\otimes\mathbf{n})\cdot\mathbf{t}^\tau$.

3.5.2   Temporal Discretization and Linearization

The time derivatives, $\partial \mathbf{v}/\partial t$ which appears in the expression for $\mathbf{a}$ in eq.(2.11.2), and $\partial J/\partial t$ which similarly appears in $\dot{J}$, may be discretized upon the choice of a time integration scheme, such as the generalized-α method [36] (Section 3.7). The solution of the nonlinear equation $\delta W = 0$ is obtained by linearizing this relation as

$$\delta W + D\delta W\left[\Delta \mathbf{v}\right] + D\delta W\left[\Delta J\right] \approx 0\,, \tag{3.5.4}$$

where the operator $D\delta W\left[\cdot\right]$ represents the directional derivative of δW at $(\mathbf{v}, J)$ along an increment $\Delta \mathbf{v}$ of $\mathbf{v}$, or ΔJ of J [19]. Using the split form of δW between external and internal work contributions, this relation may be expanded as

$$\begin{aligned} D\delta W_{int}\left[\Delta \mathbf{v}\right] + D\delta W_{int}\left[\Delta J\right] - D\delta W_{ext}\left[\Delta \mathbf{v}\right] \\ - D\delta W_{ext}\left[\Delta J\right] \approx \delta W_{ext} - \delta W_{int}\,. \end{aligned} \tag{3.5.5}$$

In this framework the finite element mesh is defined on the spatial domain Ω, which is fixed (time-invariant) in conventional CFD treatments. Thus, we can linearize δW_{int} along increments $\Delta \mathbf{v}$ in the velocity and ΔJ in the volume ratio, by simply bringing the directional derivative operator into the integrals of eqs.(3.5.2)-(3.5.3). The linearization of $\partial \mathbf{v}/\partial t$ and $\partial J/\partial t$ is given by

$$D\left(\frac{\partial \mathbf{v}}{dt}\right)\left[\Delta \mathbf{v}\right] = \xi\frac{\Delta \mathbf{v}}{\Delta t}\,, \tag{3.5.6}$$

$$D\left(\frac{\partial J}{\partial t}\right)\left[\Delta \mathbf{v}\right] = \xi\frac{\Delta J}{\Delta t}\,. \tag{3.5.7}$$

Here, Δt is the current time increment and ξ is a parameter chosen as described in [36]; for example, $\xi = 1$ yields the backward Euler scheme, in which case $\partial \mathbf{v}/\partial t \approx \left(\mathbf{v} - \mathbf{v}^{-\Delta t}\right)/\Delta t$ and $\partial J/\partial t \approx \left(J - J^{-\Delta t}\right)/\Delta t$, where $\mathbf{v}^{-\Delta t}$ and $J^{-\Delta t}$ are the velocity and volume ratio, respectively, at the previous time $t - \Delta t$. More generally, ξ is evaluated from the spectral radius for an infinite time step, ρ_∞ (Section 3.7).

The linearization of δW_{int} along an increment $\Delta \mathbf{v}$ is then

$$\begin{aligned} D\left(\delta W_{int}\right)\left[\Delta \mathbf{v}\right] = &\int_\Omega \operatorname{grad}\delta \mathbf{v} : \boldsymbol{\mathcal{C}}^\tau : \operatorname{grad}\Delta \mathbf{v}\,dv \\ &+ \int_\Omega \delta \mathbf{v} \cdot \rho\left(\left(\frac{\xi\mathbf{I}}{\Delta t} + \mathbf{L}\right) \cdot \Delta \mathbf{v} + \operatorname{grad}\Delta \mathbf{v}\cdot \mathbf{v}\right)dv \\ &- \int_\Omega \left(\frac{\delta J}{J}\operatorname{grad}J + \operatorname{grad}\delta J\right)\cdot \Delta \mathbf{v}\,dv \end{aligned} \tag{3.5.8}$$

where we have introduced the fourth-order tensor $\boldsymbol{\mathcal{C}}^\tau$ representing the tangent of the viscous stress with respect to the rate of deformation,

$$\boldsymbol{\mathcal{C}}^\tau = \frac{\partial \boldsymbol{\tau}}{\partial \mathbf{D}}\,. \tag{3.5.9}$$

Note that $\boldsymbol{\mathcal{C}}^\tau$ exhibits minor symmetries because of the symmetries of $\boldsymbol{\tau}$ and $\mathbf{D}$; in Cartesian components, we have $\mathcal{C}^\tau_{ijkl} = \mathcal{C}^\tau_{jikl}$ and $\mathcal{C}^\tau_{ijkl} = \mathcal{C}^\tau_{ijlk}$. In general, $\boldsymbol{\mathcal{C}}^\tau$ does not exhibit major symmetry ($\mathcal{C}^\tau_{ijkl} \neq \mathcal{C}^\tau_{klij}$), though the common constitutive relations adopted in fluid mechanics produce such symmetry as shown below.

The linearization of δW_{int} along an increment ΔJ is

$$D\left(\delta W_{int}\right)[\Delta J] = \int_b \Delta J\,\boldsymbol{\tau}'_J : \operatorname{grad}\delta\mathbf{v}\,dv - \int_\Omega \delta\mathbf{v}\cdot\Delta J\frac{\rho}{J}\mathbf{a}\,dv$$
$$+ \int_\Omega \delta\mathbf{v}\cdot\left(p'\operatorname{grad}\Delta J + \Delta J\,p''\operatorname{grad}J\right)\,dv \qquad (3.5.10)$$
$$- \int_\Omega \frac{\delta J}{J}\left(\left(\frac{\xi}{\Delta t} - \frac{\dot{J}}{J}\right)\Delta J + \operatorname{grad}\Delta J\cdot\mathbf{v}\right)\,dv$$

where we have used $DJ\left[\Delta J\right] = \Delta J$; p' and p'' respectively represent the first and second derivatives of $p\left(J\right)$. We have also defined $\boldsymbol{\tau}'_J$ as the tangent of the viscous stress $\boldsymbol{\tau}$ with respect to J,

$$\boldsymbol{\tau}'_J = \frac{\partial\boldsymbol{\tau}}{\partial J}\,. \qquad (3.5.11)$$

For the external work, when $\mathbf{t}^\tau$, $\mathbf{b}$ and v_n are prescribed, these linearizations simplify to

$$D\left(\delta W_{ext}\right)[\Delta\mathbf{v}] = 0\,, \qquad (3.5.12)$$

and

$$D\left(\delta W_{ext}\right)[\Delta J] = -\int_b \delta\mathbf{v}\cdot\Delta J\frac{\rho}{J}\mathbf{b}\,dv\,. \qquad (3.5.13)$$

We may define the fluid dilatation $e = J - 1$ as an alternative essential variable, since initial and boundary conditions $e = 0$ are more convenient to handle in a numerical scheme than $J = 1$. It follows that $\operatorname{grad}J = \operatorname{grad}e$ and $\partial J/\partial t = \partial e/\partial t$. Therefore the changes to the above equations are minimal, simply requiring the substitution $J = 1 + e$ and $\Delta J = \Delta e$. Steady-state analyses may be obtained by setting the terms involving Δt^{-1} to zero in eqs.(3.5.6)-(3.5.7), (3.5.8) and (3.5.10).

3.5.3 Spatial Discretization

The velocity $\mathbf{v}\left(\mathbf{x}, t\right)$ and Jacobian $J\left(\mathbf{x}, t\right)$ are spatially interpolated over the domain Ω using the same interpolation functions $N_a\left(\mathbf{x}\right)$, with $a = 1$ to n where n is the number of nodes in an element),

$$\mathbf{v}\left(\mathbf{x}, t\right) = \sum_{a=1}^n N_a\left(\mathbf{x}\right)\mathbf{v}_a\,, \quad J\left(\mathbf{x}, t\right) = \sum_{a=1}^n N_a\left(\mathbf{x}\right)J_a\,. \qquad (3.5.14)$$

Here, $\mathbf{v}_a$ and J_a are nodal values of $\mathbf{v}$ and J that evolve with time. In contrast to classical mixed formulations for incompressible flow [53], which solve for the pressure p using $\operatorname{div}\mathbf{v} = 0$ instead of eq.(2.11.6), equal order interpolation is acceptable in this formulation since the governing equations for $\mathbf{v}$ and J involve spatial derivatives of both variables ($\operatorname{grad}\mathbf{v}$ and $\operatorname{grad}J$). The expressions of eq.(3.5.14) may be used to evaluate $\mathbf{L}$, $\operatorname{div}\mathbf{v}$, $\mathbf{a}$, $\operatorname{grad}J$, $\dot{J}$, etc. Similar interpolations are used for virtual increments $\delta\mathbf{v}$ and δJ, as well as real increments $\Delta\mathbf{v}$ and ΔJ.

When substituted into eq.(4.2.32), we find that the discretized form of δW_{int} may be written as

$$\delta W_{int} = \sum_a \delta\mathbf{v}_a\cdot\left(\mathbf{f}_a^\sigma + \mathbf{f}_a^\rho\right) + f_a^J\delta J_a\,, \qquad (3.5.15)$$

where

$$\mathbf{f}_a^\sigma = \int_\Omega \left(\boldsymbol{\tau} \cdot \operatorname{grad} N_a + N_a \operatorname{grad} p\right) dv\,,$$

$$\mathbf{f}_a^\rho = \int_\Omega N_a \rho \mathbf{a}\, dv\,,$$

(3.5.16)

$$f_a^J = \int_\Omega -\left(N_a \frac{\dot{J}}{J} + \operatorname{grad} N_a \cdot \mathbf{v}\right) dv\,.$$

Similarly, the discretized form of $D\delta W_{int}\left[\Delta \mathbf{v}\right]$ in eq.(3.5.8) becomes

$$D\left(\delta W_{int}\right)\left[\Delta \mathbf{v}\right] = \sum_a \delta \mathbf{v}_a \cdot \sum_b \left(\mathbf{K}_{ab}^{vv} + \mathbf{M}_{ab}^{vv}\right) \cdot \Delta \mathbf{v}_b$$
$$+ \sum_a \delta J_a \sum_b \mathbf{k}_{ab}^{Jv} \cdot \Delta \mathbf{v}_b\,,$$

(3.5.17)

where

$$\mathbf{K}_{ab}^{vv} = \int_\Omega \operatorname{grad} N_a \cdot \boldsymbol{\mathcal{C}}^v \cdot \operatorname{grad} N_b\, dv\,,$$

$$\mathbf{M}_{ab}^{vv} = \int_\Omega N_a \rho \left(N_b \left(\frac{\xi}{\Delta t}\mathbf{I} + \operatorname{grad} \mathbf{v}\right) + \left(\operatorname{grad} N_b \cdot \mathbf{v}\right)\mathbf{I}\right) dv\,,$$

(3.5.18)

$$\mathbf{k}_{ab}^{Jv} = \int_\Omega -\left(\frac{N_a}{J}\operatorname{grad} J + \operatorname{grad} N_a\right) N_b\, dv\,,$$

whereas that of $D\delta W_{int}\left[\Delta J\right]$ in eq.(3.5.10) becomes

$$D\left(\delta W_{int}\right)\left[\Delta J\right] = \sum_a \delta \mathbf{v}_a \cdot \sum_b \left(\mathbf{k}_{ab}^{vJ} + \mathbf{m}_{ab}^{vJ}\right) \Delta J_b$$
$$+ \sum_a \delta J_a \sum_b k_{ab}^{JJ}\, \Delta J_b$$

(3.5.19)

where

$$\mathbf{k}_{ab}^{vJ} = \int_\Omega \left[N_b \boldsymbol{\tau}'_J \cdot \operatorname{grad} N_a + N_a \left(p' \operatorname{grad} N_b + N_b p'' \operatorname{grad} J\right)\right] dv\,,$$

$$\mathbf{m}_{ab}^{vJ} = \int_\Omega -N_a N_b \frac{\rho}{J}\mathbf{a}\, dv\,,$$

(3.5.20)

$$k_{ab}^{JJ} = \int_\Omega -\frac{N_a}{J}\left(\left(\frac{\xi}{\Delta t} - \frac{\dot{J}}{J}\right)N_b + \operatorname{grad} N_b \cdot \mathbf{v}\right) dv\,.$$

For the external work in eq.(4.2.34), its discretized form is

$$\delta W_{ext} = \sum_a \delta \mathbf{v}_a \cdot \left(\mathbf{f}_a^t + \mathbf{f}_a^b\right) + \delta J_a f_a^v\,,$$

(3.5.21)

where

$$\mathbf{f}_a^t = \int_{\partial\Omega} N_a \mathbf{t}^\tau\, da\,,$$

$$\mathbf{f}_a^b = \int_\Omega N_a \rho \mathbf{b}\, dv\,,$$

(3.5.22)

$$f_a^v = \int_\Omega -N_a v_n\, da\,.$$

The discretized form of $D\left(\delta W_{ext}\right)[\Delta J]$ in eq.(3.5.13) is

$$D\left(\delta W_{ext}\right)[\Delta J] = \sum_a \delta\mathbf{v}_a \cdot \sum_b \mathbf{k}_{ab}^{\mathsf{b}}\,\Delta J_b\,, \tag{3.5.23}$$

where

$$\mathbf{k}_{ab}^{\mathsf{b}} = \int_\Omega -N_a N_b \frac{\rho}{J}\mathbf{b}\,dv\,. \tag{3.5.24}$$

3.5.4 Special Boundary Conditions

3.5.4.1 Backflow Stabilization

For arterial blood flow, backflow stabilization has been proposed previously to deal with truncated domains where the entire artery is not modeled explicitly [16, 25]; for these types of problems, letting $\mathbf{t} = \mathbf{0}$ or prescribing a constant pressure at the outflow boundary may not prevent flow reversals that compromise convergence of an analysis. Instead, these authors proposed a velocity-dependent traction boundary condition, $\mathbf{t} = \beta\rho\left(\mathbf{v}\otimes\mathbf{v}\right)\cdot\mathbf{n}$ with a tensile normal component, that counters the backflow (only when $v_n < 0$). Here, β is a non-dimensional user-defined parameter; a value of $\beta = 0$ turns off this feature, while a value of $\beta = 1$ generally shows good numerical performance. We adapt this previously proposed formulation by letting the normal component of the viscous traction be given by

$$t_n^\tau = \begin{cases} \beta\rho_r v_n^2 & v_n < 0 \\ 0 & v_n \geq 0 \end{cases}. \tag{3.5.25}$$

The choice of ρ_r in lieu of ρ is for convenience, to avoid the dependence of ρ on J (which is negligible for nearly incompressible flow). Then, the contribution of this traction to the virtual external work δW_{ext} is

$$\delta G = \int_{\partial\Omega} \delta\mathbf{v} \cdot t_n^\tau \mathbf{n}\,da\,. \tag{3.5.26}$$

The linearization of δG along an increment $\Delta\mathbf{v}$ in the velocity is given by

$$D\delta G\left[\Delta\mathbf{v}\right] = \int_{\partial\Omega} \delta\mathbf{v}\cdot\mathbf{K}_n\cdot\Delta\mathbf{v}\,da\,, \tag{3.5.27}$$

where

$$\mathbf{K}_n = \begin{cases} 2\beta\rho_r v_n\left(\mathbf{n}\otimes\mathbf{n}\right) & v_n < 0 \\ \mathbf{0} & v_n \geq 0 \end{cases}. \tag{3.5.28}$$

The discretized form of δG is

$$\delta G = \sum_a \delta\mathbf{v}_a \cdot \mathbf{f}_a^n\,, \quad \mathbf{f}_a^n = \int_{\partial\Omega} N_a t_n^\tau \mathbf{n}\,da\,, \tag{3.5.29}$$

whereas the discretized form of $D\delta G\left[\Delta\mathbf{v}\right]$ is

$$D\delta G\left[\Delta\mathbf{v}\right] = \sum_a \delta\mathbf{v}_a \cdot \sum_b \mathbf{K}_{ab}^n\cdot\Delta\mathbf{v}_b\,, \quad \mathbf{K}_{ab}^n = \int_{\partial\Omega} N_a N_b \mathbf{K}_n\,da\,. \tag{3.5.30}$$

A (viscous) tangential traction is implemented as a separate flow stabilization method in the next section, applicable to inlet or outlet surfaces, without a conditional requirement based on the sign of v_n.

3.5.4.2 Tangential Flow Stabilization

For certain outlet conditions, using the natural boundary condition $\mathbf{t}_t^\tau = \mathbf{0}$ may lead to flow instabilities. It is possible to minimize these effects by prescribing a tangential viscous traction onto the boundary surface, which opposes this tangential flow. Optionally, this condition may be combined with the backflow stabilization described above.

Similar to the previous section, we introduce a non-dimensional parameter β, with the tangential traction given by

$$\mathbf{t}_t^\tau = -\beta\rho_r \left|\mathbf{v}_t\right| \mathbf{v}_t \,. \tag{3.5.31}$$

This form shows that $\mathbf{t}_t^\tau$ opposes tangential flow. The external virtual work for this traction is

$$\delta G = \int_{\partial\Omega} \delta\mathbf{v} \cdot \mathbf{t}_t^\tau \, da \,. \tag{3.5.32}$$

Its linearization along an increment $\Delta\mathbf{v}$ is

$$D\delta G\left[\Delta\mathbf{v}\right] = \int_{\partial\Omega} \delta\mathbf{v} \cdot \mathbf{K}_t \cdot \Delta\mathbf{v} \, da \,, \tag{3.5.33}$$

where it can be shown that

$$\mathbf{K}_t = -\beta\rho_r \left|\mathbf{v}_t\right| \left(\mathbf{I} - \mathbf{n} \otimes \mathbf{n} + \frac{\mathbf{v}_t}{\left|\mathbf{v}_t\right|} \otimes \frac{\mathbf{v}_t}{\left|\mathbf{v}_t\right|} \right) \,. \tag{3.5.34}$$

The discretized form of δG is

$$\delta G = \sum_a \delta\mathbf{v}_a \cdot \mathbf{f}_a^\tau \,, \quad \mathbf{f}_a^\tau = \int_{\partial\Omega} N_a \mathbf{t}_t^\tau \, da \,. \tag{3.5.35}$$

The discretized form of $D\delta G\left[\Delta\mathbf{v}\right]$ is

$$D\delta G\left[\Delta\mathbf{v}\right] = \sum_a \delta\mathbf{v}_a \cdot \sum_b \mathbf{K}_{ab}^t \cdot \Delta\mathbf{v}_b \,, \quad \mathbf{K}_{ab}^t = \int_{\partial\Omega} N_a N_b \mathbf{K}_t \, da \,. \tag{3.5.36}$$

3.5.4.3 Flow Resistance

Flow resistance is typically implemented when modeling arterial flow, where the finite element domain only describes a portion of an arterial network [63]. A flow resistance may be imposed on downstream boundaries to simulate the resistance produced by the vascular network with its branches and bifurcations. The resistance is equivalent to a mean pressure which is proportional to the volumetric flow rate Q,

$$p = RQ \,, \quad Q = \int_{\partial\Omega} v_n \, da \,,$$

where R is the resistance. Using the pressure-dilatation relation (5.14.5), equivalent to $p = -K \cdot e$, this pressure may be prescribed as an essential boundary condition on the dilatation e.

3.6 Newton-Raphson Method

The Newton-Raphson method (also known as "Newton's method", "Full Newton method" or "the Newton method") is the basis for solving the nonlinear finite element equations. This section will describe the *Full Newton method* and the Broyden-Fletcher-Goldfarb-Shanno (BFGS) method [44]. The latter variation is actually a *quasi-Newton method*. It is important since it provides several advantages over the full Newton method and it is this method that is implemented in FEBio [44].

3.6.1 Full Newton Method

The Newton-Raphson equation (3.1.3) can be written in terms of the discretized equilibrium equations that were derived in the previous section as follows:

$$\delta \mathbf{v}^T \cdot \mathbf{K} \cdot \mathbf{u} = -\delta \mathbf{v}^T \cdot \mathbf{R}. \tag{3.6.1}$$

Since the virtual velocities $\delta \mathbf{v}$ are arbitrary, a discretized Newton-Raphson scheme can be formulated as follows:

$$\mathbf{K}\left(\mathbf{x}_k\right) \cdot \mathbf{u} = -\mathbf{R}\left(\mathbf{x}_k\right); \quad \mathbf{x}_{k+1} = \mathbf{x}_k + \mathbf{u} \ . \tag{3.6.2}$$

This is the basis of the Newton-Raphson method. For each iteration k, both the stiffness matrix and the residual vector are re-evaluated and a displacement increment $\mathbf{u}$ is calculated by pre-multiplying both sides of the above equation by $\mathbf{K}^{-1}$. This procedure is repeated until some convergence criteria are satisfied.

The formation of the stiffness matrix and, especially, calculation of its inverse, are computationally expensive. Quasi-Newton methods do not require the reevaluation of the stiffness matrix for every iteration. Instead, a quick update is calculated. One particular method that has been quite successful in the field of computational solid mechanics is the BFGS method, which is described in the next section.

3.6.2 BFGS Method

The BFGS method updates the stiffness matrix (or rather its inverse) to provide an approximation to the exact matrix. A displacement increment is defined as

$$\mathbf{d}_k = \mathbf{x}_k - \mathbf{x}_{k-1} \ , \tag{3.6.3}$$

and an increment in the residual is defined as

$$\mathbf{G}_k = \mathbf{R}_{k-1} - \mathbf{R}_k \ . \tag{3.6.4}$$

The updated matrix $\mathbf{K}_k$ should satisfy the quasi-Newton equation:

$$\mathbf{K}_k \mathbf{d}_k = \mathbf{G}_k \ . \tag{3.6.5}$$

In order to calculate this update, as displacement increment is first calculated:

$$\mathbf{u} = \mathbf{K}_{k-1}^{-1} \mathbf{R}_{k-1} \ . \tag{3.6.6}$$

This displacement vector defines a "direction" for the actual displacement increment. A line search (see next section) can now be applied to determine the optimal displacement increment:

$$\mathbf{x}_k = \mathbf{x}_{k-1} + s\mathbf{u} \ , \tag{3.6.7}$$

where s is determined from the line search. With the updated position calculated, $\mathbf{R}_k$ can be evaluated. Also, using equations (3.6.3) and (3.6.4), $\mathbf{d}_k$ and $\mathbf{G}_k$ can be evaluted. The stiffness update can now be expressed as

$$\mathbf{K}_k^{-1} = \mathbf{A}_k^T \mathbf{K}_{k-1}^{-1} \mathbf{A}_k \ , \tag{3.6.8}$$

where the matrix $\mathbf{A}$ is an $n \times n$ matrix of the simple form:

$$\mathbf{A}_k = \mathbf{1} + \mathbf{v}_k \mathbf{w}_k^T \ . \tag{3.6.9}$$

The vectors $\mathbf{v}$ and $\mathbf{w}$ are given by

$$\mathbf{v}_k = -\left(\frac{\mathbf{d}_k^T \mathbf{G}_k}{\mathbf{d}_k^T \mathbf{K}_{k-1} \mathbf{d}_k}\right)^{1/2} \mathbf{K}_{k-1} \mathbf{d}_k - \mathbf{G}_k \,, \tag{3.6.10}$$

$$\mathbf{w}_k = \frac{\mathbf{d}_k}{\mathbf{d}_k^T \mathbf{G}_k} \,. \tag{3.6.11}$$

The vector $\mathbf{K}_{k-1} \mathbf{d}_k$ is equal to $s\mathbf{R}_{k-1}$ and has already been calculated.

To avoid numerically dangerous updates, the condition number c of the updating matrix $\mathbf{A}$ is calculated:

$$c = \left(\frac{\mathbf{d}_k^T \mathbf{G}_k}{\mathbf{d}_k^T \mathbf{K}_{k-1} \mathbf{d}_k}\right)^{1/2} \,. \tag{3.6.12}$$

The update is not performed when this number exceeds a preset tolerance.

Considering the actual computations involved, it should be noted that using the matrix updates defined above, the calculation of the search direction in (3.6.6) can be rewritten as,

$$\mathbf{u} = \left(\mathbf{1} + \mathbf{w}_{k-1} \mathbf{v}_{k-1}^T\right) \cdots \left(\mathbf{1} + \mathbf{w}_1 \mathbf{v}_1^T\right) \mathbf{K}_0^{-1} \left(\mathbf{1} + \mathbf{v}_1 \mathbf{w}_1^T\right) \cdots \left(\mathbf{1} + \mathbf{v}_{k-1} \mathbf{w}_{k-1}^T\right) \mathbf{R}_{k-1} \,. \tag{3.6.13}$$

Hence, the search direction can be computed without explicitly calculating the updated matrices or performing any additional costly matrix factorizations as required in the full Newton-Raphson method.

3.6.3 Line Search Method

A powerful technique often used to improve the convergence rate of Newton based methods is the *line search method*. In this method, the direction of the displacement vector $\mathbf{u}$ is considered as optimal, but the magnitude is controlled by a parameter s:

$$\mathbf{x}_{k+1} = \mathbf{x}_k + s\mathbf{u} \,. \tag{3.6.14}$$

The value of s is usually chosen so that the total potential energy $W(s) = W(\mathbf{x}_k + s\mathbf{u})$ at the end of the iteration is minimized in the direction of $\mathbf{u}$. This is equivalent to the requirement that the residual force $\mathbf{R}(\mathbf{x}_k + s\mathbf{u})$ at the end of the iteration is orthogonal to $\mathbf{u}$:

$$R(s) = \mathbf{u}^T \mathbf{R}(\mathbf{x}_k + s\mathbf{u}) = 0 \,. \tag{3.6.15}$$

However, in practice it is sufficient to obtain a value of s such that,

$$|R(s)| < \rho |R(0)| \,, \tag{3.6.16}$$

where typically a value of $\rho = 0.9$ is used. Under normal conditions the value $s = 1$ automatically satisfies equation (3.6.16) and therefore few extra operations are involved. However, when this is not the case, a more suitable value for s needs to be obtained. For this reason it is convenient to approximate $R(s)$ as a quadratic in s:

$$R(s) \approx (1 - s) R(0) + R(1) s^2 = 0 \,, \tag{3.6.17}$$

which yields a value for s as

$$s = \frac{r}{2} \pm \sqrt{\left(\frac{r}{2}\right)^2 - r} \,, \quad r = \frac{R(0)}{R(1)} \,. \tag{3.6.18}$$

If $r < 0$, the square root is positive and a first improved value for s is obtained:

$$s_1 = \frac{r}{2} + \sqrt{\left(\frac{r}{2}\right)^2 - r}.$$ (3.6.19)

If $r > 0$ the s can be obtained by using the value that minimizes the quadratic function, that is, $s_1 = r/2$. This procedure is now repeated with $R(1)$ replaced by $R(s_1)$ until equation (3.6.16) is satisfied.

3.7 Generalized $\alpha-$Method

The generalized $\alpha-$method is used for temporal discretization of governing equations in fluid mechanics. For this method we combine the degrees of freedom into $\mathbf{Y}_n = \{\mathbf{v}, J\}_n$, where the subscript n denotes time t_n; similarly, we let $\dot{\mathbf{Y}}_n = \left\{\frac{\partial \mathbf{v}}{\partial t}, \frac{\partial J}{\partial t}\right\}_n$. According to this method [36], the virtual work is evaluated at $\delta W\left(\dot{\mathbf{Y}}_{n+\alpha_m}, \mathbf{Y}_{n+\alpha_f}\right)$, where $t_{n+\alpha} = t_n + \alpha\Delta t$ and $\Delta t = t_{n+1} - t_n$. The parameters α_f and α_m are evaluated from a single parameter ρ_∞ using

$$\alpha_f = \frac{1}{1 + \rho_\infty}, \quad \alpha_m = \frac{1}{2}\frac{3 - \rho_\infty}{1 + \rho_\infty},$$ (3.7.1)

where $0 \leq \rho_\infty \leq 1$. This parameter is the spectral radius for an infinite time step, which controls the amount of damping of high frequencies; a value of zero produces the greatest amount of damping, anihilating the highest frequency in one step, whereas a value of one preserves the highest frequency.

The linearization of δW reported in Section 3.5.2 is effectively performed along $\Delta\mathbf{Y}_{n+\alpha_f}$ so that the solution to $\delta W = 0$ produces $\mathbf{Y}_{n+\alpha_f}$. The parameter ξ used in eqs.(3.5.6)-(3.5.7) is given by

$$\xi = \frac{\alpha_m}{\gamma\alpha_f}, \quad \gamma = \frac{1}{2} + \alpha_m - \alpha_f.$$ (3.7.2)

In this scheme, $\dot{\mathbf{Y}}_{n+\alpha_m}$ is evaluated from

$$\dot{\mathbf{Y}}_{n+\alpha_m} = \left(1 - \frac{\alpha_m}{\gamma}\right)\dot{\mathbf{Y}}_n + \frac{\xi}{\Delta t}\left(\mathbf{Y}_{n+\alpha_f} - \mathbf{Y}_n\right).$$ (3.7.3)

Given the solution $\left(\dot{\mathbf{Y}}_{n+\alpha_m}, \mathbf{Y}_{n+\alpha_f}\right)$, the solution at t_{n+1} is evaluated from

$$\mathbf{Y}_{n+1} = \mathbf{Y}_n + \frac{\mathbf{Y}_{n+\alpha_f} - \mathbf{Y}_n}{\alpha_f},$$

$$\dot{\mathbf{Y}}_{n+1} = \dot{\mathbf{Y}}_n + \frac{\dot{\mathbf{Y}}_{n+\alpha_m} - \dot{\mathbf{Y}}_n}{\alpha_m}.$$ (3.7.4)

Four different options are presented in [36] for initializing $\mathbf{Y}_{n+1}$ and $\dot{\mathbf{Y}}_{n+1}$ at the beginning of time step t_{n+1}; the first three of these have been implemented in FEBio. For steady flows these authors recommend disregarding ρ_∞ and setting $\alpha_f = \alpha_m = \gamma = 1$ to recover the backward Euler scheme.

Chapter 4

Element Library

FEBio provides several element types for finite element discretization. This chapter describes these elements in more detail.

4.1 Solid Elements

The 3D solid elements available in FEBio are *isoparametric elements*. All of the solid elements are formulated in a global Cartesian coordinate system. For all these elements, a local coordinate system (so-called *isoparametric coordinates*) is defined as well. The global position vector $\mathbf{x}$ can be written as a function of the isoparametric coordinates in the following sense:

$$\mathbf{x}\left(r,s,t\right) = \sum_{i=1}^{n} N_i\left(r,s,t\right)\mathbf{x}_i.\tag{4.1.1}$$

Here, n is the number of nodes, r, s and t are the isoparametric coordinates, N_i are the element shape functions and $\mathbf{x}_i$ are the spatial coordinates of the element nodes. The same parametric interpolation is used for the interpolation of other scalar and vector quantities.

All elements in FEBio are integrated numerically. This implies that integrals over the volume of the element v^e are approximated by a sum:

$$\int_{v^e} f\left(\mathbf{x}\right)\,dv = \int_{\square^e} f\left(\mathbf{r}\right) J(\mathbf{r})d\square \cong \sum_{i=1}^{m} f\left(\mathbf{r}_i\right) J_i w_i\,.\tag{4.1.2}$$

Here, $\square$ is the biunit cube, m is the number of integration points, $\mathbf{r}_i$ are the location of the integration points in isoparametric coordinates, J is the Jacobian of the transformation $\mathbf{x} = \mathbf{x}\left(r,s,t\right)$, and w_i is a weight associated with the integration point. The integration is performed over the element's volume in the natural coordinate system.

Most fully integrated solid elements are unsuitable for the analysis of (nearly-) incompressible material behavior. To deal with this type of deformation, a three-field element implementation is available in FEBio [55].

4.1.1 Hexahedral Elements

FEBio implements an 8-node trilinear hexahedral element. This element is also known as a *brick* element. The shape functions for these elements are defined in function of the isoparametric

coordinates r, s and t, and are given below.

$$N_1 = \frac{1}{8} (1 - r) (1 - s) (1 - t)$$
$$N_2 = \frac{1}{8} (1 + r) (1 - s) (1 - t)$$
$$N_3 = \frac{1}{8} (1 + r) (1 + s) (1 - t)$$
$$N_4 = \frac{1}{8} (1 - r) (1 + s) (1 - t)$$
$$N_5 = \frac{1}{8} (1 - r) (1 - s) (1 + t)$$
$$N_6 = \frac{1}{8} (1 + r) (1 - s) (1 + t)$$
$$N_7 = \frac{1}{8} (1 + r) (1 + s) (1 + t)$$
$$N_8 = \frac{1}{8} (1 - r) (1 + s) (1 + t)$$

(4.1.3)

The following integration rule is implemented for this element type.

8-point Gauss rule			
r	s	t	w
-0.577350269	-0.577350269	-0.577350269	1
0.577350269	-0.577350269	-0.577350269	1
0.577350269	0.577350269	-0.577350269	1
-0.577350269	0.577350269	-0.577350269	1
-0.577350269	-0.577350269	0.577350269	1
0.577350269	-0.577350269	0.577350269	1
0.577350269	0.577350269	0.577350269	1
-0.577350269	0.577350269	0.577350269	1

4.1.2   Pentahedral Elements

Pentahedral elements (also knows as "wedge" elements) consist of six nodes and five faces. Their shape functions are defined in function of the isoparametric coordinates r, s and t and are given

as follows.

$$N_1 = \frac{1}{2}\left(1 - r - s\right)\left(1 - t\right)$$
$$N_2 = \frac{1}{2}r\left(1 - t\right)$$
$$N_3 = \frac{1}{2}s\left(1 - t\right)$$
$$N_4 = \frac{1}{2}\left(1 - r - s\right)\left(1 + t\right) \qquad (4.1.4)$$
$$N_5 = \frac{1}{2}r\left(1 + t\right)$$
$$N_6 = \frac{1}{2}s\left(1 + t\right)$$

The following integration rule is implemented for this element type.

6-point Gauss rule			
r	s	t	w
0.166666667	0.166666667	-0.577350269	0.166666667
0.666666667	0.166666667	-0.577350269	0.166666667
0.166666667	0.666666667	-0.577350269	0.166666667
0.166666667	0.166666667	0.577350269	0.166666667
0.666666667	0.166666667	0.577350269	0.166666667
0.166666667	0.666666667	0.577350269	0.166666667

4.1.3 Tetrahedral Elements

Linear 4-node tetrahedral elements are also available in FEBio. Their shape functions are defined in function of the isoparametric coordinates r, s and t.

$$N_1 = 1 - r - s - t$$
$$N_2 = r$$
$$N_3 = s \qquad (4.1.5)$$
$$N_4 = t$$

The following integration rules are implemented for this element type.

1-point Gauss rule			
r	s	t	w
0.25	0.25	0.25	0.166666667

4-point Gauss rule			
r	s	t	w
0.13819660	0.13819660	0.13819660	0.041666667
0.58541020	0.13819660	0.13819660	0.041666667
0.13819660	0.58541020	0.13819660	0.041666667
0.13819660	0.13819660	0.58541020	0.041666667
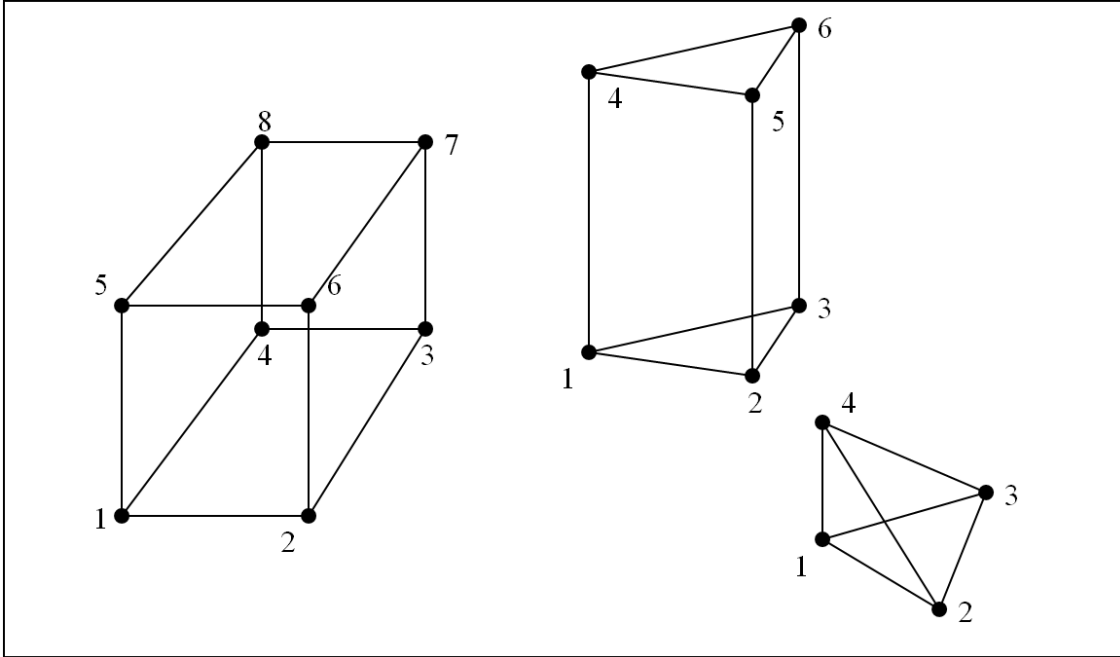
Different solid element types that are available in FEBio

4.1.4   Quadratic Tetrahedral Elements

FEBio implements a 10-node quadratic tetrahedral element. It has four corner nodes and six nodes located at the midpoint of the edges. The shape functions in terms area coordinates are given below. The area coordinates relate to the isoparametric coordinates as follows.

$$
\begin{aligned}
t_1 &= 1 - r - s - t \\
t_2 &= r \\
t_3 &= s \\
t_4 &= t
\end{aligned}
\qquad (4.1.6)
$$

The shape functions follow.

$$
\begin{aligned}
H_i &= t_i\left(2t_i - 1\right), \; i = 1 \cdots 4 \\
H_5 &= 4t_1 t_2 \\
H_6 &= 4t_2 t_3 \\
H_7 &= 4t_3 t_1 \\
H_8 &= 4t_1 t_4 \\
H_9 &= 4t_2 t_4 \\
H_{10} &= 4t_3 t_4
\end{aligned}
\qquad (4.1.7)
$$

The following integration rules are implemented for this element type.

4-point Gauss rule			
r	s	t	w

0.58541020	0.13819660	0.13819660	0.041666667
0.13819660	0.58541020	0.13819660	0.041666667
0.13819660	0.13819660	0.58541020	0.041666667
0.13819660	0.13819660	0.13819660	0.041666667

8-point Gauss rule			
r	s	t	w
0.01583591	0.328054697	0.328054697	0.023087995
0.328054697	0.01583591	0.328054697	0.023087995
0.328054697	0.328054697	0.01583591	0.023087995
0.328054697	0.328054697	0.328054697	0.023087995
0.679143178	0.106952274	0.106952274	0.018578672
0.106952274	0.679143178	0.106952274	0.018578672
0.106952274	0.106952274	0.679143178	0.018578672
0.106952274	0.106952274	0.106952274	0.018578672

11-point Gauss-Lobatto rule			
r	s	t	w
0	0	0	0.002777778
1	0	0	0.002777778
0	1	0	0.002777778
0	0	1	0.002777778
0.5	0	0	0.011111111
0.5	0.5	0	0.011111111
0	0.5	0	0.011111111
0	0	0.5	0.011111111
0.5	0	0.5	0.011111111
0	0.5	0.5	0.011111111
0.25	0.25	0.25	0.088888889

FEBio also implements a 15-node quadratic tetrahedral element.
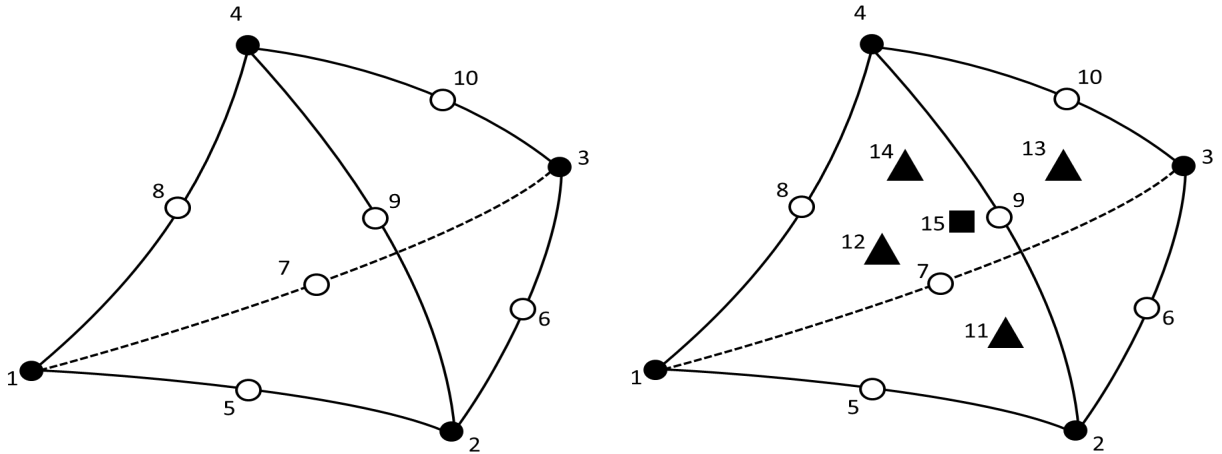
Quadratic tetrahedral elements available in FEBio. Left, a 10-node quadratic tet. Right, a 15-node quadratic tet.

The following integration rules are implemented for this element type.

8-point Gauss rule[1]			
r	**s**	**t**	**w**
0.0158359099	0.3280546970	0.3280546970	0.138527967
0.3280546970	0.0158359099	0.3280546970	0.138527967
0.3280546970	0.3280546970	0.0158359099	0.138527967
0.3280546970	0.3280546970	0.3280546970	0.138527967
0.6791431780	0.1069522740	0.1069522740	0.111472033
0.1069522740	0.6791431780	0.1069522740	0.111472033
0.1069522740	0.1069522740	0.6791431780	0.111472033
0.1069522740	0.1069522740	0.1069522740	0.111472033

11-point Gauss rule			
r	**s**	**t**	**w**
0.25	0.25	0.25	-0.01315555556
0.071428571428571	0.071428571428571	0.071428571428571	0.007622222222
0.785714285714286	0.071428571428571	0.071428571428571	0.007622222222
0.071428571428571	0.785714285714286	0.071428571428571	0.007622222222
0.071428571428571	0.071428571428571	0.785714285714286	0.007622222222
0.399403576166799	0.100596423833201	0.100596423833201	0.024888888889
0.100596423833201	0.399403576166799	0.100596423833201	0.024888888889
0.100596423833201	0.100596423833201	0.399403576166799	0.024888888889
0.399403576166799	0.399403576166799	0.100596423833201	0.024888888889
0.399403576166799	0.100596423833201	0.399403576166799	0.024888888889
0.100596423833201	0.399403576166799	0.399403576166799	0.024888888889

[1] Note that weights sum up to one and not to the volume of the tet in the natural coordinate system (i.e. 1/6).

15-point Gauss rule			
r	s	t	w
0.25	0.25	0.25	0.030283678097089
0.333333333333333	0.333333333333333	0.333333333333333	0.006026785714286
0.000000000000000	0.333333333333333	0.333333333333333	0.006026785714286
0.333333333333333	0.000000000000000	0.333333333333333	0.006026785714286
0.333333333333333	0.333333333333333	0.000000000000000	0.006026785714286
0.090909090909091	0.090909090909091	0.090909090909091	0.011645249086029
0.727272727272727	0.090909090909091	0.090909090909091	0.011645249086029
0.090909090909091	0.727272727272727	0.090909090909091	0.011645249086029
0.090909090909091	0.090909090909091	0.727272727272727	0.011645249086029
0.433449846426336	0.066550153573664	0.066550153573664	0.010949141561386
0.066550153573664	0.433449846426336	0.066550153573664	0.010949141561386
0.066550153573664	0.066550153573664	0.433449846426336	0.010949141561386
0.066550153573664	0.433449846426336	0.433449846426336	0.010949141561386
0.433449846426336	0.066550153573664	0.433449846426336	0.010949141561386
0.433449846426336	0.433449846426336	0.066550153573664	0.010949141561386

4.2 Shell Elements

Historically, shells have been formulated using two different approaches [33]. The difference between these approaches lies in the way the rotational degrees of freedom are defined. In the first approach, the rotational degrees of freedom are defined as angles. In addition, the plane stress condition needs to be enforced to take thickness variations into account. This approach is very useful for infinitesimal strains, but becomes very difficult to pursue in finite deformation due to the fact that finite rotations do not commute. Another disadvantage of this approach is that it requires a modification to the material formulation to enforce the plane stress condition. For complex materials this modification is very difficult or even impossible to obtain.

The alternative approach is to use an *extensible director* to describe the rotational degrees of freedom. With this approach it is not necessary to enforce the plane-stress condition and the full 3D constitutive relations can be employed. This approach is adapted in FEBio as described here.

The shell formulation implemented in FEBio is still a work in progress. The goal is to implement an extensible director formulation with strain enhancements to deal with the well-known locking effect in incompressible and bending problems [18]. With the current state of the implementation, it is advised to use quadratic elements in such problems.

Starting with FEBio 2.6, two shell formulations have become available: The original formulation, where nodes are located at the mid-surface through the thickness of the shell, and a new formulation where nodes are located on the front face of the shell. The original formulation uses nodal displacements and directors as degrees of freedom; the new formulation uses front and back face nodal displacements. The new formulation is designed to properly accommodate shells attached to the surface of a solid element, or shells sandwiched between two solid elements, with

minimal alterations to the rest of the code. The original formulation does not strictly enforce continuity of all the relevant degrees of freedom in those situations. However, this original formulation is maintained in the code for backward compatibility.

4.2.1   Shell with mid-surface nodal displacements

We create a shell formulation by reducing a solid element interpolation which is linear along the parametric coordinate ξ_3. We start with the general interpolation for a solid element,

$$\mathbf{x}\left(\xi_i\right) = \sum_{a=1}^{n} N_a\left(\xi_i\right)\mathbf{x}_a, \tag{4.2.1}$$

where $i = 1, 2, 3$ and n is the number of nodes, and specialize it to the case of a shell as

$$N_a\left(\xi_i\right) = \begin{cases} \frac{1-\xi_3}{2}M_a\left(\xi_\alpha\right) & 1 \leqslant a \leqslant m \\ \frac{1+\xi_3}{2}M_a\left(\xi_\alpha\right) & m+1 \leqslant a \leqslant n \end{cases}, \tag{4.2.2}$$

where $\alpha = 1, 2$, $m = n/2$ is the number of shell element nodes, and $M_a\left(\xi_\alpha\right)$ are the interpolation functions within the mid-shell surface. The description of the mid-shell surface is thus given by

$$\hat{\mathbf{x}}\left(\xi_\alpha\right) = \sum_{a=1}^{n} N_a\left(\xi_1, \xi_2, 0\right)\mathbf{x}_a \equiv \sum_{b=1}^{m} M_b\left(\xi_\alpha\right)\hat{\mathbf{x}}_b, \tag{4.2.3}$$

where

$$\hat{\mathbf{x}}_b = \frac{1}{2}\left(\mathbf{x}_b + \mathbf{x}_{b+m}\right) \tag{4.2.4}$$

are the nodal positions for the mid-shell surface.
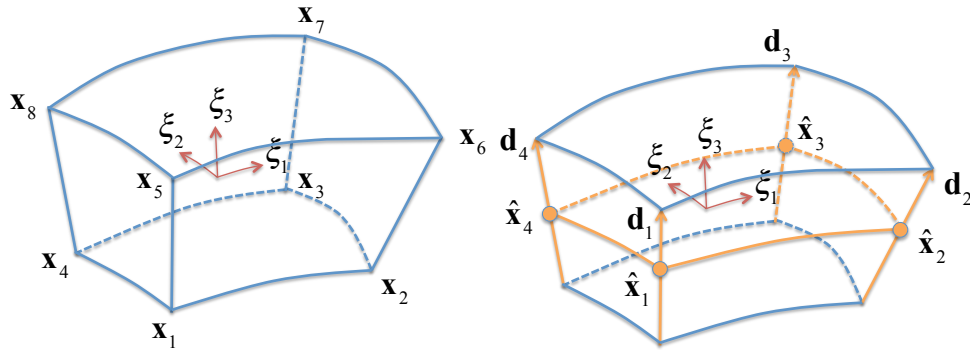
Example of shell elements with four mid-surface nodal positions $\hat{\mathbf{x}}_b$ and directors $\mathbf{d}_b$ ($b = 1 - 4$), reduced from a solid element.

We also define the director across the shell surface as

$$\mathbf{d}\left(\xi_\alpha\right) = \mathbf{x}\left(\xi_1, \xi_2, 1\right) - \mathbf{x}\left(\xi_1, \xi_2, -1\right) = \sum_{b=1}^{m} M_b\left(\xi_\alpha\right)\mathbf{d}_b, \tag{4.2.5}$$

where

$$\mathbf{d}_b = \mathbf{x}_{b+m} - \mathbf{x}_b, \quad b = 1 - m \tag{4.2.6}$$

are the nodal directors. Note that the magnitude of the nodal director represents the shell thickness, $h(\xi_\alpha) = \|\mathbf{d}(\xi_\alpha)\|$ and the shell thicknesses at the nodes are $h_b = \|\mathbf{d}_b\|$. With these definitions we find that the interpolation across the parametric space of the shell element is

$$\mathbf{x}(\xi_i) = \hat{\mathbf{x}}(\xi_\alpha) + \frac{1}{2}\xi_3\mathbf{d}(\xi_\alpha) = \sum_{b=1}^{m} M_b(\xi_\alpha)\left(\hat{\mathbf{x}}_b + \frac{1}{2}\xi_3\mathbf{d}_b\right). \tag{4.2.7}$$

From this relation we can obtain the covariant basis vectors as

$$\begin{aligned} \mathbf{g}_\alpha(\xi_i) &= \frac{\partial\mathbf{x}}{\partial\xi_\alpha} = \sum_{b=1}^{m}\frac{\partial M_b}{\partial\xi_\alpha}\left(\hat{\mathbf{x}}_b + \frac{1}{2}\xi_3\mathbf{d}_b\right) \\ \mathbf{g}_3(\xi_i) &= \frac{\partial\mathbf{x}}{\partial\xi_3} = \frac{1}{2}\sum_{b=1}^{m}M_b(\xi_\alpha)\mathbf{d}_b \end{aligned}, \tag{4.2.8}$$

from which we may evaluate the contravariant basis vectors $\mathbf{g}^j$ using the identity $\mathbf{g}_i \cdot \mathbf{g}^j = \delta_i^j$. Then, the gradients of the shape functions are given by

$$\operatorname{grad} M_b = \frac{\partial M_b}{\partial\xi_\alpha}\mathbf{g}^\alpha, \quad \operatorname{grad}\left(\frac{1}{2}\xi_3 M_b\right) = \frac{1}{2}\left(\xi_3\operatorname{grad} M_b + M_b\mathbf{g}^3\right). \tag{4.2.9}$$

It follows from (4.2.7) that the virtual displacement is

$$\delta\mathbf{u}(\xi_i) = \sum_{a=1}^{m}M_a(\xi_\alpha)\left(\delta\hat{\mathbf{u}}_a + \frac{1}{2}\xi_3\delta\mathbf{d}_a\right), \tag{4.2.10}$$

and the incremental displacement is

$$\Delta\mathbf{u}(\xi_i) = \sum_{b=1}^{m}M_b(\xi_\alpha)\left(\Delta\hat{\mathbf{u}}_b + \frac{1}{2}\xi_3\Delta\mathbf{d}_b\right). \tag{4.2.11}$$

In FEBio, for historical reasons, the nodal director $\mathbf{d}_b$ is currently called *rotation*. This is a misnomer and users should treat this *rotation* as the vector $\mathbf{d}_a$ whose components have units of length. Thus, fixing or prescribing *rotation* components in the input file effectively places these constraints on the components of the nodal director; similarly, requesting *rotation* in the output files will produce the components of the director.

When this type of shell is connected face-to-face with a solid element, the nodes located at $\hat{\mathbf{x}}_b$ automatically share their displacement degrees of freedom $\mathbf{u}_b$ with the corresponding nodes from the face of the solid element. However, no continuity is enforced between the directors $\mathbf{d}_b$ and the solid element deformation. One consequence of this condition is that a shell sandwiched between two solid elements will not detect out-of-plane shear and normal stresses transmitted by the solid element(s). Another consequence is that bending of the solid element(s) will not produce a bending moment in the shell. Therefore, these shell elements are best used as shell-only structures.

4.2.1.1 Elastic Shell

For an elastic shell, the internal virtual work becomes

$$\delta W_{\text{int}}^e = \int_{\Omega^e} \boldsymbol{\sigma} : \operatorname{grad}\delta\mathbf{u}\, dv = \sum_{a=1}^{n}\begin{bmatrix}\delta\hat{\mathbf{u}}_a & \delta\mathbf{d}_a\end{bmatrix}\cdot\begin{bmatrix}\mathbf{f}_a^u \\ \mathbf{f}_a^d\end{bmatrix}, \tag{4.2.12}$$

where

$$\mathbf{f}_a^u = \int_{\Omega^e} \boldsymbol{\sigma} \cdot \operatorname{grad} M_a \, dv, \quad \mathbf{f}_a^d = \int_{\Omega^e} \boldsymbol{\sigma} \cdot \operatorname{grad} \left(\frac{1}{2} \xi_3 M_a \right) \, dv . \tag{4.2.13}$$

The linearization of the internal virtual work is

$$\begin{aligned} D\left(\delta W_{\mathsf{int}}^e\right)[\Delta \mathbf{u}] &= \int_{\Omega^e} \operatorname{tr}\left(\operatorname{grad} \Delta \mathbf{u} \cdot \boldsymbol{\sigma} \cdot \operatorname{grad}^T \delta \mathbf{u}\right) \, dv \\ &+ \int_{\Omega^e} \operatorname{grad} \delta \mathbf{u} : \boldsymbol{\mathcal{C}} : \operatorname{grad}^T \Delta \mathbf{u} \, dv \end{aligned} \tag{4.2.14}$$

The first of these integrals may be discretized as

$$\int_{\Omega^e} \operatorname{tr}\left(\operatorname{grad} \Delta \mathbf{u} \cdot \boldsymbol{\sigma} \cdot \operatorname{grad}^T \delta \mathbf{u}\right) \, dv = \sum_{a=1}^{m} \sum_{b=1}^{m} \begin{bmatrix} \delta \hat{\mathbf{u}}_a & \delta \mathbf{d}_a \end{bmatrix} \begin{bmatrix} \mathbf{K}_{ab}^{uu} & \mathbf{K}_{ab}^{ud} \\ \mathbf{K}_{ab}^{du} & \mathbf{K}_{ab}^{dd} \end{bmatrix} \begin{bmatrix} \Delta \hat{\mathbf{u}}_b \\ \Delta \mathbf{d}_b \end{bmatrix}, \tag{4.2.15}$$

where

$$\mathbf{K}_{ab}^{uu} = \int_{\Omega^e} \left(\operatorname{grad} M_a \cdot \boldsymbol{\sigma} \cdot \operatorname{grad} M_b \right) \mathbf{I} \, dv$$

$$\mathbf{K}_{ab}^{ud} = \int_{\Omega^e} \left(\operatorname{grad} M_a \cdot \boldsymbol{\sigma} \cdot \operatorname{grad} \left(\frac{1}{2} \xi_3 M_b \right) \right) \mathbf{I} \, dv$$

$$\mathbf{K}_{ab}^{du} = \int_{\Omega^e} \left(\operatorname{grad} \left(\frac{1}{2} \xi_3 M_a \right) \cdot \boldsymbol{\sigma} \cdot \operatorname{grad} M_b \right) \mathbf{I} \, dv \tag{4.2.16}$$

$$\mathbf{K}_{ab}^{dd} = \int_{\Omega^e} \left(\operatorname{grad} \left(\frac{1}{2} \xi_3 M_a \right) \cdot \boldsymbol{\sigma} \cdot \operatorname{grad} \left(\frac{1}{2} \xi_3 M_b \right) \right) \mathbf{I} \, dv$$

The second integral in (4.2.14) becomes

$$\int_{\Omega^e} \operatorname{grad} \delta \mathbf{u} : \boldsymbol{\mathcal{C}} : \operatorname{grad}^T \Delta \mathbf{u} \, dv = \sum_{a=1}^{m} \sum_{b=1}^{m} \begin{bmatrix} \delta \hat{\mathbf{u}}_a & \delta \mathbf{d}_a \end{bmatrix} \begin{bmatrix} \mathbf{K}_{ab}^{uu} & \mathbf{K}_{ab}^{ud} \\ \mathbf{K}_{ab}^{du} & \mathbf{K}_{ab}^{dd} \end{bmatrix} \begin{bmatrix} \Delta \hat{\mathbf{u}}_b \\ \Delta \mathbf{d}_b \end{bmatrix}, \tag{4.2.17}$$

where

$$\mathbf{K}_{ab}^{uu} = \int_{\Omega^e} \operatorname{grad} M_a \cdot \boldsymbol{\mathcal{C}} \cdot \operatorname{grad} M_b \, dv$$

$$\mathbf{K}_{ab}^{ud} = \int_{\Omega^e} \operatorname{grad} M_a \cdot \boldsymbol{\mathcal{C}} \cdot \operatorname{grad} \left(\frac{1}{2} \xi_3 M_b \right) \, dv$$

$$\mathbf{K}_{ab}^{du} = \int_{\Omega^e} \operatorname{grad} \left(\frac{1}{2} \xi_3 M_a \right) \cdot \boldsymbol{\mathcal{C}} \cdot \operatorname{grad} M_b \, dv \tag{4.2.18}$$

$$\mathbf{K}_{ab}^{dd} = \int_{\Omega^e} \operatorname{grad} \left(\frac{1}{2} \xi_3 M_a \right) \cdot \boldsymbol{\mathcal{C}} \cdot \operatorname{grad} \left(\frac{1}{2} \xi_3 M_b \right) \, dv$$

Similar expressions may be derived for the external work and inertia forces.

In FEBio a 3-point Gaussian quadrature rule is used for the through-the-thickness integration. FEBio currently supports four- and eight-node quadrilateral and three- and six-node triangular shell elements.

4.2.1.2 Quadrilateral shells

For four-node quadrilateral shells, the shape functions are given by

$$
\begin{aligned}
M_1 &= \frac{1}{4}\left(1-r\right)\left(1-s\right) \\
M_2 &= \frac{1}{4}\left(1+r\right)\left(1-s\right) \\
M_3 &= \frac{1}{4}\left(1+r\right)\left(1+s\right) \\
M_4 &= \frac{1}{4}\left(1-r\right)\left(1+s\right)
\end{aligned}
\tag{4.2.19}
$$

For eight-node quadrilateral shells the shape functions are

$$
\begin{aligned}
M_1 &= \frac{1}{4}\left(1-r\right)\left(1-s\right)-\frac{1}{2}\left(M_8+M_5\right) & M_5 &= \frac{1}{2}\left(1-r^2\right)\left(1-s\right) \\
M_2 &= \frac{1}{4}\left(1+r\right)\left(1-s\right)-\frac{1}{2}\left(M_5+M_6\right) & M_6 &= \frac{1}{2}\left(1-s^2\right)\left(1+r\right) \\
M_3 &= \frac{1}{4}\left(1+r\right)\left(1+s\right)-\frac{1}{2}\left(M_6+M_7\right) & M_7 &= \frac{1}{2}\left(1-r^2\right)\left(1+s\right) \\
M_4 &= \frac{1}{4}\left(1-r\right)\left(1+s\right)-\frac{1}{2}\left(M_7+M_8\right) & M_8 &= \frac{1}{2}\left(1-s^2\right)\left(1-r\right)
\end{aligned}
\tag{4.2.20}
$$

4.2.1.3 Triangular shells

For three-node triangular shell elements, the shape functions are given by

$$
\begin{aligned}
M_1 &= 1-r-s \\
M_2 &= r \\
M_3 &= s
\end{aligned}
\tag{4.2.21}
$$

For six-node triangular shell elements they are

$$
\begin{aligned}
M_1 &= r_1\left(2r_1-1\right) & M_4 &= 4r_1 r_2 \\
M_2 &= r_2\left(2r_2-1\right) & M_5 &= 4r_2 r_3 \\
M_3 &= r_3\left(2r_3-1\right) & M_6 &= 4r_3 r_1 \\
r_1 &= 1-r-s & r_2 &= r & r_3 &= s
\end{aligned}
\tag{4.2.22}
$$
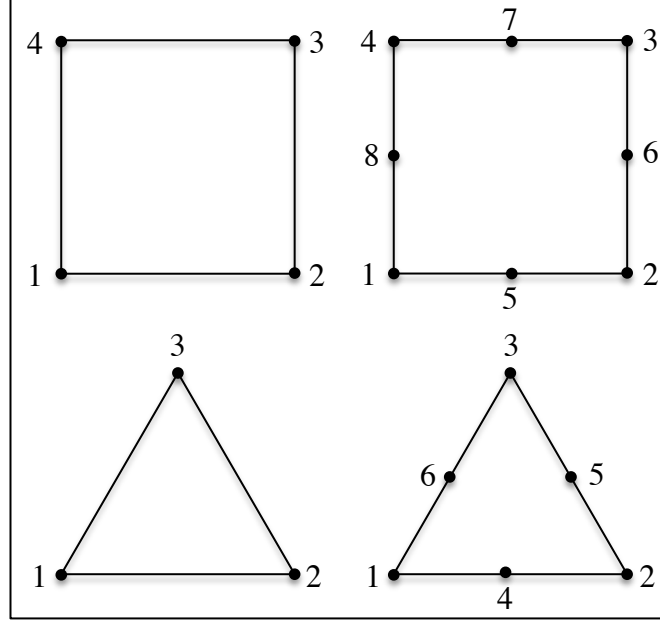
Different shell elements available in FEBio.

4.2.2   Shells with front and back face nodal displacements

We create a shell formulation by reducing a 3D element interpolation which is linear along ξ_3. The nodal positions at the back of the shell ($\xi_3 = -1$) are denoted by $\mathbf{y}_a$ and those on the front of the shell ($\xi_3 = +1$) are denoted by $\mathbf{x}_a$, thus

$$\mathbf{x}(\xi_i) = \sum_a M_a(\xi_1, \xi_2) \left(\frac{1 + \xi_3}{2} \mathbf{x}_a + \frac{1 - \xi_3}{2} \mathbf{y}_a \right) = \sum_a M_a(\xi_1, \xi_2) \left(\mathbf{x}_a - \frac{1 - \xi_3}{2} \mathbf{d}_a \right) \qquad (4.2.23)$$

The vector from $\mathbf{y}_a$ to $\mathbf{x}_a$ is the director, $\mathbf{d}_a$,

$$\mathbf{d}_a = \mathbf{x}_a - \mathbf{y}_a$$

From this relation we can get the shell covariant basis vectors,

$$\mathbf{g}_\alpha(\xi_i) = \frac{\partial \mathbf{x}}{\partial \xi_\alpha} = \sum_a \frac{\partial M_a}{\partial \xi_\alpha} \left(\frac{1 + \xi_3}{2} \mathbf{x}_a + \frac{1 - \xi_3}{2} \mathbf{y}_a \right) = \sum_a \frac{\partial M_a}{\partial \xi_\alpha} \left(\mathbf{x}_a - \frac{1 - \xi_3}{2} \mathbf{d}_a \right)$$

$$\mathbf{g}_3(\xi_i) = \frac{\partial \mathbf{x}}{\partial \xi_3} = \sum_a \frac{1}{2} M_a(\xi_1, \xi_2)(\mathbf{x}_a - \mathbf{y}_a) = \sum_a \frac{1}{2} M_a(\xi_1, \xi_2) \mathbf{d}_a$$

$$(4.2.24)$$

from which we may evaluate the contravariant basis vectors $\mathbf{g}^i$. Let the front-face and back-face displacements be denoted by $\mathbf{u}$ and $\mathbf{w}$, respectively. It follows that $\mathbf{x}_a = \mathbf{X}_a + \mathbf{u}_a$ and $\mathbf{y}_a = \mathbf{Y}_a + \mathbf{w}_a$, where $\mathbf{X}_a$ represents the shell nodal positions in the reference configuration, provided as nodal coordinates in the input file, and $\mathbf{Y}_a = \mathbf{X}_a - \mathbf{D}_a$ is evaluated from the user-defined referential shell thickness, and the surface surface normals evaluated at each node. If the shell surface is not planar in the reference configuration, users must be careful to select shell thicknesses that don't produce inverted elements (negative Jacobians) as a result of this extrapolation.
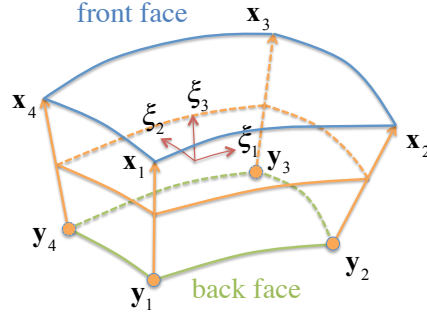
Example of shell element with front-face nodal positions $\mathbf{x}_b$ and back-face nodal positions $\mathbf{y}_b$ ($b = 1 - 4$), reduced from a solid element.

It follows that the virtual displacement is

$$\delta \mathbf{u}\left(\xi_i\right) = \sum_a M_a \left(\frac{1+\xi_3}{2}\delta \mathbf{u}_a + \frac{1-\xi_3}{2}\delta \mathbf{w}_a\right), \tag{4.2.25}$$

and the incremental displacement is

$$\Delta \mathbf{u}\left(\xi_i\right) = \sum_b M_b \left(\frac{1+\xi_3}{2}\Delta \mathbf{u}_b + \frac{1-\xi_3}{2}\Delta \mathbf{w}_b\right), \tag{4.2.26}$$

so that

$$\operatorname{grad} \delta \mathbf{u} = \sum_a \delta \mathbf{u}_a \otimes \operatorname{grad}\left(\frac{1+\xi_3}{2}M_a\right) + \delta \mathbf{w}_a \otimes \operatorname{grad}\left(\frac{1-\xi_3}{2}M_a\right), \tag{4.2.27}$$

and

$$\operatorname{grad} \Delta \mathbf{u} = \sum_b \Delta \mathbf{u}_b \otimes \operatorname{grad}\left(\frac{1+\xi_3}{2}M_b\right) + \Delta \mathbf{w}_b \otimes \operatorname{grad}\left(\frac{1-\xi_3}{2}M_b\right) \tag{4.2.28}$$

Note that

$$\operatorname{grad} M_b = \frac{\partial M_b}{\partial \xi_\alpha}\mathbf{g}^\alpha, \tag{4.2.29}$$

so that

$$\operatorname{grad}\left(\frac{1+\xi_3}{2}M_b\right) = \frac{1}{2}\left((1+\xi_3)\operatorname{grad} M_b + M_b \mathbf{g}^3\right) \tag{4.2.30}$$

and

$$\operatorname{grad}\left(\frac{1-\xi_3}{2}M_b\right) = \frac{1}{2}\left((1-\xi_3)\operatorname{grad} M_b - M_b \mathbf{g}^3\right) \tag{4.2.31}$$

To evaluate the deformation gradient in this shell element, we use

$$\mathbf{F} = \operatorname{Grad}\mathbf{x} = \sum_b \mathbf{u}_b \otimes \operatorname{Grad}\left(\frac{1+\xi_3}{2}M_b\right) + \mathbf{w}_b \otimes \operatorname{grad}\left(\frac{1-\xi_3}{2}M_b\right)$$

For this formulation, when a shell element is connected face-to-face with a solid element, the nodal displacements of the solid element face are set to coincide with the back-face nodal displacements $\mathbf{w}_b$ of the shell. When a user prescribes displacement components on that shared face, they apply to the front-face displacements $\mathbf{u}_b$. Similarly, prescribed pressures and contact pressures act on the shell front face.

When a shell element is sandwiched between two solid elements, the nodal displacements of the solid element facing the shell back face are set to coincide with the shell back-face nodal displacements $\mathbf{w}_b$, whereas the nodal displacements of the solid element facing the shell front face are set to coincide with the shell front-face nodal displacements $\mathbf{u}_a$. If the shell thickness exceeds the thickness of the solid element connected to its back face, results become unpredictable.

4.2.2.1   Elastic Shell

For an elastic solid, the internal virtual work is

$$
\begin{aligned}
\delta W_{int} &= \int_v \boldsymbol{\sigma} : \operatorname{grad} \delta \mathbf{u} \, dv \\
&= \sum_a \begin{bmatrix} \delta \mathbf{u}_a & \delta \mathbf{w}_a \end{bmatrix} \begin{bmatrix} \mathbf{f}_a^u \\ \mathbf{f}_a^w \end{bmatrix},
\end{aligned}
\tag{4.2.32}
$$

where

$$
\begin{aligned}
\mathbf{f}_a^u &= \int_v \boldsymbol{\sigma} \cdot \operatorname{grad} \left(\frac{1 + \xi_3}{2} M_a \right) dv \\
\mathbf{f}_a^w &= \int_v \boldsymbol{\sigma} \cdot \operatorname{grad} \left(\frac{1 - \xi_3}{2} M_a \right) dv
\end{aligned}.
\tag{4.2.33}
$$

For the external work of body forces,

$$
\begin{aligned}
\delta W_{ext} &= \int_v \delta \mathbf{u} \cdot \rho \mathbf{b} \, dv \\
&= \sum_{a=1}^m \delta \mathbf{u}_a \cdot \mathbf{f}_a^u + \delta \mathbf{w}_a \cdot \mathbf{f}_a^w,
\end{aligned}
\tag{4.2.34}
$$

where

$$
\begin{aligned}
\mathbf{f}_a^u &= \int_v \frac{1 + \xi_3}{2} M_a \rho \mathbf{b} \, dv \\
\mathbf{f}_a^w &= \int_v \frac{1 - \xi_3}{2} M_a \rho \mathbf{b} \, dv
\end{aligned}.
\tag{4.2.35}
$$

The linearization of the internal virtual work is

$$
\begin{aligned}
D \left(\delta W_{int} \right) [\Delta \mathbf{u}] &= \int_v \operatorname{tr} \left(\operatorname{grad} \Delta \mathbf{u} \cdot \boldsymbol{\sigma} \cdot \operatorname{grad}^T \delta \mathbf{u} \right) dv \\
&+ \int_v \operatorname{grad} \delta \mathbf{u} : \boldsymbol{\mathcal{C}} : \operatorname{grad}^T \Delta \mathbf{u} \, dv
\end{aligned}.
\tag{4.2.36}
$$

So

$$
\int_v \operatorname{tr} \left(\operatorname{grad} \Delta \mathbf{u} \cdot \boldsymbol{\sigma} \cdot \operatorname{grad}^T \delta \mathbf{u} \right) dv = \sum_a \sum_b \begin{bmatrix} \delta \mathbf{u}_a & \delta \mathbf{w}_a \end{bmatrix} \begin{bmatrix} \mathbf{K}_{ab}^{uu} & \mathbf{K}_{ab}^{uw} \\ \mathbf{K}_{ab}^{wu} & \mathbf{K}_{ab}^{ww} \end{bmatrix} \begin{bmatrix} \Delta \mathbf{u}_b \\ \Delta \mathbf{w}_b \end{bmatrix},
\tag{4.2.37}
$$

where

$$\mathbf{K}_{ab}^{uu} = \int_v \left(\operatorname{grad} \left(\frac{1+\xi_3}{2} M_a \right) \cdot \boldsymbol{\sigma} \cdot \operatorname{grad} \left(\frac{1+\xi_3}{2} M_b \right) \right) \mathbf{I} \, dv$$

$$\mathbf{K}_{ab}^{uw} = \int_v \left(\operatorname{grad} \left(\frac{1+\xi_3}{2} M_a \right) \cdot \boldsymbol{\sigma} \cdot \operatorname{grad} \left(\frac{1-\xi_3}{2} M_b \right) \right) \mathbf{I} \, dv$$

$$\mathbf{K}_{ab}^{wu} = \int_v \left(\operatorname{grad} \left(\frac{1-\xi_3}{2} M_a \right) \cdot \boldsymbol{\sigma} \cdot \operatorname{grad} \left(\frac{1+\xi_3}{2} M_b \right) \right) \mathbf{I} \, dv$$

$$\mathbf{K}_{ab}^{ww} = \int_v \left(\operatorname{grad} \left(\frac{1-\xi_3}{2} M_a \right) \cdot \boldsymbol{\sigma} \cdot \operatorname{grad} \left(\frac{1-\xi_3}{2} M_b \right) \right) \mathbf{I} \, dv$$

(4.2.38)

Similarly,

$$\int_v \operatorname{grad} \delta \mathbf{u} : \boldsymbol{\mathcal{C}} : \operatorname{grad}^T \Delta \mathbf{u} \, dv = \sum_a \sum_b \left[\begin{array}{cc} \delta \mathbf{u}_a & \delta \mathbf{w}_a \end{array} \right] \left[\begin{array}{cc} \mathbf{K}_{ab}^{uu} & \mathbf{K}_{ab}^{uw} \\ \mathbf{K}_{ab}^{wu} & \mathbf{K}_{ab}^{ww} \end{array} \right] \left[\begin{array}{c} \Delta \mathbf{u}_b \\ \Delta \mathbf{w}_b \end{array} \right], \qquad (4.2.39)$$

where

$$\mathbf{K}_{ab}^{uu} = \int_v \operatorname{grad} \left(\frac{1+\xi_3}{2} M_a \right) \cdot \boldsymbol{\mathcal{C}} \cdot \operatorname{grad} \left(\frac{1+\xi_3}{2} M_b \right) \, dv$$

$$\mathbf{K}_{ab}^{uw} = \int_v \operatorname{grad} \left(\frac{1+\xi_3}{2} M_a \right) \cdot \boldsymbol{\mathcal{C}} \cdot \operatorname{grad} \left(\frac{1-\xi_3}{2} M_b \right) \, dv$$

$$\mathbf{K}_{ab}^{wu} = \int_v \operatorname{grad} \left(\frac{1-\xi_3}{2} M_a \right) \cdot \boldsymbol{\mathcal{C}} \cdot \operatorname{grad} \left(\frac{1+\xi_3}{2} M_b \right) \, dv$$

$$\mathbf{K}_{ab}^{ww} = \int_v \operatorname{grad} \left(\frac{1-\xi_3}{2} M_a \right) \cdot \boldsymbol{\mathcal{C}} \cdot \operatorname{grad} \left(\frac{1-\xi_3}{2} M_b \right) \, dv$$

(4.2.40)

The linearization of the external work is

$$D\left(\delta W_{ext} \right) = \sum_{a=1}^m \sum_{b=1}^m \int_v \left(\frac{1+\xi_3}{2} M_a \delta \mathbf{u}_a + \frac{1-\xi_3}{2} M_a \delta \mathbf{w}_a \right) \cdot \rho \operatorname{grad} \mathbf{b} \cdot \left(\frac{1+\xi_3}{2} \Delta \mathbf{u}_b + \frac{1-\xi_3}{2} M_b \Delta \mathbf{w}_b \right) \, dv$$

$$= \sum_a \sum_b \left[\begin{array}{cc} \delta \mathbf{u}_a & \delta \mathbf{w}_a \end{array} \right] \left[\begin{array}{cc} \mathbf{K}_{ab}^{uu} & \mathbf{K}_{ab}^{uw} \\ \mathbf{K}_{ab}^{wu} & \mathbf{K}_{ab}^{ww} \end{array} \right] \left[\begin{array}{c} \Delta \mathbf{u}_b \\ \Delta \mathbf{w}_b \end{array} \right]$$

(4.2.41)

where

$$\mathbf{K}_{ab}^{uu} = \int_V \left(\frac{1+\xi_3}{2} \right)^2 M_a M_b \rho_0 \operatorname{grad} \mathbf{b} \, dV$$

$$\mathbf{K}_{ab}^{uw} = \int_V \left(\frac{1+\xi_3}{2} \right) \left(\frac{1-\xi_3}{2} \right) M_a M_b \rho_0 \operatorname{grad} \mathbf{b} \, dV$$

$$\mathbf{K}_{ab}^{wu} = \int_V \left(\frac{1+\xi_3}{2} \right) \left(\frac{1-\xi_3}{2} \right) M_a M_b \rho_0 \operatorname{grad} \mathbf{b} \, dV$$

$$\mathbf{K}_{ab}^{ww} = \int_V \left(\frac{1-\xi_3}{2} \right)^2 M_a M_b \rho_0 \operatorname{grad} \mathbf{b} \, dV$$

(4.2.42)

4.2.2.2 External work of surface forces

We assume that surface forces are applied on the shell front face ($\xi_3 = +1$). Therefore, the external work of surface forces has the form

$$\delta W_{ext} = \int_{\partial v} \delta \mathbf{u} \left(\xi_1, \xi_2, +1 \right) \cdot \mathbf{t} \, da = \sum_a \delta \mathbf{u}_a \cdot \int_{\partial v} M_a \left(\xi_1, \xi_2 \right) \mathbf{t} \, da \qquad (4.2.43)$$

In other words, the treatment of surface forces on a shell becomes identical to the treatment of surface forces on the face of a solid. No special treatment is needed.

4.2.2.3 Shell on top of solid element

When a shell is coincident with the face of a solid element, we assume that the face of the solid element coincides with the back face ($\xi_3 = -1$) of the shell element. This means that the solid element nodal displacements $\mathbf{u}_b$ on that face coincide with the shell nodal displacements $\mathbf{w}_b$. Therefore, when we use UnpackLM for those solid elements, we should reassign the DOF ID's of the $\mathbf{u}_b$ displacements to those of the $\mathbf{w}_b$ displacements stored in that same node.

4.2.2.4 Shell sandwiched between solid elements

When a shell is sandwiched between two solid elements, we reassign the DOF ID's of the the solid $\mathbf{u}_b$ displacements facing the back of the shell to those of the shell $\mathbf{w}_b$ displacements stored in that same node. The DOF ID's of solid $\mathbf{u}_b$ displacements facing the front of the shell remain unchanged; they will coincide with those of the corresponding solid element nodes.

4.2.2.5 Rigid-Shell Interface

When the node of a deformable shell belongs to a rigid body, we need to substitute the nodal degrees of freedom with the rigid body degrees of freedom. The positions of the shell front face and back face nodes are

$$
\begin{aligned}
\mathbf{x}_b &= \mathbf{r} + \mathbf{\Lambda} \cdot (\mathbf{X}_b - \mathbf{R}) \equiv \mathbf{r} + \mathbf{a}_b \\
\mathbf{y}_b &= \mathbf{r} + \mathbf{\Lambda} \cdot (\mathbf{Y}_b - \mathbf{R}) \equiv \mathbf{r} + \mathbf{b}_b
\end{aligned},
\tag{4.2.44}
$$

where $\mathbf{r}$ is the current position of the rigid body center of mass and $\mathbf{R}$ is its initial position; $\mathbf{\Lambda}$ is the rotation tensor for the rigid body. We assume that $\mathbf{x}_b$ and $\mathbf{y}_b$ are connected to the same rigid body. From these relations it follows that virtual displacements are

$$
\begin{aligned}
\delta\mathbf{u}_a &= \delta\mathbf{r} - \hat{\mathbf{a}}_a \cdot \delta\boldsymbol{\theta} \\
\delta\mathbf{w}_b &= \delta\mathbf{r} - \hat{\mathbf{b}}_a \cdot \delta\boldsymbol{\theta}
\end{aligned},
\tag{4.2.45}
$$

and incremental displacements are

$$
\begin{aligned}
\Delta\mathbf{u}_b &= \Delta\mathbf{r} - \hat{\mathbf{a}}_b \cdot \Delta\boldsymbol{\theta} \\
\Delta\mathbf{w}_b &= \Delta\mathbf{r} - \hat{\mathbf{b}}_b \cdot \Delta\boldsymbol{\theta}
\end{aligned},
\tag{4.2.46}
$$

where $\hat{\mathbf{a}}$ is the skew-symmetric tensor whose dual vector is $\mathbf{a}$, such that $\hat{\mathbf{a}} \cdot \mathbf{v} = \mathbf{a} \times \mathbf{v}$ for any vector $\mathbf{v}$. When nodes are flexible (when they do not belong to any rigid body), the virtual work has the general form

$$
\delta W = \sum_{a=1}^{m} \delta\mathbf{u}_a \cdot \mathbf{f}_a^u + \delta\mathbf{w}_a \cdot \mathbf{f}_a^w + \delta p_a \, f_a^p = \sum_{a=1}^{m} \begin{bmatrix} \delta\mathbf{v}_a & \delta\mathbf{w}_a & \delta p_a \end{bmatrix} \begin{bmatrix} \mathbf{f}_a^u \\ \mathbf{f}_a^w \\ f_a^p \end{bmatrix},
\tag{4.2.47}
$$

where p denotes any additional degree-of-freedom at that node. If node a is rigid we get

$$
\begin{bmatrix} \delta\mathbf{u}_a & \delta\mathbf{w}_a & \delta p_a \end{bmatrix} = \begin{bmatrix} \delta\mathbf{r} & \delta\boldsymbol{\theta} & \delta p_a \end{bmatrix} \begin{bmatrix} \mathbf{I} & \mathbf{I} & \mathbf{0} \\ \hat{\mathbf{a}}_a & \hat{\mathbf{b}}_a & \mathbf{0} \\ \mathbf{0} & \mathbf{0} & 1 \end{bmatrix}.
\tag{4.2.48}
$$

If node b is rigid we get

$$
\begin{bmatrix} \Delta\mathbf{u}_b \\ \Delta\mathbf{w}_b \\ \Delta p_b \end{bmatrix} = \begin{bmatrix} \mathbf{I} & -\hat{\mathbf{a}}_b & \mathbf{0} \\ \mathbf{I} & -\hat{\mathbf{b}}_b & \mathbf{0} \\ \mathbf{0} & \mathbf{0} & 1 \end{bmatrix} \begin{bmatrix} \Delta\mathbf{r} \\ \Delta\boldsymbol{\theta} \\ \Delta p_b \end{bmatrix} .
\tag{4.2.49}
$$

When node a belongs to a rigid body, the expression for δW must be substituted with

$$
\delta W = \sum_{a=1}^{m} \begin{bmatrix} \delta\mathbf{u}_a & \delta\mathbf{w}_a & \delta p_a \end{bmatrix} \begin{bmatrix} \mathbf{f}_a^u \\ \mathbf{f}_a^w \\ f_a^p \end{bmatrix}
$$
$$
= \sum_{a=1}^{m} \begin{bmatrix} \delta\mathbf{r} & \delta\boldsymbol{\omega} & \delta p_a \end{bmatrix} \begin{bmatrix} \mathbf{f}_a^u + \mathbf{f}_a^w \\ \hat{\mathbf{a}}_a^{n+\alpha} \cdot \mathbf{f}_a^u + \hat{\mathbf{b}}_a^{n+\alpha} \cdot \mathbf{f}_a^w \\ f_a^p \end{bmatrix} .
\tag{4.2.50}
$$

Similarly, the linearized virtual work has the general form

$$
D\delta W = \sum_a \sum_b \begin{bmatrix} \delta\mathbf{u}_a & \delta\mathbf{w}_a & \delta p_a \end{bmatrix} \begin{bmatrix} \mathbf{K}_{ab}^{uu} & \mathbf{K}_{ab}^{uw} & \mathbf{k}_{ab}^{up} \\ \mathbf{K}_{ab}^{wu} & \mathbf{K}_{ab}^{ww} & \mathbf{k}_{ab}^{wp} \\ \mathbf{k}_{ab}^{pu} & \mathbf{k}_{ab}^{pw} & k_{ab}^{pp} \end{bmatrix} \begin{bmatrix} \Delta\mathbf{u}_b \\ \Delta\mathbf{w}_b \\ \Delta p_b \end{bmatrix} .
\tag{4.2.51}
$$

When node a is rigid but node b is not,

$$
D\delta W = \sum_a \sum_b \begin{bmatrix} \delta\mathbf{r} & \delta\boldsymbol{\theta} & \delta p_a \end{bmatrix} \times
$$
$$
\begin{bmatrix} \mathbf{K}_{ab}^{uu} + \mathbf{K}_{ab}^{wu} & \mathbf{K}_{ab}^{uw} + \mathbf{K}_{ab}^{ww} & \mathbf{k}_{ab}^{up} + \mathbf{k}_{ab}^{wp} \\ \hat{\mathbf{a}}_a \cdot \mathbf{K}_{ab}^{uu} + \hat{\mathbf{b}}_a \cdot \mathbf{K}_{ab}^{wu} & \hat{\mathbf{a}}_a \cdot \mathbf{K}_{ab}^{uw} + \hat{\mathbf{b}}_a \cdot \mathbf{K}_{ab}^{ww} & \hat{\mathbf{a}}_a \cdot \mathbf{k}_{ab}^{up} + \hat{\mathbf{b}}_a \cdot \mathbf{k}_{ab}^{wp} \\ \mathbf{k}_{ab}^{pu} & \mathbf{k}_{ab}^{pw} & k_{ab}^{pp} \end{bmatrix} .
$$
$$
\times \begin{bmatrix} \Delta\mathbf{u}_b \\ \Delta\mathbf{w}_b \\ \Delta p_b \end{bmatrix}
\tag{4.2.52}
$$

If nodes a and b are both rigid,

$$
D\delta W = \sum_a \sum_b \begin{bmatrix} \delta\mathbf{r} & \delta\boldsymbol{\theta} & \delta p_a \end{bmatrix} \times
$$
$$
\begin{bmatrix} \mathbf{K}_{ab}^{uu} + \mathbf{K}_{ab}^{wu} + \mathbf{K}_{ab}^{uw} + \mathbf{K}_{ab}^{ww} & \begin{pmatrix} -(\mathbf{K}_{ab}^{uu} + \mathbf{K}_{ab}^{wu}) \cdot \hat{\mathbf{a}}_b \\ -(\mathbf{K}_{ab}^{uw} + \mathbf{K}_{ab}^{ww}) \cdot \hat{\mathbf{b}}_b \end{pmatrix} & \mathbf{k}_{ab}^{up} + \mathbf{k}_{ab}^{wp} \\ \begin{pmatrix} \hat{\mathbf{a}}_a \cdot (\mathbf{K}_{ab}^{uu} + \mathbf{K}_{ab}^{uw}) \\ +\hat{\mathbf{b}}_a \cdot (\mathbf{K}_{ab}^{wu} + \mathbf{K}_{ab}^{ww}) \end{pmatrix} & \begin{pmatrix} -\left(\hat{\mathbf{a}}_a \cdot \mathbf{K}_{ab}^{uu} + \hat{\mathbf{b}}_a \cdot \mathbf{K}_{ab}^{wu}\right) \cdot \hat{\mathbf{a}}_b \\ -\left(\hat{\mathbf{a}}_a \cdot \mathbf{K}_{ab}^{uw} + \hat{\mathbf{b}}_a \cdot \mathbf{K}_{ab}^{ww}\right) \cdot \hat{\mathbf{b}}_b \end{pmatrix} & \hat{\mathbf{a}}_a \cdot \mathbf{k}_{ab}^{up} + \hat{\mathbf{b}}_a \cdot \mathbf{k}_{ab}^{wp} \\ \mathbf{k}_{ab}^{pu} + \mathbf{k}_{ab}^{pw} & \hat{\mathbf{a}}_b \cdot \mathbf{k}_{ab}^{pu} + \hat{\mathbf{b}}_b \cdot \mathbf{k}_{ab}^{pw} & k_{ab}^{pp} \end{bmatrix} .
$$
$$
\times \begin{bmatrix} \Delta\mathbf{r} \\ \Delta\boldsymbol{\theta} \\ \Delta p_b \end{bmatrix}
\tag{4.2.53}
$$

If node a is not rigid and node b is rigid,

$$
D\delta W = \sum_a \sum_b \begin{bmatrix} \delta\mathbf{u}_a & \delta\mathbf{w}_a & \delta p_a \end{bmatrix} \times
$$
$$
\begin{bmatrix} \mathbf{K}_{ab}^{uu} + \mathbf{K}_{ab}^{wu} & -\mathbf{K}_{ab}^{uu} \cdot \hat{\mathbf{a}}_b - \mathbf{K}_{ab}^{uw} \cdot \hat{\mathbf{b}}_b & \mathbf{k}_{ab}^{up} \\ \mathbf{K}_{ab}^{wu} + \mathbf{K}_{ab}^{ww} & -\mathbf{K}_{ab}^{wu} \cdot \hat{\mathbf{a}}_b - \mathbf{K}_{ab}^{ww} \cdot \hat{\mathbf{b}}_b & \mathbf{k}_{ab}^{wp} \\ \mathbf{k}_{ab}^{pu} + \mathbf{k}_{ab}^{pw} & \hat{\mathbf{a}}_b \cdot \mathbf{k}_{ab}^{pu} + \hat{\mathbf{b}}_b \cdot \mathbf{k}_{ab}^{pw} & k_{ab}^{pp} \end{bmatrix} \begin{bmatrix} \Delta\mathbf{r} \\ \Delta\boldsymbol{\theta} \\ \Delta p_b \end{bmatrix} .
\tag{4.2.54}
$$

Chapter 5

Constitutive Models

This chapter describes the theoretical background behind the constitutive models that are available in FEBio. Most materials are derived from a hyperelastic strain-energy function. Please consult Section 2.4 for more background information on this class of materials.

5.1   Linear Elasticity

In the theory of linear elasticity the Cauchy stress tensor is a linear function of the small strain tensor ε:

$$\boldsymbol{\sigma} = \boldsymbol{\mathcal{C}} : \boldsymbol{\varepsilon} \, . \tag{5.1.1}$$

Here, $\boldsymbol{\mathcal{C}}$ is the fourth-order elasticity tensor that contains the material properties. In the most general case this tensor has 21 independent parameters. However, in the presence of material symmetry the number of independent parameters is greatly reduced. For example, in the case of isotropic linear elasticity only two independent parameters remain. In this case, the elasticity tensor is given by $\boldsymbol{\mathcal{C}} = \lambda \mathbf{I} \otimes \mathbf{I} + 2\mu \mathbf{I} \,\overline{\otimes}\, \mathbf{I}$, or equivalently,

$$\mathcal{C}_{ijkl} = \lambda \delta_{ij}\delta_{kl} + \mu \left(\delta_{ik}\delta_{jl} + \delta_{il}\delta_{jk} \right) \, . \tag{5.1.2}$$

The material coefficients λ and μ are known as the Lamé parameters. Using this equation, the stress-strain relationship can be written as

$$\sigma_{ij} = \lambda \varepsilon_{kk} \delta_{ij} + 2\mu \varepsilon_{ij} \, . \tag{5.1.3}$$

If the stress and strain are represented inVoigt notation, the constitutive equation can be rewritten in matrix form as

$$
\begin{bmatrix} \sigma_{11} \\ \sigma_{22} \\ \sigma_{33} \\ \sigma_{12} \\ \sigma_{23} \\ \sigma_{13} \end{bmatrix} = \begin{bmatrix} \lambda + 2\mu & \lambda & \lambda & 0 & 0 & 0 \\ \lambda & \lambda + 2\mu & \lambda & 0 & 0 & 0 \\ \lambda & \lambda & \lambda + 2\mu & 0 & 0 & 0 \\ 0 & 0 & 0 & \mu & 0 & 0 \\ 0 & 0 & 0 & 0 & \mu & 0 \\ 0 & 0 & 0 & 0 & 0 & \mu \end{bmatrix} \begin{bmatrix} \varepsilon_{11} \\ \varepsilon_{22} \\ \varepsilon_{33} \\ \gamma_{12} \\ \gamma_{23} \\ \gamma_{13} \end{bmatrix} \, . \tag{5.1.4}
$$

The shear strain measures $\gamma_{ij} = 2\varepsilon_{ij}$ are called the *engineering strains*.

The following table relates the Lamé parameters to the more familiar Young's modulus E and Poisson's ratio ν or to the bulk modulus K and shear modulus G.

	E, ν	λ, μ	K, G
E, ν		$E = \frac{\mu}{\lambda+\mu}(2\mu+3\lambda)$ $\nu = \frac{\lambda}{2(\lambda+\mu)}$	$E = \frac{9KG}{3K+G}$ $\nu = \frac{3K-2G}{6K+2G}$
λ, μ	$\lambda = \frac{\nu E}{(1+\nu)(1-2\nu)}$ $\mu = \frac{E}{2(1+\nu)}$		$\lambda = K - \frac{2}{3}G$ $\mu = G$
K, G	$K = \frac{E}{3(1-2v)}$ $G = \frac{E}{2(1+v)}$	$K = \lambda + \frac{2}{3}\mu$ $G = \mu$	

The theoretical range of the Young's modulus and Poisson's ratio for an isotropic material have the ranges

$$0 < E < \infty \,, \tag{5.1.5}$$

$$-1 \leqslant \nu < 0.5 \,. \tag{5.1.6}$$

Materials with Poisson's ratio (close to) 0.5 are known as (nearly-) incompressible materials. For these materials, the bulk modulus approaches infinity. Most materials have a positive Poisson's ratio. However there do exist some materials with a negative ratio. These materials are known as *auxetic* materials and they have the remarkable property that they expand under tension.

The linear stress-strain relationship can also be derived from a strain-energy function such as in the case of hyperelastic materials. In this case the linear strain-energy is given by

$$W = \frac{1}{2}\varepsilon : \mathcal{C} : \varepsilon \,. \tag{5.1.7}$$

The stress is then similarly derived from $\sigma = \frac{\partial W}{\partial \varepsilon}$. In the case of isotropic elasticity, (5.1.7) can be simplified:

$$W = \frac{1}{2}\lambda \left(\operatorname{tr}\varepsilon\right)^2 + \mu\varepsilon : \varepsilon \,. \tag{5.1.8}$$

The Cauchy stress is now given in tensor form by

$$\boldsymbol{\sigma} = \lambda\left(\operatorname{tr}\varepsilon\right)\mathbf{I} + 2\mu\varepsilon \,. \tag{5.1.9}$$

5.2 Compressible Materials

5.2.1 Isotropic Elasticity

The linear elastic material model as described in Section 5.1 is only valid for small strains and small rotations. A first modification to this model to the range of nonlinear deformations is given by the St. Venant-Kirchhoff model [19], which in FEBio is referred to as *isotropic elasticity*. This model is objective for large strains and rotations. For the isotropic case it can be derived from the following hyperelastic strain-energy function:

$$W = \frac{1}{2}\lambda \left(\operatorname{tr}\mathbf{E}\right)^2 + \mu\mathbf{E} : \mathbf{E}\,. \tag{5.2.1}$$

The second Piola-Kirchhoff stress can be derived from this:

$$\mathbf{S} = \frac{\partial W}{\partial \mathbf{E}} = \lambda \left(\operatorname{tr}\mathbf{E}\right)\mathbf{I} + 2\mu\mathbf{E}\,. \tag{5.2.2}$$

Note that these equations are similar to the corresponding equations in the linear elastic case, except that the small strain tensor is replaced by the Green-Lagrange elasticity tensor $\mathbf{E}$. The material elasticity tensor is then given by,

$$\mathbb{C} = \frac{\partial \mathbf{S}}{\partial \mathbf{E}} = \lambda\mathbf{I}\otimes\mathbf{I} + 2\mu\mathbf{I}\,\overline{\underline{\otimes}}\,\mathbf{I}\,. \tag{5.2.3}$$

It is important to note that although this model is objective, it should only be used for small strains. For large strains, the response can be somewhat strange if not completely unrealistic. For example, it can be shown that under uni-axial tension the stress becomes infinite and the volume tends to zero for finite strains. Therefore, for large strains it is highly recommended to avoid this material and instead use one of the other non-linear material models described below. The Cauchy stress is

$$\boldsymbol{\sigma} = \frac{1}{J}\left(\lambda\operatorname{tr}\mathbf{E} - \mu\right)\mathbf{b} + \frac{\mu}{J}\mathbf{b}^2\,, \tag{5.2.4}$$

where $\operatorname{tr}\mathbf{E} = \left(\operatorname{tr}\mathbf{b} - 3\right)/2$, whereas the spatial elasticity tensor is

$$\mathcal{C} = \frac{\lambda}{J}\mathbf{b}\otimes\mathbf{b} + \frac{2}{J}\mu\mathbf{b}\,\overline{\underline{\otimes}}\,\mathbf{b}\,. \tag{5.2.5}$$

5.2.2 Orthotropic Elasticity

An extension of the St. Venant-Kirchhoff model [19] to orthotropic symmetry is provided in FEBio, referred to as *orthotropic elasticity*. This model is objective for large strains and rotations. It can be derived from the following hyperelastic strain-energy function:

$$W = \sum_{a=1}^{3}\mu_a\mathbf{A}_a^0 : \mathbf{E}^2 + \frac{1}{2}\sum_{b=1}^{3}\lambda_{ab}\left(\mathbf{A}_a^0 : \mathbf{E}\right)\left(\mathbf{A}_b^0 : \mathbf{E}\right)\,, \tag{5.2.6}$$

where $\mathbf{A}_a^0 = \mathbf{a}_a^0 \otimes \mathbf{a}_a^0$ is the structural tensor corresponding to one of the three mutually orthogonal planes of symmetry whose unit outward normal is $\mathbf{a}_a^0$ ($\mathbf{a}_a^0 \cdot \mathbf{a}_b^0 = \delta_{ab}$). The material constants are

the three shear moduli μ_a and six moduli λ_{ab}, where $\lambda_{ba} = \lambda_{ab}$. They may be related to the Young's moduli E_a, shear moduli G_{ab} and Poisson's ratios ν_{ab} via

$$
\begin{bmatrix}
\lambda_{11}+2\mu_1 & \lambda_{12} & \lambda_{13} & 0 & 0 & 0 \\
\lambda_{12} & \lambda_{22}+2\mu_2 & \lambda_{23} & 0 & 0 & 0 \\
\lambda_{13} & \lambda_{23} & \lambda_{33}+2\mu_3 & 0 & 0 & 0 \\
0 & 0 & 0 & (\mu_1+\mu_2)/2 & 0 & 0 \\
0 & 0 & 0 & 0 & (\mu_2+\mu_3)/2 & 0 \\
0 & 0 & 0 & 0 & 0 & (\mu_3+\mu_1)/2
\end{bmatrix}^{-1} =
$$
$$
\begin{bmatrix}
1/E_1 & -\nu_{12}/E_1 & -\nu_{13}/E_1 & 0 & 0 & 0 \\
-\nu_{21}/E_2 & 1/E_2 & -\nu_{23}/E_2 & 0 & 0 & 0 \\
-\nu_{31}/E_3 & -\nu_{32}/E_3 & 1/E_3 & 0 & 0 & 0 \\
0 & 0 & 0 & 1/G_{12} & 0 & 0 \\
0 & 0 & 0 & 0 & 1/G_{23} & 0 \\
0 & 0 & 0 & 0 & 0 & 1/G_{31}
\end{bmatrix} . \tag{5.2.7}
$$

The second Piola-Kirchhoff stress can be derived from this strain energy density function:

$$
\mathbf{S} = \frac{\partial W}{\partial \mathbf{E}} = \sum_{a=1}^{3} \mu_a \left(\mathbf{A}_a^0 \cdot \mathbf{E} + \mathbf{E} \cdot \mathbf{A}_a^0 \right)
$$
$$
+ \frac{1}{2} \sum_{b=1}^{3} \lambda_{ab} \left[\left(\mathbf{A}_a^0 : \mathbf{E} \right) \mathbf{A}_b^0 + \left(\mathbf{A}_b^0 : \mathbf{E} \right) \mathbf{A}_a^0 \right] . \tag{5.2.8}
$$

Note that these equations are similar to the corresponding equations in the linear orthotropic elastic case, except that the small strain tensor is replaced by the Green-Lagrange elasticity tensor $\mathbf{E}$. The material elasticity tensor is then given by,

$$
\mathbb{C} = \frac{\partial \mathbf{S}}{\partial \mathbf{E}} = \sum_{a=1}^{3} \mu_a \left(\mathbf{A}_a^0 \,\overline{\underline{\otimes}}\, \mathbf{I} + \mathbf{I} \,\overline{\underline{\otimes}}\, \mathbf{A}_a^0 \right) + \frac{1}{2} \sum_{b=1}^{3} \lambda_{ab} \left(\mathbf{A}_a^0 \otimes \mathbf{A}_b^0 + \mathbf{A}_b^0 \otimes \mathbf{A}_a^0 \right) . \tag{5.2.9}
$$

It is important to note that although this model is objective, it should only be used for small strains. For large strains, the response can be somewhat strange if not completely unrealistic. For example, it can be shown that under uni-axial tension the stress becomes infinite and the volume tends to zero for finite strains. Therefore, for large strains it is highly recommended to avoid this material and instead use one of the other non-linear material models described below. The Cauchy stress is

$$
\boldsymbol{\sigma} = \sum_{a=1}^{3} \frac{\mu_a}{2J} \left(\mathbf{A}_a \cdot (\mathbf{b} - \mathbf{I}) + (\mathbf{b} - \mathbf{I}) \cdot \mathbf{A}_a \right)
$$
$$
+ \frac{1}{2} \sum_{b=1}^{3} \frac{\lambda_{ab}}{2J} \left[(\mathbf{A}_a : \mathbf{I} - 1) \mathbf{A}_b + (\mathbf{A}_b : \mathbf{I} - 1) \mathbf{A}_a \right] , \tag{5.2.10}
$$

where $\mathbf{A}_a = \mathbf{F} \cdot \mathbf{A}_a^0 \cdot \mathbf{F}^T$ and the spatial elasticity tensor is

$$
\boldsymbol{\mathcal{C}} = \sum_{a=1}^{3} \frac{\mu_a}{J} \left(\mathbf{A}_a \,\overline{\underline{\otimes}}\, \mathbf{b} + \mathbf{b} \,\overline{\underline{\otimes}}\, \mathbf{A}_a \right) + \frac{1}{2} \sum_{b=1}^{3} \frac{\lambda_{ab}}{J} \left(\mathbf{A}_a \otimes \mathbf{A}_b + \mathbf{A}_b \otimes \mathbf{A}_a \right) . \tag{5.2.11}
$$

5.2.3 Neo-Hookean Hyperelasticity

This is a compressible neo-Hookean material. It is derived from the following hyperelastic strain energy function [19]:

$$W = \frac{\mu}{2}\left(I_1 - 3\right) - \mu \ln J + \frac{\lambda}{2}\left(\ln J\right)^2 . \tag{5.2.12}$$

The parameters μ and λ are the Lamé parameters from linear elasticity. This model reduces to the isotropic linear elastic model for small strains and rotations.

The Cauchy stress is given by,

$$\boldsymbol{\sigma} = \frac{\mu}{J}\left(\mathbf{b} - \mathbf{I}\right) + \frac{\lambda}{J}\left(\ln J\right)\mathbf{I} , \tag{5.2.13}$$

and the spatial elasticity tensor is given by

$$\mathcal{C} = \frac{\lambda}{J}\mathbf{I} \otimes \mathbf{I} + \frac{2}{J}\left(\mu - \lambda \ln J\right)\mathbf{I}\,\overline{\otimes}\,\mathbf{I} . \tag{5.2.14}$$

The neo-Hookean material is an extension of Hooke's law for the case of large deformations. It is useable for certain plastics and rubber-like substances. A generalization of this model is the Mooney-Rivlin material, which is often used to describe the elastic response of biological tissue.

In FEBio this constitutive model uses a standard displacement-based element formulation and a "coupled" strain energy, so care must be taken when modeling materials with nearly-incompressible material behavior to avoid element locking.

5.2.4 Ogden Unconstrained

The Ogden unconstrained material is defined using the following hyperelastic strain energy function:

$$W\left(\lambda_1, \lambda_2, \lambda_3\right) = \frac{1}{2}c_p\left(J - 1\right)^2 + \sum_{k=1}^{N}\frac{c_k}{m_k^2}\left(\lambda_1^{m_k} + \lambda_2^{m_k} + \lambda_3^{m_k} - 3 - m_k \ln J\right) . \tag{5.2.15}$$

Here, λ_i are the principal stretches and c_p, c_k and m_k are material parameters.

The Cauchy stress tensor for this material may be obtained using the general formula for isotropic elasticity in principal directions given in (2.4.18), with

$$\sigma_i = c_p\left(J - 1\right) + \sum_{k=1}^{N}\frac{1}{J}\frac{c_k}{m_k}\left(\lambda_i^{m_k} - 1\right) . \tag{5.2.16}$$

Similarly, the spatial elasticity tensor is given by

$$\begin{aligned}
\mathcal{C} = &\sum_{i=1}^{3}\left(c_p + \sum_{k=1}^{N}\frac{1}{J}\frac{c_k}{m_k}\left[\left(m_k - 2\right)\lambda_i^{m_k} + 2\right]\right)\mathbf{a}_i \otimes \mathbf{a}_i \\
&+ \sum_{i=1}^{3}\sum_{j=i+1}^{3}c_p\left(2J - 1\right)\left(\mathbf{a}_i \otimes \mathbf{a}_j + \mathbf{a}_j \otimes \mathbf{a}_i\right) \\
&+ \sum_{i=1}^{3}\sum_{j=i+1}^{3}2\frac{\lambda_j^2\sigma_i - \lambda_i^2\sigma_j}{\lambda_i^2 - \lambda_j^2}\left(\mathbf{a}_i\,\overline{\otimes}\,\mathbf{a}_j + \mathbf{a}_j\,\overline{\otimes}\,\mathbf{a}_i\right) ,
\end{aligned} \tag{5.2.17}$$

where $\mathbf{a}_i = \mathbf{n}_i \otimes \mathbf{n}_i$ and $\mathbf{n}_i$ are the eigenvectors of $\mathbf{b}$. In the limit when eigenvalues coincide,

$$\lim_{\lambda_j \to \lambda_i} 2 \frac{\sigma_i \lambda_j^2 - \sigma_j \lambda_i^2}{\lambda_i^2 - \lambda_j^2} = 2c_p \left(1 - J\right) + \sum_{k=1}^{N} \frac{1}{J} \frac{c_k}{m_k} \left[2 + \left(m_k - 2\right) \lambda_i^{m_k}\right] . \tag{5.2.18}$$

In the reference configuration the elasticity tensor reduces to

$$\mathcal{C}|_{\mathbf{b}=\mathbf{I}} = c_p \mathbf{I} \otimes \mathbf{I} + \left(\sum_{k=1}^{N} c_k\right) \mathbf{I} \,\overline{\underline{\otimes}}\, \mathbf{I} , \tag{5.2.19}$$

which has the form of Hooke's law for infinitesimal isotropic elasticity (see Section 5.1), with equivalent Lamé coefficients $c_p \equiv \lambda$ and $2\mu \equiv \sum_{k=1}^{N} c_k$.

5.2.5   Holmes-Mow

The coupled hyperelastic strain-energy function for this material is given by [30],

$$\Psi\left(I_1, I_2, J\right) = \frac{1}{2} c \left(e^Q - 1\right) , \tag{5.2.20}$$

where I_1 and I_2 are the first and second invariants of the right Cauchy-Green tensor and J the jacobian of the deformation. Furthermore,

$$\begin{aligned} Q &= \frac{\beta}{\lambda + 2\mu} \left[\left(2\mu - \lambda\right)\left(I_1 - 3\right) + \lambda\left(I_2 - 3\right) - \left(\lambda + 2\mu\right) \ln J^2\right] , \\ c &= \frac{\lambda + 2\mu}{2\beta} , \end{aligned} \tag{5.2.21}$$

and λ and μ are the Lamé parameters. The corresponding Cauchy stress tensor is

$$\boldsymbol{\sigma} = \frac{1}{2J} e^Q \left(\left[2\mu + \lambda\left(I_1 - 1\right)\right] \mathbf{b} - \lambda \mathbf{b}^2 - \left(\lambda + 2\mu\right) \mathbf{I}\right) , \tag{5.2.22}$$

and the spatial elasticity tensor is

$$\mathcal{C} = \frac{4\beta}{\lambda + 2\mu} J e^{-Q} \boldsymbol{\sigma} \otimes \boldsymbol{\sigma} + J^{-1} e^Q \left[\lambda \left(\mathbf{b} \otimes \mathbf{b} - \mathbf{b} \,\overline{\underline{\otimes}}\, \mathbf{b}\right) + \left(\lambda + 2\mu\right) \mathbf{I} \,\overline{\underline{\otimes}}\, \mathbf{I}\right] . \tag{5.2.23}$$

5.2.6   Conewise Linear Elasticity

Curnier et al. [23] formulated a model for describing bimodular elastic solids exhibiting orthotropic material symmetry. This can be derived from the following hyperelastic strain-energy function:

$$W = \sum_{a=1}^{3} \mu_a \mathbf{A}_a^0 : \mathbf{E}^2 + \frac{1}{2} \lambda_{aa} \left[\mathbf{A}_a^0 : \mathbf{E}\right] \left(\mathbf{A}_a^0 : \mathbf{E}\right) + \sum_{b=1, b \neq a}^{3} \frac{1}{2} \lambda_{ab} \left(\mathbf{A}_a^0 : \mathbf{E}\right) \left(\mathbf{A}_b^0 : \mathbf{E}\right) , \tag{5.2.24}$$

where $\mathbf{A}_a^0 = \mathbf{a}_a^0 \otimes \mathbf{a}_a^0$ is the structural tensor corresponding to one of the three mutually orthogonal planes of symmetry whose unit outward normal is $\mathbf{a}_a^0$ ($\mathbf{a}_a^0 \cdot \mathbf{a}_b^0 = \delta_{ab}$). The bimodular response is described by

$$\lambda_{aa} \left[\mathbf{A}_a^0 : \mathbf{E}\right] = \begin{cases} \lambda_{+aa} & \mathbf{A}_a^0 : \mathbf{E} \geqslant 0 \\ \lambda_{-aa} & \mathbf{A}_a^0 : \mathbf{E} < 0 \end{cases} . \tag{5.2.25}$$

The material constants are the three shear moduli μ_a, three tensile moduli λ_{+aa}, three compressive moduli λ_{-aa}, and three moduli λ_{ab} ($b \neq a$), where $\lambda_{ba} = \lambda_{ab}$. The second Piola-Kirchhoff stress can be derived from this strain energy density function:

$$\mathbf{S} = \frac{\partial W}{\partial \mathbf{E}} = \sum_{a=1}^{3} \mu_a \left(\mathbf{A}_a^0 \cdot \mathbf{E} + \mathbf{E} \cdot \mathbf{A}_a^0 \right)$$
$$+ \lambda_{aa} \left[\mathbf{A}_a^0 : \mathbf{E} \right] \left(\mathbf{A}_a^0 : \mathbf{E} \right) \mathbf{A}_a^0 + \sum_{b=1,\, b\neq a}^{3} \lambda_{ab} \left(\mathbf{A}_a^0 : \mathbf{E} \right) \mathbf{A}_b^0 . \tag{5.2.26}$$

The material elasticity tensor is then given by,

$$\mathbb{C} = \frac{\partial \mathbf{S}}{\partial \mathbf{E}} = \sum_{a=1}^{3} \mu_a \left(\mathbf{A}_a^0 \,\overline{\underline{\otimes}}\, \mathbf{I} + \mathbf{I} \,\overline{\underline{\otimes}}\, \mathbf{A}_a^0 \right)$$
$$+ \lambda_{aa} \left[\mathbf{A}_a^0 : \mathbf{E} \right] \mathbf{A}_a^0 \otimes \mathbf{A}_a^0 + \sum_{b=1,\, b\neq a}^{3} \lambda_{ab} \mathbf{A}_a^0 \otimes \mathbf{A}_b^0 . \tag{5.2.27}$$

It is important to note that although this model is objective, it should only be used for small strains. For large strains, the response may be unrealistic. The Cauchy stress is

$$\boldsymbol{\sigma} = J^{-1} \left(\sum_{a=1}^{3} \frac{\mu_a}{2} \left(\mathbf{A}_a \cdot (\mathbf{b} - \mathbf{I}) + (\mathbf{b} - \mathbf{I}) \cdot \mathbf{A}_a \right) \right.$$
$$\left. + \lambda_{aa} \left[K_a \right] K_a \mathbf{A}_a + \sum_{b=1,\, b\neq a}^{3} \lambda_{ab} K_a \mathbf{A}_b \right) , \tag{5.2.28}$$

where $\mathbf{A}_a = \mathbf{F} \cdot \mathbf{A}_a^0 \cdot \mathbf{F}^T$ and $K_a = \frac{1}{2} \left(\mathbf{A}_a : \mathbf{I} - 1 \right)$. The spatial elasticity tensor is

$$\mathcal{C} = J^{-1} \left(\sum_{a=1}^{3} \mu_a \left(\mathbf{A}_a \,\overline{\underline{\otimes}}\, \mathbf{b} + \mathbf{b} \,\overline{\underline{\otimes}}\, \mathbf{A}_a \right) + \lambda_{aa} \left[K_a \right] \mathbf{A}_a \otimes \mathbf{A}_a + \sum_{b=1,\, b\neq a}^{3} \lambda_{ab} \mathbf{A}_a \otimes \mathbf{A}_b \right) . \tag{5.2.29}$$

In the special case of cubic symmetry the number of material constants reduces to four,

$$\begin{aligned}
\lambda_{+11} &= \lambda_{+22} = \lambda_{+33} \equiv \lambda_{+1} \\
\lambda_{-11} &= \lambda_{-22} = \lambda_{-33} \equiv \lambda_{-1} \\
\lambda_{12} &= \lambda_{23} = \lambda_{31} \equiv \lambda_2 \\
\mu_1 &= \mu_2 = \mu_3 \equiv \mu
\end{aligned} . \tag{5.2.30}$$

5.2.7 Donnan Equilibrium Swelling

The swelling pressure is described by the equations for ideal Donnan equilibrium, assuming that the material is porous, with a charged solid matrix, and the external bathing environment consists of a salt solution of monovalent counter-ions. Since osmotic swelling must be resisted by a solid material, this material is not stable on its own. It must be combined with an elastic material that resists the swelling.

The Cauchy stress for this material is the stress from the Donnan equilibrium response [7]:

$$\boldsymbol{\sigma} = -\pi\,\mathbf{I}\,, \tag{5.2.31}$$

where π is the osmotic pressure, given by

$$\pi = R\theta\left(\sqrt{(c^F)^2 + (\bar{c}^*)^2} - \bar{c}^*\right), \tag{5.2.32}$$

$\bar{c}^*$ is the bath osmolarity (twice the concentration) and c^F is the fixed charge density in the current configuration, related to the reference configuration via,

$$c^F = \frac{\varphi_0^w}{J - 1 + \varphi_0^w}c_0^F\,, \tag{5.2.33}$$

where $J = \det \mathbf{F}$ is the relative volume, R is the universal gas constant and θ is the absolute temperature.

Note that c_0^F may be negative or positive. The gel porosity φ_0^w is unitless and must be in the range $0 < \varphi_0^w < 1$. The corresponding spatial elasticity tensor is [14]

$$\begin{aligned}
\mathcal{C} &= \frac{R\theta J\left(c^F\right)^2}{(J - 1 + \varphi_0^w)\sqrt{(c^F)^2 + (\bar{c}^*)^2}}\mathbf{I} \otimes \mathbf{I} \\
&\quad + R\theta\left[\sqrt{(c^F)^2 + (\bar{c}^*)^2} - \bar{c}^*\right]\left(2\mathbf{I}\,\overline{\underline{\otimes}}\,\mathbf{I} - \mathbf{I} \otimes \mathbf{I}\right).
\end{aligned} \tag{5.2.34}$$

5.2.8 Perfect Osmometer Equilibrium Osmotic Pressure

The swelling pressure is described by the equations for a perfect osmometer, assuming that the material is porous, containing an interstitial solution whose solutes cannot be exchanged with the external bathing environment. Similarly, solutes in the external bathing solution cannot be exchanged with the interstitial fluid of the porous material. Therefore, osmotic pressurization occurs when there is an imbalance between the interstitial and bathing solution osmolarities. Since osmotic swelling must be resisted by a solid matrix, this material is not stable on its own. It must be combined with an elastic material that resists the swelling.

The Cauchy stress for this material is the stress from the perfect osmometer equilibrium response [6]:

$$\boldsymbol{\sigma} = -\pi\,\mathbf{I}\,, \tag{5.2.35}$$

where π is the osmotic pressure, given by

$$\pi = R\theta\left(\bar{c} - \bar{c}^*\right). \tag{5.2.36}$$

Here, R is the universal gas constant and θ is the absolute temperature, $\bar{c}^*$ is the external bath osmolarity and $\bar{c}$ is the interstitial fluid osmolarity in the current configuration, related to the reference configuration osmolarity $\bar{c}_0$ via,

$$\bar{c} = \frac{\varphi_0^w}{J - 1 + \varphi_0^w}\bar{c}_0\,. \tag{5.2.37}$$

Though this material is porous, this is not a full-fledged poroelastic material. The behavior described by this material is strictly valid only after the transient response of interstitial fluid and solute fluxes has subsided. The corresponding spatial elasticity tensor is

$$\mathcal{C} = R\theta\left[\frac{J\,\bar{c}}{J - 1 + \varphi_0^w}\mathbf{I} \otimes \mathbf{I} + (\bar{c} - \bar{c}^*)\left(2\mathbf{I}\,\overline{\underline{\otimes}}\,\mathbf{I} - \mathbf{I} \otimes \mathbf{I}\right)\right]. \tag{5.2.38}$$

5.2.9 Large Poisson's Ratio Ligament

This material captures the transversely isotropic behavior of tendon and ligaments while enforcing a large Poisson's ratio. The material utilizes a three part strain energy equation:

$$W = W_{\text{fiber}} + W_{\text{matrix}} + W_{\text{vol}} \,,$$

where:

$$W_{\text{fiber}} = \frac{1}{2} \frac{c_1}{c_2} \left(e^{c_2(\lambda-1)^2} - 1 \right) \,,$$

$$W_{\text{matrix}} = \frac{\mu}{2} (I_1 - 3) - \mu \ln \left(\sqrt{I_3} \right) \,,$$

$$W_{\text{vol}} = \frac{\kappa}{2} \left(\ln \left(\frac{I_5 - I_1 I_4 + I_2}{I_4^{2(m-v_0)} e^{-4m(\lambda-1)}} \right) \right)^2 \,.$$

The transversely isotropic strain energy W_{fiber} takes into account the behavior of the collagen fibers. The isotropic strain energy W_{matrix} takes into account the mechanical contribution of the extrafibrillar matrix and provides the majority of support when loaded transverse to the fiber direction. The variables c_1, c_2 and μ are material parameters controlling the stress-strain response of the material.

The volumetric strain energy W_{vol} acts as a penalty term which enforces a Poisson's ratio based on user selection of the parameters m and v_0. The variable κ acts as a penalty parameter. Raising κ will cause the prescribed Poisson's ratio to be enforced. The Poisson's ratio in question is given by the following function:

$$v_{\text{apparent}} = -\frac{\lambda^{m-v_0} e^{-m(\lambda-1)} - 1}{\lambda - 1} \,.$$

5.3 Nearly-Incompressible Materials

5.3.1 Mooney-Rivlin Hyperelasticity

This material model is a hyperelastic Mooney-Rivlin type with uncoupled deviatoric and volumetric behavior. The uncoupled strain energy W is given by:

$$W = c_1 \left(\tilde{I}_1 - 3 \right) + c_2 \left(\tilde{I}_2 - 3 \right) + \frac{1}{2} K \left(\ln J \right)^2 \,. \tag{5.3.1}$$

Here, c_1 and c_2 are the Mooney-Rivlin material coefficients, $\tilde{I}_1$ and $\tilde{I}_2$ are the invariants of the deviatoric part of the right Cauchy-Green deformation tensor, $\tilde{\mathbf{C}} = \tilde{\mathbf{F}}^T \cdot \tilde{\mathbf{F}}$, where $\tilde{\mathbf{F}} = J^{-1/3} \mathbf{F}$, $\mathbf{F}$ is the deformation gradient and $J = \det \mathbf{F}$ is the Jacobian of the deformation. When $c_2 = 0$, this model reduces to an uncoupled version of the incompressible neo-Hookean constitutive model.

The Cauchy stress is given by

$$\boldsymbol{\sigma} = p\mathbf{I} + \frac{2}{J} \left[\left(c_1 + c_2 \tilde{I}_1 \right) \tilde{\mathbf{b}} - c_2 \tilde{\mathbf{b}}^2 - \frac{1}{3} \left(c_1 \tilde{I}_1 + 2 c_2 \tilde{I}_2 \right) \mathbf{I} \right] \,. \tag{5.3.2}$$

The spatial elasticity tensor is given by

$$\mathcal{C} = p \left(\mathbf{I} \otimes \mathbf{I} - 2 \mathbf{I} \,\overline{\underline{\otimes}}\, \mathbf{I} \right) - \frac{2}{3} \left(\operatorname{dev} \boldsymbol{\sigma} \otimes \mathbf{I} + \mathbf{I} \otimes \operatorname{dev} \boldsymbol{\sigma} \right) + \mathcal{C}_w \,, \tag{5.3.3}$$

where,

$$\mathcal{C}_w = \frac{4}{3J}\left(c_1\tilde{I}_1 + 2c_2\tilde{I}_2\right)\left(\mathbf{I}\,\overline{\otimes}\,\mathbf{I} - \frac{1}{3}\mathbf{I}\otimes\mathbf{I}\right) + \frac{4c_2}{J}\left(\tilde{\mathbf{b}}\otimes\tilde{\mathbf{b}} - \tilde{\mathbf{b}}\,\overline{\otimes}\,\tilde{\mathbf{b}}\right)$$
$$- \frac{4c_2}{3J}\left[\left(\tilde{I}_1\tilde{\mathbf{b}} - \tilde{\mathbf{b}}^2\right)\otimes\mathbf{I} + \mathbf{I}\otimes\left(\tilde{I}_1\tilde{\mathbf{b}} - \tilde{\mathbf{b}}^2\right)\right] + \frac{8c_2\tilde{I}_2}{9J}\mathbf{I}\otimes\mathbf{I}\,. \tag{5.3.4}$$

This material model uses a three-field element formulation, interpolating displacements as linear field variables and pressure and volume ratio as piecewise constant in each element [55].

5.3.2 Ogden Hyperelastic

The Ogden material is defined using the following hyperelastic strain energy function:

$$W(\lambda_1, \lambda_2, \lambda_3, J) = \sum_{i=1}^{N}\frac{c_i}{m_i^2}\left(\tilde{\lambda}_1^{m_i} + \tilde{\lambda}_2^{m_i} + \tilde{\lambda}_3^{m_i} - 3\right) + U(J)\,. \tag{5.3.5}$$

Here, $\tilde{\lambda}_i$ are the deviatoric principal stretches and c_i and m_i are material parameters. The term $U(J)$ is the volumetric component and J is the determinant of the deformation gradient.

Note that the neo-Hookean and Mooney-Rivlin models can also be obtained from the general Ogden strain energy function using special choices for c_i and m_i.

5.3.3 Veronda-Westmann Hyperelasticity

This model is similar to the Mooney-Rivlin model in that it also uses an uncoupled strain energy. However, in this case the strain energy is given by an exponential form:

$$W = C_1\left[e^{\left(C_2\left(\tilde{I}_1 - 3\right)\right)} - 1\right] - \frac{C_1C_2}{2}\left(\tilde{I}_2 - 3\right) + U(J)\,. \tag{5.3.6}$$

The dilatational term U is identical to the Mooney-Rivlin model.

The Cauchy stress $\boldsymbol{\sigma}$ is found from

$$\boldsymbol{\sigma} = p\mathbf{I} + \mathrm{dev}\,\tilde{\boldsymbol{\sigma}}\,, \tag{5.3.7}$$

where

$$\tilde{\boldsymbol{\sigma}} = \frac{2}{J}\left[\left(W_1 + I_1W_2\right)\tilde{\mathbf{b}} - W_2\tilde{\mathbf{b}}^2\right]\,. \tag{5.3.8}$$

The strain energy derivatives are given by

$$W_1 = C_1C_2e^{C_2(I_1 - 3)}\,, \tag{5.3.9}$$

$$W_2 = -\frac{C_1C_2}{2}\,. \tag{5.3.10}$$

This material model was the result from the research of the elastic response of skin tissue [62].

5.3.4 Arruda-Boyce Hyperelasticity

Arruda and Boyce proposed a model for the deformation of rubber materials [3]. Their main motivation was to develop a model that accurately captures the behavior of rubbers in different loading scenarios and that can be described with a limited number of physically motivated parameters. Their model is based on the Langevin chain statistics, which models a rubber chain segment between chemical crosslinks as a number N of rigid links of equal length l. The parameter N is related to the locking stretch λ_L, the stretch at which the chains reach their full extended state, $\lambda_L = \sqrt{N}$.

Their proposed strain-energy is a truncated Taylor series of the inverse Langevin function. A formulation that retains the first five terms of this function takes on the following form:

$$\tilde{W} = \mu \sum_{i=1}^{5} \frac{\alpha_i}{N^{i-1}} \left(\tilde{I}_1^i - 3^i \right) + U(J) , \tag{5.3.11}$$

where μ is a shear-modulus like parameter and the coefficients α_i are

$$\alpha_1 = \frac{1}{2}, \quad \alpha_2 = \frac{1}{20}, \quad \alpha_3 = \frac{11}{1050}, \quad \alpha_4 = \frac{19}{7000}, \quad \alpha_5 = \frac{519}{673750} . \tag{5.3.12}$$

The Cauchy stress is given by

$$\boldsymbol{\sigma} = p\mathbf{I} + \frac{2}{J} \operatorname{dev}\left(W_1 \tilde{\mathbf{b}} \right) = p\mathbf{I} + \frac{2W_1}{J} \left(\tilde{\mathbf{b}} - \frac{1}{3}\tilde{I}_1 \mathbf{I} \right) , \tag{5.3.13}$$

where,

$$W_1 = \frac{\partial \tilde{W}}{\partial \tilde{I}_1} = \mu \sum_{i=1}^{5} \alpha_i i \left(\frac{\tilde{I}_1}{N} \right)^{i-1} . \tag{5.3.14}$$

5.3.5 Transversely Isotropic Hyperelastic

This constitutive model can be used to represent a material that has a single preferred fiber direction and was developed for application to biological soft tissues [64, 49, 51]. It can be used to model tissues such as tendons, ligaments and muscle. The elastic response of the tissue is assumed to arise from the resistance of the fiber family and an isotropic matrix. It is assumed that the strain energy function can be written as follows:

$$W = F_1 \left(\tilde{I}_1, \tilde{I}_2 \right) + F_2 \left(\tilde{\lambda} \right) + \frac{K}{2} \left[\ln(J) \right]^2 . \tag{5.3.15}$$

Here, $\tilde{I}_1$ and $\tilde{I}_2$ are the first and second invariants of the deviatoric version of the right Cauchy Green deformation tensor $\tilde{\mathbf{C}}$ and $\tilde{\lambda}$ is the deviatoric part of the stretch along the fiber direction ($\tilde{\lambda}^2 = \mathbf{A} \cdot \tilde{\mathbf{C}} \cdot \mathbf{A}$, where $\mathbf{A}$ is the initial fiber direction). The function F_1 represents the material response of the isotropic ground substance matrix, while F_2 represents the contribution from the fiber family. The strain energy of the fiber family is as follows:

$$\tilde{\lambda} \frac{\partial F_2}{\partial \tilde{\lambda}} = \begin{cases} 0 & \tilde{\lambda} \leqslant 1 \\ C_3 \left(e^{C_4(\tilde{\lambda}-1)} - 1 \right) & 1 < \tilde{\lambda} < \lambda_m \\ C_5 + C_6 \tilde{\lambda} & \tilde{\lambda} \geqslant \lambda_m \end{cases} . \tag{5.3.16}$$

Here, λ_m is the stretch at which the fibers are straightened, C_3 scales the exponential stresses, C_4 is the rate of uncrimping of the fibers, and C_5 is the modulus of the straightened fibers. C_6 is determined from the requirement that the stress is continuous at λ_m,

$$C_6 = \frac{1}{\lambda_m} \left[C_3 \left(e^{C_4(\lambda_m - 1)} - 1 \right) - C_5 \right] . \tag{5.3.17}$$

It also follows that

$$F_2 \left(\tilde{\lambda} \right) = \begin{cases} 0 & \tilde{\lambda} \leqslant 1 \\ C_3 \left(e^{-C_4} \left[\mathrm{Ei} \left(C_4 \tilde{\lambda} \right) - \mathrm{Ei} \left(C_4 \right) \right] - \ln \tilde{\lambda} \right) & 1 < \tilde{\lambda} < \lambda_m \\ \left(C_5 + \frac{C_6}{2} \tilde{\lambda} \right) \tilde{\lambda} + C_7 & \tilde{\lambda} \geqslant \lambda_m \end{cases}, \tag{5.3.18}$$

where

$$C_7 = C_3 \left(e^{-C_4} \left[\mathrm{Ei} \left(C_4 \lambda_m \right) - \mathrm{Ei} \left(C_4 \right) \right] - \ln \lambda_m \right) - \left(C_5 + \frac{C_6}{2} \lambda_m \right) \lambda_m . \tag{5.3.19}$$

This material model uses a three-field element formulation, interpolating displacements as linear field variables and pressure and volume ratio as piecewise constant on each element [55].

5.3.6   Ellipsoidal Fiber Distribution

This constitutive model describes a material that is composed of an ellipsoidal continuous fiber distribution in an uncoupled formulation. The deviatoric part of the stress is given by [7, 4, 39],

$$\tilde{\boldsymbol{\sigma}} = \int_0^{2\pi} \int_0^{\pi} H \left(\tilde{I}_n - 1 \right) \tilde{\boldsymbol{\sigma}}_n \left(\mathbf{n} \right) \sin \varphi \, d\varphi \, d\theta , \tag{5.3.20}$$

and the corresponding elasticity tensor is

$$\tilde{\boldsymbol{\mathcal{C}}} = \int_0^{2\pi} \int_0^{\pi} H \left(\tilde{I}_n - 1 \right) \tilde{\boldsymbol{\mathcal{C}}}_n \left(\mathbf{n} \right) \sin \phi \, d\phi \, d\theta . \tag{5.3.21}$$

$\tilde{I}_n = \tilde{\lambda}_n^2 = \mathbf{N} \cdot \tilde{\mathbf{C}} \cdot \mathbf{N}$ is the square of the fiber stretch $\mathbf{F}$, $\mathbf{N}$ is the unit vector along the fiber direction (in the reference configuration), which in spherical angles is directed along (θ, φ), $\mathbf{n} = \tilde{\mathbf{F}} \cdot \mathbf{N} / \tilde{\lambda}_n$ and $H \left(\cdot \right)$ is the unit step function that enforces the tension-only contribution. The fiber stress is determined from a fiber strain energy function in the usual manner:

$$\tilde{\boldsymbol{\sigma}}_n \left(\mathbf{n} \right) = 2 J^{-1} \tilde{I}_n \frac{\partial \tilde{\Psi}}{\partial \tilde{I}_n} \mathbf{n} \otimes \mathbf{n} , \tag{5.3.22}$$

whereas the fiber elasticity tensor is

$$\tilde{\boldsymbol{\mathcal{C}}}_n \left(\mathbf{n} \right) = 4 J^{-1} \tilde{I}_n^2 \frac{\partial^2 \tilde{\Psi}}{\partial \tilde{I}_n^2} \mathbf{n} \otimes \mathbf{n} \otimes \mathbf{n} \otimes \mathbf{n} , \tag{5.3.23}$$

where in this material

$$\tilde{\Psi} \left(\mathbf{n}, \tilde{I}_n \right) = \xi \left(\mathbf{n} \right) \left(\tilde{I}_n - 1 \right)^{\beta(\mathbf{n})} . \tag{5.3.24}$$

The materials parameters β and ξ are determined from:

$$\xi\left(\mathbf{n}\right) = \left(\frac{\cos^2\theta\sin^2\varphi}{\xi_1^2} + \frac{\sin^2\theta\sin^2\varphi}{\xi_2^2} + \frac{\cos^2\varphi}{\xi_3^2}\right)^{-1/2},$$

$$\beta\left(\mathbf{n}\right) = \left(\frac{\cos^2\theta\sin^2\varphi}{\beta_1^2} + \frac{\sin^2\theta\sin^2\varphi}{\beta_2^2} + \frac{\cos^2\varphi}{\beta_3^2}\right)^{-1/2}.$$

(5.3.25)

Since fibers can only sustain tension, this material is not stable on its own. It must be combined with a material that acts as the ground matrix. The total stress is then given by the sum of the fiber stress and the ground matrix stress:

$$\tilde{\boldsymbol{\sigma}} = \tilde{\boldsymbol{\sigma}}_m + \tilde{\boldsymbol{\sigma}}_f.$$

(5.3.26)

5.3.7 Fiber with Exponential Power law

This material model describes a constitutive model for fibers, where a single fiber family follows an exponential power law strain energy function. The deviatoric part of the Cauchy stress is given by:

$$\tilde{\boldsymbol{\sigma}} = 2J^{-1}H\left(\tilde{I}_n - 1\right)\tilde{I}_n\frac{\partial\tilde{\Psi}}{\partial\tilde{I}_n}\mathbf{n}\otimes\mathbf{n},$$

(5.3.27)

and the corresponding spatial elasticity tensor is

$$\tilde{\boldsymbol{\mathcal{C}}} = 4J^{-1}H\left(\tilde{I}_n - 1\right)\tilde{I}_n^2\frac{\partial^2\tilde{\Psi}}{\partial\tilde{I}_n^2}\mathbf{n}\otimes\mathbf{n}\otimes\mathbf{n}\otimes\mathbf{n},$$

(5.3.28)

where $\tilde{I}_n = \tilde{\lambda}_n^2 = \mathbf{N}\cdot\tilde{\mathbf{C}}\cdot\mathbf{N}$ is the square of the fiber stretch, $\mathbf{N}$ is the fiber orientation in the reference configuration,

$$\mathbf{N} = \sin\varphi\cos\theta\,\mathbf{e}_1 + \sin\varphi\sin\theta\,\mathbf{e}_2 + \cos\varphi\,\mathbf{e}_3,$$

(5.3.29)

and $\mathbf{n} = \tilde{\mathbf{F}}\cdot\mathbf{N}/\tilde{\lambda}_n$ and $H\left(\cdot\right)$ is the unit step function that enforces the tension-only contribution. The fiber strain energy density is given by

$$\tilde{\Psi} = \frac{\xi}{\alpha\beta}\left(\exp\left[\alpha\left(\tilde{I}_n - 1\right)^\beta\right] - 1\right),$$

(5.3.30)

where $\xi > 0$, $\alpha \geqslant 0$ and $\beta \geqslant 2$.

Note: In the limit when $\alpha \to 0$, this expression produces a power law,

$$\lim_{\alpha\to 0}\tilde{\Psi} = \frac{\xi}{\beta}\left(\tilde{I}_n - 1\right)^\beta.$$

(5.3.31)

Note: When $\beta > 2$, the fiber modulus is zero at the strain origin ($\tilde{I}_n = 1$). Therefore, use $\beta > 2$ when a smooth transition in the stress is desired from compression to tension.

5.3.8 Fung Orthotropic

The hyperelastic strain energy function for a Fung Orthotropic material is given by [26, 27]

$$\tilde{\Psi} = \frac{1}{2}c\left(e^{\tilde{Q}} - 1\right) + U\left(J\right),$$

(5.3.32)

where

$$\tilde{Q} = c^{-1} \sum_{a=1}^{3} \left[2\mu_a \mathbf{M}_a : \tilde{\mathbf{E}}^2 + \sum_{b=1}^{3} \lambda_{ab} \left(\mathbf{M}_a : \tilde{\mathbf{E}} \right) \left(\mathbf{M}_b : \tilde{\mathbf{E}} \right) \right] . \tag{5.3.33}$$

Here, $\tilde{\mathbf{E}} = \frac{1}{2} \left(\tilde{\mathbf{C}} - \mathbf{I} \right)$ and $\mathbf{M}_a = \mathbf{A}_a \otimes \mathbf{A}_a$, where $\mathbf{A}_a$ are orthonormal vectors that define the initial direction of material axes. The orthotropic Lamé coefficients should be chosen such that the stiffness matrix,

$$\begin{bmatrix} \lambda_{11} + 2\mu_1 & \lambda_{12} & \lambda_{13} & 0 & 0 & 0 \\ \lambda_{12} & \lambda_{22} + 2\mu_2 & \lambda_{23} & 0 & 0 & 0 \\ \lambda_{13} & \lambda_{23} & \lambda_{33} + 2\mu_3 & 0 & 0 & 0 \\ 0 & 0 & 0 & \frac{1}{2}(\mu_1 + \mu_2) & 0 & 0 \\ 0 & 0 & 0 & 0 & \frac{1}{2}(\mu_2 + \mu_3) & 0 \\ 0 & 0 & 0 & 0 & 0 & \frac{1}{2}(\mu_1 + \mu_3) \end{bmatrix} \tag{5.3.34}$$

is positive definite.

5.3.9 Tension-Compression Nonlinear Orthotropic

This material model is based on the following uncoupled hyperelastic strain energy function [12]:

$$\Psi \left(\mathbf{C}, \lambda_1, \lambda_2, \lambda_3 \right) = \tilde{\Psi}_{\text{iso}} \left(\tilde{\mathbf{C}} \right) + \sum_{i=1}^{3} \tilde{\Psi}_i^{TC} \left(\tilde{\lambda}_i \right) + U \left(J \right) . \tag{5.3.35}$$

The isotropic strain energy $\tilde{\Psi}_{\text{iso}}$ and the dilatational energy U are the same as for the Mooney-Rivlin material (Section 5.3.1). The tension-compression term is defined as follows:

$$\tilde{\Psi}_i^{TC} \left(\tilde{\lambda}_i \right) = \begin{cases} \xi_i \left(\tilde{\lambda}_i - 1 \right)^{\beta_i} & \tilde{\lambda}_i > 1 \\ 0 & \tilde{\lambda}_i \leqslant 1 \end{cases} , \xi_i \geqslant 0 \quad \text{(no sum over } i\text{).} \tag{5.3.36}$$

The $\tilde{\lambda}_i$ parameters are the deviatoric fiber stretches of the local material fibers,

$$\tilde{\lambda}_i = \left(\mathbf{A}_i \cdot \tilde{\mathbf{C}} \cdot \mathbf{A}_i \right)^{1/2} . \tag{5.3.37}$$

The local material fibers are defined (in the reference frame) as an orthonormal set of vectors $\mathbf{A}_i$. The corresponding deviatoric part of the Cauchy stress is

$$\tilde{\boldsymbol{\sigma}} = J^{-1} \sum_{i=1}^{3} \frac{1}{\tilde{\lambda}_i} \frac{\partial \tilde{\Psi}}{\partial \tilde{\lambda}_i} \mathbf{a}_i \otimes \mathbf{a}_i , \tag{5.3.38}$$

and the spatial elasticity tensor is

$$\tilde{\mathcal{C}} = J^{-1} \sum_{i=1}^{3} \frac{1}{\tilde{\lambda}_i} \frac{\partial}{\partial \tilde{\lambda}_i} \left(\frac{1}{\tilde{\lambda}_i} \frac{\partial \tilde{\Psi}}{\partial \tilde{\lambda}_i} \right) \mathbf{a}_i \otimes \mathbf{a}_i \otimes \mathbf{a}_i \otimes \mathbf{a}_i , \tag{5.3.39}$$

where $\mathbf{a}_i = \tilde{\mathbf{F}} \cdot \mathbf{A}_i$.

5.4 Viscoelasticity

For a viscoelastic material the second Piola Kirchhoff stress can be written as follows [49]:

$$\mathbf{S}(t) = \int\limits_{-\infty}^{t} G(t-s) \frac{d\mathbf{S}^e}{ds} \, ds , \tag{5.4.1}$$

where $\mathbf{S}^e$ is the elastic stress and $G(t)$ is the relaxation function. Here we consider the special case where the relaxation function is given by

$$G(t) = \gamma_0 + \sum_{i=1}^{N} \gamma_i \exp(-t/\tau_i) . \tag{5.4.2}$$

With this function chosen for the relaxation function, we can write the total stress as

$$\mathbf{S}(t) = \int\limits_{-\infty}^{t} \left(\gamma_0 + \sum_{i=1}^{N} \gamma_i \exp\left((-t+s)/\tau_i\right) \frac{d\mathbf{S}^e}{ds} \right) ds . \tag{5.4.3}$$

Introducing the internal variables,

$$\mathbf{H}^{(i)}(t) = \int\limits_{-\infty}^{t} \exp\left[-(t-s)/\tau_i\right] \frac{d\mathbf{S}^e}{ds} \, ds , \tag{5.4.4}$$

we can rewrite (5.4.3) as follows,

$$\mathbf{S}(t) = \gamma_0 \mathbf{S}^e(t) + \sum_{i=1}^{N} \gamma_i \mathbf{H}^{(i)}(t) . \tag{5.4.5}$$

In FEBio, $\gamma_0 = 1$, so $\mathbf{S}^e$ is the long-term elastic response of the material.

The question now remains how to evaluate the internal variables. From equation (5.4.4) it appears that we have to integrate over the entire time domain. However, we can find a recurrence relationship that will allow us to evaluate the internal variables at a time $t + \Delta t$ given the values at time t.

$$\mathbf{H}^{(i)}(t + \Delta t) = \int\limits_{-\infty}^{t+\Delta t} \exp\left[-(t+\Delta t-s)/\tau_i\right] \frac{d\mathbf{S}^e}{ds} \, ds$$

$$= \exp(-\Delta t/\tau_i) \int\limits_{-\infty}^{t} \exp\left[-(t-s)/\tau_i\right] \frac{d\mathbf{S}^e}{ds} \, ds + \int\limits_{t}^{t+\Delta t} \exp\left[-(t+\Delta t-s)/\tau_i\right] \frac{d\mathbf{S}^e}{ds} \, ds$$

$$= \exp(-\Delta t/\tau_i) \mathbf{H}^{(i)}(t) + \int\limits_{t}^{t+\Delta t} \exp\left[-(t+\Delta t-s)/\tau_i\right] \frac{d\mathbf{S}^e}{ds} \, ds .$$

$$\tag{5.4.6}$$

The last term can now be simplified using the midpoint rule to approximate the derivate. In that case we find the recurrence relation:

$$\mathbf{H}^{(i)}(t + \Delta t) = \exp(-\Delta t/\tau_i) \mathbf{H}^{(i)}(t) + \frac{1 - \exp(-\Delta t/\tau_i)}{\Delta t/\tau_i} \left(\mathbf{S}^e(t + \Delta t) - \mathbf{S}^e(t)\right) . \tag{5.4.7}$$

The following procedure can now be applied to calculate the new stress. Given $\mathbf{S}_n^e$ and $\mathbf{H}_n^{(i)}$ corresponding to time t, find $\mathbf{S}_{n+1}^e$ and $\mathbf{H}_{n+1}^{(i)}$ corresponding to time $t + \Delta t$:

1. calculate elastic stress:

$$\mathbf{S}_{n+1}^e = \frac{\partial W^e}{\partial \mathbf{C}_{n+1}} \, ,$$

2. evaluate internal variables:

$$\mathbf{H}_{n+1}^i = \exp\left(-\Delta t/\tau_i\right) \mathbf{H}_n^i + \frac{1 - \exp\left(-\Delta t/\tau_i\right)}{\Delta t/\tau_i} \left(\mathbf{S}_{n+1}^e - \mathbf{S}_n^e\right) \, ,$$

3. find the total stress:

$$\mathbf{S}_{n+1} = \gamma_0 \mathbf{S}_{n+1}^e + \sum_{i=1}^{N} \gamma_i \mathbf{H}_{n+1}^i \, .$$

5.5 Reactive Viscoelasticity

Reactive viscoelasticity models a material as a mixture of strong bonds, which are permanent, and weak bonds, which break and reform in response to loading [11]. Strong bonds produce the equilibrium elastic response, whereas weak bonds produce the transient viscous response. Strong bonds are in a stress-free state when in their reference configuration $\mathbf{X}$. Their deformation gradient is defined as usual, $\mathbf{F}(\mathbf{X}, t) = \partial\chi(\mathbf{X}, t) / \partial\mathbf{X}$. When weak bonds break in response to loading at some time u, they reform instantaneously in a stress-free configuration $\mathbf{X}^u$ that coincides with the current configuration at time u, thus, $\mathbf{X}^u = \chi(\mathbf{X}, u)$. Therefore, a reaction transforms intact loaded bonds into reformed unloaded bonds. Weak bonds that reform at time u may be called $u-$generation bonds. The deformation gradient of $u-$generation weak bonds relative to their reference configuration $\mathbf{X}^u$ is denoted by $\mathbf{F}^u(\mathbf{X}, t)$, which may be evaluated from the chain rule,

$$\mathbf{F}(\mathbf{X}, t) = \mathbf{F}^u(\mathbf{X}, t) \cdot \mathbf{F}(\mathbf{X}, u) . \tag{5.5.1}$$

The strain energy density Ψ_r in a reactive viscoelastic material is given by

$$\Psi_r(\mathbf{F}) = \Psi_r^e(\mathbf{F}) + \sum_u w^u \Psi_0^b(\mathbf{F}^u) , \tag{5.5.2}$$

where Ψ_r^e is the strain energy density of strong bonds and Ψ_0^b is the strain energy density of weak bonds, when they all belong to the same generation. In this expression, $w^u(\mathbf{X}, t)$ is the mass fraction of $u-$generation weak bonds, which evolves over time as described below. The summation is taken over all generations u that were created prior to the current time t. The Cauchy stress σ in a reactive viscoelastic material is similarly given by

$$\boldsymbol{\sigma}(\mathbf{F}) = \boldsymbol{\sigma}^e(\mathbf{F}) + \sum_u w^u \boldsymbol{\sigma}^b(\mathbf{F}^u) , \tag{5.5.3}$$

where σ^e is the stress in the strong bonds and σ^b is the stress in the weak bonds. These stresses are related to the respective strain energy densities of strong and weak bonds according to

$$\boldsymbol{\sigma}^e(\mathbf{F}) = \frac{1}{J}\frac{\partial\Psi_r^e(\mathbf{F})}{\partial\mathbf{F}} \cdot \mathbf{F}^T, \quad \boldsymbol{\sigma}^b(\mathbf{F}^u) = \frac{1}{J}\frac{\partial\Psi_0^b(\mathbf{F}^u)}{\partial\mathbf{F}^u} \cdot (\mathbf{F}^u)^T . \tag{5.5.4}$$

The mass fractions $w^u(\mathbf{X}, t)$ are obtained by solving the equation of mass balance for reactive constrained mixtures,

$$\frac{\partial w^u}{\partial t} = \hat{w}^u(\mathbf{F}, w^\gamma) , \tag{5.5.5}$$

where the mass fraction supply $\hat{w}^u$ must be specified as a constitutive function of the deformation gradient $\mathbf{F}$ and the mass fractions w^γ from all generations. Since mass must be conserved over all generations, it follows that

$$\sum_u \hat{w}^u = 0, \quad \sum_u w^u = 1 . \tag{5.5.6}$$

Any number of valid solutions may exist for w^u, based on constitutive assumptions for $\hat{w}^u$. For example, for $u-$generation bonds reforming in an unloaded state during the time interval $u \leqslant t < v$, and subsequently breaking in response to loading at $t = v$, Type I bond kinetics provides a solution of the form

$$w^u(\mathbf{X}, t) = \begin{cases} 0 & t < u \\ f^u(\mathbf{X}, t) & u \leqslant t < v \\ f^u(\mathbf{X}, v) \, g(\mathbf{F}^u(v); \mathbf{X}, t - v) & v \leqslant t \end{cases} , \tag{5.5.7}$$

where

$$f^u \left(\mathbf{X}, t \right) = 1 - \sum_{\gamma < u} w^\gamma \left(\mathbf{X}, t \right) , \tag{5.5.8}$$

and $g \left(\mathbf{F}^u \left(v \right); \mathbf{X}, t - v \right)$ is a reduced relaxation function which may assume any number of valid forms. (A reduced relaxation function $g \left(t \right)$ satisfies $g \left(0 \right) = 1$ and $g \left(t \to \infty \right) = 0$, and decreases monotonically with t.) In particular, g may depend on the strain at time v relative to the reference configuration of the $u-$generation. In the recursive expression of (5.5.7), the earliest generation $u = -\infty$, which is initially at rest, produces $w^u \left(t \right) = 1$ for $t < v$ and $w^u \left(t \right) = g \left(\mathbf{F}^u \left(v \right); \mathbf{X}, t - v \right)$ for $t \geqslant v$; this latter expression seeds the recursion for subsequent generations. Therefore, providing a functional form for g suffices to produce the solution for all bond generations u.

For Type II bond kinetics, the solution for the mass fractions is given by

$$w^u \left(t \right) = \begin{cases} 0 & t < u \\ 1 - g \left(t - u \right) & u \leqslant t < v \\ g \left(t - v \right) - g \left(t - u \right) & v \leqslant t \end{cases} . \tag{5.5.9}$$

For this type of bond kinetics, the reduced relaxation function g cannot depend on the magnitude of the strain, because strain-dependence might violate the constraint $0 \leqslant w^u \leqslant 1$.

For all bond kinetics, it is also possible to constrain the occurrence of the breaking-and-reforming reaction to specific forms of the strain. For example, the reaction may be allowed to proceed only in the case of dilatational strain, or only in the case of distortional strain.

The finite element implementation of reactive viscoelasticity stores the value of $\mathbf{F}^{-1} \left(\mathbf{X}, u \right)$ every time that a bond-breaking deformation is detected; this value can be used to evaluate $\mathbf{F}^u \left(\mathbf{X}, t \right)$ using (5.5.1). It also stores $w^u \left(\mathbf{X}, v \right) = f^u \left(\mathbf{X}, v \right)$, where v is the time step immediately following u, which is then used for evaluating w^u for subsequent time steps $t > v$ when using Type I bond kinetics, using the expressions of (5.5.7) and (5.5.8). These measures are then used to evaluate the stress from (5.5.3), with the summation taken over the time steps that correspond to bond-reforming generations.

5.6 Hydraulic Permeability

Hydraulic permeability is a material function needed for biphasic and biphasic-solute materials.

5.6.1 Constant Isotropic Permeability

When the permeability is isotropic,

$$\mathbf{k} = k\,\mathbf{I}\,. \tag{5.6.1}$$

For this material model, k is constant. Generally, this assumption is only reasonable when strains are small.

5.6.2 Holmes-Mow

This isotropic material is similar to the constant isotropic permeability material described above, except that it uses a strain-dependent permeability tensor [30]:

$$\mathbf{k} = k\left(J\right)\mathbf{I}\,, \tag{5.6.2}$$

where,

$$k\left(J\right) = k_0 \left(\frac{J - \varphi_0}{1 - \varphi_0}\right)^{\alpha} e^{\frac{1}{2}M\left(J^2 - 1\right)}\,. \tag{5.6.3}$$

5.6.3 Referentially Isotropic Permeability

This material uses a strain-dependent permeability tensor that accommodates strain-induced anisotropy [9]:

$$\mathbf{k} = \left(k_{0r}\mathbf{I} + \frac{k_{1r}}{J^2}\mathbf{b} + \frac{k_{2r}}{J^4}\mathbf{b}^2\right)\left(\frac{J - \varphi_r^s}{1 - \varphi_r^s}\right)e^{M\left(J^2 - 1\right)/2}\,, \tag{5.6.4}$$

Note that the permeability in the reference state ($\mathbf{F} = \mathbf{I}$) is isotropic and given by $\mathbf{k} = \left(k_{0r} + k_{1r} + k_{2r}\right)\mathbf{I}$.

5.6.4 Referentially Orthotropic Permeability

This material uses a strain-dependent permeability tensor that is orthotropic in the reference configuration, and accommodates strain-induced anisotropy [9]:

$$\mathbf{k} = k_0\mathbf{I} + \sum_{a=1}^{3} k_1^a\mathbf{m}_a + k_2^a\left(\mathbf{m}_a \cdot \mathbf{b} + \mathbf{b} \cdot \mathbf{m}_a\right)\,, \tag{5.6.5}$$

where,

$$
\begin{aligned}
k_0 &= k_{0r}\left(\frac{J - \varphi_r^s}{1 - \varphi_r^s}\right)^{\alpha_0} e^{M_0\left(J^2 - 1\right)/2}\,, \\
k_1^a &= \frac{k_{1r}^a}{J^2}\left(\frac{J - \varphi_r^s}{1 - \varphi_r^s}\right)^{\alpha_a} e^{M_a\left(J^2 - 1\right)/2}\,, \quad a = 1, 2, 3 \\
k_2^a &= \frac{k_{2r}^a}{2J^4}\left(\frac{J - \varphi_r^s}{1 - \varphi_r^s}\right)^{\alpha_a} e^{M_a\left(J^2 - 1\right)/2}\,.
\end{aligned}
\tag{5.6.6}
$$

Here, $\mathbf{m}_a$ are second order tensors representing the spatial structural tensors describing the orthogonal planes of symmetry, given by

$$\mathbf{m}_a = \mathbf{F} \cdot (\mathbf{V}_a \otimes \mathbf{V}_a) \cdot \mathbf{F}^T, \quad a = 1 - 3, \tag{5.6.7}$$

where $\mathbf{V}_a$ are orthonormal vectors normal to the planes of symmetry. Note that the permeability in the reference state ($\mathbf{F} = \mathbf{I}$) is given by $\mathbf{k} = k_{0r}\mathbf{I} + \sum_{a=1}^{3} (k_{1r}^a + k_{2r}^a) \mathbf{V}_a \otimes \mathbf{V}_a$.

5.6.5   Referentially Transversely Isotropic Permeability

This material uses a strain-dependent permeability tensor that is transversely isotropic in the reference configuration, and accommodates strain-induced anisotropy [9]:

$$
\begin{aligned}
\mathbf{k} = {} & k_{0r} \left(\frac{J - \varphi_r^s}{1 - \varphi_r^s} \right)^{\alpha_0} e^{M_0 \left(J^2 - 1 \right)/2} \mathbf{I} \\
& + \left(\frac{k_{1r}^T}{J^2} (\mathbf{b} - \mathbf{m}) + \frac{k_{2r}^T}{2J^4} \left[2\mathbf{b}^2 - (\mathbf{m} \cdot \mathbf{b} + \mathbf{b} \cdot \mathbf{m}) \right] \right) \left(\frac{J - \varphi_r^s}{1 - \varphi_r^s} \right)^{\alpha_T} e^{M_T \left(J^2 - 1 \right)/2} \\
& + \left(\frac{1}{J^2} k_{1r}^A \mathbf{m} + \frac{1}{2J^4} k_{2r}^A (\mathbf{m} \cdot \mathbf{b} + \mathbf{b} \cdot \mathbf{m}) \right) \left(\frac{J - \varphi_r^s}{1 - \varphi_r^s} \right)^{\alpha_A} e^{M_A \left(J^2 - 1 \right)/2},
\end{aligned}
\tag{5.6.8}
$$

where $\mathbf{m}$ is a second order tensor representing the spatial structural tensor describing the axial direction, given by

$$\mathbf{m} = \mathbf{F} \cdot (\mathbf{V} \otimes \mathbf{V}) \cdot \mathbf{F}^T, \tag{5.6.9}$$

and $\mathbf{V}$ is a unit vector along the axial direction. Note that the permeability in the reference state ($\mathbf{F} = \mathbf{I}$) is given by $\mathbf{k} = \left(k_{0r} + k_{1r}^T + k_{2r}^T \right) \mathbf{I} + \left(k_{1r}^A - k_{1r}^T + k_{2r}^A - k_{2r}^T \right) (\mathbf{V} \otimes \mathbf{V})$.

5.7 Solute Diffusivity

Diffusivity materials provide a constitutive relation for the solute diffusivity in a biphasic-solute material. In general, the diffusivity tensor $\mathbf{d}$ may be a function of strain and solute concentration.

5.7.1 Constant Isotropic Diffusivity

When the permeability is isotropic,

$$\mathbf{d} = d\,\mathbf{I}. \tag{5.7.1}$$

For this material model, d is constant. This assumption is only true when strains are small. Note that the user must specify $d \leqslant d_0$, where d_0 is the solute diffusivity in free solution, since a solute cannot diffuse through the biphasic-solute mixture faster than in free solution.

5.7.2 Constant Orthotropic Diffusivity

When the permeability is orthotropic,

$$\mathbf{d} = \sum_{a=1}^{3} d^a \mathbf{V}_a \otimes \mathbf{V}_a\,, \tag{5.7.2}$$

where $\mathbf{V}_a$ are orthonormal vectors normal to the planes of symmetry. For this material model, the d^a are constant. Therefore this model should be used only when strains are small. Note that the user must specify $d^a \leqslant d_0$, where d_0 is the solute diffusivity in free solution, since a solute cannot diffuse through the biphasic-solute mixture faster than in free solution.

5.7.3 Referentially Isotropic Diffusivity

This material uses a strain-dependent diffusivity tensor that is isotropic in the reference configuration and accommodates strain-induced anisotropy:

$$\mathbf{d} = \left(d_{0r}\mathbf{I} + \frac{d_{1r}}{J^2}\mathbf{b} + \frac{d_{2r}}{J^4}\mathbf{b}^2 \right) \left(\frac{J - \varphi_r^s}{1 - \varphi_r^s} \right) e^{M\left(J^2-1\right)/2}, \tag{5.7.3}$$

where J is the jacobian of the deformation, i.e. $J = \det \mathbf{F}$ where $\mathbf{F}$ is the deformation gradient, and $\mathbf{b} = \mathbf{F} \cdot \mathbf{F}^T$ is the left Cauchy-Green tensor. Note that the diffusivity in the reference state $(\mathbf{F} = \mathbf{I})$ is isotropic and given by $\mathbf{d} = \left(d_{0r} + d_{1r} + d_{2r} \right) \mathbf{I}$.

5.7.4 Referentially Orthotropic Diffusivity

This material uses a strain-dependent diffusivity tensor that is orthotropic in the reference configuration and accommodates strain-induced anisotropy:

$$\mathbf{d} = d_0\mathbf{I} + \sum_{a=1}^{3} d_1^a \mathbf{m}_a + d_2^a \left(\mathbf{m}_a \cdot \mathbf{b} + \mathbf{b} \cdot \mathbf{m}_a \right)\,, \tag{5.7.4}$$

where

$$d_0 = d_{0r} \left(\frac{J - \varphi_r^s}{1 - \varphi_r^s} \right)^{\alpha_0} e^{M_0 \left(J^2 - 1 \right)/2},$$

$$d_1^a = \frac{d_{1r}^a}{J^2} \left(\frac{J - \varphi_r^s}{1 - \varphi_r^s} \right)^{\alpha_a} e^{M_a \left(J^2 - 1 \right)/2}, \quad a = 1, 2, 3 \tag{5.7.5}$$

$$d_2^a = \frac{d_{2r}^a}{2 J^4} \left(\frac{J - \varphi_r^s}{1 - \varphi_r^s} \right)^{\alpha_a} e^{M_a \left(J^2 - 1 \right)/2}.$$

Here, J is the Jacobian of the deformation, i.e. $J = \det \mathbf{F}$ where $\mathbf{F}$ is the deformation gradient. $\mathbf{m}_a$ are second order tensor representing the spatial structural tensors describing the orthogonal planes of symmetry, given by

$$\mathbf{m}_a = \mathbf{F} \cdot (\mathbf{V}_a \otimes \mathbf{V}_a) \cdot \mathbf{F}^T, \quad a = 1 - 3, \tag{5.7.6}$$

where $\mathbf{V}_a$ are orthonormal vectors normal to the planes of symmetry. Note that the permeability in the reference state ($\mathbf{F} = \mathbf{I}$) is given by $\mathbf{k} = k_{0r} \mathbf{I} + \sum_{a=1}^{3} (k_{1r}^a + k_{2r}^a) \mathbf{V}_a \otimes \mathbf{V}_a$.

5.8 Solute Solubility

Solubility constitutive equations provide a relation for $\tilde{\kappa}$ as a function of solid matrix strain and effective solute concentrations.

5.8.1 Constant Solubility

For this material model, $\tilde{\kappa}$ is constant.

5.9   Osmotic Coefficient

Osmotic coefficient constitutive equations provide a relation for Φ as a function of solid matrix strain and effective solute concentrations.

5.9.1   Constant Osmotic Coefficient

For this material model, Φ is constant.

5.10 Active Contraction Model

A time varying "elastance" active contraction model [29] was added to the transversely isotropic materials. When active contraction is activated, the total Cauchy stress σ is defined as the sum of the active stress tensor $\boldsymbol{\sigma}^a = T^a \mathbf{a} \otimes \mathbf{a}$ and the passive stress tensor $\boldsymbol{\sigma}^p$:

$$\boldsymbol{\sigma} = \boldsymbol{\sigma}^p + \boldsymbol{\sigma}^a, \tag{5.10.1}$$

where *a* is the deformed fiber vector (unit length), defined as $\lambda \mathbf{a} = \mathbf{F} \cdot \mathbf{a}$. The time varying elastance model is a modification of the standard Hill equation that scales the standard equation by an activation curve $C(t)$. The active fiber stress T^a is defined as:

$$T^a = T_{\max} \frac{Ca_0^2}{Ca_0^2 + ECa_{50}^2} C(t), \tag{5.10.2}$$

where $T_{max} = 135.7\,\text{kPa}$ is the isometric tension under maximal activation at the peak intracellular calcium concentration of $Ca_0 = 4.35\,\mu M$. The length dependent calcium sensitivity is governed by the following equation:

$$ECa_{50} = \frac{(\text{Ca}_0)_{\max}}{\sqrt{\exp\left[B(l - l_0)\right] - 1}}, \tag{5.10.3}$$

where $(\text{Ca}_0)_{\max} = 4.35\,\mu\text{M}$ is the maximum peak intracellular calcium concentration, $B = 4.75\,\mu\text{m}^{-1}$ governs the shape of the peak isometric tension-sarcomere length relation, $l_0 = 1.58\,\mu\text{m}$ is the sarcomere length at which no active tension develops, and l is the sarcomere length which is the product of the fiber stretch λ and the sarcomere unloaded length $l_r = 2.04\,\mu\text{m}$.

5.11   Prescribed Active Contraction

Prescribed active contraction models allow the user to directly specify the time history of the active contractile stress.

5.11.1   Uniaxial Active Contraction

For this model, the active stress is acting along a prescribed direction given by the unit vector $\mathbf{a}_r$ in the reference configuration. The 2nd Piola-Kirchhoff stress is

$$\mathbf{S}^a = T^a \mathbf{a}_r \otimes \mathbf{a}_r \,, \tag{5.11.1}$$

and the Cauchy stress is

$$\boldsymbol{\sigma}^a = J^{-1} T^a \mathbf{a} \otimes \mathbf{a} \,, \tag{5.11.2}$$

where T^a is the prescribed contractile stress and $\mathbf{a} = \mathbf{F} \cdot \mathbf{a}_r$. Since $\mathbf{S}^a$ is not a function of deformation, the material and spatial tangents are both zero.

5.11.2   Transversely Isotropic Active Contraction

In this case, the active stress is isotropic in a plane transverse to the direction $\mathbf{a}_r$,

$$\mathbf{S}^a = T^a \left(\mathbf{I} - \mathbf{a}_r \otimes \mathbf{a}_r \right) \,, \tag{5.11.3}$$

and the corresponding Cauchy stress is

$$\boldsymbol{\sigma}^a = J^{-1} T^a \left(\mathbf{B} - \mathbf{a} \otimes \mathbf{a} \right) \,, \tag{5.11.4}$$

where $\mathbf{B} = \mathbf{F} \cdot \mathbf{F}^T$ is the left Cauchy-Green tensor. The material and spatial tangents are zero.

5.11.3   Isotropic Active Contraction

An isotropic active contractile stress is given by

$$\mathbf{S}^a = T^a \mathbf{I} \tag{5.11.5}$$

and the corresponding Cauchy stress is

$$\boldsymbol{\sigma}^a = J^{-1} T^a \mathbf{B} \,. \tag{5.11.6}$$

The material and spatial tangents are zero.

5.12 Chemical Reaction Production Rate

Production rate constitutive equations provide a relation for $\hat{\zeta}$ as a function of solid matrix strain, solute concentrations, and the concentrations of solid-bound molecular species.

5.12.1 Mass Action Forward

According to the law of mass action for forward reactions,

$$\hat{\zeta} = k\left(\theta, \mathbf{F}, \rho_r^\sigma\right) \prod_\alpha (c^\alpha)^{\nu_R^\alpha} \,. \tag{5.12.1}$$

A constitutive relation for the specific reaction rate $k\left(\theta, \mathbf{F}, \rho_r^\sigma\right)$ must also be provided.

5.12.2 Mass Action Reversible

According to the law of mass action for reversible reactions,

$$\hat{\zeta}_F = k_F\left(\theta, \mathbf{F}, \rho_r^\sigma\right) \prod_\alpha (c^\alpha)^{\nu_R^\alpha}$$

$$\hat{\zeta}_R = k_R\left(\theta, \mathbf{F}, \rho_r^\sigma\right) \prod_\alpha (c^\alpha)^{\nu_P^\alpha} \tag{5.12.2}$$

$$\hat{\zeta} = \hat{\zeta}_F - \hat{\zeta}_R = \hat{\zeta}_F \left[1 - K_c\left(\theta, \mathbf{F}, \rho_r^\sigma\right) \prod_\alpha (c^\alpha)^{\nu^\alpha} \right] \,,$$

where $K_c = k_R/k_F$ is a function that reduces to the equilibrium constant of the reversible reaction at chemical equilibrium (when $\hat{\zeta} = 0$). Constitutive relations for the specific forward and reverse reaction rates, $k_F\left(\theta, \mathbf{F}, \rho_r^\sigma\right)$ and $k_R\left(\theta, \mathbf{F}, \rho_r^\sigma\right)$ respectively, must also be provided.

5.12.3 Michaelis-Menten

Michaelis-Menten is a model for enzyme kinetics as represented by the reactions

$$\mathcal{E}^e + \mathcal{E}^s \rightleftharpoons \mathcal{E}^{es} \rightarrow \mathcal{E}^e + \mathcal{E}^p \,, \tag{5.12.3}$$

where $\mathcal{E}^e$ is the enzyme, $\mathcal{E}^s$ is the substrate, $\mathcal{E}^{es}$ is the enzyme-substrate complex, and $\mathcal{E}^p$ is the product. The molar mass supply $\hat{c}^p$ producing $\mathcal{E}^p$ is related to the concentration of the substrate $\mathcal{E}^s$ via

$$\hat{c}^p = \frac{V_{max} c^s}{K_m + c^s} \,, \tag{5.12.4}$$

where V_{max} is the maximum rate achieved by the system, at maximum (saturating) substrate concentrations. K_m is the substrate concentration at which the reaction rate is half of V_{max}.

This relation may be derived by applying the law of mass action to the two reactions in (5.12.3). under the simplifying assumption that the reversible reaction between the enzyme and substrate reaches steady state much faster than the subsequent forward reaction forming the product. If the first and second reactions are denoted by subscripts 1 and 2, respectively, the law of mass action for the first (reversible) and second (forwar) reaction produces

$$\hat{\zeta}_1 = k_{F1} c^e c^s - k_{R1} c^{es}, \quad \hat{\zeta}_2 = k_{F2} c^{es} \,,$$
$$\hat{c}^s = -\hat{\zeta}_1, \quad \hat{c}^p = \hat{\zeta}_2, \quad \hat{c}^{es} = \hat{\zeta}_1 - \hat{\zeta}_2 \,. \tag{5.12.5}$$

The total enzyme concentration remains constant at $c_0^e = c^e + c^{es}$, so that $\hat{\zeta}_1 = k_{F1}c_0^e c^s - (k_{F1}c^s + k_{R1})\,c^{es}$. Assuming that the first reaction equilibrates much faster than the second is equivalent to letting $\hat{\zeta}_1 \approx 0$, in which case

$$c^{es} \approx \frac{c_0^e c^s}{c^s + K_m}\,, \tag{5.12.6}$$

where $K_m = k_{R1}/k_{F1}$. Then,

$$\hat{\zeta}_2 = \frac{V_{\max}c^s}{c^s + K_m}\,,$$

where $V_{\max} = k_{F2}c_0^e$ represents the maximum value of $\hat{\zeta}_2$, when $K_m \ll c^s$. In practice, choosing $k_{F1} \gg k_{F2}$ can produce the desired effect.

5.13   Specific Reaction Rate

Specific reaction rate constitutive equations provide a relation for k as a function of solid matrix strain and the concentrations of solid-bound molecular species.

5.13.1   Constant Specific Reaction Rate

For this material model, k is constant.

5.13.2   Huiskes Remodeling

For this material, the specific reaction rate depends on the deviation of the specific strain energy from a threshold value,

$$k\left(\mathbf{F}, \rho_r^s\right) = \frac{B}{\left(J - \varphi_r^s\right)M^s}\left(\frac{\Psi_r}{\rho_r^s} - \psi_0\right)\,, , \tag{5.13.1}$$

where B is a constant, Ψ_r is the strain energy density of the solid, ρ_r^s is the referential mass density of the solid, ψ_0 is the threshold value for the specific strain energy. In this relation, $J = \det\mathbf{F}$ is evaluated from the solid deformation and φ_r^s is evaluated from (2.10.7).

5.14   Viscous Fluids

The most common family of constitutive relations employed for viscous fluids, including Newtonian fluids, is given by

$$\boldsymbol{\tau}\left(J, \mathbf{D}\right) = \left(\kappa - \frac{2}{3}\mu\right)\left(\operatorname{tr}\mathbf{D}\right)\mathbf{I} + 2\mu\,\mathbf{D}\,, \tag{5.14.1}$$

where μ and κ are, respectively, the dynamic shear and bulk viscosity coefficients (both positive), which may generally depend on J and, for non-Newtonian fluids, on invariants of $\mathbf{D}$. In practice, most constitutive models for non-Newtonian viscous fluids only use a dependence on $\dot{\gamma} = \sqrt{2\mathbf{D}:\mathbf{D}}$, since it is the only non-zero invariant in viscometric flows [52]. In this case, substituting eq.(5.14.1) into eq.(3.5.9) produces

$$\begin{aligned}
\boldsymbol{\mathcal{C}}^\tau = {} & \left(\kappa - \frac{2}{3}\mu\right)\mathbf{I}\otimes\mathbf{I} + \frac{2}{\dot{\gamma}}\left(\frac{\partial\kappa}{\partial\dot{\gamma}} - \frac{2}{3}\frac{\partial\mu}{\partial\dot{\gamma}}\right)\left(\operatorname{tr}\mathbf{D}\right)\mathbf{I}\otimes\mathbf{D} \\
& + 2\left(\frac{2}{\dot{\gamma}}\frac{\partial\mu}{\partial\dot{\gamma}}\mathbf{D}\otimes\mathbf{D} + \mu\,\mathbf{I}\,\overline{\otimes}\,\mathbf{I}\right)\,.
\end{aligned} \tag{5.14.2}$$

The term containing $\mathbf{I} \otimes \mathbf{D}$ is the only one that does not exhibit major symmetry. In Newtonian fluids, μ and κ are independent of $\mathbf{D}$; in incompressible fluids they are independent of J (since $J = 1$ remains constant and $\operatorname{tr} \mathbf{D} = 0$). Thus, for both of these cases the term containing $\mathbf{I} \otimes \mathbf{D}$ drops out and $\mathcal{C}^\tau$ exhibits major symmetry.

Similarly, using eq.(5.14.1), the tangent $\boldsymbol{\tau}'_J$ in eq.(3.5.11) reduces to

$$\boldsymbol{\tau}'_J = \left(\frac{\partial \kappa}{\partial J} - \frac{2}{3} \frac{\partial \mu}{\partial J} \right) (\operatorname{tr} \mathbf{D}) \, \mathbf{I} + 2 \frac{\partial \mu}{\partial J} \, \mathbf{D} \, . \tag{5.14.3}$$

Explicit forms for the dependence of μ or κ on J are not illustrated here, since viscosity generally shows negligible dependence on pressure (thus J) over typical ranges of pressures in fluids, hence $\boldsymbol{\tau}'_J \approx \mathbf{0}$ in most analyses.

Many fluid mechanics textbooks employ Stoke's condition ($\kappa = 0$) for the purpose of equating the elastic pressure p with the mean normal stress $-\frac{1}{3} \operatorname{tr} \boldsymbol{\sigma}$ [48]; in FEBio, κ is kept as a user-defined material property, which may be set to zero if desired. A common example of a non-Newtonian fluid is the Carreau model, where $\boldsymbol{\tau} = 2\mu\left(\dot{\gamma}\right) \mathbf{D}$, which is a special case of eq.(5.14.1), with $\kappa = 2\mu/3$ and

$$\mu = \mu_\infty + (\mu_0 - \mu_\infty) \left(1 + (\lambda\dot{\gamma})^2 \right)^{(n-1)/2} \, , \tag{5.14.4}$$

where λ is a time constant, n is a parameter governing the power-law response, μ_0 is the viscosity when $\dot{\gamma} = 0$ and μ_∞ is the viscosity as $\dot{\gamma} \to \infty$. Other common models of non-Newtonian viscous fluids are summarized in [22], though it should be noted that some of these models produce infinite values when evaluating $\dot{\gamma}^{-1} \partial\mu/\partial\dot{\gamma}$ as $\dot{\gamma} \to 0$, which is problematic in the evaluation of $\mathcal{C}^\tau$ in eq.(5.14.2).

For nearly incompressible fluids, a simple constitutive relation may be adopted for the pressure,

$$p\left(J\right) = K\left(1 - J\right) \, , \tag{5.14.5}$$

where K is the bulk modulus of the fluid in the limit when $J = 1$. It follows that $p'\left(J\right) = -K$ and $p''\left(J\right) = 0$ in eq.(3.5.10). This constitutive relation is adopted for nearly-incompressible CFD analyses in FEBio, though alternative formulations may be easily implemented.

Chapter 6

Contact and Coupling

FEBio allows the user to connect the different parts of the model in various ways. Deformable parts can be connected to rigid bodies. Deformable objects can be brought in contact with each other. Rigid bodies can be connected with rigid joints. This chapter describes the different ways to couple parts together.

6.1 Rigid-Deformable Coupling

In FEBio deformable bodies can be coupled with rigid bodies. The coupling requires a modification of the global stiffness matrix and residual vector. Additionally, degrees of freedom need to be introduced for the rigid bodies [42]. This section describes the coupling between rigid and deformable bodies.

6.1.1 Kinematics

The position vector $\mathbf{x}$ of a finite element node may be denoted as,

$$\mathbf{x} = \mathbf{X} + \mathbf{u}, \tag{6.1.1}$$

where $\mathbf{X}$ is the initial position of the node and **u** the displacement vector. If this node is connected to a rigid body the position can alternatively be written as,

$$\mathbf{x} = \mathbf{r} + \mathbf{a}, \tag{6.1.2}$$

where $\mathbf{r}$ is the current position of the center of mass of the rigid body and $\mathbf{a}$ is the relative position of the node to the center of mass. The vector $\mathbf{a}$ may be written in terms of its initial value $\mathbf{a}_0$ in the undeformed state and a rotation matrix,

$$\mathbf{a} = \mathbf{Q}\mathbf{a}_0. \tag{6.1.3}$$

In an incremental displacement formulation equation (6.1.2) must be linearized:

$$\Delta\mathbf{u} = \Delta\mathbf{r} + \Delta\mathbf{Q}\mathbf{a}_0, \tag{6.1.4}$$

where the linearization of the rotation matrix can be expressed in a more convenient form,

$$\Delta\mathbf{Q} = \hat{\mathbf{a}}\Delta\boldsymbol{\theta}. \tag{6.1.5}$$

Here is $\Delta\boldsymbol{\theta}^T = [\Delta\theta_1, \Delta\theta_2, \Delta\theta_3]$ and the matrix $\hat{\mathbf{a}}$ is

$$\hat{\mathbf{a}} = \begin{bmatrix} 0 & a_3 & -a_2 \\ -a_3 & 0 & a_1 \\ a_2 & -a_1 & 0 \end{bmatrix} . \tag{6.1.6}$$

For a model containing both deformable and rigid nodes the nodal degrees of freedom may be grouped, and the above expressions used to obtain a condensed set of unknowns:

$$\left\{ \begin{array}{c} \Delta\mathbf{u}^D \\ \Delta\mathbf{u}^R \end{array} \right\} = \begin{bmatrix} \mathbf{I} & \mathbf{0} & \mathbf{0} \\ \mathbf{0} & \mathbf{I} & \hat{\mathbf{a}} \end{bmatrix} \left\{ \begin{array}{c} \Delta\mathbf{u}^D \\ \Delta\mathbf{r} \\ \Delta\boldsymbol{\theta} \end{array} \right\} = \mathbf{A}\Delta\tilde{\mathbf{u}} . \tag{6.1.7}$$

Substituting this into the discrete form of the principle of virtual work yields expressions for the condensed finite element stiffness matrix and residual vector for the coupled rigid-deformable system:

$$\tilde{\mathbf{K}}\Delta\tilde{\mathbf{u}} = -\tilde{\mathbf{R}}, \quad \tilde{\mathbf{K}} = \mathbf{A}^T\mathbf{K}\mathbf{A}, \quad \tilde{\mathbf{R}} = \mathbf{A}^T\mathbf{R} \quad . \tag{6.1.8}$$

Equation (6.1.8) is now solved for the incremental update vector $\Delta\tilde{\mathbf{u}}$. The nodal positions of the deformable nodes can now be updated in the usual way,

$$\mathbf{u}_{n+1}^{D,k+1} = \mathbf{u}_{n+1}^{D,k} + \Delta\mathbf{u}^D . \tag{6.1.9}$$

Here, k is the iteration index of the Newon-Raphson iterations. The center of mass of the rigid body can now also be updated in a similar way,

$$\mathbf{r}_{n+1}^{k+1} = \mathbf{r}_{n+1}^k + \Delta\mathbf{r} . \tag{6.1.10}$$

To update the rotational degrees of freedom we employ quaternion algebra. The orientation of the rigid body at time $n+1$ is represented by the (unit) quaternion $\mathbf{q}_{n+1} = (w_{n+1}, \mathbf{x}_{n+1})$. The rotational update vector $\Delta\boldsymbol{\theta}$ can be written as a quaternion as follows,

$$\Delta\mathbf{q} = \left(\cos\alpha, \frac{1}{2\alpha}\sin\alpha\Delta\boldsymbol{\theta} \right)$$
$$\alpha = \frac{1}{2}\left(\Delta\theta_1^2 + \Delta\theta_2^2 + \Delta\theta_3^2 \right)^{1/2} \tag{6.1.11}$$

The updated orientation quaternion is then given by the quaternion product,

$$\tilde{\mathbf{q}}_{n+1}^{k+1} = \Delta\mathbf{q} \cdot \mathbf{q}_{n+1}^k . \tag{6.1.12}$$

Finally, we must ensure that the updated quaternion is a unit quaternion. To accomplish this we normalize the quaternion.

$$\mathbf{q} = \tilde{\mathbf{q}}/\|\tilde{\mathbf{q}}\| . \tag{6.1.13}$$

Normalizing the quaternion guarantees that it represents a proper rotation.

6.1.2   A single rigid body

The global system of equations can now be written as follows (for a single rigid body coupled to a deformable body),

$$\begin{bmatrix} \mathbf{K}^D & \mathbf{K}^{DR} \\ (\mathbf{K}^{DR})^T & \mathbf{K}^R \end{bmatrix} \left\{ \begin{array}{c} \Delta\mathbf{u}^D \\ \Delta\mathbf{r} \\ \Delta\boldsymbol{\theta} \end{array} \right\} = -\left\{ \begin{array}{c} \mathbf{R}^D \\ \mathbf{F}^R \\ \mathbf{M}^R \end{array} \right\} . \tag{6.1.14}$$

Here $\mathbf{F}^R$ is formed by adding all the residual vectors of all interface nodes that connect the deformable body to the rigid body,

$$\mathbf{F}^R = \sum_i \mathbf{R}_i^D \, , \tag{6.1.15}$$

where i sums over all interface nodes, and

$$\mathbf{M}^R = \sum_i \hat{\mathbf{a}}_i \mathbf{R}_i^D \, . \tag{6.1.16}$$

It is recognized that $\mathbf{F}^R$ is simply the total residual force that is applied to the rigid body and $\mathbf{M}^R$ is the total residual torque.

Constructing the stiffness matrix is accomplished in a similar manner. Assume n nodes per element, then the normal element stiffness matrix (in absence of rigid nodes) is given by,

$$\mathbf{k}^{(e)} = \begin{bmatrix} \mathbf{k}_{11} & \cdots & \mathbf{k}_{1n} \\ \vdots & \ddots & \vdots \\ \mathbf{k}_{n1} & \cdots & \mathbf{k}_{nn} \end{bmatrix} \, , \tag{6.1.17}$$

where $\mathbf{k}_{ij}$ is the nodal stiffness matrix connecting node i to node j. These nodal stiffness matrices are now assembled into the global stiffness matrix. If node i and j are neither interface nodes their nodal stiffness matrix is assembled into $\mathbf{K}^D$ in the usual manner,

$$\mathbf{K}^D = \sum_e \mathbf{k}_{ij}^{(e)} \, , \tag{6.1.18}$$

where the sum now has to interpreted as the finite element assembly operator.

If node j is an interface node, than the nodal stiffness matrix gets assembled in the $\mathbf{K}^{DR}$ matrix:

$$\mathbf{K}^{DR} = \sum_e \begin{bmatrix} \mathbf{k}_{ij}^{(e)} & \mathbf{k}_{ij}^{(e)} \hat{\mathbf{a}}_j \end{bmatrix} \, . \tag{6.1.19}$$

If both nodes belong to the rigid body than the nodal element matrix gets assembled in $\mathbf{K}^R$ as follows,

$$\mathbf{K}^R = \sum_e \begin{bmatrix} \mathbf{k}_{ij}^{(e)} & \mathbf{k}_{ij}^{(e)} \hat{\mathbf{a}}_j \\ \hat{\mathbf{a}}_i^T \mathbf{k}_{ij}^{(e)T} & \hat{\mathbf{a}}_i^T \mathbf{k}_{ij}^{(e)} \hat{\mathbf{a}}_j \end{bmatrix} \, . \tag{6.1.20}$$

6.1.3   Multiple Rigid Bodies

The previous results can easily be extended if there are multiple rigid bodies. The following section presents the approach for two rigid bodies, but the results can easily be generalized to N rigid bodies.

For two rigid bodies, the global system of equations takes the following form,

$$\begin{bmatrix} \mathbf{K}^D & \mathbf{K}_1^{DR} & \mathbf{K}_2^{DR} \\ (\mathbf{K}_1^{DR})^T & \mathbf{K}_{11}^R & \mathbf{K}_{12}^R \\ (\mathbf{K}_2^{DR})^T & \mathbf{K}_{21}^R & \mathbf{K}_{22}^R \end{bmatrix} \begin{Bmatrix} \Delta \mathbf{u}^D \\ \Delta \mathbf{r}_1 \\ \Delta \boldsymbol{\theta}_1 \\ \Delta \mathbf{r}_2 \\ \Delta \boldsymbol{\theta}_2 \end{Bmatrix} = - \begin{Bmatrix} \mathbf{R}^R \\ \mathbf{F}_1 \\ \mathbf{M}_1 \\ \mathbf{F}_2 \\ \mathbf{M}_2 \end{Bmatrix} \, . \tag{6.1.21}$$

Care must be taken to assemble the nodal stiffness matrix in the correct global sub-matrix. If node i is not an interface node and node j is connected to rigid body 1, then their nodal stiffness matrix

goes into $\mathbf{K}_1^{DR}$. If, however, node j is attached to rigid body 2 then their nodal stiffness matrix goes into $\mathbf{K}_2^{DR}$. If node i is connected to rigid body 1 and node j is connected to rigid body 2, then their nodal stiffness matrix goes into $\mathbf{K}_{12}^R$, and so on. Note that it is assumed here that a node may only connect to a single rigid body.

6.2 Rigid Joints

A rigid joint is a location in space where two rigid bodies connect. The joint enforces a constraint on the system. This constraint can be written as,

$$\mathbf{c}\left(\mathbf{Y}^c\right) = \boldsymbol{\varphi}^{(1)}\left(\mathbf{Y}^c\right) - \boldsymbol{\varphi}^{(2)}\left(\mathbf{Y}^c\right) = \mathbf{0}\,. \tag{6.2.1}$$

Here $\mathbf{Y}^c$ is the location of the joint in the reference configuration and $\boldsymbol{\varphi}^{(i)}$ ($i = 1, 2$) is the deformation map of rigid body i. Equation (6.2.1) is a constraint equation that will be added to the total balance of virtual work.

$$G\left(\boldsymbol{\varphi}, \mathbf{w}\right) = \sum_{i=1}^{2} G^{\text{int,ext}}\left(\boldsymbol{\varphi}^{(i)}, \mathbf{w}^{(i)}\right) - \underbrace{\sum_{i=1}^{2} \mathbf{w}^{(i)}\left(\mathbf{Y}^c\right) \cdot \mathbf{T}^{(i)}}_{G^c} = 0\,. \tag{6.2.2}$$

Here, the $\mathbf{T}^{(i)}$'s are the forces that will prevent the rigid bodies to separate at the joint position and $\mathbf{w}^{(i)} = \delta\boldsymbol{\varphi}^{(i)}$. First we note that due to the third law of Newton $\mathbf{T}^{(1)} = -\mathbf{T}^{(2)}$, so that we can write the constraint term as,

$$G^c\left(\boldsymbol{\varphi}, \mathbf{w}\right) = -\mathbf{T}^{(1)} \cdot \left(\mathbf{w}^{(1)} - \mathbf{w}^{(2)}\right)\left(\mathbf{Y}^c\right)\,. \tag{6.2.3}$$

Note that we can also write this as,

$$G^c\left(\boldsymbol{\varphi}, \mathbf{w}\right) = -\mathbf{T}^{(1)} \cdot \delta\mathbf{c}\,. \tag{6.2.4}$$

The constraint forces are determined by the augmented Lagrangian method and are given by,

$$\mathbf{T} = \boldsymbol{\lambda} + \varepsilon_c \mathbf{c}\,, \tag{6.2.5}$$

where $\boldsymbol{\lambda}$ is the Lagrange multiplier and ε_c is a user-defined penalty factor.

The linearization of (6.2.4) is given by,

$$\begin{aligned}
\Delta G^c\left(\boldsymbol{\varphi}, \mathbf{w}\right) &= -\Delta\left(\varepsilon_c \mathbf{c} \cdot \delta\mathbf{c}\right) \\
&= -\varepsilon_c \Delta\mathbf{c} \cdot \delta\mathbf{c}
\end{aligned}\,. \tag{6.2.6}$$

Using the rigid body assumption, the quantity $\Delta\mathbf{c}$ can be written as follows,

$$\begin{aligned}
\Delta\mathbf{c} &= \Delta\boldsymbol{\varphi}^{(1)}\left(\mathbf{Y}^c\right) - \Delta\boldsymbol{\varphi}^{(2)}\left(\mathbf{Y}^c\right) \\
&= \Delta\mathbf{r}_1 + \hat{\mathbf{y}}_1^c \Delta\boldsymbol{\theta}_1 - \Delta\mathbf{r}_2 - \hat{\mathbf{y}}_2^c \Delta\boldsymbol{\theta}_2
\end{aligned}\,. \tag{6.2.7}$$

And similarly for $\delta\mathbf{c}$. If we now introduce the vectors,

$$\delta\boldsymbol{\Phi} = \begin{bmatrix} \delta\mathbf{r}_1 \\ \delta\boldsymbol{\theta}_1 \\ \delta\mathbf{r}_2 \\ \delta\boldsymbol{\theta}_2 \end{bmatrix} \qquad \mathbf{N} = \begin{bmatrix} \mathbf{T} \\ \hat{\mathbf{y}}_1^T \mathbf{T} \\ -\mathbf{T} \\ -\hat{\mathbf{y}}_2^T \mathbf{T} \end{bmatrix}\,. \tag{6.2.8}$$

Then we can write the constraint work as,

$$G^c = -\delta \boldsymbol{\Phi}^T \mathbf{N} . \tag{6.2.9}$$

And the stiffness contribution as,

$$\Delta G^c = -\delta \boldsymbol{\Phi}^T \mathbf{K}^c \Delta \boldsymbol{\Phi} . \tag{6.2.10}$$

$$\mathbf{K}^c = \varepsilon_c \begin{bmatrix} \mathbf{I} & \hat{\mathbf{y}}_1 & -\mathbf{I} & -\hat{\mathbf{y}}_2 \\ \hat{\mathbf{y}}_1^T & \hat{\mathbf{y}}_1^T \mathbf{y}_1 & -\mathbf{y}_1^T & -\mathbf{y}_1^T \mathbf{y}_2 \\ -\mathbf{I} & -\mathbf{y}_1 & \mathbf{I} & \mathbf{y}_2 \\ -\mathbf{y}_2^T & -\mathbf{y}_2^T \mathbf{y}_1 & \mathbf{y}_2^T & \mathbf{y}_2^T \mathbf{y}_2 \end{bmatrix} . \tag{6.2.11}$$

6.3 Sliding Interfaces

This section summarizes the theoretical developments of the two body contact problem. After introducing some notation and terminology, the contact integral is presented, which contains the contribution to the virtual work equation from the contact tractions. Since the nonlinear contact problem is solved using a Newton based iterative method, the contact integral is linearized. Next, anticipating a finite element implementation, the contact integral and its linearization are discretized using a standard finite element approach. Finally the augmented Lagrangian method for enforcing the contact constraints is described.

6.3.1 Contact Kinematics

For the most part the notation of this section follows [41], with a few simplifications here and there since the implementation in FEBio is currently for quasi-static, frictionless, two body contact problem.

The volume occupied by body i in the reference configuration is denoted by $\Omega^{(i)} \subset \mathbb{R}^3$ where $i = 1, 2$. The boundary of body i is denoted by $\Gamma^{(i)}$ and is divided into three regions $\Gamma^{(i)} = \Gamma_\sigma^{(i)} \cup \Gamma_u^{(i)} \cup \Gamma_c^{(i)}$, where $\Gamma_\sigma^{(i)}$ is the boundary where tractions are applied, $\Gamma_u^{(i)}$ the boundary where the solution is prescribed and $\Gamma_c^{(i)}$ the part of the boundary that will be in contact with the other body. It is assumed that $\Gamma_\sigma^{(i)} \cap \Gamma_u^{(i)} \cap \Gamma_c^{(i)} = \emptyset$.

The deformation of body i is defined by $\boldsymbol{\varphi}^{(i)}$. The boundary of the deformed body i, that is the boundary of $\boldsymbol{\varphi}^{(i)} \left(\Omega^{(i)} \right)$ is denoted by $\gamma^{(i)} = \gamma_\sigma^{(i)} \cup \gamma_u^{(i)} \cup \gamma_c^{(i)}$ where $\gamma_\sigma^{(i)} = \boldsymbol{\varphi}^{(i)} \left(\Gamma_\sigma^{(i)} \right)$ is the boundary in the current configuration where the tractions are applied and similar definitions for $\gamma_u^{(i)}$ and $\gamma_c^{(i)}$. See the figure below for a graphical illustration of the defined regions.
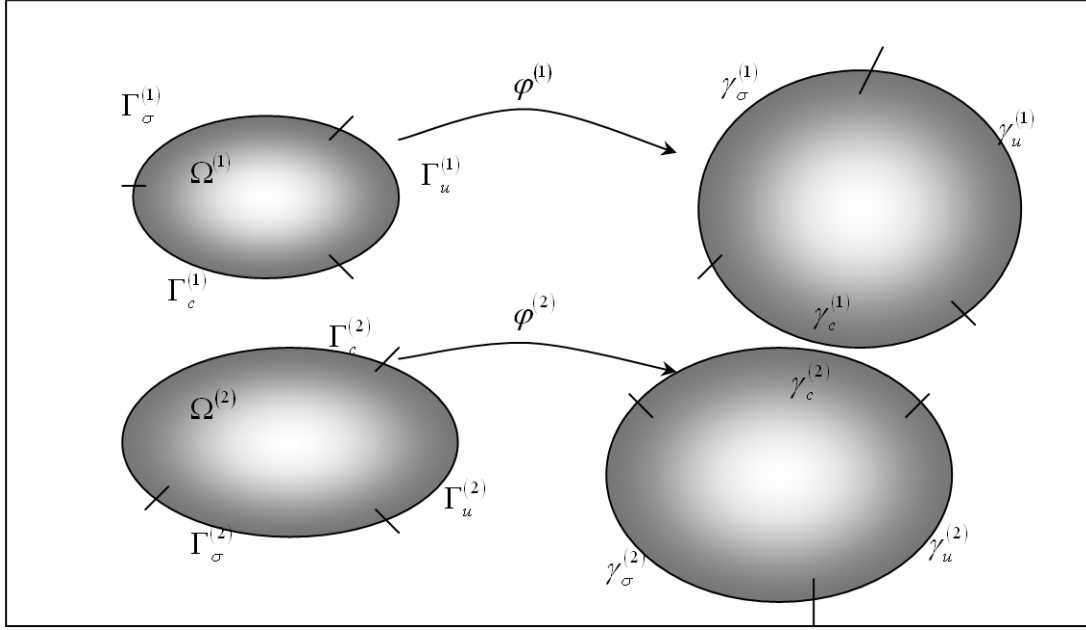
The two-body contact problem.

Points in body 1 are denoted by $\mathbf{X}$ in the reference configuration and $\mathbf{x}$ in the current configuration. For body 2 these points are denoted by $\mathbf{Y}$ and $\mathbf{y}$. To define contact, the location where the two bodies are in contact with each other must be established. If body 1 is the *slave body* and body 2 is the *master body*, then for a given point $\mathbf{X}$ on the slave reference contact surface there is a point $\bar{\mathbf{Y}}(\mathbf{X})$ on the master contact surface that is in some sense closest to point $\mathbf{X}$. This closest point is defined in a closest point projection sense:

$$\bar{\mathbf{Y}}(\mathbf{X}) = \arg \min_{\mathbf{Y}\in\Gamma_c^{(2)}} \left\| \boldsymbol{\varphi}^{(1)}(\mathbf{X}) - \boldsymbol{\varphi}^{(2)}(\mathbf{Y}) \right\| . \tag{6.3.1}$$

With the definition of $\bar{\mathbf{Y}}(\mathbf{X})$ established the *gap function* can be defined, which is a measure for the distance between $\mathbf{X}$ and $\bar{\mathbf{Y}}(\mathbf{X})$,

$$g(\mathbf{X}) = -\boldsymbol{\nu} \cdot \left(\boldsymbol{\varphi}^{(1)}(\mathbf{X}) - \boldsymbol{\varphi}^{(2)}\left(\bar{\mathbf{Y}}(\mathbf{X})\right) \right) , \tag{6.3.2}$$

where $\boldsymbol{\nu}$ is the local surface normal of surface $\gamma_c^{(2)}$ evaluated at $\bar{\mathbf{y}} = \boldsymbol{\varphi}^{(2)}\left(\bar{\mathbf{Y}}(\mathbf{X})\right)$. Note that $g > 0$ when $\mathbf{X}$ has penetrated body 2, so that the constraint condition to be satisfied at all time is $g \leqslant 0$.

6.3.2   Weak Form of Two Body Contact

The balance of linear momentum can be written for each of the two bodies in the reference configuration,

$$G^{(i)}\left(\boldsymbol{\varphi}^{(i)}, \mathbf{w}^{(i)}\right) = \int_{\Omega^{(i)}} \mathrm{Grad}\, \mathbf{w}^{(i)} : \mathbf{P}^{(i)}\, d\Omega - \int_{\Omega^{(i)}} \mathbf{w}^{(i)}\cdot\mathbf{F}^{(i)}\, d\Omega - \int_{\Gamma_s^{(i)}} \mathbf{w}^{(i)}\cdot\mathbf{T}^{(i)}\, d\Gamma - \int_{\Gamma_c^{(i)}} \mathbf{w}^{(i)}\cdot\mathbf{T}^{(i)}\, d\Gamma = 0,$$

$$\tag{6.3.3}$$

where $\mathbf{w}^{(i)}$ is a weighting function and $\mathbf{P}$ is the 1$^{\text{st}}$ Piola-Kirchhoff stress tensor. The last term corresponds to the virtual work of the contact tractions on body i. For notational convenience, the

notations φ and w are introduced to denote the collection of the respective mappings $\varphi^{(i)}$ and $\mathbf{w}^{(i)}$ (for $i =$ 1,2). In other words,

$$\varphi : \bar{\Omega}^{(1)} \cup \bar{\Omega}^{(2)} \rightarrow \mathbb{R}^3 \,,$$
$$w : \bar{\Omega}^{(1)} \cup \bar{\Omega}^{(2)} \rightarrow \mathbb{R}^3 \,. \tag{6.3.4}$$

The variational principle for the two body system is the sum of (6.3.3) for body 1 and 2 and can be expressed as,

$$
\begin{aligned}
G\left(\varphi, \mathbf{w}\right) &:= \sum_{i=1}^{2} G^{(i)}\left(\varphi^{(i)}, \mathbf{w}^{(i)}\right) \\
&= \sum_{i=1}^{2} \underbrace{\left\{ \int_{\Omega^{(i)}} \operatorname{Grad} \mathbf{w}^{(i)} : \mathbf{P}^{(i)} \, d\Omega - \int_{\Omega^{(i)}} \mathbf{w}^{(i)} \cdot \mathbf{F}^{(i)} \, d\Omega - \int_{\Gamma_s^{(i)}} \mathbf{w}^{(i)} \cdot \mathbf{T}^{(i)} \, d\Gamma \right\}}_{G^{\text{int,ext}}(\varphi,\mathbf{w})} \\
&\quad - \underbrace{\sum_{i=1}^{2} \int_{\Gamma_c^{(i)}} \mathbf{w}^{(i)} \cdot \mathbf{T}^{(i)} \, d\Gamma}_{G^c(\varphi,\mathbf{w})} \,.
\end{aligned}
\tag{6.3.5}
$$

Or in short,

$$G\left(\varphi, \mathbf{w}\right) = G^{\text{int,ext}}\left(\varphi, \mathbf{w}\right) + G^c\left(\varphi, \mathbf{w}\right) \,. \tag{6.3.6}$$

Note that the minus sign is included in the definition of the contact integral G^c. The contact integral can be written as an integration over the contact surface of body 1 by balancing linear momentum across the contact surface:

$$\mathbf{t}^{(2)}\left(\bar{\mathbf{y}}\left(\mathbf{x}\right)\right) d\Gamma^{(2)} = -\mathbf{t}^{(1)}\left(\mathbf{x}\right) d\Gamma^{(1)} \,. \tag{6.3.7}$$

The contact integral can now be rewritten over the contact surface of body 1:

$$G^c = - \int_{\Gamma_c^{(1)}} \mathbf{t}^{(1)}\left(\mathbf{x}\right) \cdot \left[\mathbf{w}^{(1)}\left(\mathbf{x}\right) - \mathbf{w}^{(2)}\left(\bar{\mathbf{y}}\left(\mathbf{x}\right)\right)\right] d\Gamma \,. \tag{6.3.8}$$

In the case of frictionless contact, the contact traction is taken as perpendicular to surface 2 and therefore can be written as, $\mathbf{t}^{(1)} = t_N \boldsymbol{\nu}$ where $\boldsymbol{\nu}$ is the (outward) surface normal and t_N is to be determined from the solution strategy. For example in a Lagrange multiplier method the t_N's would be the Lagrange multipliers.

By noting that the variation of the gap function is given by

$$\delta g = -\boldsymbol{\nu} \cdot \left(\mathbf{w}^{(1)}\left(\mathbf{x}\right) - \mathbf{w}^{(2)}\left(\bar{\mathbf{y}}\left(\mathbf{x}\right)\right)\right) \,, \tag{6.3.9}$$

equation (6.3.8) can be simplified as,

$$G^c = \int_{\Gamma_c^{(1)}} t_N \delta g \, d\Gamma \,. \tag{6.3.10}$$

6.3.3   Linearization of the Contact Integral

In a Newton-Raphson implementation the contact integral must be linearized with respect to the current configuration:

$$\Delta G^c \left(\boldsymbol{\varphi}, \mathbf{w} \right) = \int_{\Gamma_c^{(1)}} \Delta \left(t_N \delta g \right) d\Gamma \,. \tag{6.3.11}$$

Examining the normal contact term first, the directional derivative of t_N is given (for the case of the penalty regularization) by:

$$\begin{aligned} \Delta t_N &= \Delta \left\{ \varepsilon_N \left\langle g \right\rangle \right\} \\ &= H \left(g \right) \varepsilon_N \Delta g \end{aligned}, \tag{6.3.12}$$

where ε_N is the penalty factor and $H \left(g \right)$ is the Heaviside function. The quantity $\Delta \left(\delta g \right)$ is given by

$$\begin{aligned} \Delta \left(\delta g \right) = g &\left[\boldsymbol{\nu} \cdot \delta \boldsymbol{\varphi}_{,\gamma}^{(2)} \left(\bar{\mathbf{Y}} \left(\mathbf{X} \right) \right) + \kappa_{\alpha\gamma} \left(\bar{\mathbf{Y}} \left(\mathbf{X} \right) \right) \delta \bar{\xi}_\alpha \right] m^{\gamma\beta} \\ &\left[\boldsymbol{\nu} \cdot \Delta \boldsymbol{\varphi}_{,\beta}^{(2)} \left(\bar{\mathbf{Y}} \left(\mathbf{X} \right) \right) + \kappa_{\alpha\beta} \left(\bar{\mathbf{Y}} \left(\mathbf{X} \right) \right) \Delta \bar{\xi}^\alpha \right] \\ &+ \delta \bar{\xi}^\beta \boldsymbol{\nu} \cdot \left[\Delta \boldsymbol{\varphi}_{,\beta}^{(2)} \left(\bar{\mathbf{Y}} \left(\mathbf{X} \right) \right) \right] + \Delta \bar{\xi}^\beta \boldsymbol{\nu} \cdot \left[\delta \boldsymbol{\varphi}_{,\beta}^{(2)} \left(\bar{\mathbf{Y}} \left(\mathbf{X} \right) \right) \right] \\ &+ \kappa_{\alpha\beta} \left(\bar{\mathbf{Y}} \left(\mathbf{X} \right) \right) \delta \bar{\xi}^\beta \Delta \bar{\xi}^\alpha \,. \end{aligned} \tag{6.3.13}$$

6.3.4   Discretization of the Contact Integral

The contact integral, which is repeated here,

$$G^c \left(\boldsymbol{\varphi}, \mathbf{w} \right) = \int_{\Gamma^{(1)}} t_N \delta g \, d\Gamma \,, \tag{6.3.14}$$

will now be discretized using a standard finite element procedure. First it is noted that the integration can be written as a sum over the surface element areas:

$$G^c \left(\boldsymbol{\varphi}, \mathbf{w} \right) = \sum_{e=1}^{N_{sel}} \int_{\Gamma^{(1)e}} t_N \delta g \, d\Gamma \,, \tag{6.3.15}$$

where N_{sel} is the number of surface elements. The integration can be approximated using a quadrature rule,

$$G^c \left(\boldsymbol{\varphi}, \mathbf{w} \right) \cong \sum_{e=1}^{N_{sel}} \left\{ \sum_{i=1}^{N_{int}^e} w^i j \left(\boldsymbol{\xi}_i \right) t_N \left(\boldsymbol{\xi}_i \right) \delta g \left(\boldsymbol{\xi}_i \right) \right\} \,, \tag{6.3.16}$$

where N_{int}^e are the number of integration points for element e. It is now assumed that the integration points coincide with the element's nodes (e.g. for a quadrilateral surface element we have $\boldsymbol{\xi}_1 = \left(-1, -1 \right)$, $\boldsymbol{\xi}_2 = \left(1, -1 \right)$, $\boldsymbol{\xi}_3 = \left(1, 1 \right)$ and $\boldsymbol{\xi}_4 = \left(-1, 1 \right)$). With this quadrature rule, we have

$$\begin{aligned} w^{(1)} \left(\boldsymbol{\xi}_i \right) &= \mathbf{c}_i^{(1)} \\ w^{(2)} \left(\bar{\boldsymbol{\xi}}_i \right) &= \sum_{j=1}^n N_j \left(\bar{\boldsymbol{\xi}}_i \right) \mathbf{c}_j^{(2)} \end{aligned}, \tag{6.3.17}$$

so that,

$$\delta g\left(\boldsymbol{\xi}_i\right) = -\boldsymbol{\nu} \cdot \left(\mathbf{c}_i^{(1)} - \sum_{j=1}^{n} N_j^{(2)}\left(\bar{\boldsymbol{\xi}}_i\right) \mathbf{c}_j^{(2)} \right) . \tag{6.3.18}$$

If the following vectors are defined,

$$\begin{aligned} \delta \boldsymbol{\Phi}^T &= \left[\begin{array}{cccc} \mathbf{c}_i^{(1)} & \mathbf{c}_1^{(2)} & \cdots & \mathbf{c}_n^{(2)} \end{array} \right] \\ \mathbf{N}^T &= \left[\begin{array}{cccc} \boldsymbol{\nu} & -\boldsymbol{\nu} N_1^{(2)} & \cdots & -\boldsymbol{\nu} N_n^{(2)} \end{array} \right] \end{aligned}, \tag{6.3.19}$$

equation (6.3.16) can then be rewritten as follows,

$$G^c\left(\boldsymbol{\varphi}, \mathbf{w}\right) \cong \sum_{e=1}^{N_{sel}} \left\{ \sum_{i=1}^{N_{int}^e} w^i j\left(\boldsymbol{\xi}_i\right) t_N\left(\boldsymbol{\xi}_i\right) \delta \boldsymbol{\Phi}^T \mathbf{N}^T \right\} . \tag{6.3.20}$$

The specific form for t_N will depend on the method employed for enforcing the contact constraint.

6.3.5 Discretization of the Contact Stiffness

A similar procedure can now be used to calculate the discretized contact stiffness matrix. The linearization of the contact integral is repeated here:

$$\begin{aligned} \Delta G^c\left(\boldsymbol{\varphi}, \mathbf{w}\right) &= \sum_{e=1}^{N_{sel}} \int_{\Gamma^{(1)e}} \Delta\left(t_N \delta g\right) \, d\Gamma \\ &= \sum_{e=1}^{N_{sel}} \sum_{i=1}^{N_{int}^e} w_i j\left(\boldsymbol{\xi}_i\right) \Delta\left(t_N \delta g\right)\left(\boldsymbol{\xi}_i\right) \end{aligned}. \tag{6.3.21}$$

Using matrix notation we can rewrite equation (6.3.21) as,

$$\Delta W^c\left(\boldsymbol{\varphi}, \mathbf{w}\right) = \sum_{e=1}^{N_{sel}} \sum_{i}^{N_{int}^e} w_i j\left(\xi_i\right) \delta \boldsymbol{\Phi} \cdot \mathbf{k}^c \Delta \boldsymbol{\Phi} , \tag{6.3.22}$$

where $\delta \boldsymbol{\Phi}$ is as above and $\Delta \boldsymbol{\Phi}$ similar to $\delta \boldsymbol{\Phi}$ with δ replaced with Δ, and $\mathbf{k}^c$ is

$$\begin{aligned} \mathbf{k}^c &= \varepsilon_N H\left(\lambda_N^k + \varepsilon_N g\right) \mathbf{N}\mathbf{N}^T + t_N \left\{ g\left[m^{11}\bar{\mathbf{N}}_1\bar{\mathbf{N}}_1^T \right.\right. \\ &\quad + m^{12}\left(\bar{\mathbf{N}}_1\bar{\mathbf{N}}_2^T + \bar{\mathbf{N}}_2\bar{\mathbf{N}}_1^T\right) + m^{22}\bar{\mathbf{N}}_2\bar{\mathbf{N}}_2^T\left] - \mathbf{D}_1\mathbf{N}_1^T \right. \\ &\quad \left. - \mathbf{D}_2\mathbf{N}_2^T - \mathbf{N}_1\mathbf{D}_1^T - \mathbf{N}_2\mathbf{D}_2^T + \kappa_{12}\left(\mathbf{D}_1\mathbf{D}_2^T + \mathbf{D}_2\mathbf{D}_1^T\right) \right\} \end{aligned}, \tag{6.3.23}$$

where,

$$\mathbf{N} = \begin{bmatrix} \boldsymbol{\nu} \\ -N_1\left(\bar{\boldsymbol{\xi}}\right)\boldsymbol{\nu} \\ \vdots \\ -N_4\left(\bar{\boldsymbol{\xi}}\right)\boldsymbol{\nu} \end{bmatrix}, \quad \mathbf{T}_\alpha = \begin{bmatrix} \boldsymbol{\tau}_\alpha \\ -N_1\left(\bar{\boldsymbol{\xi}}\right)\boldsymbol{\tau}_\alpha \\ \vdots \\ -N_4\left(\bar{\boldsymbol{\xi}}\right)\boldsymbol{\tau}_\alpha \end{bmatrix}, \quad \mathbf{N}_\alpha = \begin{bmatrix} \mathbf{0} \\ -N_{1,\alpha}\left(\bar{\boldsymbol{\xi}}\right)\boldsymbol{\nu} \\ \vdots \\ -N_{4,\alpha}\left(\bar{\boldsymbol{\xi}}\right)\boldsymbol{\nu} \end{bmatrix}. \tag{6.3.24}$$

The following vectors are also defined which depend on the vectors of (6.3.24):

$$\mathbf{D}_1 = \frac{1}{\det \mathbf{A}} \left[A_{22} \left(\mathbf{T}_1 + g\mathbf{N}_1 \right) - A_{12} \left(\mathbf{T}_2 + g\mathbf{N}_2 \right) \right]$$

$$\mathbf{D}_2 = \frac{1}{\det \mathbf{A}} \left[A_{11} \left(\mathbf{T}_2 + g\mathbf{N}_2 \right) - A_{12} \left(\mathbf{T}_1 + g\mathbf{N}_1 \right) \right],$$

$$\bar{\mathbf{N}}_1 = \mathbf{N}_1 - \kappa_{12}\mathbf{D}_2$$

$$\bar{\mathbf{N}}_2 = \mathbf{N}_2 - \kappa_{12}\mathbf{D}_1$$

$$(6.3.25)$$

where the matrix $\mathbf{A}$ is defined as,

$$A_{ij} = m_{ij} + g\kappa_{ij}. \tag{6.3.26}$$

Here, $m_{ij} = \boldsymbol{\tau}_i \cdot \boldsymbol{\tau}_j$ is the surface metric tensor and $\kappa_{ij} = \boldsymbol{\nu} \cdot \boldsymbol{\varphi}^{(2)}_{t,ij} \left(\bar{\mathbf{Y}} \right)$ denotes the components of the surface curvature at $\bar{\boldsymbol{\xi}}$.

6.3.6 Augmented Lagrangian Method

The augmented Lagrangian method is used in FEBio to enforce the contact constraints to a user-specified tolerance. This implies that the normal contact tractions are given by,

$$t_N = \langle \lambda_N + \varepsilon_N g \rangle . \tag{6.3.27}$$

Note that this assumption is consistent with the approach that was used in establishing the discretization of the linearization of the contact integral (6.3.23). In (6.3.27) ε_N is a penalty factor that is chosen arbitrarily.

The Newton-Raphson iterative method is now used to solve the nonlinear contact problem where Uzawa's method (REF) is employed to calculate the Lagrange multipliers λ_N. This implies that the Lagrange multipliers are kept fixed during the Newton-Raphson iterations. After convergence the multipliers are updated and a new NR procedure is started. This procedure can be summarized by the following four steps.

1. **Initialize** the augmented Lagrangian iteration counter k, and the initial guesses for the multipliers:

$$\lambda_{N_{n+1}}^{(0)} = \lambda_{N_n} ,$$

$$k = 0 . \tag{6.3.28}$$

2. **Solve** for $\mathbf{d}_{n+1}^{(k)}$, the solution vector corresponding to the fixed kth iterate for the multipliers,

$$\mathbf{F}^{int} \left(\mathbf{d}_{n+1}^{(k)} \right) + \mathbf{F}^c \left(\mathbf{d}_{n+1}^{(k)} \right) = \mathbf{F}_{n+1}^{ext} , \tag{6.3.29}$$

where the contact tractions used to compute $\mathbf{F}^c$, the contact force, are governed by

$$t_{N_{n+1}}^{(k)} = \left\langle \lambda_{N_{n+1}}^{(k)} + \varepsilon_N g_{n+1}^k \right\rangle . \tag{6.3.30}$$

3. **Update** the Lagrange multipliers and iteration counters:

$$\lambda_{N_{n+1}}^{(k+1)} = \left\langle \lambda_{N_{n+1}}^{(k)} + \varepsilon_N g_{n+1}^{(k)} \right\rangle ,$$

$$k = k + 1 . \tag{6.3.31}$$

4. **Return** to the solution phase.

Steps 2-4 of the above algorithm are generally repeated until all contact constraints are satisfied to a user-specified tolerance or little change in the solution vector from augmentation to augmentation is noted.

6.3.7 Automatic Penalty Calculation

The determination of the penalty factor ε_N can be a difficult task, since a good value may depend on both material parameters and geometrical factors. In FEBio the value of this penalty factor can be determined automatically. In this case FEBio will calculate a penalty factor for each facet using the following formula.

$$\varepsilon_i = \frac{f_{SI} E_i A_i^2}{V_i} \, . \tag{6.3.32}$$

Here, E_i is the effective Young's modulus along the facet normal, A_i the surface area of the facet, V_i the volume of the element to which this facet belongs and f_{SI} a user defined scale factor. The parameter E_i is evaluated from the elasticity tensor $\mathcal{C}$ and the facet unit normal $\mathbf{n}$ according to

$$\frac{1}{E_i} = (\mathbf{n} \otimes \mathbf{n}) : \mathcal{C}^{-1} : (\mathbf{n} \otimes \mathbf{n}) \, , \tag{6.3.33}$$

where $\mathcal{C}^{-1}$ is the compliance tensor.

6.3.8 Alternative Formulations

6.3.8.1 Facet-To-Facet Sliding

As of FEBio version 1.2, two alternative formulations for sliding contact are available. The first method, which is referred to as the *facet-to-facet sliding*, is very similar to the formulation described above. It only differs in that it uses a Gaussian quadrature rule instead of nodal integration. Because of the more accurate integration rule, it was noted that this method in many situations was more stable and resulted in better convergence.

6.3.8.2 Sliding-Tension-Compression

The second alternative differs more significantly from the method described above. It also begins with the definition of a single contact integral over the slave surface.

$$G_c = - \int_{\gamma^{(1)}} \mathbf{t}_c \cdot \left(\delta\boldsymbol{\varphi}^{(1)} - \delta\bar{\boldsymbol{\varphi}}^{(2)} \right) \, da \, . \tag{6.3.34}$$

But a different derivation is followed to obtain the linearization of this contact integral. The main reason for this difference is a subtly alternative definition for the gap function. In this method, it is defined as follows.

$$g(\mathbf{X}) = \boldsymbol{\nu}^{(1)} \cdot \left(\boldsymbol{\varphi}^{(1)}(\mathbf{X}) - \boldsymbol{\varphi}^{(2)}\left(\bar{\mathbf{Y}}(\mathbf{X})\right) \right) \, , \tag{6.3.35}$$

where, $\boldsymbol{\nu}^{(1)}$ is the normal of the slave surface (opposed to the master normal as used in the derivation above). In this case, the point $\bar{\mathbf{Y}}(\mathbf{X})$ is no longer the closest point projection of $\mathbf{X}$ onto the master surface, but instead is the normal projection along $\boldsymbol{\nu}^{(1)}$. The linearization of equation (6.3.35) now becomes,

$$\delta g = \boldsymbol{\nu}^{(1)} \cdot \left(\delta\boldsymbol{\varphi}^{(1)}(\mathbf{X}) - \delta\bar{\boldsymbol{\varphi}}^{(2)}(\mathbf{X}) - \boldsymbol{\tau}_i^{(2)}\delta\xi_i \right) \, , \tag{6.3.36}$$

where, $\boldsymbol{\tau}_i^{(2)} = \frac{\partial\bar{\boldsymbol{\varphi}}^{(2)}}{\partial\eta_i}$ are the tangent vectors to the master surface at $\bar{\mathbf{Y}}(\mathbf{X})$. Note that since $\boldsymbol{\nu}^{(1)}$ is normal to the slave surface, equation (6.3.36) does not reduce to equation (6.3.9).

In one assumes frictionless contact, the contact traction can be written as follows,

$$\mathbf{t}_c = t_n \boldsymbol{\nu}^{(1)} = t_n \frac{\boldsymbol{\tau}_1^{(1)} \times \boldsymbol{\tau}_2^{(1)}}{\left\| \boldsymbol{\tau}_1^{(1)} \times \boldsymbol{\tau}_2^{(1)} \right\|} \,, \tag{6.3.37}$$

where, $\boldsymbol{\tau}_i^{(1)}$ are the tangent vectors to $\gamma^{(1)}$ evaluated at $\mathbf{X}$. Using (6.3.37) we can rewrite the contact integral as follows.

$$G_c = - \int\limits_{\xi^{(1)}} t_n \left(\delta\boldsymbol{\varphi}^{(1)} - \delta\bar{\boldsymbol{\varphi}}^{(2)} \right) \cdot \left(\boldsymbol{\tau}_1^{(1)} \times \boldsymbol{\tau}_2^{(1)} \right) d\xi \,, \tag{6.3.38}$$

where we assumed that the integration domain can be mapped to a 2D parametric domain, $\mathbf{x} = \mathbf{x}(\xi_\alpha)$.

The linearization of (6.3.38) now proceeds in the usual fashion. Omitting the details, it can be shown that the linearization of the contact integral results in,

$$\begin{aligned}
DG_c = & \int\limits_{\xi^{(1)}} \varepsilon\boldsymbol{\nu}^{(1)} \cdot \left(\mathbf{u}_2 - \mathbf{u}_1 + \bar{\boldsymbol{\tau}}_\alpha^{(2)} \Delta\bar{\xi}_{(2)}^\alpha \right) (\delta\boldsymbol{\varphi}_1 - \delta\bar{\boldsymbol{\varphi}}_2) \cdot \left(\boldsymbol{\tau}_1^{(1)} \times \boldsymbol{\tau}_2^{(1)} \right) d\xi \\
& - \int\limits_{\xi^{(1)}} t_n \frac{\partial\mathbf{u}_1}{\partial\xi_\alpha} \left((\mathbf{u}_1 - \mathbf{u}_2) \cdot a^{\alpha\beta} \boldsymbol{\tau}_\beta^{(1)} - a^{\alpha\beta} g\boldsymbol{\nu}^{(1)} \cdot \frac{\partial\mathbf{u}_1}{\partial\xi_\beta} \right) d\xi \\
& + \int\limits_{\xi^{(1)}} t_n (\delta\boldsymbol{\varphi}_1 - \delta\bar{\boldsymbol{\varphi}}_2) \cdot \left(\frac{\partial\mathbf{u}_1}{\partial\xi_1} \times \boldsymbol{\tau}_2^{(1)} + \boldsymbol{\tau}_1^{(1)} \times \frac{\partial\mathbf{u}_1}{\partial\xi_2} \right) d\xi \,,
\end{aligned} \tag{6.3.39}$$

where, $a_{\alpha\beta} = \boldsymbol{\tau}_\alpha^{(1)} \times \boldsymbol{\tau}_\beta^{(2)}$ and $a^{\alpha\beta} = \left(a^{-1} \right)_{\alpha\beta}$.

The discretization of the contact integral and its linearization now proceeds as usual. We will not derive the details, but it is important to point out that the resulting stiffness matrix for this particular contact formulation is not symmetric. Although this method has shown to give good results, especially in large compression problems, it was desirable to derive a symmetric version as well. Because of this, a slightly different formulation was also developed that does reduce to a symmetric stiffness matrix although this symmetric version did not seem to perform as well as the non-symmetric one.

6.4 Biphasic Contact

6.4.1 Contact Integral

See Section 2.5 for a review of biphasic materials, and [10] for additional details on biphasic contact. The contact interface is defined between surfaces $\gamma^{(1)}$ and $\gamma^{(2)}$. Due to continuity requirements on the traction and fluxes, the external virtual work resulting from contact tractions $\mathbf{t}^{(i)}$ and solvent fluxes $w_n^{(i)}$ $(i = 1, 2)$, may be combined into the contact integral

$$\begin{aligned}
\delta G_c = & \int_{\gamma^{(1)}} \left(\delta\mathbf{v}^{(1)} - \delta\mathbf{v}^{(2)} \right) \cdot \mathbf{t}^{(1)} \, da^{(1)} \\
& + \int_{\gamma^{(1)}} \left(\delta p^{(1)} - \delta p^{(2)} \right) w_n^{(1)} \, da^{(1)} \,.
\end{aligned} \tag{6.4.1}$$

In the current implementation, only frictionless contact is taken into consideration, so that the contact traction has only a normal component, $\mathbf{t}^{(i)} = t_n \mathbf{n}^{(i)}$. To evaluate and linearize δG_c, define the covariant basis vectors on each surface as

$$\mathbf{g}_\alpha^{(i)} = \frac{\partial \mathbf{x}^{(i)}}{\partial \eta_{(i)}^\alpha}, \quad \alpha = 1, 2, \tag{6.4.2}$$

where $\mathbf{x}^{(i)}$ represents the spatial position of points on $\gamma^{(i)}$, and $\eta_{(i)}^\alpha$ represent the parametric coordinates of that point. The unit outward normal on each surface is then given by

$$\mathbf{n}^{(i)} = \frac{\mathbf{g}_1^{(i)} \times \mathbf{g}_2^{(i)}}{\left| \mathbf{g}_1^{(i)} \times \mathbf{g}_2^{(i)} \right|}. \tag{6.4.3}$$

Now the contact integral may be rewritten as

$$\begin{aligned}
\delta G_c = &\int_{\gamma^{(1)}} \left(\delta \mathbf{v}^{(1)} - \delta \mathbf{v}^{(2)} \right) t_n \mathbf{g}_1^{(1)} \times \mathbf{g}_2^{(1)} \, d\eta_{(1)}^1 d\eta_{(1)}^2 \\
&+ \int_{\gamma^{(1)}} \left(\delta p^{(1)} - \delta p^{(2)} \right) w_n^{(1)} \left| \mathbf{g}_1^{(1)} \times \mathbf{g}_2^{(1)} \right| \, d\eta_{(1)}^1 d\eta_{(1)}^2,
\end{aligned} \tag{6.4.4}$$

and the linearization $D\delta G_c$ of δG_c has the form

$$D\delta G_c = \sum_{i=1}^{2} D\delta G_c \left[\Delta \mathbf{u}^{(i)} \right] + D\delta G_c \left[\Delta p^{(i)} \right]. \tag{6.4.5}$$

6.4.2 Gap Function

The gap function g, representing the distance between the contact surfaces, is defined by

$$\mathbf{x}^{(2)} = \mathbf{x}^{(1)} + g\mathbf{n}^{(1)}, \quad g = \left(\mathbf{x}^{(2)} - \mathbf{x}^{(1)} \right) \cdot \mathbf{n}^{(1)}. \tag{6.4.6}$$

The linearization of variables associated with motion, pressure, and concentration, is given by

$$\begin{aligned}
D\mathbf{x}^{(1)} &= \Delta \mathbf{u}^{(1)}, & D\mathbf{x}^{(2)} &= \Delta \mathbf{u}^{(2)} + \mathbf{g}_\alpha^{(2)} \Delta \eta_{(2)}^\alpha \\
Dp^{(1)} &= \Delta p^{(1)}, & Dp^{(2)} &= \Delta p^{(2)} + \frac{\partial p^{(2)}}{\partial \eta_{(2)}^\alpha} \Delta \eta_{(2)}^\alpha \\
D\delta \mathbf{v}^{(1)} &= \mathbf{0}, & D\mathbf{v}^{(2)} &= \frac{\partial \delta \mathbf{v}^{(2)}}{\partial \eta_{(2)}^\alpha} \Delta \eta_{(2)}^\alpha \\
D\delta p^{(1)} &= 0, & D\delta p^{(2)} &= \frac{\partial \delta p^{(2)}}{\partial \eta_{(2)}^\alpha} \Delta \eta_{(2)}^\alpha
\end{aligned} \tag{6.4.7}$$

where

$$\Delta \eta_{(2)}^\alpha = \left(\Delta \mathbf{u}^{(1)} - \Delta \mathbf{u}^{(2)} \right) \cdot a^{\alpha\beta} \mathbf{g}_\beta^{(1)} - a^{\alpha\beta} g \mathbf{n}^{(1)} \cdot \frac{\partial \Delta \mathbf{u}^{(1)}}{\partial \eta_{(1)}^\beta}, \tag{6.4.8}$$

with $a^{\alpha\beta} = (A_{\alpha\beta})^{-1}$ and $A_{\alpha\beta} = \mathbf{g}_\alpha^{(1)} \cdot \mathbf{g}_\beta^{(2)}$.

6.4.3   Penalty Method

Let the normal component of the contact traction be described by the penalty function,

$$t_n = \begin{cases} \varepsilon_n g & g < 0 \\ 0 & g \geq 0 \end{cases}, \tag{6.4.9}$$

where ε_n is a penalty factor associated with t_n. Similarly, let

$$\begin{cases} w_n = \varepsilon_p \pi = \varepsilon_p \left(p^{(1)} - p^{(2)} \right) & t_n < 0 \\ p^{(i)} = 0 & t_n = 0 \end{cases}, \tag{6.4.10}$$

where ε_p is a penalty factor associated with w_n. It follows that

$$Dt_n = \varepsilon_n \left(\Delta \mathbf{u}^{(2)} - \Delta \mathbf{u}^{(1)} + \mathbf{g}_\alpha^{(2)} \Delta \eta_{(2)}^\alpha \right) \cdot \mathbf{n}^{(1)} ,$$

$$Dw_n = \varepsilon_p \left(\Delta p^{(1)} - \Delta p^{(2)} - \frac{\partial p^{(2)}}{\partial \eta_{(2)}^\alpha} \Delta \eta_{(2)}^\alpha \right) . \tag{6.4.11}$$

Given these relations, it can be shown that the directional derivatives of the various terms appearing in the integrand of δG_c are

$$D \left(t_n \left(\delta \mathbf{v}^{(1)} - \delta \mathbf{v}^{(2)} \right) \cdot \mathbf{g}_1^{(1)} \times \mathbf{g}_2^{(1)} \right) =$$
$$- J_\eta^{(1)} \varepsilon_n \left(\delta \mathbf{v}^{(1)} - \delta \mathbf{v}^{(2)} \right) \cdot \left(\mathbf{n}^{(1)} \otimes \mathbf{n}^{(1)} \right) \cdot \left(\Delta \mathbf{u}^{(1)} - \Delta \mathbf{u}^{(2)} \right)$$
$$+ J_\eta^{(1)} t_n \frac{\partial \delta \mathbf{v}^{(2)}}{\partial \eta_{(2)}^\alpha} \cdot \left(\mathbf{n}^{(2)} \otimes \mathbf{g}_{(2)}^\alpha \right) \cdot \left(\Delta \mathbf{u}^{(1)} - \Delta \mathbf{u}^{(2)} \right) \tag{6.4.12}$$
$$+ t_n \left(\delta \mathbf{v}^{(1)} - \delta \mathbf{v}^{(2)} \right) \cdot \left(\frac{\partial \Delta \mathbf{u}^{(1)}}{\partial \eta_{(1)}^1} \times \mathbf{g}_2^{(1)} + \mathbf{g}_1^{(1)} \times \frac{\partial \Delta \mathbf{u}^{(1)}}{\partial \eta_{(1)}^2} \right)$$

$$D \left(w_n \left(\delta p^{(1)} - \delta p^{(2)} \right) \left| \mathbf{g}_1^{(1)} \times \mathbf{g}_2^{(1)} \right| \right) =$$
$$J_\eta^{(1)} \varepsilon_p \left(\delta p^{(1)} - \delta p^{(2)} \right) \left(\Delta p^{(1)} - \Delta p^{(2)} \right)$$
$$- J_\eta^{(1)} \left[\varepsilon_p \left(\delta p^{(1)} - \delta p^{(2)} \right) \frac{\partial p^{(1)}}{\partial \eta_{(1)}^\alpha} \mathbf{g}_{(1)}^\alpha + w_n \frac{\partial \delta p^{(2)}}{\partial \eta_{(2)}^\alpha} \mathbf{g}_{(2)}^\alpha \right] \cdot \left(\Delta \mathbf{u}^{(1)} - \Delta \mathbf{u}^{(2)} \right) , \tag{6.4.13}$$
$$+ w_n \left(\delta p^{(1)} - \delta p^{(2)} \right) \mathbf{n}^{(1)} \cdot \left(\frac{\partial \Delta \mathbf{u}^{(1)}}{\partial \eta_{(1)}^1} \times \mathbf{g}_2^{(1)} + \mathbf{g}_1^{(1)} \times \frac{\partial \Delta \mathbf{u}^{(1)}}{\partial \eta_{(1)}^2} \right)$$

where $J_\eta^{(1)} = \left| \mathbf{g}_1^{(1)} \times \mathbf{g}_2^{(1)} \right|$.

6.4.4   Discretization

The contact integral may be discretized as

$$\delta G_c = \sum_{e=1}^{n_e^{(1)}} \sum_{k=1}^{n_{\text{int}}^{(e)}} W_k J_\eta^{(1)} \left[t_n \left(\delta \mathbf{v}^{(1)} - \delta \mathbf{v}^{(2)} \right) \cdot \mathbf{n}^{(1)} + w_n \left(\delta p^{(1)} - \delta p^{(2)} \right) \right] . \tag{6.4.14}$$

The variables may be interpolated over each element face according to

$$
\begin{aligned}
\delta\mathbf{v}^{(1)} &= \sum_{a=1}^{m^{(1)}} N_a^{(1)}\delta\mathbf{v}_a^{(1)}, &\quad \delta\mathbf{v}^{(2)} &= \sum_{b=1}^{m^{(2)}} N_b^{(2)}\delta\mathbf{v}_b^{(2)} \\
\Delta\mathbf{u}^{(1)} &= \sum_{c=1}^{m^{(1)}} N_c^{(1)}\Delta\mathbf{u}_c^{(1)}, &\quad \Delta\mathbf{u}^{(2)} &= \sum_{d=1}^{m^{(2)}} N_d^{(2)}\Delta\mathbf{u}_d^{(2)} \\
\delta p^{(1)} &= \sum_{a=1}^{m^{(1)}} N_a^{(1)}\delta p_a^{(1)}, &\quad \delta p^{(2)} &= \sum_{b=1}^{m^{(2)}} N_b^{(2)}\delta p_b^{(2)} \\
\Delta p^{(1)} &= \sum_{c=1}^{m^{(1)}} N_c^{(1)}\Delta p_c^{(1)}, &\quad \Delta p^{(2)} &= \sum_{d=1}^{m^{(2)}} N_d^{(2)}\Delta p_d^{(2)}
\end{aligned}
\tag{6.4.15}
$$

Then,

$$
\begin{aligned}
\delta G_c = \sum_{e=1}^{n_e^{(1)}} \sum_{k=1}^{n_{\text{int}}^{(e)}} W_k J_\eta^{(1)} & \left(\sum_{a=1}^{m^{(1)}} \begin{bmatrix} \delta\mathbf{v}_a^{(1)} & \delta p_a^{(1)} \end{bmatrix} \cdot \begin{bmatrix} \mathbf{f}_a^{(1)} \\ w_a^{(1)} \end{bmatrix} \right. \\
& \left. + \sum_{b=1}^{m_k^{(2)}} \begin{bmatrix} \delta\mathbf{v}_{b,k}^{(1)} & \delta p_{b,k}^{(1)} \end{bmatrix} \cdot \begin{bmatrix} \mathbf{f}_{b,k}^{(1)} \\ w_{b,k}^{(1)} \end{bmatrix} \right),
\end{aligned}
\tag{6.4.16}
$$

where

$$
\begin{aligned}
\mathbf{f}_a^{(1)} &= N_a^{(1)} t_n \mathbf{n}^{(1)} & \mathbf{f}_{b,k}^{(2)} &= -N_b^{(2)} t_n \mathbf{n}^{(1)} \\
w_a^{(1)} &= N_a^{(1)} w_n & w_{b,k}^{(2)} &= -N_b^{(2)} w_n
\end{aligned}
\tag{6.4.17}
$$

Similarly,

$$
\begin{aligned}
-D\delta G_c = \sum_{e=1}^{n_e^{(1)}} \sum_{k=1}^{n_{\text{int}}^{(e)}} W_k J_\eta^{(1)} & \\
\times \left(\sum_{a=1}^{m^{(1)}} \begin{bmatrix} \delta\mathbf{v}_a^{(1)} & \delta p_a^{(1)} \end{bmatrix} \cdot \right. & \left(\sum_{c=1}^{m^{(1)}} \begin{bmatrix} \mathbf{K}_{ac}^{(1,1)} & \mathbf{0} \\ \mathbf{g}_{ac}^{(1,1)} & g_{ac}^{(1,1)} \end{bmatrix} \cdot \begin{bmatrix} \Delta\mathbf{u}_c^{(1)} \\ \Delta p_c^{(1)} \end{bmatrix} \right. \\
& \left. + \sum_{d=1}^{m_k^{(2)}} \begin{bmatrix} \mathbf{K}_{ad,k}^{(1,2)} & \mathbf{0} \\ \mathbf{g}_{ad,k}^{(1,2)} & g_{ad,k}^{(1,2)} \end{bmatrix} \cdot \begin{bmatrix} \Delta\mathbf{u}_d^{(2)} \\ \Delta p_d^{(2)} \end{bmatrix} \right) \\
+ \sum_{b=1}^{m_k^{(2)}} \begin{bmatrix} \delta\mathbf{v}_{b,k}^{(2)} & \delta p_{b,k}^{(2)} \end{bmatrix} \cdot & \left(\sum_{c=1}^{m^{(1)}} \begin{bmatrix} \mathbf{K}_{bc,k}^{(2,1)} & \mathbf{0} \\ \mathbf{g}_{bc,k}^{(2,1)} & g_{bc,k}^{(2,1)} \end{bmatrix} \cdot \begin{bmatrix} \Delta\mathbf{u}_c^{(1)} \\ \Delta p_c^{(1)} \end{bmatrix} \right. \\
& \left. \left. + \sum_{d=1}^{m_k^{(2)}} \begin{bmatrix} \mathbf{K}_{bd,k}^{(2,2)} & \mathbf{0} \\ \mathbf{g}_{bd,k}^{(2,2)} & g_{bd,k}^{(2,2)} \end{bmatrix} \cdot \begin{bmatrix} \Delta\mathbf{u}_d^{(2)} \\ \Delta p_d^{(2)} \end{bmatrix} \right) \right),
\end{aligned}
\tag{6.4.18}
$$

where

$$\mathbf{K}_{ac}^{(1,1)} = N_a^{(1)} \left(\varepsilon_n N_c^{(1)} \mathbf{N}^{(1)} + t_n \mathbf{A}_c^{(1)} \right)$$

$$\mathbf{K}_{ad,k}^{(1,2)} = -\varepsilon_n N_a^{(1)} N_d^{(2)} \mathbf{N}^{(1)}$$

$$\mathbf{K}_{bc,k}^{(2,1)} = -N_c^{(1)} \left(\varepsilon_n N_b^{(2)} \mathbf{N}^{(1)} + t_n \mathbf{M}_b^{(2)} \right) - t_n N_b^{(2)} \mathbf{A}_c^{(1)}$$

$$\mathbf{K}_{bd,k}^{(2,2)} = N_d^{(2)} \left(\varepsilon_n N_b^{(2)} \mathbf{N}^{(1)} + t_n \mathbf{M}_b^{(2)} \right)$$

(6.4.19)

$$\mathbf{g}_{ac}^{(1,1)} = N_a^{(1)} \left(\varepsilon_p N_c^{(1)} \mathbf{p}^{(1)} - w_n \mathbf{A}_c^{(1)} \cdot \mathbf{n}^{(1)} \right)$$

$$\mathbf{g}_{ad,k}^{(1,2)} = -\varepsilon_p N_a^{(1)} N_d^{(2)} \mathbf{p}^{(1)}$$

$$\mathbf{g}_{bc,k}^{(2,1)} = N_c^{(1)} \left(-\varepsilon_p N_b^{(2)} \mathbf{p}^{(1)} + w_n \mathbf{m}_b^{(2)} \right) + w_n N_b^{(2)} \mathbf{A}_c^{(1)} \cdot \mathbf{n}^{(1)}$$

$$\mathbf{g}_{bd,k}^{(2,2)} = N_d^{(2)} \left(\varepsilon_p N_b^{(2)} \mathbf{p}^{(1)} - w_n \mathbf{m}_b^{(2)} \right)$$

(6.4.20)

$$g_{ac}^{(1,1)} = -\varepsilon_p N_a^{(1)} N_c^{(1)}$$

$$g_{ad,k}^{(1,2)} = \varepsilon_p N_a^{(1)} N_d^{(2)}$$

$$g_{bc,k}^{(2,1)} = \varepsilon_p N_b^{(2)} N_c^{(1)}$$

$$g_{bd,k}^{(2,2)} = -\varepsilon_p N_b^{(2)} N_d^{(2)}$$

(6.4.21)

and

$$\mathbf{N}^{(1)} = \mathbf{n}^{(1)} \otimes \mathbf{n}^{(1)}$$

$$\mathbf{A}_c^{(1)} = \frac{1}{J_\eta^{(1)}} \mathcal{A} \left\{ \frac{\partial N_c^{(1)}}{\partial \eta_{(1)}^1} \mathbf{g}_2^{(1)} - \frac{\partial N_c^{(1)}}{\partial \eta_{(1)}^2} \mathbf{g}_1^{(1)} \right\}$$

$$\mathbf{M}_b^{(2)} = \mathbf{n}^{(2)} \otimes \mathbf{m}_b^{(2)}$$

$$\mathbf{m}_b^{(2)} = \frac{\partial N_b^{(2)}}{\partial \eta_{(2)}^\alpha} \mathbf{g}_{(2)}^\alpha$$

$$\mathbf{p}^{(1)} = \frac{\partial p^{(1)}}{\partial \eta_{(1)}^\alpha} \mathbf{g}_{(1)}^\alpha$$

(6.4.22)

6.5 Biphasic-Solute Contact

6.5.1 Contact Integral

See Section 2.6 for a review of biphasic-solute materials. The contact interface is defined between surfaces $\gamma^{(1)}$ and $\gamma^{(2)}$. Due to continuity requirements on the traction and fluxes, the external virtual work resulting from contact tractions $\mathbf{t}^{(i)}$, solvent fluxes $w_n^{(i)}$ and solute fluxes $j_n^{(i)}$ ($i = 1, 2$), may be combined into the contact integral

$$\delta G_c = \int_{\gamma^{(1)}} \left(\delta \mathbf{v}^{(1)} - \delta \mathbf{v}^{(2)} \right) \cdot \mathbf{t}^{(1)} \, da^{(1)}$$

$$+ \int_{\gamma^{(1)}} \left(\delta \tilde{p}^{(1)} - \delta \tilde{p}^{(2)} \right) w_n^{(1)} \, da^{(1)}$$

(6.5.1)

$$+ \int_{\gamma^{(1)}} \left(\delta \tilde{c}^{(1)} - \delta \tilde{c}^{(2)} \right) j_n^{(1)} \, da^{(1)} \, .$$

In the current implementation, only frictionless contact is taken into consideration, so that the contact traction has only a normal component, $\mathbf{t}^{(i)} = t_n \mathbf{n}^{(i)}$. To evaluate and linearize δG_c, define the covariant basis vectors on each surface as

$$\mathbf{g}_\alpha^{(i)} = \frac{\partial \mathbf{x}^{(i)}}{\partial \eta_{(i)}^\alpha}, \quad \alpha = 1, 2, \tag{6.5.2}$$

where $\mathbf{x}^{(i)}$ represents the spatial position of points on $\gamma^{(i)}$, and $\eta_{(i)}^\alpha$ represent the parametric coordinates of that point. The unit outward normal on each surface is then given by

$$\mathbf{n}^{(i)} = \frac{\mathbf{g}_1^{(i)} \times \mathbf{g}_2^{(i)}}{\left| \mathbf{g}_1^{(i)} \times \mathbf{g}_2^{(i)} \right|}. \tag{6.5.3}$$

Now the contact integral may be rewritten as

$$
\begin{aligned}
\delta G_c = & \int_{\gamma^{(1)}} \left(\delta \mathbf{v}^{(1)} - \delta \mathbf{v}^{(2)} \right) t_n \mathbf{g}_1^{(1)} \times \mathbf{g}_2^{(1)} \, d\eta_{(1)}^1 d\eta_{(1)}^2 \\
& + \int_{\gamma^{(1)}} \left(\delta \tilde{p}^{(1)} - \delta \tilde{p}^{(2)} \right) w_n^{(1)} \left| \mathbf{g}_1^{(1)} \times \mathbf{g}_2^{(1)} \right| \, d\eta_{(1)}^1 d\eta_{(1)}^2 \\
& + \int_{\gamma^{(1)}} \left(\delta \tilde{c}^{(1)} - \delta \tilde{c}^{(2)} \right) j_n^{(1)} \left| \mathbf{g}_1^{(1)} \times \mathbf{g}_2^{(1)} \right| \, d\eta_{(1)}^1 d\eta_{(1)}^2 ,
\end{aligned}
\tag{6.5.4}
$$

and the linearization $D\delta G_c$ of δG_c has the form

$$D\delta G_c = \sum_{i=1}^{2} D\delta G_c \left[\Delta \mathbf{u}^{(i)} \right] + D\delta G_c \left[\Delta \tilde{p}^{(i)} \right] + D\delta G_c \left[\Delta \tilde{c}^{(i)} \right]. \tag{6.5.5}$$

6.5.2 Gap Function

The gap function g, representing the distance between the contact surfaces, is defined by

$$\mathbf{x}^{(2)} = \mathbf{x}^{(1)} + g\mathbf{n}^{(1)}, \quad g = \left(\mathbf{x}^{(2)} - \mathbf{x}^{(1)} \right) \cdot \mathbf{n}^{(1)}. \tag{6.5.6}$$

The linearization of variables associated with motion, pressure, and concentration, is given by

$$
\begin{aligned}
D\mathbf{x}^{(1)} &= \Delta \mathbf{u}^{(1)} & D\mathbf{x}^{(2)} &= \Delta \mathbf{u}^{(2)} + \mathbf{g}_\alpha^{(2)} \Delta \eta_{(2)}^\alpha \\[4pt]
D\tilde{p}^{(1)} &= \Delta \tilde{p}^{(1)} & D\tilde{p}^{(2)} &= \Delta \tilde{p}^{(2)} + \frac{\partial \tilde{p}^{(2)}}{\partial \eta_{(2)}^\alpha} \Delta \eta_{(2)}^\alpha \\[4pt]
D\tilde{c}^{(1)} &= \Delta \tilde{c}^{(1)} & D\tilde{c}^{(2)} &= \Delta \tilde{c}^{(2)} + \frac{\partial \tilde{c}^{(2)}}{\partial \eta_{(2)}^\alpha} \Delta \eta_{(2)}^\alpha \\[4pt]
D\delta \mathbf{v}^{(1)} &= \mathbf{0} & D\mathbf{v}^{(2)} &= \frac{\partial \delta \mathbf{v}^{(2)}}{\partial \eta_{(2)}^\alpha} \Delta \eta_{(2)}^\alpha \\[4pt]
D\delta \tilde{p}^{(1)} &= 0 & D\delta \tilde{p}^{(2)} &= \frac{\partial \delta \tilde{p}^{(2)}}{\partial \eta_{(2)}^\alpha} \Delta \eta_{(2)}^\alpha \\[4pt]
D\delta \tilde{c}^{(1)} &= 0 & D\delta \tilde{c}^{(2)} &= \frac{\partial \delta \tilde{c}^{(2)}}{\partial \eta_{(2)}^\alpha} \Delta \eta_{(2)}^\alpha
\end{aligned}
\tag{6.5.7}
$$

where

$$\Delta\eta_{(2)}^\alpha = \left(\Delta\mathbf{u}^{(1)} - \Delta\mathbf{u}^{(2)}\right) \cdot a^{\alpha\beta}\mathbf{g}_\beta^{(1)} - a^{\alpha\beta}gn^{(1)} \cdot \frac{\partial\Delta\mathbf{u}^{(1)}}{\partial\eta_{(1)}^\beta}, \tag{6.5.8}$$

with $a^{\alpha\beta} = (A_{\alpha\beta})^{-1}$ and $A_{\alpha\beta} = \mathbf{g}_\alpha^{(1)} \cdot \mathbf{g}_\beta^{(2)}$.

6.5.3   Penalty Method

Let the normal component of the contact traction be described by the penalty function,

$$t_n = \begin{cases} \varepsilon_n g & g < 0 \\ 0 & g \geqslant 0 \end{cases}, \tag{6.5.9}$$

where ε_n is a penalty factor associated with t_n. Similarly, let

$$\begin{cases} w_n = \varepsilon_p\pi = \varepsilon_p\left(\tilde{p}^{(1)} - \tilde{p}^{(2)}\right) & t_n < 0 \\ \tilde{p}^{(i)} = \tilde{p}^* & t_n = 0 \end{cases}, \tag{6.5.10}$$

and

$$\begin{cases} j_n = \varepsilon_c\chi = \varepsilon_c\left(\tilde{c}^{(1)} - \tilde{c}^{(2)}\right) & t_n < 0 \\ \tilde{c}^{(i)} = \tilde{c}^* & t_n = 0 \end{cases}, \tag{6.5.11}$$

where ε_p and ε_c are penalty factors associated with w_n and j_n, respectively. It follows that

$$Dt_n = \varepsilon_n\left(\Delta\mathbf{u}^{(2)} - \Delta\mathbf{u}^{(1)} + \mathbf{g}_\alpha^{(2)}\Delta\eta_{(2)}^\alpha\right) \cdot \mathbf{n}^{(1)}$$

$$Dw_n = \varepsilon_p\left(\Delta\tilde{p}^{(1)} - \Delta\tilde{p}^{(2)} - \frac{\partial\tilde{p}^{(2)}}{\partial\eta_{(2)}^\alpha}\Delta\eta_{(2)}^\alpha\right) \tag{6.5.12}$$

$$Dj_n = \varepsilon_c\left(\Delta\tilde{c}^{(1)} - \Delta\tilde{c}^{(2)} - \frac{\partial\tilde{c}^{(2)}}{\partial\eta_{(2)}^\alpha}\Delta\eta_{(2)}^\alpha\right)$$

Given these relations, it can be shown that the directional derivatives of the various terms appearing in the integrand of δG_c are

$$D\left(t_n\left(\delta\mathbf{v}^{(1)} - \delta\mathbf{v}^{(2)}\right) \cdot \mathbf{g}_1^{(1)} \times \mathbf{g}_2^{(1)}\right) =$$

$$- J_\eta^{(1)}\varepsilon_n\left(\delta\mathbf{v}^{(1)} - \delta\mathbf{v}^{(2)}\right) \cdot \left(\mathbf{n}^{(1)} \otimes \mathbf{n}^{(1)}\right) \cdot \left(\Delta\mathbf{u}^{(1)} - \Delta\mathbf{u}^{(2)}\right)$$

$$+ J_\eta^{(1)}t_n\frac{\partial\delta\mathbf{v}^{(2)}}{\partial\eta_{(2)}^\alpha} \cdot \left(\mathbf{n}^{(2)} \otimes \mathbf{g}_{(2)}^\alpha\right) \cdot \left(\Delta\mathbf{u}^{(1)} - \Delta\mathbf{u}^{(2)}\right) \tag{6.5.13}$$

$$+ t_n\left(\delta\mathbf{v}^{(1)} - \delta\mathbf{v}^{(2)}\right) \cdot \left(\frac{\partial\Delta\mathbf{u}^{(1)}}{\partial\eta_{(1)}^1} \times \mathbf{g}_2^{(1)} + \mathbf{g}_1^{(1)} \times \frac{\partial\Delta\mathbf{u}^{(1)}}{\partial\eta_{(1)}^2}\right)$$

$$D\left(w_n\left(\delta\tilde{p}^{(1)} - \delta\tilde{p}^{(2)}\right)\left|\mathbf{g}_1^{(1)} \times \mathbf{g}_2^{(1)}\right|\right) =$$

$$J_\eta^{(1)}\varepsilon_p\left(\delta\tilde{p}^{(1)} - \delta\tilde{p}^{(2)}\right)\left(\Delta\tilde{p}^{(1)} - \Delta\tilde{p}^{(2)}\right)$$

$$- J_\eta^{(1)}\left[\varepsilon_p\left(\delta\tilde{p}^{(1)} - \delta\tilde{p}^{(2)}\right)\frac{\partial\tilde{p}^{(1)}}{\partial\eta_{(1)}^\alpha}\mathbf{g}_{(1)}^\alpha + w_n\frac{\partial\delta\tilde{p}^{(2)}}{\partial\eta_{(2)}^\alpha}\mathbf{g}_{(2)}^\alpha\right] \cdot \left(\Delta\mathbf{u}^{(1)} - \Delta\mathbf{u}^{(2)}\right), \tag{6.5.14}$$

$$+ w_n\left(\delta\tilde{p}^{(1)} - \delta\tilde{p}^{(2)}\right)\mathbf{n}^{(1)} \cdot \left(\frac{\partial\Delta\mathbf{u}^{(1)}}{\partial\eta_{(1)}^1} \times \mathbf{g}_2^{(1)} + \mathbf{g}_1^{(1)} \times \frac{\partial\Delta\mathbf{u}^{(1)}}{\partial\eta_{(1)}^2}\right)$$

$$D \left(j_n \left(\delta \tilde{c}^{(1)} - \delta \tilde{c}^{(2)} \right) \left| \mathbf{g}_1^{(1)} \times \mathbf{g}_2^{(1)} \right| \right) =$$

$$J_\eta^{(1)} \varepsilon_c \left(\delta \tilde{c}^{(1)} - \delta \tilde{c}^{(2)} \right) \left(\Delta \tilde{c}^{(1)} - \Delta \tilde{c}^{(2)} \right)$$

$$- J_\eta^{(1)} \left[\varepsilon_c \left(\delta \tilde{c}^{(1)} - \delta \tilde{c}^{(2)} \right) \frac{\partial \tilde{c}^{(1)}}{\partial \eta_{(1)}^\alpha} \mathbf{g}_{(1)}^\alpha + j_n \frac{\partial \delta \tilde{c}^{(2)}}{\partial \eta_{(2)}^\alpha} \mathbf{g}_{(2)}^\alpha \right] \cdot \left(\Delta \mathbf{u}^{(1)} - \Delta \mathbf{u}^{(2)} \right), \qquad (6.5.15)$$

$$+ j_n \left(\delta \tilde{c}^{(1)} - \delta \tilde{c}^{(2)} \right) \mathbf{n}^{(1)} \cdot \left(\frac{\partial \Delta \mathbf{u}^{(1)}}{\partial \eta_{(1)}^1} \times \mathbf{g}_2^{(1)} + \mathbf{g}_1^{(1)} \times \frac{\partial \Delta \mathbf{u}^{(1)}}{\partial \eta_{(1)}^2} \right)$$

where $J_\eta^{(1)} = \left| \mathbf{g}_1^{(1)} \times \mathbf{g}_2^{(1)} \right|$.

6.5.4 Discretization

The contact integral may be discretized as

$$\delta G_c = \sum_{e=1}^{n_e^{(1)}} \sum_{k=1}^{n_{\text{int}}^{(e)}} W_k J_\eta^{(1)} \left[t_n \left(\delta \mathbf{v}^{(1)} - \delta \mathbf{v}^{(2)} \right) \cdot \mathbf{n}^{(1)} + w_n \left(\delta \tilde{p}^{(1)} - \delta \tilde{p}^{(2)} \right) + j_n \left(\delta \tilde{c}^{(1)} - \delta \tilde{c}^{(2)} \right) \right] \cdot \tag{6.5.16}$$

The variables may be interpolated over each element face according to

$$\delta \mathbf{v}^{(1)} = \sum_{a=1}^{m^{(1)}} N_a^{(1)} \delta \mathbf{v}_a^{(1)} \qquad \delta \mathbf{v}^{(2)} = \sum_{b=1}^{m^{(2)}} N_b^{(2)} \delta \mathbf{v}_b^{(2)}$$

$$\Delta \mathbf{u}^{(1)} = \sum_{c=1}^{m^{(1)}} N_c^{(1)} \Delta \mathbf{u}_c^{(1)} \quad \Delta \mathbf{u}^{(2)} = \sum_{d=1}^{m^{(2)}} N_d^{(2)} \Delta \mathbf{u}_d^{(2)}$$

$$\delta \tilde{p}^{(1)} = \sum_{a=1}^{m^{(1)}} N_a^{(1)} \delta \tilde{p}_a^{(1)} \qquad \delta \tilde{p}^{(2)} = \sum_{b=1}^{m^{(2)}} N_b^{(2)} \delta \tilde{p}_b^{(2)}$$

$$\Delta \tilde{p}^{(1)} = \sum_{c=1}^{m^{(1)}} N_c^{(1)} \Delta \tilde{p}_c^{(1)} \quad \Delta \tilde{p}^{(2)} = \sum_{d=1}^{m^{(2)}} N_d^{(2)} \Delta \tilde{p}_d^{(2)} \tag{6.5.17}$$

$$\delta \tilde{c}^{(1)} = \sum_{a=1}^{m^{(1)}} N_a^{(1)} \delta \tilde{c}_a^{(1)} \qquad \delta \tilde{c}^{(2)} = \sum_{b=1}^{m^{(2)}} N_b^{(2)} \delta \tilde{c}_b^{(2)}$$

$$\Delta \tilde{c}^{(1)} = \sum_{c=1}^{m^{(1)}} N_c^{(1)} \Delta \tilde{c}_c^{(1)} \quad \Delta \tilde{c}^{(2)} = \sum_{d=1}^{m^{(2)}} N_d^{(2)} \Delta \tilde{c}_d^{(2)}$$

Then,

$$\delta G_c = \sum_{e=1}^{n_e^{(1)}} \sum_{k=1}^{n_{\text{int}}^{(e)}} W_k J_\eta^{(1)} \left(\sum_{a=1}^{m^{(1)}} \begin{bmatrix} \delta \mathbf{v}_a^{(1)} & \delta \tilde{p}_a^{(1)} & \delta \tilde{c}_a^{(1)} \end{bmatrix} \cdot \begin{bmatrix} \mathbf{f}_a^{(1)} \\ w_a^{(1)} \\ j_a^{(1)} \end{bmatrix} \right.$$

$$\left. + \sum_{b=1}^{m_k^{(2)}} \begin{bmatrix} \delta \mathbf{v}_{b,k}^{(1)} & \delta \tilde{p}_{b,k}^{(1)} & \delta \tilde{c}_{b,k}^{(1)} \end{bmatrix} \cdot \begin{bmatrix} \mathbf{f}_{b,k}^{(1)} \\ w_{b,k}^{(1)} \\ j_{b,k}^{(1)} \end{bmatrix} \right), \tag{6.5.18}$$

where

$$
\begin{aligned}
\mathbf{f}_a^{(1)} &= N_a^{(1)} t_n \mathbf{n}^{(1)} \qquad \mathbf{f}_{b,k}^{(2)} = -N_b^{(2)} t_n \mathbf{n}^{(1)} \\
w_a^{(1)} &= N_a^{(1)} w_n \qquad\quad w_{b,k}^{(2)} = -N_b^{(2)} w_n \\
j_a^{(1)} &= N_a^{(1)} j_n \qquad\quad\; j_{b,k}^{(2)} = -N_b^{(2)} j_n
\end{aligned}
\tag{6.5.19}
$$

Similarly,

$$
\begin{aligned}
-D\delta G_c = \sum_{e=1}^{n_e^{(1)}} \sum_{k=1}^{n_{\text{int}}^{(e)}} W_k J_\eta^{(1)} \\
\times \Bigg(\sum_{a=1}^{m^{(1)}} \left[\begin{array}{ccc} \delta\mathbf{v}_a^{(1)} & \delta\tilde{p}_a^{(1)} & \delta\tilde{c}_a^{(1)} \end{array} \right] \cdot \Bigg(\sum_{c=1}^{m^{(1)}} \left[\begin{array}{ccc} \mathbf{K}_{ac}^{(1,1)} & \mathbf{0} & \mathbf{0} \\ \mathbf{g}_{ac}^{(1,1)} & g_{ac}^{(1,1)} & 0 \\ \mathbf{h}_{ac}^{(1,1)} & 0 & h_{ac}^{(1,1)} \end{array} \right] \cdot \left[\begin{array}{c} \Delta\mathbf{u}_c^{(1)} \\ \Delta\tilde{p}_c^{(1)} \\ \Delta\tilde{c}_c^{(1)} \end{array} \right] \\
+ \sum_{d=1}^{m_k^{(2)}} \left[\begin{array}{ccc} \mathbf{K}_{ad,k}^{(1,2)} & \mathbf{0} & \mathbf{0} \\ \mathbf{g}_{ad,k}^{(1,2)} & g_{ad,k}^{(1,2)} & 0 \\ \mathbf{h}_{ad,k}^{(1,2)} & 0 & h_{ad,k}^{(1,2)} \end{array} \right] \cdot \left[\begin{array}{c} \Delta\mathbf{u}_d^{(2)} \\ \Delta\tilde{p}_d^{(2)} \\ \Delta\tilde{c}_d^{(2)} \end{array} \right] \Bigg) \\
+ \sum_{b=1}^{m_k^{(2)}} \left[\begin{array}{ccc} \delta\mathbf{v}_{b,k}^{(2)} & \delta\tilde{p}_{b,k}^{(2)} & \delta\tilde{c}_{b,k}^{(2)} \end{array} \right] \cdot \Bigg(\sum_{c=1}^{m^{(1)}} \left[\begin{array}{ccc} \mathbf{K}_{bc,k}^{(2,1)} & \mathbf{0} & \mathbf{0} \\ \mathbf{g}_{bc,k}^{(2,1)} & g_{bc,k}^{(2,1)} & 0 \\ \mathbf{h}_{bc,k}^{(2,1)} & 0 & h_{bc,k}^{(2,1)} \end{array} \right] \cdot \left[\begin{array}{c} \Delta\mathbf{u}_c^{(1)} \\ \Delta\tilde{p}_c^{(1)} \\ \Delta\tilde{c}_c^{(1)} \end{array} \right] \\
+ \sum_{d=1}^{m_k^{(2)}} \left[\begin{array}{ccc} \mathbf{K}_{bd,k}^{(2,2)} & \mathbf{0} & \mathbf{0} \\ \mathbf{g}_{bd,k}^{(2,2)} & g_{bd,k}^{(2,2)} & 0 \\ \mathbf{h}_{bd,k}^{(2,2)} & 0 & h_{bd,k}^{(2,2)} \end{array} \right] \cdot \left[\begin{array}{c} \Delta\mathbf{u}_d^{(2)} \\ \Delta\tilde{p}_d^{(2)} \\ \Delta\tilde{c}_d^{(2)} \end{array} \right] \Bigg) \Bigg),
\end{aligned}
\tag{6.5.20}
$$

where

$$
\begin{aligned}
\mathbf{K}_{ac}^{(1,1)} &= N_a^{(1)} \left(\varepsilon_n N_c^{(1)} \mathbf{N}^{(1)} + t_n \mathbf{A}_c^{(1)} \right) \\
\mathbf{K}_{ad,k}^{(1,2)} &= -\varepsilon_n N_a^{(1)} N_d^{(2)} \mathbf{N}^{(1)} \\
\mathbf{K}_{bc,k}^{(2,1)} &= -N_c^{(1)} \left(\varepsilon_n N_b^{(2)} \mathbf{N}^{(1)} + t_n \mathbf{M}_b^{(2)} \right) - t_n N_b^{(2)} \mathbf{A}_c^{(1)} \\
\mathbf{K}_{bd,k}^{(2,2)} &= N_d^{(2)} \left(\varepsilon_n N_b^{(2)} \mathbf{N}^{(1)} + t_n \mathbf{M}_b^{(2)} \right)
\end{aligned}
\tag{6.5.21}
$$

$$
\begin{aligned}
\mathbf{g}_{ac}^{(1,1)} &= N_a^{(1)} \left(\varepsilon_p N_c^{(1)} \mathbf{p}^{(1)} - w_n \mathbf{A}_c^{(1)} \cdot \mathbf{n}^{(1)} \right) \\
\mathbf{g}_{ad,k}^{(1,2)} &= -\varepsilon_p N_a^{(1)} N_d^{(2)} \mathbf{p}^{(1)} \\
\mathbf{g}_{bc,k}^{(2,1)} &= N_c^{(1)} \left(-\varepsilon_p N_b^{(2)} \mathbf{p}^{(1)} + w_n \mathbf{m}_b^{(2)} \right) + w_n N_b^{(2)} \mathbf{A}_c^{(1)} \cdot \mathbf{n}^{(1)} \\
\mathbf{g}_{bd,k}^{(2,2)} &= N_d^{(2)} \left(\varepsilon_p N_b^{(2)} \mathbf{p}^{(1)} - w_n \mathbf{m}_b^{(2)} \right)
\end{aligned}
\tag{6.5.22}
$$

$$
\begin{aligned}
g_{ac}^{(1,1)} &= -\varepsilon_p N_a^{(1)} N_c^{(1)} \\
g_{ad,k}^{(1,2)} &= \varepsilon_p N_a^{(1)} N_d^{(2)} \\
g_{bc,k}^{(2,1)} &= \varepsilon_p N_b^{(2)} N_c^{(1)} \\
g_{bd,k}^{(2,2)} &= -\varepsilon_p N_b^{(2)} N_d^{(2)}
\end{aligned}
\tag{6.5.23}
$$

$$\mathbf{h}_{ac}^{(1,1)} = N_a^{(1)} \left(\varepsilon_c N_c^{(1)} \mathbf{q}^{(1)} - j_n \mathbf{A}_c^{(1)} \cdot \mathbf{n}^{(1)} \right)$$

$$\mathbf{h}_{ad,k}^{(1,2)} = -\varepsilon_c N_a^{(1)} N_d^{(2)} \mathbf{q}^{(1)}$$

$$\mathbf{h}_{bc,k}^{(2,1)} = N_c^{(1)} \left(-\varepsilon_c N_b^{(2)} \mathbf{q}^{(1)} + j_n \mathbf{m}_b^{(2)} \right) + j_n N_b^{(2)} \mathbf{A}_c^{(1)} \cdot \mathbf{n}^{(1)}$$

$$\mathbf{h}_{bd,k}^{(2,2)} = N_d^{(2)} \left(\varepsilon_c N_b^{(2)} \mathbf{q}^{(1)} - j_n \mathbf{m}_b^{(2)} \right)$$

$$(6.5.24)$$

$$h_{ac}^{(1,1)} = -\varepsilon_c N_a^{(1)} N_c^{(1)}$$

$$h_{ad,k}^{(1,2)} = \varepsilon_c N_a^{(1)} N_d^{(2)}$$

$$h_{bc,k}^{(2,1)} = \varepsilon_c N_b^{(2)} N_c^{(1)}$$

$$h_{bd,k}^{(2,2)} = -\varepsilon_c N_b^{(2)} N_d^{(2)}$$

$$(6.5.25)$$

and

$$\mathbf{N}^{(1)} = \mathbf{n}^{(1)} \otimes \mathbf{n}^{(1)}$$

$$\mathbf{A}_c^{(1)} = \frac{1}{J_\eta^{(1)}} \mathcal{A} \left\{ \frac{\partial N_c^{(1)}}{\partial \eta_{(1)}^1} \mathbf{g}_2^{(1)} - \frac{\partial N_c^{(1)}}{\partial \eta_{(1)}^2} \mathbf{g}_1^{(1)} \right\}$$

$$\mathbf{M}_b^{(2)} = \mathbf{n}^{(2)} \otimes \mathbf{m}_b^{(2)}$$

$$\mathbf{m}_b^{(2)} = \frac{\partial N_b^{(2)}}{\partial \eta_{(2)}^\alpha} \mathbf{g}_{(2)}^\alpha$$

$$\mathbf{p}^{(1)} = \frac{\partial \tilde{p}^{(1)}}{\partial \eta_{(1)}^\alpha} \mathbf{g}_{(1)}^\alpha$$

$$\mathbf{q}^{(1)} = \frac{\partial \tilde{c}^{(1)}}{\partial \eta_{(1)}^\alpha} \mathbf{g}_{(1)}^\alpha$$

$$(6.5.26)$$

6.6 Multiphasic Contact

6.6.1 Contact Integral

See Section 2.7 for a review of multiphasic materials. The contact interface is defined between surfaces $\gamma^{(1)}$ and $\gamma^{(2)}$. Due to continuity requirements on the traction and fluxes, the external virtual work resulting from contact tractions $\mathbf{t}^{(i)}$, solvent fluxes $w_n^{(i)}$ and solute fluxes $j_n^{\alpha(i)}$ for solute α $(i = 1, 2)$, may be combined into the contact integral

$$\delta G_c = \int_{\gamma^{(1)}} \left(\delta \mathbf{v}^{(1)} - \delta \mathbf{v}^{(2)} \right) \cdot \mathbf{t}^{(1)} \, da^{(1)}$$

$$+ \int_{\gamma^{(1)}} \left(\delta \tilde{p}^{(1)} - \delta \tilde{p}^{(2)} \right) w_n^{(1)} \, da^{(1)} \qquad . \qquad (6.6.1)$$

$$+ \sum_\alpha \int_{\gamma^{(1)}} \left(\delta \tilde{c}^{\alpha(1)} - \delta \tilde{c}^{\alpha(2)} \right) j_n^{\alpha(1)} \, da^{(1)}$$

In the current implementation, only frictionless contact is taken into consideration, so that the contact traction has only a normal component, $\mathbf{t}^{(i)} = t_n \mathbf{n}^{(i)}$. To evaluate and linearize δG_c, define

the covariant basis vectors on each surface as

$$\mathbf{g}_\alpha^{(i)} = \frac{\partial \mathbf{x}^{(i)}}{\partial \eta_{(i)}^\alpha}, \quad \alpha = 1, 2, \tag{6.6.2}$$

where $\mathbf{x}^{(i)}$ represents the spatial position of points on $\gamma^{(i)}$, and $\eta_{(i)}^\alpha$ represent the parametric coordinates of that point. The unit outward normal on each surface is then given by

$$\mathbf{n}^{(i)} = \frac{\mathbf{g}_1^{(i)} \times \mathbf{g}_2^{(i)}}{\left| \mathbf{g}_1^{(i)} \times \mathbf{g}_2^{(i)} \right|}. \tag{6.6.3}$$

Now the contact integral may be rewritten as

$$\begin{aligned}
\delta G_c = &\int_{\gamma^{(1)}} \left(\delta \mathbf{v}^{(1)} - \delta \mathbf{v}^{(2)} \right) t_n \mathbf{g}_1^{(1)} \times \mathbf{g}_2^{(1)} \, d\eta_{(1)}^1 d\eta_{(1)}^2 \\
&+ \int_{\gamma^{(1)}} \left(\delta \tilde{p}^{(1)} - \delta \tilde{p}^{(2)} \right) w_n^{(1)} \left| \mathbf{g}_1^{(1)} \times \mathbf{g}_2^{(1)} \right| \, d\eta_{(1)}^1 d\eta_{(1)}^2 \\
&+ \sum_\alpha \int_{\gamma^{(1)}} \left(\delta \tilde{c}^{\alpha(1)} - \delta \tilde{c}^{\alpha(2)} \right) j_n^{\alpha(1)} \left| \mathbf{g}_1^{(1)} \times \mathbf{g}_2^{(1)} \right| \, d\eta_{(1)}^1 d\eta_{(1)}^2
\end{aligned} \tag{6.6.4}$$

and the linearization $D\delta G_c$ of δG_c has the form

$$D\delta G_c = \sum_{i=1}^2 D\delta G_c \left[\Delta \mathbf{u}^{(i)} \right] + D\delta G_c \left[\Delta \tilde{p}^{(i)} \right] + \sum_\alpha D\delta G_c \left[\Delta \tilde{c}^{\alpha(i)} \right]. \tag{6.6.5}$$

6.6.2   Gap Function

The gap function g, representing the distance between the contact surfaces, is defined by

$$\mathbf{x}^{(2)} = \mathbf{x}^{(1)} + g\mathbf{n}^{(1)}, \quad g = \left(\mathbf{x}^{(2)} - \mathbf{x}^{(1)} \right) \cdot \mathbf{n}^{(1)}. \tag{6.6.6}$$

The linearization of variables associated with motion, pressure, and concentration, is given by

$$\begin{aligned}
D\mathbf{x}^{(1)} &= \Delta \mathbf{u}^{(1)} & D\mathbf{x}^{(2)} &= \Delta \mathbf{u}^{(2)} + \mathbf{g}_\alpha^{(2)} \Delta \eta_{(2)}^\alpha \\[2mm]
D\tilde{p}^{(1)} &= \Delta \tilde{p}^{(1)} & D\tilde{p}^{(2)} &= \Delta \tilde{p}^{(2)} + \frac{\partial \tilde{p}^{(2)}}{\partial \eta_{(2)}^\alpha} \Delta \eta_{(2)}^\alpha \\[2mm]
D\tilde{c}^{\gamma(1)} &= \Delta \tilde{c}^{\gamma(1)} & D\tilde{c}^{\gamma(2)} &= \Delta \tilde{c}^{\gamma(2)} + \frac{\partial \tilde{c}^{\gamma(2)}}{\partial \eta_{(2)}^\alpha} \Delta \eta_{(2)}^\alpha \\[2mm]
D\delta \mathbf{v}^{(1)} &= \mathbf{0} & D\mathbf{v}^{(2)} &= \frac{\partial \delta \mathbf{v}^{(2)}}{\partial \eta_{(2)}^\alpha} \Delta \eta_{(2)}^\alpha \\[2mm]
D\delta \tilde{p}^{(1)} &= 0 & D\delta \tilde{p}^{(2)} &= \frac{\partial \delta \tilde{p}^{(2)}}{\partial \eta_{(2)}^\alpha} \Delta \eta_{(2)}^\alpha \\[2mm]
D\delta \tilde{c}^{\gamma(1)} &= 0 & D\delta \tilde{c}^{\gamma(2)} &= \frac{\partial \delta \tilde{c}^{\gamma(2)}}{\partial \eta_{(2)}^\alpha} \Delta \eta_{(2)}^\alpha
\end{aligned} \tag{6.6.7}$$

where

$$\Delta \eta_{(2)}^\alpha = \left(\Delta \mathbf{u}^{(1)} - \Delta \mathbf{u}^{(2)} \right) \cdot a^{\alpha\beta} \mathbf{g}_\beta^{(1)} - a^{\alpha\beta} g \mathbf{n}^{(1)} \cdot \frac{\partial \Delta \mathbf{u}^{(1)}}{\partial \eta_{(1)}^\beta}, \tag{6.6.8}$$

with $a^{\alpha\beta} = (A_{\alpha\beta})^{-1}$ and $A_{\alpha\beta} = \mathbf{g}_\alpha^{(1)} \cdot \mathbf{g}_\beta^{(2)}$.

6.6.3 Penalty Method

Let the normal component of the contact traction be described by the penalty function,

$$t_n = \begin{cases} \varepsilon_n g & g < 0 \\ 0 & g \geqslant 0 \end{cases} , \tag{6.6.9}$$

where ε_n is a penalty factor associated with t_n. Similarly, let

$$\begin{cases} w_n = \varepsilon_p \pi = \varepsilon_p \left(\tilde{p}^{(1)} - \tilde{p}^{(2)} \right) & t_n < 0 \\ \tilde{p}^{(i)} = \tilde{p}^* & t_n = 0 \end{cases} , \tag{6.6.10}$$

and

$$\begin{cases} j_n^\alpha = \varepsilon_c \chi^\alpha = \varepsilon_c \left(\tilde{c}^{\alpha(1)} - \tilde{c}^{\alpha(2)} \right) & t_n < 0 \\ \tilde{c}^{\alpha(i)} = \tilde{c}^{\alpha*} & t_n = 0 \end{cases} , \tag{6.6.11}$$

where ε_p and ε_c are penalty factors associated with $w_n \equiv w_n^{(1)}$ and $j_n^\alpha \equiv j_n^{\alpha(1)}$, respectively. It follows that

$$Dt_n = \varepsilon_n \left(\Delta \mathbf{u}^{(2)} - \Delta \mathbf{u}^{(1)} + \mathbf{g}_\alpha^{(2)} \Delta \eta_{(2)}^\alpha \right) \cdot \mathbf{n}^{(1)}$$

$$Dw_n = \varepsilon_p \left(\Delta \tilde{p}^{(1)} - \Delta \tilde{p}^{(2)} - \frac{\partial \tilde{p}^{(2)}}{\partial \eta_{(2)}^\alpha} \Delta \eta_{(2)}^\alpha \right) \tag{6.6.12}$$

$$Dj_n^\gamma = \varepsilon_c \left(\Delta \tilde{c}^{\gamma(1)} - \Delta \tilde{c}^{\gamma(2)} - \frac{\partial \tilde{c}^{\gamma(2)}}{\partial \eta_{(2)}^\alpha} \Delta \eta_{(2)}^\alpha \right)$$

Given these relations, it can be shown that the directional derivatives of the various terms appearing in the integrand of δG_c are

$$- D \left(t_n \left(\delta \mathbf{v}^{(1)} - \delta \mathbf{v}^{(2)} \right) \cdot \mathbf{g}_1^{(1)} \times \mathbf{g}_2^{(1)} \right) =$$

$$J_\eta^{(1)} \varepsilon_n \left(\delta \mathbf{v}^{(1)} - \delta \mathbf{v}^{(2)} \right) \cdot \left(\mathbf{n}^{(1)} \otimes \mathbf{n}^{(1)} \right) \cdot \left(\Delta \mathbf{u}^{(1)} - \Delta \mathbf{u}^{(2)} \right)$$

$$- J_\eta^{(1)} t_n \frac{\partial \delta \mathbf{v}^{(2)}}{\partial \eta_{(2)}^\alpha} \cdot \left(\mathbf{n}^{(2)} \otimes \mathbf{g}_{(2)}^\alpha \right) \cdot \left(\Delta \mathbf{u}^{(1)} - \Delta \mathbf{u}^{(2)} \right) \tag{6.6.13}$$

$$+ t_n \left(\delta \mathbf{v}^{(1)} - \delta \mathbf{v}^{(2)} \right) \cdot \left(\mathbf{g}_2^{(1)} \times \frac{\partial \Delta \mathbf{u}^{(1)}}{\partial \eta_{(1)}^1} - \mathbf{g}_1^{(1)} \times \frac{\partial \Delta \mathbf{u}^{(1)}}{\partial \eta_{(1)}^2} \right)$$

$$- D \left(w_n \left(\delta \tilde{p}^{(1)} - \delta \tilde{p}^{(2)} \right) \left| \mathbf{g}_1^{(1)} \times \mathbf{g}_2^{(1)} \right| \right) =$$

$$- J_\eta^{(1)} \varepsilon_p \left(\delta \tilde{p}^{(1)} - \delta \tilde{p}^{(2)} \right) \left(\Delta \tilde{p}^{(1)} - \Delta \tilde{p}^{(2)} \right)$$

$$+ J_\eta^{(1)} \left[\varepsilon_p \left(\delta \tilde{p}^{(1)} - \delta \tilde{p}^{(2)} \right) \frac{\partial \tilde{p}^{(1)}}{\partial \eta_{(1)}^\alpha} \mathbf{g}_{(1)}^\alpha + w_n \frac{\partial \delta \tilde{p}^{(2)}}{\partial \eta_{(2)}^\alpha} \mathbf{g}_{(2)}^\alpha \right] \cdot \left(\Delta \mathbf{u}^{(1)} - \Delta \mathbf{u}^{(2)} \right), \tag{6.6.14}$$

$$+ w_n \left(\delta \tilde{p}^{(1)} - \delta \tilde{p}^{(2)} \right) \mathbf{n}^{(1)} \cdot \left(\mathbf{g}_2^{(1)} \times \frac{\partial \Delta \mathbf{u}^{(1)}}{\partial \eta_{(1)}^1} - \mathbf{g}_1^{(1)} \times \frac{\partial \Delta \mathbf{u}^{(1)}}{\partial \eta_{(1)}^2} \right)$$

$$- D \left(j_n^\gamma \left(\delta \tilde{c}^{\gamma(1)} - \delta \tilde{c}^{\gamma(2)} \right) \left| \mathbf{g}_1^{(1)} \times \mathbf{g}_2^{(1)} \right| \right) =$$

$$- J_\eta^{(1)} \varepsilon_c \left(\delta \tilde{c}^{\gamma(1)} - \delta \tilde{c}^{\gamma(2)} \right) \left(\Delta \tilde{c}^{\gamma(1)} - \Delta \tilde{c}^{\gamma(2)} \right)$$

$$+ J_\eta^{(1)} \varepsilon_c \left(\delta \tilde{c}^{\gamma(1)} - \delta \tilde{c}^{\gamma(2)} \right) \frac{\partial \tilde{c}^{\gamma(1)}}{\partial \eta_{(1)}^\alpha} \mathbf{g}_\alpha^{(1)} \cdot \left(\Delta \mathbf{u}^{(1)} - \Delta \mathbf{u}^{(2)} \right)$$

$$+ J_\eta^{(1)} j_n^\gamma \frac{\partial \delta \tilde{c}^{\gamma(1)}}{\partial \eta_{(1)}^\alpha} \mathbf{g}_\alpha^{(1)} \cdot \left(\Delta \mathbf{u}^{(1)} - \Delta \mathbf{u}^{(2)} \right)$$

$$+ j_n^\gamma \left(\delta \tilde{c}^{\gamma(1)} - \delta \tilde{c}^{\gamma(2)} \right) \mathbf{n}^{(1)} \cdot \left(\mathbf{g}_2^{(1)} \times \frac{\partial \Delta \mathbf{u}^{(1)}}{\partial \eta_{(1)}^1} - \mathbf{g}_1^{(1)} \times \frac{\partial \Delta \mathbf{u}^{(1)}}{\partial \eta_{(1)}^2} \right)$$

$$(6.6.15)$$

where $J_\eta^{(1)} = \left| \mathbf{g}_1^{(1)} \times \mathbf{g}_2^{(1)} \right|$.

6.6.4   Discretization

The contact integral may be discretized as

$$\delta G_c = \sum_{e=1}^{n_e^{(1)}} \sum_{k=1}^{n_{\text{int}}^{(e)}} W_k J_\eta^{(1)} \left[t_n \left(\delta \mathbf{v}^{(1)} - \delta \mathbf{v}^{(2)} \right) \cdot \mathbf{n}^{(1)} + w_n \left(\delta \tilde{p}^{(1)} - \delta \tilde{p}^{(2)} \right) + \sum_\gamma j_n^\gamma \left(\delta \tilde{c}^{\gamma(1)} - \delta \tilde{c}^{\gamma(2)} \right) \right] \cdot$$

$$(6.6.16)$$

The variables may be interpolated over each element face according to

$$\delta \mathbf{v}^{(1)} = \sum_{a=1}^{m^{(1)}} N_a^{(1)} \delta \mathbf{v}_a^{(1)} \qquad \delta \mathbf{v}^{(2)} = \sum_{b=1}^{m^{(2)}} N_b^{(2)} \delta \mathbf{v}_b^{(2)}$$

$$\Delta \mathbf{u}^{(1)} = \sum_{c=1}^{m^{(1)}} N_c^{(1)} \Delta \mathbf{u}_c^{(1)} \qquad \Delta \mathbf{u}^{(2)} = \sum_{d=1}^{m^{(2)}} N_d^{(2)} \Delta \mathbf{u}_d^{(2)}$$

$$\delta \tilde{p}^{(1)} = \sum_{a=1}^{m^{(1)}} N_a^{(1)} \delta \tilde{p}_a^{(1)} \qquad \delta \tilde{p}^{(2)} = \sum_{b=1}^{m^{(2)}} N_b^{(2)} \delta \tilde{p}_b^{(2)}$$

$$\Delta \tilde{p}^{(1)} = \sum_{c=1}^{m^{(1)}} N_c^{(1)} \Delta \tilde{p}_c^{(1)} \qquad \Delta \tilde{p}^{(2)} = \sum_{d=1}^{m^{(2)}} N_d^{(2)} \Delta \tilde{p}_d^{(2)} \qquad (6.6.17)$$

$$\delta \tilde{c}^{\gamma(1)} = \sum_{a=1}^{m^{(1)}} N_a^{(1)} \delta \tilde{c}_a^{\gamma(1)} \qquad \delta \tilde{c}^{\gamma(2)} = \sum_{b=1}^{m^{(2)}} N_b^{(2)} \delta \tilde{c}_b^{\gamma(2)}$$

$$\Delta \tilde{c}^{\gamma(1)} = \sum_{c=1}^{m^{(1)}} N_c^{(1)} \Delta \tilde{c}_c^{\gamma(1)} \qquad \Delta \tilde{c}^{\gamma(2)} = \sum_{d=1}^{m^{(2)}} N_d^{(2)} \Delta \tilde{c}_d^{\gamma(2)}$$

Then,

$$
\delta G_c = \sum_{e=1}^{n_e^{(1)}} \sum_{k=1}^{n_{\text{int}}^{(e)}} W_k J_\eta^{(1)} \left(\sum_{a=1}^{m^{(1)}} \left[\begin{array}{cccc} \delta \mathbf{v}_a^{(1)} & \delta \tilde{p}_a^{(1)} & \delta \tilde{c}_a^{\alpha(1)} & \delta \tilde{c}_a^{\beta(1)} \end{array} \right] \cdot \left[\begin{array}{c} \mathbf{f}_a^{(1)} \\ w_a^{(1)} \\ j_a^{\alpha(1)} \\ j_a^{\beta(1)} \end{array} \right] \right.
$$
$$
\left. + \sum_{b=1}^{m^{(2)}} \left[\begin{array}{cccc} \delta \mathbf{v}_b^{(2)} & \delta \tilde{p}_b^{(2)} & \delta \tilde{c}_b^{\alpha(2)} & \delta \tilde{c}_b^{\beta(2)} \end{array} \right] \cdot \left[\begin{array}{c} \mathbf{f}_{b,k}^{(2)} \\ w_{b,k}^{(2)} \\ j_{b,k}^{\alpha(2)} \\ j_{b,k}^{\beta(2)} \end{array} \right] \right),
$$

(6.6.18)

where

$$
\begin{array}{ll}
\mathbf{f}_a^{(1)} = t_n N_a^{(1)} \mathbf{n}^{(1)} & \mathbf{f}_{b,k}^{(2)} = -t_n N_b^{(2)} \mathbf{n}^{(1)} \\
w_a^{(1)} = w_n N_a^{(1)} & w_{b,k}^{(2)} = -w_n N_b^{(2)} \\
j_a^{\gamma(1)} = j_n^\gamma N_a^{(1)} & j_{b,k}^{\gamma(2)} = -j_n^\gamma N_b^{(2)}
\end{array} \quad .
$$

(6.6.19)

Similarly,

$$
-D\delta G_c = \sum_{e=1}^{n_e^{(1)}} \sum_{k=1}^{n_{\text{int}}^{(e)}} W_k J_\eta^{(1)} \times \left(\sum_{a=1}^{m^{(1)}} \left[\begin{array}{cccc} \delta \mathbf{v}_a^{(1)} & \delta \tilde{p}_a^{(1)} & \delta \tilde{c}_a^{\alpha(1)} & \delta \tilde{c}_a^{\beta(1)} \end{array} \right] \cdot \right.
$$
$$
\left(\sum_{c=1}^{m^{(1)}} \left[\begin{array}{cccc} \mathbf{K}_{ac}^{(1,1)} & 0 & 0 & 0 \\ \mathbf{g}_{ac}^{(1,1)} & g_{ac}^{(1,1)} & 0 & 0 \\ \mathbf{h}_{ac}^{\alpha(1,1)} & 0 & h_{ac}^{\alpha\alpha(1,1)} & 0 \\ \mathbf{h}_{ac}^{\beta(1,1)} & 0 & 0 & h_{ac}^{\beta\beta(1,1)} \end{array} \right] \cdot \left[\begin{array}{c} \Delta \mathbf{u}_c^{(1)} \\ \Delta \tilde{p}_c^{(1)} \\ \Delta \tilde{c}_c^{\alpha(1)} \\ \Delta \tilde{c}_c^{\beta(1)} \end{array} \right] \right.
$$
$$
\left. + \sum_{d=1}^{m_k^{(2)}} \left[\begin{array}{cccc} \mathbf{K}_{ad,k}^{(1,2)} & 0 & 0 & 0 \\ \mathbf{g}_{ad,k}^{(1,2)} & g_{ad,k}^{(1,2)} & 0 & 0 \\ \mathbf{h}_{ad,k}^{\alpha(1,2)} & 0 & h_{ad,k}^{\alpha\alpha(1,2)} & 0 \\ \mathbf{h}_{ad,k}^{\beta(1,2)} & 0 & 0 & h_{ad,k}^{\beta\beta(1,2)} \end{array} \right] \cdot \left[\begin{array}{c} \Delta \mathbf{u}_d^{(2)} \\ \Delta \tilde{p}_d^{(2)} \\ \Delta \tilde{c}_d^{\alpha(2)} \\ \Delta \tilde{c}_d^{\beta(2)} \end{array} \right] \right)
$$
$$
+ \sum_{b=1}^{m_k^{(2)}} \left[\begin{array}{cccc} \delta \mathbf{v}_{b,k}^{(2)} & \delta \tilde{p}_{b,k}^{(2)} & \delta \tilde{c}_{b,k}^{\alpha(2)} & \delta \tilde{c}_{b,k}^{\beta(2)} \end{array} \right] \cdot
$$
$$
\left(\sum_{c=1}^{m^{(1)}} \left[\begin{array}{cccc} \mathbf{K}_{bc,k}^{(2,1)} & 0 & 0 & 0 \\ \mathbf{g}_{bc,k}^{(2,1)} & g_{bc,k}^{(2,1)} & 0 & 0 \\ \mathbf{h}_{bc,k}^{\alpha(2,1)} & 0 & h_{bc,k}^{\alpha\alpha(2,1)} & 0 \\ \mathbf{h}_{bc,k}^{\beta(2,1)} & 0 & 0 & h_{bc,k}^{\beta\beta(2,1)} \end{array} \right] \cdot \left[\begin{array}{c} \Delta \mathbf{u}_c^{(1)} \\ \Delta \tilde{p}_c^{(1)} \\ \Delta \tilde{c}_c^{\alpha(1)} \\ \Delta \tilde{c}_c^{\beta(1)} \end{array} \right] \right.
$$
$$
\left. \left. + \sum_{d=1}^{m_k^{(2)}} \left[\begin{array}{cccc} \mathbf{K}_{bd,k}^{(2,2)} & 0 & 0 & 0 \\ \mathbf{g}_{bd,k}^{(2,2)} & g_{bd,k}^{(2,2)} & 0 & 0 \\ \mathbf{h}_{bd,k}^{\alpha(2,2)} & 0 & h_{bd,k}^{\alpha\alpha(2,2)} & 0 \\ \mathbf{h}_{bd,k}^{\beta(2,2)} & 0 & 0 & h_{bd,k}^{\beta\beta(2,2)} \end{array} \right] \cdot \left[\begin{array}{c} \Delta \mathbf{u}_d^{(2)} \\ \Delta \tilde{p}_d^{(2)} \\ \Delta \tilde{c}_d^{\alpha(2)} \\ \Delta \tilde{c}_d^{\beta(2)} \end{array} \right] \right) \right) \right),
$$

(6.6.20)

where

$$\mathbf{K}_{ac}^{(1,1)} = N_a^{(1)} \left(\varepsilon_n N_c^{(1)} \mathbf{N}^{(1)} + t_n \mathbf{A}_c^{(1)} \right)$$

$$\mathbf{K}_{ad,k}^{(1,2)} = -\varepsilon_n N_a^{(1)} N_d^{(2)} \mathbf{N}^{(1)}$$

$$\mathbf{K}_{bc,k}^{(2,1)} = -N_c^{(1)} \left(\varepsilon_n N_b^{(2)} \mathbf{N}^{(1)} + t_n \mathbf{M}_b^{(2)} \right) - t_n N_b^{(2)} \mathbf{A}_c^{(1)}$$

$$\mathbf{K}_{bd,k}^{(2,2)} = N_d^{(2)} \left(\varepsilon_n N_b^{(2)} \mathbf{N}^{(1)} + t_n \mathbf{M}_b^{(2)} \right)$$

(6.6.21)

$$\mathbf{g}_{ac}^{(1,1)} = N_a^{(1)} \left(\varepsilon_p N_c^{(1)} \mathbf{p}^{(1)} - w_n \mathbf{A}_c^{(1)} \cdot \mathbf{n}^{(1)} \right)$$

$$\mathbf{g}_{ad,k}^{(1,2)} = -\varepsilon_p N_a^{(1)} N_d^{(2)} \mathbf{p}^{(1)}$$

$$\mathbf{g}_{bc,k}^{(2,1)} = N_c^{(1)} \left(-\varepsilon_p N_b^{(2)} \mathbf{p}^{(1)} + w_n \mathbf{m}_b^{(2)} \right) + w_n N_b^{(2)} \mathbf{A}_c^{(1)} \cdot \mathbf{n}^{(1)}$$

$$\mathbf{g}_{bd,k}^{(2,2)} = N_d^{(2)} \left(\varepsilon_p N_b^{(2)} \mathbf{p}^{(1)} - w_n \mathbf{m}_b^{(2)} \right)$$

(6.6.22)

$$g_{ac}^{(1,1)} = -\varepsilon_p N_a^{(1)} N_c^{(1)} \qquad g_{ad,k}^{(1,2)} = \varepsilon_p N_a^{(1)} N_d^{(2)}$$

$$g_{bc,k}^{(2,1)} = \varepsilon_p N_b^{(2)} N_c^{(1)} \qquad g_{bd,k}^{(2,2)} = -\varepsilon_p N_b^{(2)} N_d^{(2)}$$

(6.6.23)

$$\mathbf{h}_{ac}^{\gamma(1,1)} = N_a^{(1)} \left(N_c^{(1)} \varepsilon_c \mathbf{q}^{\gamma(1)} - \mathbf{A}_c^{(1)} \cdot j_n^\gamma \mathbf{n}^{(1)} \right)$$

$$\mathbf{h}_{ad,k}^{\gamma(1,2)} = -N_a^{(1)} N_d^{(2)} \varepsilon_c \mathbf{q}^{\gamma(1)}$$

$$\mathbf{h}_{bc,k}^{\gamma(2,1)} = N_b^{(2)} \left(-N_c^{(1)} \varepsilon_c \mathbf{q}^{\gamma(1)} + \mathbf{A}_c^{(1)} \cdot j_n^\gamma \mathbf{n}^{(1)} \right) + N_c^{(1)} j_n^\gamma \mathbf{m}_b^{(2)}$$

$$\mathbf{h}_{bd,k}^{\gamma(2,2)} = N_b^{(2)} N_d^{(2)} \varepsilon_c \mathbf{q}^{\gamma(1)} - N_d^{(2)} j_n^\gamma \mathbf{m}_b^{(2)}$$

(6.6.24)

$$h_{ac}^{\gamma\gamma(1,1)} = -\varepsilon_c N_a^{(1)} N_c^{(1)}$$

$$h_{ad,k}^{\gamma\gamma(1,2)} = \varepsilon_c N_a^{(1)} N_d^{(2)}$$

$$h_{bc,k}^{\gamma\gamma(2,1)} = \varepsilon_c N_b^{(2)} N_c^{(1)}$$

$$h_{bd,k}^{\gamma\gamma(2,2)} = -\varepsilon_c N_b^{(2)} N_d^{(2)}$$

(6.6.25)

and

$$\mathbf{N}^{(1)} = \mathbf{n}^{(1)} \otimes \mathbf{n}^{(1)} \qquad \mathbf{A}_c^{(1)} = \frac{1}{J_\eta^{(1)}} \mathcal{A} \left\{ \frac{\partial N_c^{(1)}}{\partial \eta_{(1)}^1} \mathbf{g}_2^{(1)} - \frac{\partial N_c^{(1)}}{\partial \eta_{(1)}^2} \mathbf{g}_1^{(1)} \right\}$$

$$\mathbf{M}_b^{(2)} = \mathbf{n}^{(2)} \otimes \mathbf{m}_b^{(2)} \qquad \mathbf{m}_b^{(2)} = \frac{\partial N_b^{(2)}}{\partial \eta_{(2)}^\alpha} \mathbf{g}_{(2)}^\alpha$$

$$\mathbf{p}^{(1)} = \frac{\partial \tilde{p}^{(1)}}{\partial \eta_{(1)}^\alpha} \mathbf{g}_{(1)}^\alpha \qquad \mathbf{q}^{\gamma(1)} = \frac{\partial \tilde{c}^{\gamma(1)}}{\partial \eta_{(1)}^\alpha} \mathbf{g}_{(1)}^\alpha$$

(6.6.26)

6.7   Tied Contact

In some situations it is useful to connect two non-conforming meshes together. This can be done by defining a tied contact interface. In FEBio, the tied contact works very similar to the sliding contact interface. We need to define a slave surface and a master surface, where it is assumed that the slave surface nodes will be tied to the master surface faces.

6.7.1 Gap Function

Just as in sliding contact, we need to define a gap function that measures the distance between the slave and master surface. In order to do that, we first define the projection of a slave node to the master surface.

$$\bar{\mathbf{Y}}\left(\mathbf{X}\right) = \arg\min_{\mathbf{Y}\in\Gamma^{(2)}} \|\mathbf{X} - \mathbf{Y}\| . \tag{6.7.1}$$

This definition is similar to that of the sliding interface, except that now the projection is done in the material reference frame. This implies that the projection only needs to be calculated once, at the beginning of the analysis. We can now proceed to the definition of the gap function.

$$\mathbf{g}\left(\mathbf{X}\right) = \boldsymbol{\varphi}^{(1)}\left(\mathbf{X}\right) - \boldsymbol{\varphi}^{(2)}\left(\bar{\mathbf{Y}}\left(\mathbf{X}\right)\right) . \tag{6.7.2}$$

An important observation is that the gap function is now a vector quantity since the gap needs to be closed in all direction, not just the normal direction as is the case in sliding contact.

6.7.2 Tied Contact Integral

With the definition of the gap function at hand (equation (6.7.2)), we can define the contribution to the virtual work equation from the tied contact reaction forces.

$$W_t = \int_{\Gamma_c} \mathbf{T} \cdot \delta\mathbf{g}\, d\Gamma . \tag{6.7.3}$$

Here, $\mathbf{T}$ is the reaction force that enforces the constraint $\mathbf{g}\left(\mathbf{X}\right) = 0$. Since we anticipate the use of an augmented Lagrangian formalism, we can write this reaction force as follows,

$$\mathbf{T} = \boldsymbol{\lambda} + \varepsilon\mathbf{g} . \tag{6.7.4}$$

The vector quantity $\boldsymbol{\lambda}$ is the Lagrangian multiplier and ε is a penalty factor.

6.7.3 Linearization of the Contact Integral

Since equation (6.7.3) is nonlinear we need to calculate the linearization. For tied contact, this is simply given by the following equation.

$$\Delta W_t = \int_{\Gamma_c} \varepsilon\Delta\mathbf{g} \cdot \delta\mathbf{g}\, d\Gamma . \tag{6.7.5}$$

Where

$$\delta\mathbf{g} = \mathbf{w}^{(1)} - \mathbf{w}^{(2)} \tag{6.7.6}$$

and

$$\Delta\mathbf{g} = \Delta\boldsymbol{\varphi}^{(1)}\left(\mathbf{X}\right) - \Delta\boldsymbol{\varphi}^{(2)}\left(\bar{\mathbf{Y}}\left(\mathbf{X}\right)\right) . \tag{6.7.7}$$

We also introduced the notation $\mathbf{w}^{(i)} = \delta\boldsymbol{\varphi}^{(i)}$.

The discretization of (6.7.5) will lead to a contribution to the stiffness matrix. Notice that due to symmetry between $\delta\mathbf{g}$ and $\Delta\mathbf{g}$ this matrix will be symmetric.

6.7.4 Discretization

The contact integral (6.7.3) can be discretized as follows. First, we split the integration over all the slave surface elements.

$$W_t = \sum_{e=1}^{nel} \int_{\Gamma_c^{(e)}} \mathbf{T} \cdot \delta \mathbf{g} \, d\Gamma^{(e)} . \tag{6.7.8}$$

The integration can be approximated by a quadrature rule,

$$W_t = \sum_{e=1}^{nel} \sum_{i=1}^{N_{int}^{(e)}} w^i j \left(\xi_i \right) \mathbf{T} \left(\xi_i \right) \cdot \delta \mathbf{g} \left(\xi_i \right) . \tag{6.7.9}$$

If we use a nodally integrated elements, we have

$$\begin{aligned} \mathbf{w}^{(1)} \left(\xi_i \right) &= \mathbf{c}_i^{(1)} , \\ \mathbf{w}^{(2)} \left(\xi_i \right) &= \sum_j N_j \left(\bar{\xi}_i \right) \mathbf{c}_j^{(2)} , \end{aligned} \tag{6.7.10}$$

so that,

$$\delta \mathbf{g} \left(\xi_i \right) = \mathbf{c}_i^{(1)} - \sum_j N_j \left(\bar{\xi}_i \right) \mathbf{c}_j^{(2)} . \tag{6.7.11}$$

We can now write the contact integral (6.7.8) in its final form,

$$W_t = \sum_{e=1}^{nel} \sum_{i=1}^{N_{int}^{(e)}} w^i j \left(\xi_i \right) \left(\mathbf{N} \left(\xi_i \right) \mathbf{T} \left(\xi_i \right) \right) \cdot \delta \boldsymbol{\Phi} , \tag{6.7.12}$$

where

$$\delta \boldsymbol{\Phi}^T \left(\xi_i \right) = \left[\begin{array}{ccccc} \mathbf{c}_i^{(1)} & \mathbf{c}_1^{(2)} & \mathbf{c}_2^{(2)} & \cdots & \mathbf{c}_n^{(2)} \end{array} \right] , \tag{6.7.13}$$

$$\mathbf{N} \left(\xi_i \right) = \left[\begin{array}{cccc} \mathbf{I} & -\mathbf{N}_1 & \cdots & -\mathbf{N}_n \end{array} \right] , \tag{6.7.14}$$

and

$$\mathbf{N}_i = \left[\begin{array}{ccc} N_i & 0 & 0 \\ 0 & N_i & 0 \\ 0 & 0 & N_i \end{array} \right] . \tag{6.7.15}$$

For the linearized tied contact integral (6.7.5), a similar discretization procedure leads to,

$$\Delta W_t = \sum_{e=1}^{nel} \sum_{i=1}^{N_{int}^{(e)}} w^i j \left(\xi_i \right) \Delta \boldsymbol{\Phi} \cdot \mathbf{K}_c \delta \boldsymbol{\Phi} , \tag{6.7.16}$$

where

$$\mathbf{K}_c = \varepsilon \mathbf{N}^T \mathbf{N} . \tag{6.7.17}$$

6.8 Tied Biphasic Contact

6.8.1 Contact Integral

See Section 2.5 for a review of biphasic materials, and [10] for additional details on biphasic contact. The contact interface is defined between surfaces $\gamma^{(1)}$ and $\gamma^{(2)}$. Due to continuity requirements on the traction and fluxes, the external virtual work resulting from contact tractions $\mathbf{t}^{(i)}$ and solvent fluxes $w_n^{(i)}$ $(i = 1, 2)$ may be combined into the contact integral

$$
\delta G_c = \int_{\gamma^{(1)}} \left(\delta \mathbf{v}^{(1)} - \delta \mathbf{v}^{(2)} \right) \cdot \mathbf{t}^{(1)} da^{(1)}
$$
$$
+ \int_{\gamma^{(1)}} \left(\delta p^{(1)} - \delta p^{(2)} \right) w_n^{(1)} da^{(1)} .
$$

(6.8.1)

To evaluate and linearize δG_c, define the covariant basis vectors on each surface as

$$
\mathbf{g}_\alpha^{(i)} = \frac{\partial \mathbf{x}^{(i)}}{\partial \eta_{(i)}^\alpha}, \quad \alpha = 1, 2,
$$

(6.8.2)

where $\mathbf{x}^{(i)}$ represents the spatial position of points on $\gamma^{(i)}$, and $\eta_{(i)}^\alpha$ represent the parametric coordinates of that point. The unit outward normal on each surface is then given by

$$
\mathbf{n}^{(i)} = \frac{\mathbf{g}_1^{(i)} \times \mathbf{g}_2^{(i)}}{\left| \mathbf{g}_1^{(i)} \times \mathbf{g}_2^{(i)} \right|} .
$$

(6.8.3)

Now the contact integral may be rewritten as

$$
\delta G_c = \int_{\gamma^{(1)}} \left(\delta \mathbf{v}^{(1)} - \delta \mathbf{v}^{(2)} \right) \cdot \mathbf{t} \left| \mathbf{g}_1^{(1)} \times \mathbf{g}_2^{(1)} \right| d\eta_{(1)}^1 d\eta_{(1)}^2
$$
$$
+ \int_{\gamma^{(1)}} \left(\delta p^{(1)} - \delta p^{(2)} \right) w_n \left| \mathbf{g}_1^{(1)} \times \mathbf{g}_2^{(1)} \right| d\eta_{(1)}^1 d\eta_{(1)}^2
$$

(6.8.4)

where $\mathbf{t} \equiv \mathbf{t}^{(1)}$ and $w_n \equiv w_n^{(1)}$. The linearization $D\delta G_c$ of δG_c has the form

$$
D\delta G_c = \sum_{i=1}^{2} D\delta G_c \left[\Delta \mathbf{u}^{(i)} \right] + D\delta G_c \left[\Delta p^{(i)} \right] .
$$

(6.8.5)

6.8.2 Gap Function

The vector gap function $\mathbf{g}$, representing the distance between the contact surfaces, is defined by

$$
\mathbf{g} = \mathbf{x}^{(2)} - \mathbf{x}^{(1)} .
$$

(6.8.6)

The premise of a tied interface is that the parametric coordinates of $\mathbf{x}^{(1)}$ and $\mathbf{x}^{(2)}$ are both invariants (i.e., they are determined in the reference configuration and remain unchanged over time). The parametric coordinates of $\mathbf{x}^{(1)}$ correspond to the integration points on $\gamma^{(1)}$, and those of $\mathbf{x}^{(2)}$ are

evaluated once, in the reference configuration, by shooting a ray from the integration point on $\gamma^{(1)}$ to intersect $\gamma^{(2)}$. It follows from this premise that

$$
\begin{aligned}
D\mathbf{x}^{(1)} &= \Delta\mathbf{u}^{(1)} & D\mathbf{x}^{(2)} &= \Delta\mathbf{u}^{(2)} \\
Dp^{(1)} &= \Delta p^{(1)} & Dp^{(2)} &= \Delta p^{(2)} \\
D\delta\mathbf{v}^{(1)} &= \mathbf{0} & D\delta\mathbf{v}^{(2)} &= \mathbf{0} \\
D\delta p^{(1)} &= 0 & D\delta p^{(2)} &= 0
\end{aligned}
\tag{6.8.7}
$$

If $\gamma^{(1)}$ and $\gamma^{(2)}$ are not initially conforming, continuity of fluid pressure and normal flux will only be enforced within the contact interface; unlike the sliding biphasic contact interface (Section 6.4), free-draining conditions are not set automatically on regions of $\gamma^{(1)}$ and $\gamma^{(2)}$ where a solution for $\mathbf{g}$ was not found. Therefore, these regions naturally enforce zero fluid flux (impermeable boundary), unless an explicit boundary condition on the pressure p is prescribed over those regions.

6.8.3   Penalty Method

Let the tied contact traction be described by the penalty function,

$$
\mathbf{t} = \varepsilon_n \mathbf{g} \,,
\tag{6.8.8}
$$

where ε_n is a penalty factor associated with $\mathbf{t}$. Similarly, let

$$
w_n = \varepsilon_p \pi = \varepsilon_p \left(p^{(1)} - p^{(2)} \right) \,,
\tag{6.8.9}
$$

where ε_p is a penalty factor associated with w_n. It follows that

$$
\begin{aligned}
D\mathbf{t} &= \varepsilon_n \left(\Delta\mathbf{u}^{(2)} - \Delta\mathbf{u}^{(1)} \right) \,, \\
Dw_n &= \varepsilon_p \left(\Delta p^{(1)} - \Delta p^{(2)} \right) \,.
\end{aligned}
\tag{6.8.10}
$$

Given these relations, it can be shown that the directional derivatives of the various terms appearing in the integrand of δG_c are

$$
\begin{aligned}
&- D \left(J_\eta^{(1)} \left(\delta\mathbf{v}^{(1)} - \delta\mathbf{v}^{(2)} \right) \cdot \mathbf{t} \right) = \\
&\left(\delta\mathbf{v}^{(1)} - \delta\mathbf{v}^{(2)} \right) \cdot \varepsilon_n J_\eta^{(1)} \mathbf{I} \cdot \left(\Delta\mathbf{u}^{(1)} - \Delta\mathbf{u}^{(2)} \right) \\
&+ \left(\delta\mathbf{v}^{(1)} - \delta\mathbf{v}^{(2)} \right) \cdot \mathbf{t} \otimes \left[\left(\mathbf{g}_1^{(1)} \times \mathbf{n}^{(1)} \right) \cdot \frac{\partial \Delta\mathbf{u}^{(1)}}{\partial \eta_{(1)}^2} - \left(\mathbf{g}_2^{(1)} \times \mathbf{n}^{(1)} \right) \cdot \frac{\partial \Delta\mathbf{u}^{(1)}}{\partial \eta_{(1)}^1} \right]
\end{aligned}
\tag{6.8.11}
$$

$$
\begin{aligned}
&- D \left(w_n \left(\delta p^{(1)} - \delta p^{(2)} \right) J_\eta^{(1)} \right) = \\
&- J_\eta^{(1)} \varepsilon_p \left(\delta p^{(1)} - \delta p^{(2)} \right) \left(\Delta p^{(1)} - \Delta p^{(2)} \right) \\
&+ w_n \left(\delta p^{(1)} - \delta p^{(2)} \right) \mathbf{n}^{(1)} \cdot \left(\mathbf{g}_2^{(1)} \times \frac{\partial \Delta\mathbf{u}^{(1)}}{\partial \eta_{(1)}^1} - \mathbf{g}_1^{(1)} \times \frac{\partial \Delta\mathbf{u}^{(1)}}{\partial \eta_{(1)}^2} \right)
\end{aligned}
\tag{6.8.12}
$$

where $J_\eta^{(1)} = \left| \mathbf{g}_1^{(1)} \times \mathbf{g}_2^{(1)} \right|$.

6.8.4 Discretization

The contact integral may be discretized as

$$\delta G_c = \sum_{e=1}^{n_e^{(1)}} \sum_{k=1}^{n_{\text{int}}^{(e)}} W_k J_\eta^{(1)} \left[\left(\delta \mathbf{v}^{(1)} - \delta \mathbf{v}^{(2)} \right) \cdot \mathbf{t} + w_n \left(\delta p^{(1)} - \delta p^{(2)} \right) \right] . \tag{6.8.13}$$

The variables may be interpolated over each element face according to

$$
\begin{aligned}
\delta \mathbf{v}^{(1)} &= \sum_{a=1}^{m^{(1)}} N_a^{(1)} \delta \mathbf{v}_a^{(1)} & \delta \mathbf{v}^{(2)} &= \sum_{b=1}^{m^{(2)}} N_b^{(2)} \delta \mathbf{v}_b^{(2)} \\
\Delta \mathbf{u}^{(1)} &= \sum_{c=1}^{m^{(1)}} N_c^{(1)} \Delta \mathbf{u}_c^{(1)} & \Delta \mathbf{u}^{(2)} &= \sum_{d=1}^{m^{(2)}} N_d^{(2)} \Delta \mathbf{u}_d^{(2)} \\
\delta p^{(1)} &= \sum_{a=1}^{m^{(1)}} N_a^{(1)} \delta p_a^{(1)} & \delta p^{(2)} &= \sum_{b=1}^{m^{(2)}} N_b^{(2)} \delta p_b^{(2)} \\
\Delta p^{(1)} &= \sum_{c=1}^{m^{(1)}} N_c^{(1)} \Delta p_c^{(1)} & \Delta p^{(2)} &= \sum_{d=1}^{m^{(2)}} N_d^{(2)} \Delta p_d^{(2)}
\end{aligned}
\tag{6.8.14}
$$

Then,

$$
\begin{aligned}
\delta G_c = \sum_{e=1}^{n_e^{(1)}} \sum_{k=1}^{n_{\text{int}}^{(e)}} W_k J_\eta^{(1)} \Bigg(& \sum_{a=1}^{m^{(1)}} \left[\begin{array}{cc} \delta \mathbf{v}_a^{(1)} & \delta p_a^{(1)} \end{array} \right] \cdot \left[\begin{array}{c} \mathbf{f}_a^{(1)} \\ w_a^{(1)} \end{array} \right] \\
& + \sum_{b=1}^{m_k^{(2)}} \left[\begin{array}{cc} \delta \mathbf{v}_{b,k}^{(1)} & \delta p_{b,k}^{(1)} \end{array} \right] \cdot \left[\begin{array}{c} \mathbf{f}_{b,k}^{(1)} \\ w_{b,k}^{(1)} \end{array} \right] \Bigg) ,
\end{aligned}
\tag{6.8.15}
$$

where

$$
\begin{aligned}
\mathbf{f}_a^{(1)} &= N_a^{(1)} \mathbf{t} & \mathbf{f}_{b,k}^{(2)} &= -N_b^{(2)} \mathbf{t} \\
w_a^{(1)} &= N_a^{(1)} w_n & w_{b,k}^{(2)} &= -N_b^{(2)} w_n
\end{aligned}
\tag{6.8.16}
$$

Similarly,

$$
\begin{aligned}
-D\delta G_c = {} & \sum_{e=1}^{n_e^{(1)}} \sum_{k=1}^{n_{\text{int}}^{(e)}} W_k J_\eta^{(1)} \\
& \times \left(\sum_{a=1}^{m^{(1)}} \left[\begin{array}{cc} \delta\mathbf{v}_a^{(1)} & \delta p_a^{(1)} \end{array}\right] \cdot \left(\sum_{c=1}^{m^{(1)}} \left[\begin{array}{cc} \mathbf{K}_{ac}^{(1,1)} & \mathbf{0} \\ \mathbf{k}_{ac}^{(1,1)} & k_{ac}^{(1,1)} \end{array}\right] \cdot \left[\begin{array}{c} \Delta\mathbf{u}_c^{(1)} \\ \Delta p_c^{(1)} \end{array}\right] \right. \\
& \left. + \sum_{d=1}^{m_k^{(2)}} \left[\begin{array}{cc} \mathbf{K}_{ad,k}^{(1,2)} & \mathbf{0} \\ \mathbf{0} & k_{ad,k}^{(1,2)} \end{array}\right] \cdot \left[\begin{array}{c} \Delta\mathbf{u}_d^{(2)} \\ \Delta p_d^{(2)} \end{array}\right] \right) \\
& + \sum_{b=1}^{m_k^{(2)}} \left[\begin{array}{cc} \delta\mathbf{v}_{b,k}^{(2)} & \delta p_{b,k}^{(2)} \end{array}\right] \cdot \left(\sum_{c=1}^{m^{(1)}} \left[\begin{array}{cc} \mathbf{K}_{bc,k}^{(2,1)} & \mathbf{0} \\ \mathbf{k}_{bc,k}^{(2,1)} & k_{bc,k}^{(2,1)} \end{array}\right] \cdot \left[\begin{array}{c} \Delta\mathbf{u}_c^{(1)} \\ \Delta p_c^{(1)} \end{array}\right] \right. \\
& \left.\left. + \sum_{d=1}^{m_k^{(2)}} \left[\begin{array}{cc} \mathbf{K}_{bd,k}^{(2,2)} & \mathbf{0} \\ \mathbf{0} & k_{bd,k}^{(2,2)} \end{array}\right] \cdot \left[\begin{array}{c} \Delta\mathbf{u}_d^{(2)} \\ \Delta p_d^{(2)} \end{array}\right] \right) \right),
\end{aligned}
\tag{6.8.17}
$$

where

$$
\begin{aligned}
\mathbf{K}_{ac}^{(1,1)} &= N_a^{(1)} \left(\varepsilon_n N_c^{(1)} \mathbf{I} + \mathbf{t} \otimes \mathbf{a}_c^{(1)} \right) \\
\mathbf{K}_{ad,k}^{(1,2)} &= -\varepsilon_n N_a^{(1)} N_d^{(2)} \mathbf{I} \\
\mathbf{K}_{bc,k}^{(2,1)} &= -N_b^{(2)} \left(\varepsilon_n N_c^{(1)} \mathbf{I} + \mathbf{t} \otimes \mathbf{a}_c^{(1)} \right) \\
\mathbf{K}_{bd,k}^{(2,2)} &= \varepsilon_n N_b^{(2)} N_d^{(2)} \mathbf{I}
\end{aligned}
\tag{6.8.18}
$$

$$
\begin{aligned}
\mathbf{k}_{ac}^{(1,1)} &= N_a^{(1)} w_n \mathbf{a}_c^{(1)} \\
\mathbf{k}_{bc,k}^{(2,1)} &= -N_b^{(2)} w_n \mathbf{a}_c^{(1)}
\end{aligned}
\tag{6.8.19}
$$

$$
\begin{aligned}
k_{ac}^{(1,1)} &= -\varepsilon_p N_a^{(1)} N_c^{(1)} \\
k_{ad,k}^{(1,2)} &= \varepsilon_p N_a^{(1)} N_d^{(2)} \\
k_{bc,k}^{(2,1)} &= \varepsilon_p N_b^{(2)} N_c^{(1)} \\
k_{bd,k}^{(2,2)} &= -\varepsilon_p N_b^{(2)} N_d^{(2)}
\end{aligned}
\tag{6.8.20}
$$

and

$$
\mathbf{a}_c^{(1)} = \frac{1}{J_\eta^{(1)}} \mathbf{n}^{(1)} \times \left(\mathbf{g}_2^{(1)} \frac{\partial N_c^{(1)}}{\partial \eta_{(1)}^1} - \mathbf{g}_1^{(1)} \frac{\partial N_c^{(1)}}{\partial \eta_{(1)}^2} \right).
\tag{6.8.21}
$$

6.9   Tied Multiphasic Contact

See Section 2.7 for a review of multiphasic materials, and [13] for additional details on contact interfaces involving solutes. The contact interface is defined between surfaces $\gamma^{(1)}$ and $\gamma^{(2)}$. Due to continuity requirements on the traction and fluxes, the external virtual work resulting from contact

tractions $\mathbf{t}^{(i)}$, solvent fluxes $w_n^{(i)}$ and solute fluxes $j_n^{\alpha(i)}$ $(i = 1, 2)$ may be combined into the contact integral

$$
\begin{aligned}
\delta G_c = & \int_{\gamma^{(1)}} \left(\delta\mathbf{v}^{(1)} - \delta\mathbf{v}^{(2)} \right) \cdot \mathbf{t}^{(1)} \, da^{(1)} \\
& + \int_{\gamma^{(1)}} \left(\delta\tilde{p}^{(1)} - \delta\tilde{p}^{(2)} \right) w_n^{(1)} \, da^{(1)} \\
& + \sum_\alpha \int_{\gamma^{(1)}} \left(\delta\tilde{c}^{\alpha(1)} - \delta\tilde{c}^{\alpha(2)} \right) j_n^{\alpha(1)} \, da^{(1)} .
\end{aligned}
\tag{6.9.1}
$$

Note that the summation in (6.9.1) is performed only over solutes that are present on both sides of the contact interface. No special treatment is needed for solutes that only belong to one side, since the natural boundary condition for these solutes enforces zero normal flux across the contact interface.

To evaluate and linearize δG_c, define the covariant basis vectors on each surface as

$$
\mathbf{g}_\alpha^{(i)} = \frac{\partial \mathbf{x}^{(i)}}{\partial \eta_{(i)}^\alpha}, \quad \alpha = 1, 2,
\tag{6.9.2}
$$

where $\mathbf{x}^{(i)}$ represents the spatial position of points on $\gamma^{(i)}$, and $\eta_{(i)}^\alpha$ represent the parametric coordinates of that point. The unit outward normal on each surface is then given by

$$
\mathbf{n}^{(i)} = \frac{\mathbf{g}_1^{(i)} \times \mathbf{g}_2^{(i)}}{\left| \mathbf{g}_1^{(i)} \times \mathbf{g}_2^{(i)} \right|} .
\tag{6.9.3}
$$

Now the contact integral may be rewritten as

$$
\begin{aligned}
\delta G_c = & \int_{\gamma^{(1)}} \left(\delta\mathbf{v}^{(1)} - \delta\mathbf{v}^{(2)} \right) \cdot \mathbf{t} \left| \mathbf{g}_1^{(1)} \times \mathbf{g}_2^{(1)} \right| d\eta_{(1)}^1 d\eta_{(1)}^2 \\
& + \int_{\gamma^{(1)}} \left(\delta\tilde{p}^{(1)} - \delta\tilde{p}^{(2)} \right) w_n \left| \mathbf{g}_1^{(1)} \times \mathbf{g}_2^{(1)} \right| d\eta_{(1)}^1 d\eta_{(1)}^2 \\
& + \sum_\alpha \int_{\gamma^{(1)}} \left(\delta\tilde{c}^{\alpha(1)} - \delta\tilde{c}^{\alpha(2)} \right) j_n^\alpha \left| \mathbf{g}_1^{(1)} \times \mathbf{g}_2^{(1)} \right| d\eta_{(1)}^1 d\eta_{(1)}^2
\end{aligned} \quad ,
\tag{6.9.4}
$$

where $\mathbf{t} \equiv \mathbf{t}^{(1)}$, $w_n \equiv w_n^{(1)}$ and $j_n^\alpha \equiv j_n^{\alpha(1)}$. The linearization $D\delta G_c$ of δG_c has the form

$$
D\delta G_c = \sum_{i=1}^2 D\delta G_c \left[\Delta\mathbf{u}^{(i)} \right] + D\delta G_c \left[\Delta\tilde{p}^{(i)} \right] + \sum_\alpha D\delta G_c \left[\Delta\tilde{c}^{\alpha(i)} \right] .
\tag{6.9.5}
$$

6.9.1 Gap Function

The vector gap function $\mathbf{g}$, representing the distance between the contact surfaces, is defined by

$$
\mathbf{g} = \mathbf{x}^{(2)} - \mathbf{x}^{(1)} .
\tag{6.9.6}
$$

The premise of a tied interface is that the parametric coordinates of $\mathbf{x}^{(1)}$ and $\mathbf{x}^{(2)}$ are both invariants (i.e., they are determined in the reference configuration and remain unchanged over time). The parametric coordinates of $\mathbf{x}^{(1)}$ correspond to the integration points on $\gamma^{(1)}$, and those of $\mathbf{x}^{(2)}$ are

evaluated once, in the reference configuration, by shooting a ray from the integration point on $\gamma^{(1)}$ to intersect $\gamma^{(2)}$. It follows from this premise that

$$
\begin{aligned}
D\mathbf{x}^{(i)} &= \Delta\mathbf{u}^{(i)} & D\delta\mathbf{v}^{(i)} &= \mathbf{0} \\
D\tilde{p}^{(i)} &= \Delta\tilde{p}^{(i)} & D\delta\tilde{p}^{(i)} &= 0 \quad i = 1, 2. \\
D\tilde{c}^{\alpha(i)} &= \Delta\tilde{c}^{\alpha(i)} & D\delta\tilde{c}^{\alpha(i)} &= 0
\end{aligned}
\tag{6.9.7}
$$

If $\gamma^{(1)}$ and $\gamma^{(2)}$ are not initially conforming, continuity of effective fluid pressure and solute concentration, as well as normal fluid and solute fluxes, will only be enforced within the contact interface; unlike the sliding multiphasic contact interface (Section 6.6), ambient conditions are not set automatically on regions of $\gamma^{(1)}$ and $\gamma^{(2)}$ where a solution for g was not found. Therefore, these regions naturally enforce zero fluid and solute flux (impermeable boundary), unless an explicit boundary condition on the effective pressure $\tilde{p}$ or solute concentrations $\tilde{c}^\alpha$ are prescribed over those regions.

6.9.2   Penalty Method

Let the tied contact traction be described by the penalty function,

$$
\mathbf{t} = \varepsilon_n \mathbf{g}, \tag{6.9.8}
$$

where ε_n is a penalty factor associated with $\mathbf{t}$. Similarly, let

$$
w_n = \varepsilon_p \pi = \varepsilon_p \left(\tilde{p}^{(1)} - \tilde{p}^{(2)} \right), \tag{6.9.9}
$$

where ε_p is a penalty factor associated with w_n, and

$$
j_n^\alpha = \varepsilon_c \chi^\alpha = \varepsilon_c^\alpha \left(\tilde{c}^{\alpha(1)} - \tilde{c}^{\alpha(2)} \right), \tag{6.9.10}
$$

where ε_c^α is a penalty factor associated with j_n^α. It follows that

$$
\begin{aligned}
D\mathbf{t} &= \varepsilon_n \left(\Delta\mathbf{u}^{(2)} - \Delta\mathbf{u}^{(1)} \right), \\
Dw_n &= \varepsilon_p \left(\Delta\tilde{p}^{(1)} - \Delta\tilde{p}^{(2)} \right), \\
Dj_n^\alpha &= \varepsilon_c^\alpha \left(\Delta\tilde{c}^{\alpha(1)} - \Delta\tilde{c}^{\alpha(2)} \right).
\end{aligned}
\tag{6.9.11}
$$

Given these relations, it can be shown that the directional derivatives of the various terms appearing in the integrand of δG_c are

$$
\begin{aligned}
&- D \left(J_\eta^{(1)} \left(\delta\mathbf{v}^{(1)} - \delta\mathbf{v}^{(2)} \right) \cdot \mathbf{t} \right) = \\
&\left(\delta\mathbf{v}^{(1)} - \delta\mathbf{v}^{(2)} \right) \cdot \varepsilon_n J_\eta^{(1)} \mathbf{I} \cdot \left(\Delta\mathbf{u}^{(1)} - \Delta\mathbf{u}^{(2)} \right) \\
&+ \left(\delta\mathbf{v}^{(1)} - \delta\mathbf{v}^{(2)} \right) \cdot \mathbf{t} \otimes \left[\left(\mathbf{g}_1^{(1)} \times \mathbf{n}^{(1)} \right) \cdot \frac{\partial\Delta\mathbf{u}^{(1)}}{\partial\eta_{(1)}^2} - \left(\mathbf{g}_2^{(1)} \times \mathbf{n}^{(1)} \right) \cdot \frac{\partial\Delta\mathbf{u}^{(1)}}{\partial\eta_{(1)}^1} \right]
\end{aligned}
\tag{6.9.12}
$$

$$
\begin{aligned}
&- D \left(w_n \left(\delta p^{(1)} - \delta p^{(2)} \right) J_\eta^{(1)} \right) = \\
&- J_\eta^{(1)} \varepsilon_p \left(\delta p^{(1)} - \delta p^{(2)} \right) \left(\Delta\tilde{p}^{(1)} - \Delta\tilde{p}^{(2)} \right) \\
&+ w_n \left(\delta p^{(1)} - \delta p^{(2)} \right) \mathbf{n}^{(1)} \cdot \left(\mathbf{g}_2^{(1)} \times \frac{\partial\Delta\mathbf{u}^{(1)}}{\partial\eta_{(1)}^1} - \mathbf{g}_1^{(1)} \times \frac{\partial\Delta\mathbf{u}^{(1)}}{\partial\eta_{(1)}^2} \right)
\end{aligned}
\tag{6.9.13}
$$

$$- D \left(j_n^\alpha \left(\delta \tilde{c}^{\alpha(1)} - \delta \tilde{c}^{\alpha(2)} \right) J_\eta^{(1)} \right) =$$

$$- J_\eta^{(1)} \left(\delta \tilde{c}^{\alpha(1)} - \delta \tilde{c}^{\alpha(2)} \right) \varepsilon_c^\alpha \left(\Delta \tilde{c}^{\alpha(1)} - \Delta \tilde{c}^{\alpha(2)} \right)$$

$$+ j_n^\alpha \left(\delta \tilde{c}^{\alpha(1)} - \delta \tilde{c}^{\alpha(2)} \right) \mathbf{n}^{(1)} \cdot \left(\mathbf{g}_2^{(1)} \times \frac{\partial \Delta \mathbf{u}^{(1)}}{\partial \eta_{(1)}^1} - \mathbf{g}_1^{(1)} \times \frac{\partial \Delta \mathbf{u}^{(1)}}{\partial \eta_{(1)}^2} \right)$$

$$\qquad (6.9.14)$$

where $J_\eta^{(1)} = \left| \mathbf{g}_1^{(1)} \times \mathbf{g}_2^{(1)} \right|$.

6.9.3 Discretization

The contact integral may be discretized as

$$\delta G_c = \sum_{e=1}^{n_e^{(1)}} \sum_{k=1}^{n_{\text{int}}^{(e)}} W_k J_\eta^{(1)} \left[\left(\delta \mathbf{v}^{(1)} - \delta \mathbf{v}^{(2)} \right) \cdot \mathbf{t} + w_n \left(\delta p^{(1)} - \delta p^{(2)} \right) + \sum_\alpha j_n^\alpha \left(\delta \tilde{c}^{\alpha(1)} - \delta \tilde{c}^{\alpha(2)} \right) \right].$$

$$\qquad (6.9.15)$$

The variables may be interpolated over each element face according to

$$\delta \mathbf{v}^{(1)} = \sum_{a=1}^{m^{(1)}} N_a^{(1)} \delta \mathbf{v}_a^{(1)} \qquad \delta \mathbf{v}^{(2)} = \sum_{b=1}^{m^{(2)}} N_b^{(2)} \delta \mathbf{v}_b^{(2)}$$

$$\Delta \mathbf{u}^{(1)} = \sum_{c=1}^{m^{(1)}} N_c^{(1)} \Delta \mathbf{u}_c^{(1)} \qquad \Delta \mathbf{u}^{(2)} = \sum_{d=1}^{m^{(2)}} N_d^{(2)} \Delta \mathbf{u}_d^{(2)}$$

$$\delta \tilde{p}^{(1)} = \sum_{a=1}^{m^{(1)}} N_a^{(1)} \delta \tilde{p}_a^{(1)} \qquad \delta p^{(2)} = \sum_{b=1}^{m^{(2)}} N_b^{(2)} \delta \tilde{p}_b^{(2)}$$

$$\Delta \tilde{p}^{(1)} = \sum_{c=1}^{m^{(1)}} N_c^{(1)} \Delta \tilde{p}_c^{(1)} \qquad \Delta \tilde{p}^{(2)} = \sum_{d=1}^{m^{(2)}} N_d^{(2)} \Delta \tilde{p}_d^{(2)}$$

$$\delta \tilde{c}^{\alpha(1)} = \sum_{a=1}^{m^{(1)}} N_a^{(1)} \delta \tilde{c}_a^{\alpha(1)} \qquad \delta c^{\alpha(2)} = \sum_{b=1}^{m^{(2)}} N_b^{(2)} \delta \tilde{c}_b^{\alpha(2)}$$

$$\Delta \tilde{c}^{\alpha(1)} = \sum_{c=1}^{m^{(1)}} N_c^{(1)} \Delta \tilde{c}_c^{\alpha(1)} \qquad \Delta \tilde{c}^{\alpha(2)} = \sum_{d=1}^{m^{(2)}} N_d^{(2)} \Delta \tilde{c}_d^{\alpha(2)}$$

$$\qquad (6.9.16)$$

Then,

$$\delta G_c = \sum_{e=1}^{n_e^{(1)}} \sum_{k=1}^{n_{\text{int}}^{(e)}} W_k J_\eta^{(1)} \left(\sum_{a=1}^{m^{(1)}} \left[\delta \mathbf{v}_a^{(1)} \quad \delta \tilde{p}_a^{(1)} \quad \delta \tilde{c}^{\alpha(1)} \quad \delta \tilde{c}^{\beta(1)} \right] \cdot \begin{bmatrix} \mathbf{f}_a^{(1)} \\ w_a^{(1)} \\ j_n^{\alpha(1)} \\ j_n^{\beta(1)} \end{bmatrix} \right.$$

$$\left. + \sum_{b=1}^{m_k^{(2)}} \left[\delta \mathbf{v}_{b,k}^{(1)} \quad \delta \tilde{p}_{b,k}^{(1)} \quad \delta \tilde{c}_{b,k}^{\alpha(1)} \quad \delta \tilde{c}_{b,k}^{\beta(1)} \right] \cdot \begin{bmatrix} \mathbf{f}_{b,k}^{(1)} \\ w_{b,k}^{(1)} \\ j_{b,k}^{\alpha(1)} \\ j_{b,k}^{\beta(1)} \end{bmatrix} \right),$$

$$\qquad (6.9.17)$$

where

$$\mathbf{f}_a^{(1)} = N_a^{(1)}\mathbf{t} \qquad \mathbf{f}_{b,k}^{(2)} = -N_b^{(2)}\mathbf{t}$$
$$w_a^{(1)} = N_a^{(1)}w_n \quad w_{b,k}^{(2)} = -N_b^{(2)}w_n \, . \tag{6.9.18}$$
$$j_a^{\gamma(1)} = N_a^{(1)}j_n^{\gamma} \quad j_{b,k}^{\gamma(2)} = -N_b^{(2)}j_n^{\gamma}$$

Similarly,

$$
-D\delta G_c = \sum_{e=1}^{n_e^{(1)}} \sum_{k=1}^{n_{\text{int}}^{(e)}} W_k J_\eta^{(1)}
$$

$$
\times \left(\sum_{a=1}^{m^{(1)}} \begin{bmatrix} \delta\mathbf{v}_a^{(1)} & \delta\tilde{p}_a^{(1)} & \delta\tilde{c}_a^{\alpha(1)} & \delta\tilde{c}_a^{\beta(1)} \end{bmatrix} \cdot \left(\sum_{c=1}^{m^{(1)}} \begin{bmatrix} \mathbf{K}_{ac}^{(1,1)} & \mathbf{0} & \mathbf{0} & \mathbf{0} \\ \mathbf{k}_{ac}^{(1,1)} & k_{ac}^{(1,1)} & 0 & 0 \\ \mathbf{k}_{ac}^{\alpha(1,1)} & 0 & k_{ac}^{\alpha\alpha(1,1)} & 0 \\ \mathbf{k}_{ac}^{\beta(1,1)} & 0 & 0 & k_{ac}^{\beta\beta(1,1)} \end{bmatrix} \cdot \begin{bmatrix} \Delta\mathbf{u}_c^{(1)} \\ \Delta\tilde{p}_c^{(1)} \\ \Delta\tilde{c}_c^{\alpha(1)} \\ \Delta\tilde{c}_c^{\beta(1)} \end{bmatrix} \right.
$$

$$
+ \sum_{d=1}^{m_k^{(2)}} \begin{bmatrix} \mathbf{K}_{ad,k}^{(1,2)} & \mathbf{0} & \mathbf{0} & \mathbf{0} \\ \mathbf{0} & k_{ad,k}^{(1,2)} & 0 & 0 \\ \mathbf{0} & 0 & k_{ad,k}^{\alpha\alpha(1,2)} & 0 \\ \mathbf{0} & 0 & 0 & k_{ad,k}^{\beta\beta(1,2)} \end{bmatrix} \cdot \begin{bmatrix} \Delta\mathbf{u}_d^{(2)} \\ \Delta\tilde{p}_d^{(2)} \\ \Delta\tilde{c}_d^{\alpha(2)} \\ \Delta\tilde{c}_d^{\beta(2)} \end{bmatrix} \right)
$$

$$
+ \sum_{b=1}^{m_k^{(2)}} \begin{bmatrix} \delta\mathbf{v}_{b,k}^{(2)} & \delta\tilde{p}_{b,k}^{(2)} & \delta\tilde{c}_{b,k}^{\alpha(2)} & \delta\tilde{c}_{b,k}^{\beta(2)} \end{bmatrix} \cdot \left(\sum_{c=1}^{m^{(1)}} \begin{bmatrix} \mathbf{K}_{bc,k}^{(2,1)} & \mathbf{0} & \mathbf{0} & \mathbf{0} \\ \mathbf{k}_{bc,k}^{(2,1)} & k_{bc,k}^{(2,1)} & 0 & 0 \\ \mathbf{k}_{bc,k}^{\alpha(2,1)} & 0 & k_{bc,k}^{\alpha\alpha(2,1)} & 0 \\ \mathbf{k}_{bc,k}^{\beta(2,1)} & 0 & 0 & k_{bc,k}^{\beta\beta(2,1)} \end{bmatrix} \cdot \begin{bmatrix} \Delta\mathbf{u}_c^{(1)} \\ \Delta\tilde{p}_c^{(1)} \\ \Delta\tilde{c}_c^{\alpha(1)} \end{bmatrix} \right.
$$

$$
+ \sum_{d=1}^{m_k^{(2)}} \begin{bmatrix} \mathbf{K}_{bd,k}^{(2,2)} & \mathbf{0} & \mathbf{0} & \mathbf{0} \\ \mathbf{0} & k_{bd,k}^{(2,2)} & 0 & 0 \\ \mathbf{0} & 0 & k_{bd,k}^{\alpha\alpha(2,2)} & 0 \\ \mathbf{0} & 0 & 0 & k_{bd,k}^{\beta\beta(2,2)} \end{bmatrix} \cdot \begin{bmatrix} \Delta\mathbf{u}_d^{(2)} \\ \Delta\tilde{p}_d^{(2)} \\ \Delta\tilde{c}_d^{\alpha(2)} \\ \Delta\tilde{c}_d^{\beta(2)} \end{bmatrix} \right) \right) ,
$$

$$\tag{6.9.19}$$

where

$$\mathbf{K}_{ac}^{(1,1)} = N_a^{(1)} \left(\varepsilon_n N_c^{(1)}\mathbf{I} + \mathbf{t} \otimes \mathbf{a}_c^{(1)} \right)$$
$$\mathbf{K}_{ad,k}^{(1,2)} = -\varepsilon_n N_a^{(1)} N_d^{(2)}\mathbf{I}$$
$$\mathbf{K}_{bc,k}^{(2,1)} = -N_b^{(2)} \left(\varepsilon_n N_c^{(1)}\mathbf{I} + \mathbf{t} \otimes \mathbf{a}_c^{(1)} \right) \tag{6.9.20}$$
$$\mathbf{K}_{bd,k}^{(2,2)} = \varepsilon_n N_b^{(2)} N_d^{(2)}\mathbf{I}$$

$$\mathbf{k}_{ac}^{(1,1)} = N_a^{(1)} w_n \mathbf{a}_c^{(1)}$$
$$\mathbf{k}_{bc,k}^{(2,1)} = -N_b^{(2)} w_n \mathbf{a}_c^{(1)}$$
$$\mathbf{k}_{ac}^{\alpha(1,1)} = N_a^{(1)} j_n^{\alpha} \mathbf{a}_c^{(1)} \tag{6.9.21}$$
$$\mathbf{k}_{bc,k}^{\alpha(2,1)} = -N_b^{(2)} j_n^{\alpha} \mathbf{a}_c^{(1)}$$

$$k_{ac}^{(1,1)} = -\varepsilon_p N_a^{(1)} N_c^{(1)}$$
$$k_{ad,k}^{(1,2)} = \varepsilon_p N_a^{(1)} N_d^{(2)}$$
$$k_{bc,k}^{(2,1)} = \varepsilon_p N_b^{(2)} N_c^{(1)} \qquad ,$$
$$k_{bd,k}^{(2,2)} = -\varepsilon_p N_b^{(2)} N_d^{(2)}$$

$$(6.9.22)$$

$$k_{ac}^{\gamma\gamma(1,1)} = -\varepsilon_c^\gamma N_a^{(1)} N_c^{(1)}$$
$$k_{ad,k}^{\gamma\gamma(1,2)} = \varepsilon_c^\gamma N_a^{(1)} N_d^{(2)}$$
$$k_{bc,k}^{\gamma\gamma(2,1)} = \varepsilon_c^\gamma N_b^{(2)} N_c^{(1)}$$
$$k_{bd,k}^{\gamma\gamma(2,2)} = -\varepsilon_c^\gamma N_b^{(2)} N_d^{(2)}$$

$$(6.9.23)$$

and

$$\mathbf{a}_c^{(1)} = \frac{1}{J_\eta^{(1)}} \mathbf{n}^{(1)} \times \left(\mathbf{g}_2^{(1)} \frac{\partial N_c^{(1)}}{\partial \eta_{(1)}^1} - \mathbf{g}_1^{(1)} \frac{\partial N_c^{(1)}}{\partial \eta_{(1)}^2} \right) . \qquad (6.9.24)$$

Chapter 7

Dynamics

FEBio can perform a nonlinear dynamic analysis by iteratively solving the following nonlinear semi-discrete finite element equations [15].

$$\mathbf{M}\ddot{\mathbf{d}}_{n+1}^k + \mathbf{K}\Delta\mathbf{d}^k = \mathbf{T}_{n+1}^k - \mathbf{F}_{n+1}$$
$$\mathbf{d}_{n+1}^k = \mathbf{d}_{n+1}^{k-1} + \Delta\mathbf{d}^k \tag{7.0.1}$$

Here, $\mathbf{M}$ is the mass matrix, $\mathbf{K}$ the stiffness matrix, $\mathbf{T}$ the internal force (stress) vector and $\mathbf{F}$ the externally applied loads. The upperscript index k refers to the iteration number, the subscript n refers to the time increment. The trapezoidal (or midpoint) rule is used to perform the time integration. This results in the following approximations for the displacement and velocity updates.

$$\mathbf{d}_{n+1} = \mathbf{d}_n + \frac{h}{2}\left(\dot{\mathbf{d}}_n + \dot{\mathbf{d}}_{n+1}\right)$$
$$\dot{\mathbf{d}}_{n+1} = \dot{\mathbf{d}}_n + \frac{h}{2}\left(\ddot{\mathbf{d}}_n + \ddot{\mathbf{d}}_{n+1}\right) \tag{7.0.2}$$

Using (7.0.2) we can solve for $\ddot{\mathbf{d}}_{n+1}$,

$$\ddot{\mathbf{d}}_{n+1}^k = \frac{4}{h^2}\left(\mathbf{d}_{n+1}^{k-1} - \mathbf{d}_n + \Delta\mathbf{d}^k\right) - \frac{4}{h}\dot{\mathbf{d}}_n - \ddot{\mathbf{d}}_n. \tag{7.0.3}$$

Substituting this into equation (7.0.1) results in the following linear system of equations.

$$\left(\frac{4}{h^2}\mathbf{M} + \mathbf{K}\right)\Delta\mathbf{d}^k = \mathbf{T}_{n+1}^k - \mathbf{F}_{n+1} - \mathbf{M}\left(\frac{4}{h^2}\left(\mathbf{d}_{n+1}^{k-1} - \mathbf{d}_n\right) - \frac{4}{h}\dot{\mathbf{d}}_n - \ddot{\mathbf{d}}_n\right). \tag{7.0.4}$$

Solving this equation for $\Delta\mathbf{d}^k$ and using (7.0.1) gives the new displacement vector $\mathbf{d}_{n+1}^k$. The acceleration vector $\ddot{\mathbf{d}}_{n+1}^k$ can then be found from (7.0.3) and the velocity vector $\dot{\mathbf{d}}_{n+1}^k$ from (7.0.3). This algorithm is repeated until convergence is reached.

7.1 Elastodynamics

7.1.1 Governing Equations

The linear momentum balance for elastodynamics is

$$\rho\mathbf{a} = \operatorname{div}\boldsymbol{\sigma} + \rho\mathbf{b}, \tag{7.1.1}$$

where ρ is the density, $\mathbf{a}$ is the acceleration, $\boldsymbol{\sigma}$ is the Cauchy stress, and $\mathbf{b}$ is the body force per mass. The angular momentum balance is satisfied by letting $\boldsymbol{\sigma}^T = \boldsymbol{\sigma}$. The integrated form of the mass balance equations yields

$$\rho = \frac{\rho_r}{J}, \tag{7.1.2}$$

where ρ_r is the density in the reference configuration and $J = \det \mathbf{F}$, where $\mathbf{F}$ is the deformation gradient. The acceleration is given by the material time derivative of the velocity $\mathbf{v}$, evaluated either in a spatial or a material frame,

$$\mathbf{a} = \dot{\mathbf{v}} \tag{7.1.3}$$

7.1.2 Virtual Work

The virtual work for the domain b is given by

$$\delta W = \int_b \delta \mathbf{v} \cdot (\operatorname{div} \boldsymbol{\sigma} + \rho\,(\mathbf{b} - \mathbf{a}))\; dv\,, \tag{7.1.4}$$

where $\delta \mathbf{v}$ is the virtual velocity. Using the divergence theorem, this virtual work may be expressed as the difference $\delta W = \delta W_{ext} - \delta W_{int}$ between external virtual work δW_{ext} and internal virtual work δW_{int}, where

$$\delta W_{int} = \int_b \boldsymbol{\sigma} : \operatorname{grad} \delta \mathbf{v}\, dv + \int_b \delta \mathbf{v} \cdot \rho \mathbf{a}\, dv\,,$$
$$\delta W_{ext} = \int_{\partial b} \delta \mathbf{v} \cdot \mathbf{t}\, da + \int_b \delta \mathbf{v} \cdot \rho \mathbf{b}\, dv\,, \tag{7.1.5}$$

where $\mathbf{t} = \boldsymbol{\sigma} \cdot \mathbf{n}$ is the traction on the boundary ∂b.

7.1.3 Time Integration

In the generalized $\alpha-$method, we evaluate displacements and velocities at the intermediate time $t_{n+\alpha_f} = t_n + \alpha_f\,(t_{n+1} - t_n)$, where α_f is a user-defined parameter ($0 < \alpha_f \le 1$), such that

$$\begin{aligned} \boldsymbol{\chi}_{n+\alpha_f} &= (1 - \alpha_f)\,\boldsymbol{\chi}_n + \alpha_f \boldsymbol{\chi}_{n+1}\,, \\ \mathbf{u}_{n+\alpha_f} &= (1 - \alpha_f)\,\mathbf{u}_n + \alpha_f \mathbf{u}_{n+1}\,, \\ \mathbf{v}_{n+\alpha_f} &= (1 - \alpha_f)\,\mathbf{v}_n + \alpha_f \mathbf{v}_{n+1}\,, \end{aligned} \tag{7.1.6}$$

where $\boldsymbol{\chi}$ is the motion and $\mathbf{u}$ is the displacement. In particular, it follows that the deformation gradient and its determinant are given at the intermediate time by

$$\mathbf{F}_{n+\alpha_f} = \frac{\partial \boldsymbol{\chi}_{n+\alpha_f}}{\partial \mathbf{X}} = (1 - \alpha_f)\,\mathbf{F}_n + \alpha_f \mathbf{F}_{n+1}\,, \tag{7.1.7}$$

and

$$J_{n+\alpha_f} = \det \mathbf{F}_{n+\alpha_f}\,. \tag{7.1.8}$$

The material time derivative of $J_{n+\alpha_f}$, and the velocity gradient $\mathbf{L}_{n+\alpha_f}$ are normally evaluated as

$$\dot{J}_{n+\alpha_f} = J_{n+\alpha_f} \mathbf{F}_{n+\alpha_f}^{-T} : \operatorname{Grad} \mathbf{v}_{n+\alpha_f}\,, \tag{7.1.9}$$

and

$$\mathbf{L}_{n+\alpha_f} = \operatorname{Grad} \mathbf{v}_{n+\alpha_f} \cdot \mathbf{F}_{n+\alpha_f}^{-1}\,. \tag{7.1.10}$$

In practice however, we get better numerical results when using

$$\dot{J}_{n+\alpha_f} = \frac{J_{n+1} - J_n}{\Delta t},$$ (7.1.11)

and

$$\mathbf{L}_{n+\alpha_f} = \frac{\mathbf{F}_{n+1} - \mathbf{F}_n}{\Delta t} \cdot \mathbf{F}_{n+\alpha_f}^{-1}.$$ (7.1.12)

According to the generalized$-\alpha$ method, we evaluate the velocity derivative at a different intermediate time $t_{n+\alpha_m} = t_n + \alpha_m (t_{n+1} - t_n)$, such that

$$\dot{\mathbf{v}}_{n+\alpha_m} = (1 - \alpha_m) \dot{\mathbf{v}}_n + \alpha_m \dot{\mathbf{v}}_{n+1}.$$ (7.1.13)

Since elastodynamics represent a second-order system of equations in time, the parameters α_f and α_m are evaluated from a single parameter ρ_∞ using [17]

$$\alpha_f = \frac{1}{1 + \rho_\infty}, \quad \alpha_m = \frac{2 - \rho_\infty}{1 + \rho_\infty},$$ (7.1.14)

where $0 \le \rho_\infty \le 1$. This parameter is the spectral radius for an infinite time step, which controls the amount of damping of high frequencies; a value of zero produces the greatest amount of damping, anihilating the highest frequency in one step, whereas a value of one preserves the highest frequency.

To complete the integration scheme [36], we evaluate

$$\begin{aligned} \beta &= \frac{1}{4} (1 + \alpha_m - \alpha_f)^2 \\ \gamma &= \frac{1}{2} + \alpha_m - \alpha_f \end{aligned},$$ (7.1.15)

then we use

$$\begin{aligned} \mathbf{v}_{n+1} &= \mathbf{v}_n + \Delta t \left[(1 - \gamma) \dot{\mathbf{v}}_n + \gamma \dot{\mathbf{v}}_{n+1} \right] \\ \mathbf{u}_{n+1} &= \mathbf{u}_n + \Delta t \mathbf{v}_n + \frac{\Delta t^2}{2} \left[(1 - 2\beta) \dot{\mathbf{v}}_n + 2\beta \dot{\mathbf{v}}_{n+1} \right] \\ \dot{\mathbf{v}}_{n+1} &= \frac{1}{\beta \Delta t} \left(\frac{\mathbf{u}_{n+1} - \mathbf{u}_n}{\Delta t} - \mathbf{v}_n \right) + \left(1 - \frac{1}{2\beta} \right) \dot{\mathbf{v}}_n \end{aligned}.$$ (7.1.16)

At the start of each time step, we initialize the variables as follows:

$$\begin{aligned} \mathbf{u}_{n+1} &= \mathbf{u}_n \\ \dot{\mathbf{v}}_{n+1} &= \left(1 - \frac{1}{2\beta} \right) \dot{\mathbf{v}}_n - \frac{1}{\beta \Delta t} \mathbf{v}_n \\ \mathbf{v}_{n+1} &= \left(1 - \frac{\gamma}{\beta} \right) \mathbf{v}_n + \Delta t \left(1 - \frac{\gamma}{2\beta} \right) \dot{\mathbf{v}}_n \end{aligned}.$$ (7.1.17)

7.1.4 Linearization

The solution of the nonlinear equation $\delta W = 0$ is obtained by linearizing this relation as

$$\delta W + D\delta W [\Delta \mathbf{u}] \approx 0,$$ (7.1.18)

where the operator $D\delta W [\cdot]$ represents the directional derivative of δW at $\mathbf{u}$ along an increment $\Delta \mathbf{u}$ of $\mathbf{u}_{n+1}$ [19]. According to the generalized$-\alpha$ method [36], the virtual work is evaluated using

intermediate time step values, at $t_{n+\alpha_f}$ for all parameters except $\dot{\mathbf{v}}$, which is evaluated at $t_{n+\alpha_m}$. It follows from these definitions that the linearizations of critical variables are given by

$$
\begin{aligned}
D\mathbf{u}\,[\Delta\mathbf{u}] &= \alpha_f \Delta\mathbf{u} \\
D\mathbf{F}\,[\Delta\mathbf{u}] &= \alpha_f \operatorname{Grad}\Delta\mathbf{u} \\
DJ\,[\Delta\mathbf{u}] &= \alpha_f J\,(\operatorname{div}\Delta\mathbf{u}) \\
D\dot{J}\,[\Delta\mathbf{u}] &= D\left(J\mathbf{F}^{-T}:\operatorname{Grad}\mathbf{v}\right)[\Delta\mathbf{u}] \\
&= \alpha_f J\left[\left(\operatorname{div}\mathbf{v}+\frac{\gamma}{\beta\Delta t}\right)(\operatorname{div}\Delta\mathbf{u})-(\operatorname{grad}\Delta\mathbf{u})^T:\mathbf{L}\right]^{\cdot} \\
D\mathbf{v}\,[\Delta\mathbf{u}] &= \frac{\alpha_f\gamma}{\beta\Delta t}\Delta\mathbf{u} \\
D\dot{\mathbf{v}}\,[\Delta\mathbf{u}] &= \frac{\alpha_m}{\beta\Delta t^2}\Delta\mathbf{u}
\end{aligned}
\tag{7.1.19}
$$

To linearize the virtual work, we need to express the integrals appearing in δW_{int} and δW_{ext} over the material frame of the finite element solid domain.

7.1.4.1 Internal Work

The first term in the internal work becomes

$$
\int_b \boldsymbol{\sigma}:\operatorname{grad}\delta\mathbf{v}\,dv = \int_B \mathbf{F}\cdot\mathbf{S}:\operatorname{Grad}\delta\mathbf{v}\,dV \quad,
\tag{7.1.20}
$$

where $\mathbf{S}=J\cdot\mathbf{F}^{-1}\cdot\boldsymbol{\sigma}\cdot\mathbf{F}^{-T}$ is the second Piola-Kirchhoff stress for the solid material. In general, $\boldsymbol{\sigma}$ (and thus, $\mathbf{S}$) is only a function of the solid strain, such as the right Cauchy-Green tensor $\mathbf{C}=\mathbf{F}^T\cdot\mathbf{F}$ or the Green-Lagrange strain $\mathbf{E}=(\mathbf{C}-\mathbf{I})/2$.

$$
D\mathbf{E}\,[\Delta\mathbf{u}] = \frac{\alpha_f}{2}\left(\operatorname{Grad}^T\Delta\mathbf{u}\cdot\mathbf{F}+\mathbf{F}^T\cdot\operatorname{Grad}\Delta\mathbf{u}\right).
\tag{7.1.21}
$$

Therefore, following the standard approach in solid mechanics, the linearization of $\mathbf{S}$ is

$$
\begin{aligned}
D\mathbf{S}\,[\Delta\mathbf{u}] &= \frac{\partial\mathbf{S}}{\partial\mathbf{E}}:D\mathbf{E}\,[\Delta\mathbf{u}] \\
&= \alpha_f\mathbb{C}:\frac{1}{2}\left(\operatorname{Grad}^T\Delta\mathbf{u}\cdot\mathbf{F}+\mathbf{F}^T\cdot\operatorname{Grad}\Delta\mathbf{u}\right), \\
&= \alpha_f\mathbb{C}:\left(\mathbf{F}^T\otimes\mathbf{F}^T\right):\Delta\boldsymbol{\varepsilon}
\end{aligned}
\tag{7.1.22}
$$

where $\mathbb{C}$ is the material elasticity tensor. Now, the linearization of the first term in δW_{int} is

$$
\boxed{
\begin{aligned}
&D\left(\int_B \mathbf{F}\cdot\mathbf{S}:\operatorname{Grad}\delta\mathbf{v}\,dV\right)[\Delta\mathbf{u}] \\
&= \int_v \alpha_f\left(\operatorname{grad}\delta\mathbf{v}:\operatorname{grad}\Delta\mathbf{u}\cdot\boldsymbol{\sigma}+\operatorname{grad}\delta\mathbf{v}:\boldsymbol{\mathcal{C}}:\operatorname{grad}\Delta\mathbf{u}\right)\,dv
\end{aligned}
}
\tag{7.1.23}
$$

where $\boldsymbol{\mathcal{C}}$ is the spatial elasticity tensor. Similarly, the second term in δW_{int} produces

$$
\boxed{
D\left(\int_B \delta\mathbf{v}\cdot\rho_r\mathbf{a}\,dV\right)[\Delta\mathbf{u}] = \int_b \delta\mathbf{v}\cdot\frac{\alpha_m}{\beta\Delta t^2}\rho\Delta\mathbf{u}\,dv
}.
\tag{7.1.24}
$$

7.1.4.2 External Work

The linearization of the body force term is

$$D \left(\int_B \delta \mathbf{v} \cdot \rho_r \mathbf{b} \, dV \right) [\Delta \mathbf{u}] = \int_b \delta \mathbf{v} \cdot \alpha_f \rho \operatorname{grad} \mathbf{b} \cdot \Delta \mathbf{u} \, dv . \quad (7.1.25)$$

The linearization of the traction force term is

$$\begin{aligned} D &\left(\int_{\Gamma_\eta} \delta \mathbf{v} \cdot \mathbf{t} \, |\mathbf{g}_1 \times \mathbf{g}_2| \, d\eta^1 d\eta^2 \right) [\Delta \mathbf{u}] \\ &= \int_{\Gamma_\eta} \alpha_f \delta \mathbf{v} \cdot (\mathbf{t} \otimes \mathbf{n}) \cdot \left(\mathbf{g}_1 \times \frac{\partial \Delta \mathbf{u}}{\partial \eta^2} - \mathbf{g}_2 \times \frac{\partial \Delta \mathbf{u}}{\partial \eta^1} \right) d\eta^1 d\eta^2 . \\ &+ \int_{\Gamma_\eta} \delta \mathbf{v} \cdot D\mathbf{t} \, [\Delta \mathbf{u}] \, |\mathbf{g}_1 \times \mathbf{g}_2| \, d\eta^1 d\eta^2 \end{aligned} \quad (7.1.26)$$

Note that $D\mathbf{t} \, [\Delta \mathbf{u}]$ depends on the nature of the surface traction. For a prescribed traction we have $D\mathbf{t} \, [\Delta \mathbf{u}] = \mathbf{0}$. A contact analysis needs more elaborate derivations (not yet implemented as of FEBio 2.7). In the above expression we used

$$\begin{aligned} D \, |\mathbf{g}_1 \times \mathbf{g}_2| \, [\Delta \mathbf{u}] &= \mathbf{n} \cdot D \, (\mathbf{g}_1 \times \mathbf{g}_2) \, [\Delta \mathbf{u}] \\ &= \alpha_f \mathbf{n} \cdot \left(\mathbf{g}_1 \times \frac{\partial \Delta \mathbf{u}}{\partial \eta^2} - \mathbf{g}_2 \times \frac{\partial \Delta \mathbf{u}}{\partial \eta^1} \right) \end{aligned} \quad (7.1.27)$$

where the unit outward normal is evaluated as

$$\mathbf{n} = \frac{\mathbf{g}_1 \times \mathbf{g}_2}{|\mathbf{g}_1 \times \mathbf{g}_2|} . \quad (7.1.28)$$

7.1.5 Discretization

We use the following interpolations:

$$\begin{aligned} \delta \mathbf{v} &= \sum_a N_a \delta \mathbf{v}_a & \Delta \mathbf{u} &= \sum_b N_b \Delta \mathbf{u}_b \\ \operatorname{grad} \delta \mathbf{v} &= \sum_a \delta \mathbf{v}_a \otimes \operatorname{grad} N_a & \operatorname{grad} \Delta \mathbf{u} &= \sum_b \Delta \mathbf{u}_b \otimes \operatorname{grad} N_b , \\ \operatorname{div} \delta \mathbf{v} &= \sum_a \delta \mathbf{v}_a \cdot \operatorname{grad} N_a & \operatorname{div} \Delta \mathbf{u} &= \sum_b \Delta \mathbf{u}_b \cdot \operatorname{grad} N_b \end{aligned} \quad (7.1.29)$$

where $N_a \left(\eta^1, \eta^2, \eta^3 \right)$ are shape functions of the element parametric coordinates $\left(\eta^1, \eta^2, \eta^3 \right)$. Note that the $\operatorname{grad} \equiv \frac{\partial}{\partial \mathbf{x}}$ operator should be evaluated at $t_{n+\alpha_f}$, using $\mathbf{x}_{n+\alpha_f}$. For example, in the case of a scalar function f,

$$\begin{aligned} \operatorname{grad} f &= \frac{\partial f}{\partial \mathbf{x}_{n+\alpha_f}} = \frac{\partial f}{\partial \eta^i} \mathbf{g}^i_{n+\alpha_f} \\ \mathbf{g}^i_{n+\alpha_f} &= \frac{\partial \eta^i}{\partial \mathbf{x}_{n+\alpha_f}} \end{aligned} ,$$

where the contravariant basis vectors $\mathbf{g}^i_{n+\alpha_f}$ may be evaluated from the covariant basis vectors

$$\mathbf{g}_i^{n+\alpha_f} = \frac{\partial \mathbf{x}_{n+\alpha_f}}{\partial \eta^i} = (1 - \alpha_f) \frac{\partial \mathbf{x}_n}{\partial \eta^i} + \alpha_f \frac{\partial \mathbf{x}_{n+1}}{\partial \eta^i}$$

using $\mathbf{g}_i^{n+\alpha_f} \cdot \mathbf{g}_{n+\alpha_f}^j = \delta_i^j$.

The discretization of the internal work produces

$$\delta W_{int} = \sum_a \delta \mathbf{v}_a \cdot \int_b (\mathbf{f}_a^u + \mathbf{f}_a^\rho) \, dv\,, \qquad (7.1.30)$$

where

$$\boxed{\begin{aligned} \mathbf{f}_a^u &= \boldsymbol{\sigma} \cdot \operatorname{grad} N_a \\ \mathbf{f}_a^\rho &= N_a \rho \mathbf{a} \end{aligned}}. \qquad (7.1.31)$$

The discretization of the stress and elasticity terms in the internal work is

$$\int_v \alpha_f \left(\operatorname{grad} \delta \mathbf{v} : \operatorname{grad} \Delta \mathbf{u} \cdot \boldsymbol{\sigma} + \operatorname{grad} \delta \mathbf{v} : \boldsymbol{\mathcal{C}} : \operatorname{grad} \Delta \mathbf{u} \right) \, dv$$
$$= \sum_a \delta \mathbf{v}_a \cdot \sum_b \int_v \mathbf{K}_{ab} \, dv \cdot \Delta \mathbf{u}_b$$

,

where

$$\boxed{\mathbf{K}_{ab} = \alpha_f \left(\left(\operatorname{grad} N_a \cdot \boldsymbol{\sigma} \cdot \operatorname{grad} N_b \right) \mathbf{I} + \operatorname{grad} N_a \cdot \boldsymbol{\mathcal{C}} \cdot \operatorname{grad} N_b \right)}. \qquad (7.1.32)$$

The discretization of the mass term in the internal work is

$$\int_b \delta \mathbf{v} \cdot \frac{\alpha_m}{\beta \Delta t^2} \rho \Delta \mathbf{u} \, dv = \sum_a \delta \mathbf{v}_a \cdot \sum_b \int_b \mathbf{M}_{ab} \, dv \cdot \Delta \mathbf{u}_b\,,$$

where

$$\boxed{\mathbf{M}_{ab} = \frac{\alpha_m}{\beta \Delta t^2} \rho N_a N_b \mathbf{I}}. \qquad (7.1.33)$$

For the external work of body forces,

$$\int_b \delta \mathbf{v} \cdot \rho \mathbf{b} \, dv = \sum_a \delta \mathbf{v}_a \cdot \int_b \mathbf{f}_a^{\mathbf{b}} \, dv$$

where

$$\boxed{\mathbf{f}_a^{\mathbf{b}} = N_a \rho^s \mathbf{b}}, \qquad (7.1.34)$$

and

$$\int_b \delta \mathbf{v}^s \cdot \alpha_f \rho^s \operatorname{grad} \mathbf{b} \cdot \Delta \mathbf{u} \, dv = \sum_a \delta \mathbf{v}_a^s \cdot \sum_b \int_b \mathbf{K}_{ab}^{\mathbf{b}} \, dv \cdot \Delta \mathbf{u}_b$$

where

$$\boxed{\mathbf{K}_{ab}^{\mathbf{b}} = \alpha_f N_a N_b \rho^s \operatorname{grad} \mathbf{b}}. \qquad (7.1.35)$$

For prescribed tractions,

$$\int_{\partial b} \delta \mathbf{v}^s \cdot \mathbf{t}^s \, da = \sum_a \delta \mathbf{v}_a^s \cdot \int_{\Gamma_\eta} \mathbf{f}_a^t \, d\eta^1 d\eta^2$$

where

$$\boxed{\mathbf{f}_a^t = N_a \mathbf{t}^s \, |\mathbf{g}_1 \times \mathbf{g}_2|}, \qquad (7.1.36)$$

and

$$\int_{\Gamma_\eta} \alpha_f \delta \mathbf{v}^s \cdot (\mathbf{t}^s \otimes \mathbf{n}) \cdot \left(\mathbf{g}_1 \times \frac{\partial \Delta \mathbf{u}}{\partial \eta^2} - \mathbf{g}_2 \times \frac{\partial \Delta \mathbf{u}}{\partial \eta^1} \right) d\eta^1 d\eta^2$$
$$= \sum_a \delta \mathbf{v}_a^s \cdot \sum_b \int_{\Gamma_\eta} \mathbf{K}_{ab}^t \, d\eta^1 d\eta^2 \cdot \Delta \mathbf{u}_b$$

where

$$\boxed{\mathbf{K}_{ab}^t = \alpha_f N_a (\mathbf{t}^s \otimes \mathbf{n}) \cdot \left(\frac{\partial N_b}{\partial \eta^2} \hat{\mathbf{g}}_1 - \frac{\partial N_b}{\partial \eta^1} \hat{\mathbf{g}}_2 \right)}, \qquad (7.1.37)$$

where $\hat{\mathbf{g}}$ is the skew-symmetric tensor whose dual vector is $\mathbf{g}$.

7.1.6 Energy-Momentum Conservation Scheme

The time discretization scheme may be selected in a manner that enforces linear and angular momentum, and energy conservation over consecutive time steps t_n and t_{n+1}, when boundary conditions and external loads are time-independent. Based on the prior literature [54, 28, 50], this momentum and energy conservation may be achieved by using the midpoint rule ($\rho_\infty = 1$, leading to $\alpha_f = \alpha_m = \frac{1}{2}$), and evaluating the virtual work at $t_{n+\frac{1}{2}}$. However, since the virtual work strictly enforces momentum balance only, there is no guarantee that energy conservation will be satisfied as a result of time discretization. Therefore, we need to enforce a specific scheme to satisfy energy balance.

7.1.6.1 Energy Balance

For an elastic solid, in the absence of heat exchanges (i.e., in elastodynamics), the equation of energy balance reduces

$$\rho \dot{\varepsilon} = \boldsymbol{\sigma} : \mathbf{D}, \qquad (7.1.38)$$

where ε is the specific internal energy and $\mathbf{D}$ is the rate of deformation tensor. Recall that $\varepsilon = \psi + \theta \eta$, where ψ is the specific free energy, θ is the absolute temperature and η is the specific entropy. Since $\eta = 0$ in elasticity (due to the temperature remaining constant), the above energy balance may be combined with the mass balance (7.1.2) as

$$\rho \dot{\psi} = \frac{\rho_r}{J} \dot{\psi} = \boldsymbol{\sigma} : \mathbf{D}, \qquad (7.1.39)$$

or

$$\dot{\Psi}_r = J \boldsymbol{\sigma} : \mathbf{D}, \qquad (7.1.40)$$

where $\Psi_r = \rho_r \psi$ is the free energy density (per volume of the material in the reference configuration).

In our time integration scheme, to satisfy energy balance, this equation needs to be evaluated at $t_{n+\alpha_f}$, thus

$$\left(\dot{\Psi}_r \right)_{n+\alpha_f} = J_{n+\alpha_f} \boldsymbol{\sigma}_{n+\alpha_f} : \mathbf{D}_{n+\alpha_f} . \qquad (7.1.41)$$

However, the solution for $\boldsymbol{\sigma}_{n+\alpha_f} \equiv \boldsymbol{\sigma} \left(\mathbf{F}_{n+\alpha_f} \right)$ obtained from the momentum balance may not necessarily satisfy this equation. Thus, to satisfy energy balance over consecutive time steps, we want to evaluate an effective stress $\tilde{\boldsymbol{\sigma}}_{n+\alpha_f}$ such that

$$J_{n+\alpha_f} \tilde{\boldsymbol{\sigma}}_{n+\alpha_f} : \mathbf{D}_{n+\alpha_f} = \frac{(\Psi_r)_{n+1} - (\Psi_r)_n}{\Delta t} . \qquad (7.1.42)$$

To find a solution for $\tilde{\boldsymbol{\sigma}}_{n+\alpha_f}$, we follow the procedure of Gonzalez [28] and let

$$\tilde{\boldsymbol{\sigma}}_{n+\alpha_f} = \boldsymbol{\sigma}_{n+\alpha_f} + f\mathbf{D}_{n+\alpha_f}\,, \tag{7.1.43}$$

where f is some scalar function to be determined. Substituting this relation, (7.1.43), into the previous equation, (7.1.42), produces

$$f = \left(\frac{(\Psi_r)_{n+1} - (\Psi_r)_n}{J^s_{n+\alpha_f}\Delta t} - \boldsymbol{\sigma}_{n+\alpha_f} : \mathbf{D}_{n+\alpha_f} \right) \frac{1}{\mathbf{D}_{n+\alpha_f} : \mathbf{D}_{n+\alpha_f}}\,. \tag{7.1.44}$$

Hence, the equation for an effective stress needed to satisfy energy balance between consecutive time steps is

$$\boxed{\tilde{\boldsymbol{\sigma}}_{n+\alpha_f} = \boldsymbol{\sigma}_{n+\alpha_f} + \left(\frac{(\Psi_r)_{n+1} - (\Psi_r)_n}{J_{n+\alpha_f}\Delta t} - \boldsymbol{\sigma}_{n+\alpha_f} : \mathbf{D}_{n+\alpha_f} \right) \frac{\mathbf{D}_{n+\alpha_f}}{\mathbf{D}_{n+\alpha_f} : \mathbf{D}_{n+\alpha_f}}}\,. \tag{7.1.45}$$

In the limit when $\mathbf{D}_{n+\alpha_f} : \mathbf{D}_{n+\alpha_f} = 0$, we use $\tilde{\boldsymbol{\sigma}}_{n+\alpha_f} = \boldsymbol{\sigma}_{n+\alpha_f}$. Recall that this scheme produces conservation of linear and angular momentum and total energy only with $\rho_\infty = 1$, or equivalently, $\alpha_f = \alpha_m = \frac{1}{2}$, $\beta = \frac{1}{2}$ and $\gamma = 1$. Therefore, this effective stress calculation is only applied when the user employs $\rho_\infty = 1$.

7.2   Rigid Body Dynamics

7.2.1   General Rigid Body Motion

If the point $\mathbf{x}$ is connected to a rigid body, its motion is given by

$$\mathbf{x} = \mathbf{r}\,(t) + \boldsymbol{\Lambda}\,(t) \cdot \mathbf{Z} = \mathbf{r}\,(t) + \mathbf{z}\,(t) \tag{7.2.1}$$

where $\mathbf{r}\,(t)$ is the position of the rigid body center of mass and $\boldsymbol{\Lambda}\,(t)$ is the body's rotation tensor, which satisfies $\boldsymbol{\Lambda}\,(t_0) = \mathbf{I}$ at the initial time t_0; here, $\mathbf{z}\,(t) = \boldsymbol{\Lambda}\,(t) \cdot \mathbf{Z}$ is the distance of the point from the body's center of mass, and $\mathbf{X} = \mathbf{r}\,(t_0) + \mathbf{Z}$ is the initial position. The velocity of that point is

$$\dot{\mathbf{x}} = \dot{\mathbf{r}}\,(t) + \dot{\boldsymbol{\Lambda}}\,(t) \cdot \mathbf{Z}\quad, \tag{7.2.2}$$

where

$$\dot{\boldsymbol{\Lambda}}\,(t) = \hat{\mathbf{w}}\,(t) \cdot \boldsymbol{\Lambda}\,(t) = \boldsymbol{\Lambda}\,(t) \cdot \hat{\mathbf{W}}\,(t)\,.$$

Here, $\hat{\mathbf{w}}$ is a skew-symmetric tensor with axial vector $\mathbf{w}$ which represents the spatial angular velocity vector; similarly, $\hat{\mathbf{W}}$ is a skew-symmetry tensor with axial vector $\mathbf{W}$, such that $\mathbf{w} = \boldsymbol{\Lambda} \cdot \mathbf{W}$ and

$$\hat{\mathbf{w}} = \boldsymbol{\Lambda} \cdot \hat{\mathbf{W}} \cdot \boldsymbol{\Lambda}^T\,.$$

Thus, $\mathbf{W}\,(t)$ is the material representation of the angular velocity vector at t, whereas $\mathbf{w}\,(t)$ is its spatial representation. We may now rewrite

$$\begin{aligned}
\dot{\mathbf{x}} &= \dot{\mathbf{r}}\,(t) + \hat{\mathbf{w}}\,(t) \cdot \mathbf{z}\,(t)\\
&= \dot{\mathbf{r}}\,(t) + \boldsymbol{\Lambda}\,(t) \cdot \hat{\mathbf{W}}\,(t) \cdot \mathbf{Z}
\end{aligned}$$

so that the acceleration of the point is

$$\ddot{\mathbf{x}} = \ddot{\mathbf{r}}\left(t\right) + \left(\hat{\mathbf{a}}\left(t\right) + \hat{\mathbf{w}}^2\left(t\right)\right) \cdot \mathbf{z}$$
$$= \ddot{\mathbf{r}}\left(t\right) + \mathbf{\Lambda}\left(t\right) \cdot \left(\hat{\mathbf{A}}\left(t\right) + \hat{\mathbf{W}}^2\left(t\right)\right) \cdot \mathbf{Z}^{\,\prime}$$

where $\mathbf{a} = \dot{\mathbf{w}} = \mathbf{\Lambda} \cdot \mathbf{A}$ is the spatial acceleration vector, $\mathbf{A} = \dot{\mathbf{W}}$ is the material acceleration vector, and the corresponding skew-symmetric tensors are related to the angular velocity via

$$\hat{\mathbf{a}} = \dot{\hat{\mathbf{w}}}, \quad \hat{\mathbf{A}} = \dot{\hat{\mathbf{W}}}.$$

As shown below, the time discretization is performed in the material frame.

7.2.2 Rigid Body Momentum

For a rigid body, the conservation of linear momentum is given by

$$\frac{d}{dt}\left(m\dot{\mathbf{r}}\right) = \dot{\mathbf{p}} = \mathbf{f}^{ext}\left(t\right)$$

where m is the mass of the rigid body (constant), $\dot{\mathbf{r}}$ is the velocity of the center of mass, $\mathbf{p} = m\dot{\mathbf{r}}$ is the linear momentum, and $\mathbf{f}^{ext}\left(t\right)$ represents the sum of external forces acting on the body. Here, m is constant for a rigid body. There are typically four contributions to $\mathbf{f}^{ext}\left(t\right)$: Body forces $\mathbf{f}_b^{ext}\left(t\right) = m\mathbf{b}\left(t\right)$ (where $\mathbf{b}$ represents the body force per mass, such as gravitational acceleration), other user-prescribed forces $\mathbf{f}_p^{ext}\left(t\right)$ (which act at the center of mass), forces $\mathbf{f}_c^{ext}\left(t\right)$ produced by rigid body connectors (such as revolute and prismatic joints, or contact forces), and forces $\mathbf{f}_f^{ext}\left(t\right)$ produced by rigid-flexible connections (where deformable materials interface with the rigid body), in which case $\mathbf{f}_f^{ext}$ is evaluated from the traction $\mathbf{t} = \boldsymbol{\sigma} \cdot \mathbf{n}$ over that interface, with $\boldsymbol{\sigma}$ representing the stress in the deformable material.

The conservation of angular momentum is similarly given by

$$\frac{d}{dt}\left(\mathbf{J} \cdot \boldsymbol{\omega}\right) = \dot{\mathbf{h}} = \mathbf{m}^{ext}\left(t\right)$$

where $\mathbf{J}$ is the rigid body mass moment of inertia about its center of mass, $\boldsymbol{\omega}$ is its angular velocity, $\mathbf{h} = \mathbf{J} \cdot \boldsymbol{\omega}$ is its angular momentum, and $\mathbf{m}^{ext}\left(t\right)$ is the sum of moments acting on the rigid body. External moments include contributions from user-prescribed moments/torques $\mathbf{m}_p^{ext}\left(t\right)$, from rigid body connectors, $\mathbf{m}_c^{ext}\left(t\right) = \mathbf{z}_c\left(t\right) \times \mathbf{f}_c^{ext}\left(t\right)$ where $\mathbf{z}_c\left(t\right)$ is the connector insertion relative to the rigid body center of mass, and rigid-flexible interfaces, $\mathbf{m}_f^{ext}\left(t\right) = \mathbf{z}_f\left(t\right) \times \mathbf{f}_f^{ext}\left(t\right)$ where $\mathbf{z}_f\left(t\right)$ is the position of the interface point relative to the rigid body center of mass. Since body forces $\mathbf{f}_b^{ext}$ and user-prescribed forces $\mathbf{f}_p^{ext}$ act at the center of mass, they do not contribute to $\mathbf{m}^{ext}\left(t\right)$. Note that

$$\mathbf{J}\left(t\right) = \mathbf{\Lambda}\left(t\right) \cdot \mathbf{J}_r \cdot \mathbf{\Lambda}^T\left(t\right)$$

where $\mathbf{J}_r$ is the moment of inertia in the reference configuration and $\mathbf{\Lambda}\left(t\right)$ is the rotation tensor representing the orientation of the rigid body at time t, with $\mathbf{\Lambda} = \mathbf{I}$ in the reference configuration.

The virtual work is given by

$$\delta W = \delta\mathbf{r} \cdot \left(\mathbf{f}^{ext}\left(t\right) - \dot{\mathbf{p}}\right) + \delta\boldsymbol{\theta} \cdot \left(\mathbf{m}^{ext}\left(t\right) - \dot{\mathbf{h}}\right),$$

where $\delta\mathbf{r}$ is the virtual displacement of the center of mass and $\delta\boldsymbol{\theta}$ is the virtual rotation of the rigid body.

7.2.3 Time Discretization

According to Simo and Wong [56], to solve numerically for $\delta W = 0$ over the time domain, we start from

$$\delta \mathbf{r} \cdot \dot{\mathbf{p}} + \delta \boldsymbol{\theta} \cdot \dot{\mathbf{h}} = \delta \mathbf{r} \cdot \mathbf{f}^{ext}(t) + \delta \boldsymbol{\theta} \cdot \mathbf{m}^{ext}(t)$$

and integrate this expression with respect to time using the midpoint rule, thus producing

$$\delta \mathbf{r} \cdot \left(\mathbf{f}^{ext}_{n+\frac{1}{2}} - \frac{m}{\Delta t}(\dot{\mathbf{r}}_{n+1} - \dot{\mathbf{r}}_n) \right) + \delta \boldsymbol{\theta} \cdot \left(\mathbf{m}^{ext}_{n+\frac{1}{2}} - \frac{1}{\Delta t}(\mathbf{J}_{n+1} \cdot \boldsymbol{\omega}_{n+1} - \mathbf{J}_n \cdot \boldsymbol{\omega}_n) \right) = 0,$$

or equivalently,

$$\begin{bmatrix} \delta \mathbf{r} & \delta \boldsymbol{\theta} \end{bmatrix} \cdot \begin{bmatrix} \mathbf{f}^{ext}_{n+\frac{1}{2}} - \frac{m}{\Delta t}(\dot{\mathbf{r}}_{n+1} - \dot{\mathbf{r}}_n) \\ \mathbf{m}^{ext}_{n+\frac{1}{2}} - \frac{1}{\Delta t}(\mathbf{J}_{n+1} \cdot \boldsymbol{\omega}_{n+1} - \mathbf{J}_n \cdot \boldsymbol{\omega}_n) \end{bmatrix} = 0.$$

In these expressions, the external forces and moments at the midpoint are evaluate from

$$\mathbf{f}^{ext}_{n+\frac{1}{2}} = \frac{1}{2}\left(\mathbf{f}^{ext}_{n+1} + \mathbf{f}^{ext}_n \right), \quad \mathbf{m}^{ext}_{n+\frac{1}{2}} = \frac{1}{2}\left(\mathbf{m}^{ext}_{n+1} + \mathbf{m}^{ext}_n \right).$$

Thus, the residual vector is given by

$$[\mathbf{R}(t_{n+1})] = \begin{bmatrix} \mathbf{f}^{ext}_{n+\frac{1}{2}} \\ \mathbf{m}^{ext}_{n+\frac{1}{2}} \end{bmatrix} - \begin{bmatrix} \dot{\mathbf{p}}_{n+1} \\ \dot{\mathbf{h}}_{n+1} \end{bmatrix}$$

where

$$\dot{\mathbf{p}}_{n+1} = m\frac{\dot{\mathbf{r}}_{n+1} - \dot{\mathbf{r}}_n}{\Delta t}$$
$$\dot{\mathbf{h}}_{n+1} = \frac{\mathbf{J}_{n+1} \cdot \boldsymbol{\omega}_{n+1} - \mathbf{J}_n \cdot \boldsymbol{\omega}_n}{\Delta t}.$$

According to the midpoint rule,

$$\dot{\mathbf{r}}_{n+1} = \dot{\mathbf{r}}_n + \Delta t\, \ddot{\mathbf{r}}_{n+1}$$
$$\ddot{\mathbf{r}}_{n+1} = \frac{2}{\Delta t^2}(\mathbf{r}_{n+1} - \mathbf{r}_n) - \frac{2}{\Delta t}\dot{\mathbf{r}}_n,$$

and more generally,

$$\mathbf{r}_{n+1} = \mathbf{r}_n + \Delta t\, \dot{\mathbf{r}}_n + \Delta t^2 \left[\left(\frac{1}{2} - \beta \right) \ddot{\mathbf{r}}_n + \beta \ddot{\mathbf{r}}_{n+1} \right]$$
$$\dot{\mathbf{r}}_{n+1} = \dot{\mathbf{r}}_n + \Delta t\left[(1 - \gamma)\, \ddot{\mathbf{r}}_n + \gamma \ddot{\mathbf{r}}_{n+1} \right]$$
$$\ddot{\mathbf{r}}_{n+1} = \frac{1}{\beta}\left(\frac{1}{\Delta t}\left[\frac{1}{\Delta t}(\mathbf{r}_{n+1} - \mathbf{r}_n) - \dot{\mathbf{r}}_n \right] - \left(\frac{1}{2} - \beta \right)\ddot{\mathbf{r}}_n \right)$$

where $\mathbf{r}(t)$ is the position and $\ddot{\mathbf{r}}(t)$ is the acceleration of the rigid body center of mass, such that $\mathbf{r}_{n+1} = \mathbf{r}(t_{n+1})$ and $\ddot{\mathbf{r}}_{n+1} = \ddot{\mathbf{r}}(t_{n+1})$. However, for the angular position, velocity and acceleration, the temporal discretization must be done in the rigid body (material) frame. Thus, for the midpoint rule,

$$\mathbf{W}_{n+1} = \frac{2}{\Delta t}\boldsymbol{\Theta} - \mathbf{W}_n$$
$$\mathbf{A}_{n+1} = \frac{2}{\Delta t^2}\boldsymbol{\Theta} - \frac{2}{\Delta t}\mathbf{W}_n,$$

and more generally,

$$\mathbf{W}_{n+1} = \frac{\gamma}{\beta\Delta t}\boldsymbol{\Theta} - \mathbf{W}_n + \left(2 - \frac{\gamma}{\beta}\right)\left(\mathbf{W}_n + \frac{\Delta t}{2}\mathbf{A}_n\right)$$

$$\mathbf{A}_{n+1} = \frac{1}{\gamma\Delta t}\left(\mathbf{W}_{n+1} - \mathbf{W}_n\right) + \left(1 - \frac{1}{\gamma}\right)\mathbf{A}_n$$

$$= \frac{1}{\beta\Delta t}\left(\frac{1}{\Delta t}\boldsymbol{\Theta} - \mathbf{W}_n\right) + \left(1 - \frac{1}{2\beta}\right)\mathbf{A}_n$$

where $\boldsymbol{\theta} = \boldsymbol{\Lambda}\cdot\boldsymbol{\Theta}$, $\boldsymbol{\omega} = \boldsymbol{\Lambda}\cdot\mathbf{W}$, and $\boldsymbol{\alpha} = \dot{\boldsymbol{\omega}} = \boldsymbol{\Lambda}\cdot\mathbf{A}$. Here, $\boldsymbol{\theta}$ is the spatial rotational increment from t_n to t_{n+1}, while $\boldsymbol{\Theta}$ is the corresponding material increment, thus $\boldsymbol{\theta} = \boldsymbol{\Lambda}_n\cdot\boldsymbol{\Theta}$. For the remaining terms, $\boldsymbol{\omega}_n = \boldsymbol{\Lambda}_n\cdot\mathbf{W}_n$, $\boldsymbol{\omega}_{n+1} = \boldsymbol{\Lambda}_{n+1}\cdot\mathbf{W}_{n+1}$, and $\boldsymbol{\alpha}_{n+1} = \boldsymbol{\Lambda}_{n+1}\cdot\mathbf{A}_{n+1}$. The relation between $\boldsymbol{\Lambda}_n$ and $\boldsymbol{\Lambda}_{n+1}$ is

$$\boldsymbol{\Lambda}_{n+1} = \text{rot}\,[\boldsymbol{\theta}]\cdot\boldsymbol{\Lambda}_n = \boldsymbol{\Lambda}_n\cdot\text{rot}\,[\boldsymbol{\Theta}]$$

where $\text{rot}\,[\cdot]$ may represents either the exponential map or the Cayley transform. According to Puso [50], the Cayley transform must be used to enforce conservation of momentum and energy in a midpoint rule discretization scheme, whenever the rigid body is connected to a deformable body, or whenever two rigid bodies are connected by a joint. It follows from the midpoint rule that

$$\boldsymbol{\omega}_{n+1} = \text{cay}\,[\boldsymbol{\theta}]\cdot\left(\frac{2}{\Delta t}\boldsymbol{\theta} - \boldsymbol{\omega}_n\right)$$

$$\boldsymbol{\alpha}_{n+1} = \text{cay}\,[\boldsymbol{\theta}]\cdot\left(\frac{2}{\Delta t^2}\boldsymbol{\theta} - \frac{2}{\Delta t}\boldsymbol{\omega}_n\right)$$

and more generally,

$$\boldsymbol{\omega}_{n+1} = \text{cay}\,[\boldsymbol{\theta}]\cdot\left(\frac{\gamma}{\beta\Delta t}\boldsymbol{\theta} - \boldsymbol{\omega}_n + \left(2 - \frac{\gamma}{\beta}\right)\left(\boldsymbol{\omega}_n + \frac{\Delta t}{2}\boldsymbol{\alpha}_n\right)\right)$$

$$\boldsymbol{\alpha}_{n+1} = \text{cay}\,[\boldsymbol{\theta}]\cdot\left(\frac{1}{\beta\Delta t}\left(\frac{1}{\Delta t}\boldsymbol{\theta} - \boldsymbol{\omega}_n\right) + \left(1 - \frac{1}{2\beta}\right)\boldsymbol{\alpha}_n\right)$$

The nonlinear system $\mathbf{R}\,(t_{n+1}) = \mathbf{0}$ is solved using a Newton scheme that requires linearizing $\mathbf{R}$ along increments $\Delta\mathbf{r}$ and $\Delta\boldsymbol{\theta}$. Thus,

$$\mathbf{R}\,(t_{n+1}) + D\mathbf{R}\,(t_{n+1})\,[\Delta\mathbf{r}] + D\mathbf{R}\,(t_{n+1})\,[\Delta\boldsymbol{\theta}] \approx \mathbf{0}\,.$$

The increments $\Delta\mathbf{r}$ and $\Delta\boldsymbol{\theta}$ are evaluated at t_{n+1} and the iterative Newton scheme requires updates of the form

$$\mathbf{r}_{n+1}^{j+1} = \mathbf{r}_{n+1}^j + \Delta\mathbf{r}$$

$$\text{cay}\,[\boldsymbol{\theta}^{j+1}] = \text{cay}\,[\Delta\boldsymbol{\theta}]\cdot\text{cay}\,[\boldsymbol{\theta}^j]$$

where j represents the Newton iteration. At each Newton iteration, the current value of $\text{cay}\,[\boldsymbol{\theta}^{j+1}]$ is used to perform the update

$$\boldsymbol{\Lambda}_{n+1}^{j+1} = \text{cay}\,[\boldsymbol{\theta}^{j+1}]\cdot\boldsymbol{\Lambda}_n\,,$$

until convergence is achieved.

Using the exponential map, the rotation tensor $\boldsymbol{\Lambda}\,(t)$ may alternatively be represented by the vector $\boldsymbol{\xi}\,(t)$ where

$$\boldsymbol{\Lambda} = \exp\,[\boldsymbol{\xi}]\,.$$

Thus, $\mathbf{\Lambda}_n = \exp\left[\boldsymbol{\xi}_n\right]$ and $\mathbf{\Lambda}_{n+1} = \exp\left[\boldsymbol{\xi}_{n+1}\right]$. In practice, $\boldsymbol{\xi}$ is stored as a quaternion to facilitate the multiplication of rotation tensors. Similarly, it is convenient to store $\boldsymbol{\theta}$ and $\Delta\boldsymbol{\theta}$ in quaternions, recognizing that

$$\mathrm{cay}\left[\theta\mathbf{n}\right] = \exp\left[\left(2\tan^{-1}\frac{\theta}{2}\right)\mathbf{n}\right] ,$$

where $\mathbf{n}$ is the unit vector along $\boldsymbol{\theta}$ and $\theta = \|\boldsymbol{\theta}\|$. Thus, it is $\left(2\tan^{-1}\frac{\theta}{2}\right)\mathbf{n}$ which is stored in the quaternion, instead of $\theta\mathbf{n}$.

In the linearization of $\mathbf{R}\left(t_{n+1}\right)$, the contributions from the rate of change of linear momentum $\dot{\mathbf{p}}_{n+1}$ reduce to

$$D\dot{\mathbf{p}}_{n+1}\left[\Delta\mathbf{r}\right] = m\,D\left(\ddot{\mathbf{r}}_{n+1}\right)\left[\Delta\mathbf{r}\right] = \frac{2}{\Delta t^2}m\Delta\mathbf{r}$$

$$D\dot{\mathbf{p}}_{n+1}\left[\Delta\boldsymbol{\theta}\right] = \mathbf{0}$$

To evaluate the contributions from the rate of change of angular momentum $\dot{\mathbf{h}}_{n+1}$, it is first necessary to transform the variables to the material frame,

$$\dot{\mathbf{h}}_{n+1} = \frac{1}{\Delta t}\left(\mathbf{\Lambda}_{n+1}\cdot\mathbf{J}_r\cdot\mathbf{W}_{n+1} - \mathbf{\Lambda}_n\cdot\mathbf{J}_r\cdot\mathbf{W}_n\right)$$

$$= \frac{1}{\Delta t}\mathbf{\Lambda}_n\cdot\left(\mathrm{cay}\left[\boldsymbol{\Theta}\right]\cdot\mathbf{J}_r\cdot\left(\frac{2}{\Delta t}\boldsymbol{\Theta} - \mathbf{W}_n\right) - \mathbf{J}_r\cdot\mathbf{W}_n\right)$$

It follows that

$$D\dot{\mathbf{h}}_{n+1}\left[\Delta\mathbf{r}\right] = \mathbf{0}\,.$$

Now, we first perform the linearization along an increment $\Delta\boldsymbol{\Theta}$ in the material frame,

$$D\dot{\mathbf{h}}_{n+1}\left[\Delta\boldsymbol{\Theta}\right] = \frac{1}{\Delta t}\mathbf{\Lambda}_n\cdot\left(D\left(\mathrm{cay}\left[\boldsymbol{\Theta}\right]\right)\left[\Delta\boldsymbol{\Theta}\right]\cdot\mathbf{J}_r\cdot\mathbf{W}_{n+1} + \frac{2}{\Delta t}\mathrm{cay}\left[\boldsymbol{\Theta}\right]\cdot\mathbf{J}_r\cdot D\boldsymbol{\Theta}\left[\Delta\boldsymbol{\Theta}\right]\right)$$

$$= \frac{1}{\Delta t}\mathbf{\Lambda}_{n+1}\cdot\left(\frac{2}{\Delta t}\mathbf{J}_r\cdot\mathbf{T}\left(\boldsymbol{\Theta}\right) - \mathbf{J}_r\cdot\widehat{\mathbf{W}_{n+1}}\right)\cdot\Delta\boldsymbol{\Theta}$$

,

where $\hat{\mathbf{y}} \equiv -\mathcal{E}\cdot\mathbf{y}$ is the skew-symmetric tensor with axial vector $\mathbf{y}$ and

$$\mathbf{T}\left(\boldsymbol{\Theta}\right) = \mathbf{I} + \frac{1}{2}\hat{\boldsymbol{\Theta}} + \frac{1}{4}\boldsymbol{\Theta}\otimes\boldsymbol{\Theta}\,.$$

Then, we return to the spatial frame, recognizing that $\Delta\boldsymbol{\theta} = \mathbf{\Lambda}_{n+1}\cdot\Delta\boldsymbol{\Theta}$ (since $\Delta\boldsymbol{\theta}$ is an increment taken at t_{n+1}, from Newton iterations j to $j+1$),

$$D\dot{\mathbf{h}}_{n+1}\left[\Delta\boldsymbol{\Theta}\right] = \frac{1}{\Delta t}\left(\frac{2}{\Delta t}\mathbf{J}_{n+1}\cdot\mathbf{T}\left(\boldsymbol{\theta}\right) - \widehat{\mathbf{J}_{n+1}\cdot\boldsymbol{\omega}_{n+1}}\right)\cdot\Delta\boldsymbol{\theta} \quad,$$

where we have used the identities

$$\mathbf{\Lambda}_{n+1}\cdot\mathbf{T}\left(\boldsymbol{\Theta}\right)\cdot\mathbf{\Lambda}_{n+1}^T = \mathbf{T}\left(\mathbf{\Lambda}_{n+1}\cdot\boldsymbol{\Theta}\right) = \mathbf{T}\left(\mathrm{cay}\left[\boldsymbol{\theta}\right]\cdot\boldsymbol{\theta}\right) = \mathbf{T}\left(\boldsymbol{\theta}\right)$$

$$\mathbf{\Lambda}_{n+1}\cdot\hat{\mathbf{y}}\cdot\mathbf{\Lambda}_{n+1}^T = \widehat{\mathbf{\Lambda}_{n+1}\cdot\mathbf{y}}$$

Consider that the moments $\mathbf{m}^{ext}_{n+\frac{1}{2}}$ about the rigid body center of mass are produced by the forces $\mathbf{f}^{ext}_{n+\frac{1}{2}}$ according to

$$\mathbf{m}^{ext}_{n+\frac{1}{2}} = \mathbf{z}_{n+\frac{1}{2}}\times\mathbf{f}^{ext}_{n+\frac{1}{2}} = \hat{\mathbf{z}}_{n+\frac{1}{2}}\cdot\mathbf{f}^{ext}_{n+\frac{1}{2}}\,,$$

where $\mathbf{z}_{n+\frac{1}{2}}$ is the moment arm at $t_{n+\frac{1}{2}}$. According to Puso [50],

$$\begin{aligned}
\mathbf{z}_{n+\frac{1}{2}} &= \frac{1}{2}\left(\mathbf{z}_{n+1} + \mathbf{z}_n\right) \\
&= \frac{1}{2}\left(\mathbf{\Lambda}_{n+1} + \mathbf{\Lambda}_n\right) \cdot \mathbf{Z}
\end{aligned}$$

where $\mathbf{Z}$ is the moment arm in the reference configuration. Note that

$$D\mathbf{z}_{n+\frac{1}{2}}\left[\Delta\mathbf{r}\right] = \mathbf{0}$$

$$D\mathbf{z}_{n+\frac{1}{2}}\left[\Delta\boldsymbol{\theta}\right] = \frac{1}{2}D\mathbf{\Lambda}_{n+1}\left[\Delta\boldsymbol{\theta}\right] \cdot \mathbf{Z} = -\frac{1}{2}\hat{\mathbf{z}}_{n+1} \cdot \Delta\boldsymbol{\theta}$$

Thus,

$$\left[\begin{array}{c} D\mathbf{f}^{ext}_{n+\frac{1}{2}}\left[\Delta\mathbf{r}\right] \\ D\mathbf{m}^{ext}_{n+\frac{1}{2}}\left[\Delta\mathbf{r}\right] \end{array}\right] = \left[\begin{array}{c} D\mathbf{f}^{ext}_{n+\frac{1}{2}}\left[\Delta\mathbf{r}\right] \\ \mathbf{z}_{n+\frac{1}{2}} \times D\mathbf{f}^{ext}_{n+\frac{1}{2}}\left[\Delta\mathbf{r}\right] \end{array}\right]$$

and

$$\left[\begin{array}{c} D\mathbf{f}^{ext}_{n+\frac{1}{2}}\left[\Delta\boldsymbol{\theta}\right] \\ D\mathbf{m}^{ext}_{n+\frac{1}{2}}\left[\Delta\boldsymbol{\theta}\right] \end{array}\right] = \left[\begin{array}{c} D\mathbf{f}^{ext}_{n+\frac{1}{2}}\left[\Delta\boldsymbol{\theta}\right] \\ \mathbf{z}_{n+\frac{1}{2}} \times D\mathbf{f}^{ext}_{n+\frac{1}{2}}\left[\Delta\boldsymbol{\theta}\right] - \left(\frac{1}{2}\hat{\mathbf{z}}_{n+1} \cdot \Delta\boldsymbol{\theta}\right) \times \mathbf{f}^{ext}_{n+\frac{1}{2}} \end{array}\right].$$

Bibliography

[1] M. B. Albro, N. O. Chahine, R. Li, K. Yeager, C. T. Hung, and G. A. Ateshian. Dynamic loading of deformable porous media can induce active solute transport. *J Biomech*, 41(15):3152–7, 2008.

[2] M. B. Albro, R. Li, R. E. Banerjee, C. T. Hung, and G. A. Ateshian. Validation of theoretical framework explaining active solute uptake in dynamically loaded porous media. *J Biomech*, 43(12):2267–73, 2010.

[3] E.M. Arruda and M.C. Boyce. A three-dimensional constitutive model for the large stretch behavior of rubber elastic materials. *J. Mech. Phys. Solids*, 41(2):389–412, 1993.

[4] G. A. Ateshian. Anisotropy of fibrous tissues in relation to the distribution of tensed and buckled fibers. *J Biomech Eng*, 129(2):240–9, 2007.

[5] G. A. Ateshian. On the theory of reactive mixtures for modeling biological growth. *Biomech Model Mechanobiol*, 6(6):423–45, 2007.

[6] G. A. Ateshian, M. Likhitpanichkul, and C. T. Hung. A mixture theory analysis for passive transport in osmotic loading of cells. *J Biomech*, 39(3):464–75, 2006.

[7] G. A. Ateshian, V. Rajan, N. O. Chahine, C. E. Canal, and C. T. Hung. Modeling the matrix of articular cartilage using a continuous fiber angular distribution predicts many observed phenomena. *J Biomech Eng*, 131(6):061003, 2009.

[8] G. A. Ateshian and T. Ricken. Multigenerational interstitial growth of biological tissues. *Biomech Model Mechanobiol*, 9(6):689–702, 2010.

[9] G. A. Ateshian and J. A. Weiss. Anisotropic hydraulic permeability under finite deformation. *Journal of biomechanical engineering*, 132(11):111004, 2010.

[10] GA Ateshian, SA Maas, and J.A. Weiss. Finite element algorithm for frictionless contact of porous permeable media under finite deformation and sliding. *J. Biomech. Engn.*, 132(6):1006–1019, 2010.

[11] Gerard A Ateshian. Viscoelasticity using reactive constrained solid mixtures. *J Biomech*, 48(6):941–7, Apr 2015.

[12] Gerard A Ateshian, Benjamin J Ellis, and Jeffrey A Weiss. Equivalence between short-time biphasic and incompressible elastic material responses. *J Biomech Eng*, 129(3):405–12, Jun 2007.

[13] Gerard A Ateshian, Steve Maas, and Jeffrey A Weiss. Solute transport across a contact interface in deformable porous media. *J Biomech*, 45(6):1023–7, Apr 2012.

[14] Evren U Azeloglu, Michael B Albro, Vikrum A Thimmappa, Gerard A Ateshian, and Kevin D Costa. Heterogeneous transmural proteoglycan distribution provides a mechanism for regulating residual stresses in the aorta. *Am J Physiol Heart Circ Physiol*, 294(3):H1197–205, Mar 2008.

[15] Klaus-Jürgen Bathe. *Finite element procedures in engineering analysis*. Prentice-Hall, Englewood Cliffs, N.J., 1982.

[16] Y Bazilevs, JR Gohean, TJR Hughes, RD Moser, and Y Zhang. Patient-specific isogeometric fluid–structure interaction analysis of thoracic aortic blood flow due to implantation of the Jarvik 2000 left ventricular assist device. *Comput. Methods Appl. Mech. Engrg.*, 198(45):3534–3550, 2009.

[17] Yuri Bazilevs, Victor M Calo, Thomas JR Hughes, and Yongjie Zhang. Isogeometric fluid-structure interaction: theory, algorithms, and computations. *Computational mechanics*, 43(1):3–37, 2008.

[18] P. Betsch, F. Gruttmann, and Stein E. A 4-node finite shell element for the implementation of general hyperelastic 3d-elasticity at finite strains. *Comput. Methods Appl. Mech. Engrg*, 130:57–79, 1996.

[19] Javier Bonet and Richard D. Wood. *Nonlinear continuum mechanics for finite element analysis*. Cambridge University Press, 1997.

[20] Ray M. Bowen. Incompressible porous media models by use of the theory of mixtures. *Int J Eng Sci*, 18(9):1129–1148, 1980.

[21] R.M. Bowen. Theory of mixtures. *Continuum physics*, 3(Pt I), 1976.

[22] Y I Cho and K R Kensey. Effects of the non-Newtonian viscosity of blood on flows in a diseased arterial vessel. Part 1: Steady flows. *Biorheology*, 28(3-4):241–62, 1991.

[23] A. Curnier, He Qi-Chang, and P. Zysset. Conewise linear elastic materials. *J Elasticity*, 37(1):1–38, 1994.

[24] A.C. Eringen and J.D. Ingram. Continuum theory of chemically reacting media – 1. *Int J Eng Sci*, 3:197 – 212, 1965.

[25] Mahdi Esmaily Moghadam, Yuri Bazilevs, Tain-Yen Hsia, Irene E Vignon-Clementel, and Alison L Marsden. A comparison of outlet boundary treatments for prevention of backflow divergence with relevance to blood flow simulations. *Comput. Mech.*, 48(3):277–291, 2011.

[26] Y. C. Fung. *Biomechanics : mechanical properties of living tissues*. Springer-Verlag, New York, 2nd edition, 1993.

[27] Y. C. Fung, K. Fronek, and P. Patitucci. Pseudoelasticity of arteries and the choice of its mathematical expression. *Am J Physiol*, 237(5):H620–31, 1979.

[28] Oscar Gonzalez. Exact energy and momentum conserving algorithms for general models in nonlinear elasticity. *Computer Methods in Applied Mechanics and Engineering*, 190(13):1763–1783, 2000.

[29] J. M. Guccione, A. D. McCulloch, and L. K. Waldman. Passive material properties of intact ventricular myocardium determined from a cylindrical model. *J Biomech Eng*, 113(1):42–55., 1991.

[30] M. H. Holmes and V. C. Mow. The nonlinear characteristics of soft gels and hydrated connective tissues in ultrafiltration. *J Biomech*, 23(11):1145–56, 1990.

[31] Gerhard A Holzapfel. *Nonlinear solid mechanics: a continuum approach for engineering*. Wiley, Chichester, 2000.

[32] A. Horowitz, I. Sheinman, Y. Lanir, M. Perl, and S. Sideman. Nonlinear incompressilbe finite element for simulating loading of cardiac tissue- part i: two dimensional formulation for thin myocardial strips. *Journal of Biomechanical Engineering, Transactions of the ASME*, 110(1):57–61, 1988.

[33] J.R. Hughes and Wing Kam Liu. Nonlinear finite element analysis of shells: Part i. three-dimensional shells. *Computer Methods in Applied Mechanics and Engineering*, 26:331–362, 1980.

[34] J. D. Humphrey, R. K. Strumpf, and F. C. P. Yin. Determination of a constitutive relation for passive myocardium. i. a new functional form. *Journal of Biomechanical Engineering, Transactions of the ASME*, 112(3):333–339, 1990.

[35] J. D. Humphrey and F. C. P. Yin. On constitutive relations and finite deformations of passive cardiac tissue: I. a pseudostrain-energy function. *Journal of Biomechanical Engineering, Transactions of the ASME*, 109(4):298–304, 1987.

[36] Kenneth E Jansen, Christian H Whiting, and Gregory M Hulbert. A generalized-α method for integrating the filtered Navier–Stokes equations with a stabilized finite element method. *Comput. Methods Appl. Mech. Engrg.*, 190(3):305–319, 2000.

[37] Aharon Katzir-Katchalsky and Peter F. Curran. *Nonequilibrium thermodynamics in biophysics*. Harvard University Press, Cambridge,, 1965.

[38] W. Michael Lai, David Rubin, and Erhard Krempl. *Introduction to continuum mechanics*. Butterworth-Heinemann/Elsevier, Amsterdam, 4th ed edition, 2010.

[39] Y. Lanir. Constitutive equations for fibrous connective tissues. *J Biomech*, 16(1):1–12, 1983.

[40] Torvard C. Laurent and Johan Killander. A theory of gel filtration and its experimental verification. *J Chromatogr*, 14:317–330, 1963.

[41] Tod A. Laursen. *Computational Contact and Impact Mechanics*. Springer, 2002.

[42] B. N. Maker. Rigid bodies for metal forming analysis with nike3d. *University of California, Lawrence Livermore Lab Rept*, UCRL-JC-119862:1–8, 1995.

[43] J. E. Marsden and T. J. Hughes. *Mathematical Foundations of Elasticity*. Dover Publications, 1994.

[44] H. Matthies and G. Strang. The solution of nonlinear finite element equations. *Intl J Num Meth Eng*, 14:1613–26, 1979.

[45] R. L. Mauck, C. T. Hung, and G. A. Ateshian. Modeling of neutral solute transport in a dynamically loaded porous permeable gel: implications for articular cartilage biosynthesis and tissue engineering. *J Biomech Eng*, 125(5):602–14, 2003.

[46] V.C. Mow, S.C. Kuei, W.M. Lai, and C.G. Armstrong. Biphasic creep and stress relaxation of articular cartilage in compression: Theory and experiments. *J. Biomech. Eng.*, 102:73–84, 1980.

[47] A. G. Ogston and C. F. Phelps. The partition of solutes between buffer solutions and solutions containing hyaluronic acid. *Biochem J*, 78:827–33, 1961.

[48] Ronald L Panton. *Incompressible flow*. John Wiley & Sons, 2006.

[49] M. A. Puso and J. A. Weiss. Finite element implementation of anisotropic quasi-linear viscoelasticity using a discrete spectrum approximation. *J Biomech Eng*, 120(1):62–70, 1998.

[50] Michael Anthony Puso. An energy and momentum conserving method for rigid–flexible body dynamics. *International Journal for numerical methods in engineering*, 53(6):1393–1414, 2002.

[51] K. M. Quapp and J. A. Weiss. Material characterization of human medial collateral ligament. *J Biomech Eng*, 120(6):757–63, 1998.

[52] J. N. Reddy. *An introduction to continuum mechanics : with applications*. Cambridge University Press, New York, 2008.

[53] J. N. Reddy and David K. Gartling. *The finite element method in heat transfer and fluid dynamics*. CRC Press, Boca Raton, FL, 2nd edition, 2001.

[54] JC Simo and Nils Tarnow. The discrete energy-momentum method. conserving algorithms for nonlinear elastodynamics. *Zeitschrift für angewandte Mathematik und Physik (ZAMP)*, 43(5):757–792, 1992.

[55] J.C. Simo and R.L. Taylor. Quasi-incompressible finite elasticity in principal stretches: Continuum basis and numerical algorithms. *Computer Methods in Applied Mechanics and Engineering*, 85:273–310, 1991.

[56] Juan Carlos Simo and Kachung Kevin Wong. Unconditionally stable algorithms for rigid body dynamics that exactly preserve energy and momentum. *International journal for numerical methods in engineering*, 31(1):19–52, 1991.

[57] Anthony James Merril Spencer. *Continuum Theory of the Mechanics of Fibre-Reinforced Composites*. Springer-Verlag, New York, 1984.

[58] D. N. Sun, W. Y. Gu, X. E. Guo, W. M. Lai, and V. C. Mow. A mixed finite element formulation of triphasic mechano-electrochemical theory for charged, hydrated biological soft tissues. *Int J Numer Meth Eng*, 45(10):1375–402, 1999.

[59] I. Tinoco Jr., K. Sauer, and J. C. Wang. *Physical chemistry : principles and applications in biological sciences.* Prentice Hall, 1995.

[60] C. Truesdell and R. Toupin. *The classical field theories*, volume III/1 of *Handbuch der physik*. Springer, Heidelberg, 1960.

[61] K. Un and R. L. Spilker. A penetration-based finite element method for hyperelastic 3d biphasic tissues in contact. part ii: finite element simulations. *J Biomech Eng*, 128(6):934–42, 2006.

[62] D.R. Veronda and R.A. Westmann. Mechanical characterization of skin - finite deformations. *J. Biomechanics*, Vol. 3:111–124, 1970.

[63] Irene E Vignon-Clementel, C Alberto Figueroa, Kenneth E Jansen, and Charles A Taylor. Outflow boundary conditions for three-dimensional finite element modeling of blood flow and pressure in arteries. *Comput. Methods Appl. Mech. Engrg.*, 195(29):3776–3796, 2006.

[64] J.A. Weiss, B.N. Maker, and S. Govindjee. Finite element implementation of incompressible, transversely isotropic hyperelasticity. *Computer Methods in Applications of Mechanics and Engineering*, 135:107–128, 1996.